BEARING CAPACITY AND SETTLEMENT BEHAVIOUR OF FOOTINGS SUBJECTED TO STATIC AND SEISMIC LOADING CONDITIONS IN UNSATURATED SANDY SOILS

by

Fathi Mohamed Omar Mohamed, **B.Sc., U. of Tripoli, and M.A.Sc., U. of Ottawa**

A thesis
Submitted to the faculty of graduate and postdoctoral studies
under the supervision

of

Drs. Sai K. Vanapalli and Murat Saatcioglu

In partial fulfillment of the requirements for the degree of
Doctor of Philosophy in Civil Engineering

Faculty of Engineering, Department of Civil Engineering
University of Ottawa
Ottawa, Ontario, Canada K1N 6N5

February 2014

The doctor of philosophy in Civil Engineering is a joint program between Carleton University and University of Ottawa, which is administered by the Ottawa-Carleton institute for Civil Engineering

ABSTRACT

Several studies were undertaken by various investigators during the last five decades to better understand the engineering behaviour of unsaturated soils. These studies are justified as more than 33% of soils worldwide are found in either arid or semi-arid regions with evaporation losses exceeding water infiltration. Due to this reason, the natural ground water table in these regions is typically at a greater depth and the soil above it is in a state of unsaturated conditions. Foundations of structures such as the housing subdivisions, multi-storey buildings, bridges, retaining walls, silos, and other infrastructure constructed in these regions in sandy soils are usually built within the unsaturated zone (i.e., vadose zone). Limited studies are reported in the literature to understand the influence of capillary stresses (i.e., matric suction) on the bearing capacity, settlement and liquefaction potential of unsaturated sands. The influence of matric suction in the unsaturated zone of the sandy soils is ignored while estimating or evaluating bearing capacity, settlement and liquefaction resistance in conventional engineering practice. The focus of the research presented in the thesis has been directed towards better understanding of these aspects and providing rational and yet simple tools for the design of shallow foundations (i.e., footings) in sands under both static and dynamic loading conditions.

Terzaghi (1943) or Meyerhof (1951) equations for bearing capacity and Schmertmann et al. (1978) equation for settlement are routinely used by practicing engineers for sandy soils based on saturated soil properties. The assumption of saturated conditions leads to conservative estimates for bearing capacity; however, neglecting the influence of capillary stresses contributes to unreliable estimates of settlement or differential settlement of footings in unsaturated sands. There are no studies reported in the literature on how capillary stresses influence liquefaction, bearing capacity and settlement behavior in earthquake prone regions under dynamic loading conditions. An extensive experimental program has been undertaken to study these parameters using several specially designed and constructed equipment at the University of Ottawa.

The influence of matric suction, confinement and dilation on the bearing capacity of model footings in unsaturated sand was determined using the University of Ottawa Bearing Capacity Equipment (UOBCE-2011). Several series of plate load tests (PLTs) were carried out on a sandy soil both under saturated and unsaturated conditions. Based on these studies, a semi-empirical equation has been proposed for estimating the variation of bearing capacity with respect to matric suction. The saturated shear strength parameters and the soil water characteristic curve (SWCC) are required for using the proposed equation. This equation is consistent with the bearing capacity equation originally proposed by Terzaghi (1943) and later extended by Meyerhof (1951) for saturated soils. Chapter 2 provides the details of these studies.

The cone penetration test (CPT) is conventionally used for estimating the bearing capacity of foundations because it is simple and quick, while providing continuous records with depth. In this research program, a cone penetrometer was specially designed to investigate the influence of matric suction on the cone resistance in a controlled

laboratory environment. Several series of CPTs were conducted in sand under both saturated and unsaturated conditions. Simple correlations were proposed from CPTs data to relate the bearing capacity of shallow foundations to cone resistance in saturated and unsaturated sands. The details of these studies are presented and summarized in Chapter 3.

Standard penetration tests (SPTs) and PLTs were conducted in-situ sand deposit at Carp region in Ottawa under both saturated and unsaturated conditions. The test results from the SPTs and PLTs at Carp were used along with other data from the literature for developing correlations for estimating the bearing capacity of both saturated and unsaturated sands. The proposed SPT-CPT-based technique is simple and reliable for estimation of the bearing capacity of footings in sands. Chapter 4 summarizes the details of these investigations.

Empirical relationships were proposed using the CPTs data to estimate the modulus of elasticity of sands for settlement estimation of footings in both saturated and unsaturated sands. This was achieved by modifying the Schmertmann et al. (1978) equation, which is conventionally used for settlement estimations in practice. Comparisons are provided between the three CPT-based methods that are commonly used for settlement estimations in practice and the proposed method for seven large scale footings in sandy soils. The results of the comparisons show that the proposed method provides better estimations for both saturated and unsaturated sands. Chapter 5 summarizes the details of these studies.

A Flexible Laminar Shear Box (FLSB of 800-mm^3 in size) was specially designed and constructed to simulate and better understand the behaviour of model surface footing under seismic loads taking account of the influence of matric suction in an unsaturated sandy soil. The main purpose of using the FLSB is to simulate realistic in-situ soils behaviour during earthquake ground shaking. The FLSB test setup with model footing was placed on unidirectional 1-*g* shake table (aluminum platform of 1000-mm^2 in size) during testing. The resistance of unsaturated sand to deformations and liquefaction under seismic loads was investigated. The results of the study show that matric suction offers significant resistance to liquefaction and settlement of footings in sand. Details of the equipment setup, test procedure and results of this study are presented in Chapter 6.

Simple techniques are provided in this thesis for estimating the bearing capacity and settlement behaviour of sandy soils taking account of the influence of capillary stresses (i.e., matric suction). These techniques are consistent with the methods used in conventional geotechnical engineering practice. The studies show that even low values of capillary stresses (i.e., 0 to 5 kPa) increases the bearing capacity by two to four folds, and the settlement of footings not only decreases significantly but also offers resistance to liquefaction in sands. These studies are promising and encouraging to use ground improvement techniques; such as capillary barrier techniques to maintain capillary stresses within the zone of influence below shallow foundations. Such techniques, not only contribute to the increase of bearing capacity, they reduce settlement and alleviate problems associated with earthquake effects in sandy soils.

ACKNOWLEDGMENTS

I would like to express my sincere appreciation to my advisors, Professor Sai Vanapalli and Professor Murat Saatcioglu for their support, advice and invaluable guidance throughout the research program undertaken in the thesis.

Thanks to the committee members; Professors: Adel Hanna, Siva Sivathayalan, Mamadu Fall, Julio Angel Infante Sedano for their time and invariable comments. Many thanks go to the chair of my PhD defence Professor Paul Heintzman for steering the committee.

I am grateful to C. Jean Claude, M. Majeed, technical officers at the Department of Civil Engineering, University of Ottawa for their assistance during the research program. I thank J. Perrins, senior engineer in the machine shop at the Department of Mechanical Engineering for his assistance with the construction of setups used in the research. The assistance of the supporting staff (Y. Hogan, M. Racine and L. Deschenes) at the Department of Civil Engineering, University of Ottawa is appreciated.

I am indebted to my colleagues of graduate and former graduate students; Hana, Won, Kulan, Javad, Joseph, Naiem, Nil, Othman, Lu, Afshin, Ali, Farzad and Zu at the department of Civil Engineering, University of Ottawa for their kindness and friendship.

I wish to highly appreciate my wife, kids (Maria, Mohamed and Adam), my parents, my brothers and sisters for the encouragement and continued support during my studies.

Last but not least, I thank the Libyan Ministry of Scientific Research and Higher Education for granting me the Libyan-North American Scholarship. Special thanks go to the Canadian Bureau for International Education, CBIE in Ottawa, ON, Canada for managing the scholarship program. I also acknowledge the teaching and research assistantship, part-time instructor positions, and conference travel grants received from the University of Ottawa throughout the past five years of my PhD studies.

TABLE OF CONTENTS

LIST OF FIGURES

LIST OF TABLES

LIST OF SYMBOLS

SUBSCRIPTS

sat = saturated condition

unsat = unsaturated condition

max = maximum value

min = minimum value

ABBREVIATIONS AND SYMBOLS

PLT = plate load test

CPT = cone penetration test

SPT = standard penetration test

UOBCE = University of Ottawa bearing capacity equipment

FLSB = flexible laminar shear box

CPT = cone penetration test

USCS = unified soil classification system

DST = direct shear test

DAQS = data acquisition system

GSF = general shear failure

AEV = air-entry value

AVR = average

GWT = groundwater table

BC = bearing capacity

N = standard penetration number

N_{SPT} = corrected N value

N_{60} = N value corrected to 60% of the theoretical free fall hummer energy

$(N_1)_{60}$ = N_{60} corrected to standard value of effective overburden pressure

NE = North East

NW = North West

SE = South East

SW = South West

EQ = Earthquake

$LVDT$ = Linear Variable Displacement Transducer

CDT = Cable Displacement Transducer

LC = Load Cell

ACC. = Acceleration

e = void ratio

G_s = specific gravity

q_u = ultimate bearing capacity

q_{ult} = ultimate bearing capacity

$(u_a - u_w)$ = matric suction

$(u_a - u_w)_{AVR}$ = average matric suction value

$(u_a - u_w)_b$ = air-entry value

u_a = pore-air pressure

u_w = pore-water pressure

$d\gamma_{yz}$ = change in shear strain

$d_{\varepsilon y}$ = change in normal strain

d_z = change of thickness

Ψ = angle of dilation

$\phi'_{Critical}$ = effective critical state friction angle

D_{10} = diameter corresponding to 10% finer in the particle size distribution curve

D_{30} = diameter corresponding to 30% finer in the particle size distribution curve

D_{60} = diameter corresponding to 60% finer in the particle size distribution curve

C_u = coefficient of uniformity

C_c = coefficient of curvature

γ_d = dry unit weight of soil

$\gamma_{d(min)}$ = minimum dry unit weight of soil

$\gamma_{d(max)}$ = maximum dry unit weight of soil

D_r = relative density

w or w.c. = water content

o.w.c = optimum water content

B = width of a footing

D_i = diameter of a footing

L = length of a footing

W = width of a box used for model footing test

H = height of a box used for model footing test

D = depth of a box used for model footing test

D_f = depth of footing

q = applied stress

S = degree of saturation

$\gamma or\ \gamma_t$ = total unit weight of soil

ϕ' = effective internal friction angle for saturated condition

ϕ^b = contribution of soil suction towards the shear strength of unsaturated soil

c' = effective cohesion for saturated condition

ψ_{BC} = fitting parameter for bearing capacity

N_c, N_q, N_γ = bearing capacity factors

ξ_c, ξ_q, ξ_γ = footing shape factors

F_c, F_q, F_γ = footing depth factors

ϕ'_m = modified internal friction angle

q_c = cone resistance

D_c = cone diameter

A_c = cone base area

D_{50} = diameter corresponding to 50% finer in the particle size distribution curve

IZ = influence zone

Q_C = load carried by cone

f_C = sleeve friction

Q_f = load carried by the sleeve (shaft) in saturated condition

L_{sh} = embedded length of the shaft

σ_n = normal stress

$(u_a - u_w)$ = matric suction

$(\sigma_n - u_a)$ = net normal stress

A_s = surface area of the sleeve

R_f = friction ratio

Q_{fus} = total load carried by the sleeve

$Q_{(u_a-u_w)}$ = shaft capacity (sleeve friction) due to unsaturated condition

β = constant function of lateral earth pressure ratio

K = coefficient of lateral earth pressure ratio

κ = fitting parameter as function of plasticity index (1 for sandy soils) for shear strength of unsaturated soils

φ = soil / pile interface friction angle, ^{o}

Q_t = total load carried by the sleeve and the cone

F = shape factor for CPT-based bearing capacity (Eslaamizaad and Robertson 1996)

$q_{c\ AVR}$ = average cone resistance

θ = correlation factor for saturated condition

s_1 = first fitting parameter for saturated soil for estimating bearing capacity from CPTs

s_2 = second fitting parameter for saturated soils for estimating bearing capacity from CPTs

Ω = correlation factor for unsaturated condition

u_1 = first fitting parameter for unsaturated conditions for estimating bearing capacity from CPTs

u_2 = second fitting parameter unsaturated conditions for estimating bearing capacity from CPTs

B_1 = width of the first plate load

B_2 = width of the second plate load

δ = settlement of model footing or in-situ footing

δ_{B1} = settlement of model footing corresponding to first plate load

δ_{B2} = settlement of model footing corresponding to second plate load

q_{all} = allowable bearing capacity

C_{1spt} = first fitting parameter for estimating bearing capacity from SPTs

c_{2spt} = second fitting parameter for estimating bearing capacity from SPTs

q_t = total cone resistance

$\sigma'_{z,d}$ = vertical effective stress at footing base level

E_s = elastic modulus of soil

q_a = applied stress on a footing

C_1 = depth factor

C_2 = time factor

Δ_{zi} = thickness of the soil layer

t = time

X_1 = first constant number

X_2 = second constant number

f_1 = fitting parameter for saturated condition for settlement

f_2 = fitting parameter for unsaturated conditions for settlement

Q_m = load carried by model footing

Q_p = load carried by prototype footing

λ = scaling factor

ω = angular speed

f = frequency

A = displacement amplitude

CHAPTER 1

INTRODUCTION

1.1 Statement of the Problem

One third of the worldwide soils are in either arid or semi-arid regions with more evaporation losses from soils in comparison to water infiltration. Due to this reason, the natural ground water table in these regions is typically at a greater depth and the soil above it is in a state of unsaturated condition. Foundations of structures such as the housing subdivisions, multi-storey buildings, bridges, retaining walls, silos, and other infrastructure constructed in these regions in sandy soils are usually built within the unsaturated zone (i.e., vadose zone) in semi-arid regions. The foundations (i.e., shallow foundations) are designed to transfer the loads safely from the superstructure to the supporting soil such that the settlements are within acceptable limits as per the design and construction codes. These foundations are usually placed close to the soil surface and above the groundwater table; the loads from the superstructure are distributed within the unsaturated soil zone.

The two key parameters required in the design of shallow foundations are the bearing capacity and settlement behaviour of soils. Prandtl (1921) and Reissner (1924) were the earliest investigators who studied the bearing capacity of soils by loading a strip footing until it penetrated into the soil. The bearing capacity of shallow foundations is conventionally estimated using the approaches originally presented by Terzaghi (1943) and Meyerhof (1951) assuming the state of the soil is in saturated condition. The settlement behaviour of shallow foundations is routinely estimated using Schmetrmann et al. (1978) method without taking into account of the soil state (i.e., saturated or unsaturated). In other words, the conventional approaches used in practice for estimating

the bearing capacity and settlement of footings in unsaturated soils ignore the influence of matric suction.

Compacted soils, collapsible soils, residual soils, and expansive soils are typical examples of unsaturated soils. The mechanical behaviour of a soil in a saturated state condition is significantly different from an unsaturated state. Several investigators reported limitations in extending the principles of saturated soil mechanics for unsaturated soils (Bishop 1959, Broms 1964, and Fredlund and Rahardjo 1993). Terzaghi's effective stress concept; which is applicable for saturated soils, is not valid for unsaturated soils as the influence of capillary tension is not considered (Bishop 1959). For this reason, applying the conventional theory of soil mechanics to unsaturated soils may not be reliable leading to uneconomical shallow foundation design or estimating unreliable bearing capacity or settlement values.

Considerable research focus has been directed to interpret the engineering behaviour of unsaturated soils using two independent stress state variables; namely, net normal stress, $(\sigma_n - u_a)$ and matric suction, $(u_a - u_w)$ (for example, Bishop 1959, Bishop and Blight 1963, Fredlund and Morgenstern 1977, and Alonso et al. 1990, Vanapalli et al. 1996). The matric suction is defined as the difference between the pore-air pressure, u_a and pore-water pressure, u_w (i.e., $(u_a - u_w)$).

Several studies were also undertaken during the last five decades to understand the influence of matric suction on the bearing capacity of unsaturated soils (Broms 1964, Steensen-Bach et al. 1987, Fredlund and Rahardjo 1993, Schnaid et al. 1995, Miller and Muraleetharan 1998, Oloo et al. 1997, Costa et al. 2003, Yongfu 2004, Mohamed and Vanapalli 2006, and Rojas et al. 2007). However, there are limited studies reported in the literature with respect to interpretation of the influence of matric suction both on the bearing capacity and settlement behaviour in unsaturated soils, for both static and dynamic loading conditions.

1.2 Justification of Using Mechanics of Unsaturated Soils in Practice

The bearing capacity and settlement are two key parameters required in the design of shallow foundations (e.g., footings) particularly in sandy type of soils. The shallow foundations are usually designed to support structures for a long period of time without stability and settlement failures (i.e., typically for a period of several decades). In other words, foundations should be designed such that there are no functional or service problems for the structure on which it is constructed. To achieve this objective, a conservative approach is used for estimating the bearing capacity of shallow foundations assuming the soil is in a state of saturated condition. The bearing capacity equation proposed by Terzaghi (1943) or its modifications are conventionally used in engineering practice. These equations use saturated shear strength parameters to estimate the bearing capacity. However, shallow foundations are built near ground surface and above groundwater level where soils are typically in a state of unsaturated condition. The bearing capacity estimation in terms of saturated shear strength parameters not only provides a conservative estimate; also, neglecting the influence matric suction leads to erroneous estimates of the differential settlement behavior of unsaturated sands. In many scenarios, it is the settlement behavior which is the governing criterion in the design of foundations in sandy soils. In addition, there is limited information about the liquefaction resistance contribution in sandy soils due to matric suction. Due to these reasons, it was proposed in the present research to study the influence of capillary stresses (matric suction) on the bearing capacity, settlement behavior and liquefaction resistance of unsaturated sands. These studies are valuable and of interest to the practicing engineers as well as the academicians.

Extensive experimental investigations were undertaken in the present thesis as a first step in the laboratory to reliably determine the bearing capacity and settlement behavior of unsaturated sands taking account of the influence of matric suction ($u_a - u_w$). In addition, liquefaction resistance in unsaturated is also studied. The experimental results were interpreted using the mechanics of unsaturated soils.

Based on the research undertaken in the thesis, a semi-empirical equation for predicting the bearing capacity using saturated shear strength parameters and the soil-water characteristic cure (SWCC) is developed. Empirical procedures for estimating the settlement of shallow foundations in unsaturated soils were proposed. A Flexible Laminar Shear Box (FLSB) is designed and constructed for investigating the behaviour of a model shallow footing in unsaturated sandy soils focusing on the phenomenon of liquefaction.

1.3 Objectives of the Thesis

The main objectives of the undertaken research program are as follows:

(i) To design an equipment that can be used for bearing capacity and settlement behaviour investigations using model footings in both saturated and unsaturated sands, taking account of the influence of matric suction, dilation and overburden stress;

(ii) To propose a general equation for interpreting the bearing capacity of shallow foundations in sands that are in a state of unsaturated condition;

(iii) To propose a semi-empirical equation for estimating the variation of bearing capacity with respect to matric suction using the saturated shear strength parameters and the soil water characteristic curve (SWCC);

(iv) To propose simple relationships between the CPTs data and the bearing capacity of shallow foundations in saturated and unsaturated sands for use in geotechnical engineering practice;

(v) To modify Schmertmann et al. (1978) equation proposing simple relationships for settlement estimations in both saturated and unsaturated sands;

(vi) To conduct a series of SPTs and PLTs in the field in both saturated and unsaturated sandy soil at Carp region in Ottawa and interpret the results and provide comparisons between the bearing capacity and settlement behavior using the proposed relationships;

(vii) To design and construct a FLSB to investigate the behaviour of model footing placed on saturated and unsaturated sandy soil subjected to seismic loading.

1.4 Scope of the Thesis

In this research, the influence of matric suction on the bearing capacity and settlement behaviour of shallow foundations due to static loads is investigated both in the laboratory environment and in situ. Two model footing sizes of 100 mm × 100 mm and 150 mm × 150 mm were tested in two different bearing capacity equipment's (i.e., University of Ottawa Bearing Capacity Equipment, UOBCE-2006, and modified UOBCE-2011). The equipment were specially designed and constructed for conducting the experimental program presented in this thesis. Based on the results, a semi-empirical model is proposed for predicting the variation of the bearing capacity of unsaturated sands with respect to matric suction.

Several series of cone penetration tests (CPTs) were conducted in sand under both saturated and unsaturated conditions. Simple correlations were proposed from the CPTs data to relate the bearing capacity of shallow foundations to cone resistance in saturated and unsaturated sands. Moreover, the test results from the standard penetration tests (SPTs) and plate load tests (PLTs) at Carp region in Ottawa were used along with other data from the literature for developing correlations for estimating the bearing capacity of both saturated and unsaturated sands. The proposed SPT-CPT-based technique is simple and reliable for estimation of the bearing capacity of footings in sands.

In some scenarios, soils in saturated or unsaturated conditions can also be subjected to dynamic loading (e.g., seismic or blast) (Rollins and Seed 1990 and Charlie et al. 1980). Liquefaction associated with seismic loading remains a serious concern in sandy soils and has to be taken into account while designing shallow foundations in seismically active areas. Liquefaction occurs due to loss of effective stresses in soils; this phenomenon contributes to structures collapse leading to human and financial losses in many scenarios. There are several earthquakes recorded in history where sandy soils were subjected both liquefaction and intolerable deformation; for example, Niigata EQ in 1964, Loma Prieta 1989, and Duzce EQ (Schiff 1998 and Eseller-Bayat 2009). Limited studies are reported in the literature for sandy soils towards understanding the influence

of matric suction on the liquefaction, bearing capacity and settlement and its impact on the shallow foundation design procedures and guidelines.

In this research program, a Flexible Laminar Shear Box (FLSB of 800-mm^3 in size) was specially designed and constructed. The main purpose of this equipment is to simulate and better understand the realistic behaviour of model footing under seismic loads taking account of the influence of matric suction in unsaturated sand in a controlled laboratory environment. A model footing of 150 mm × 150 mm was tested in saturated and unsaturated sand simulating seismic loading through a sinusoidal wave in the FLSB on a 1-*g* shake table of 1000 mm (width) × 1000 mm (length) driven by an MTS actuator. The experimental results from this research program show that the matric suction of the tested sand (i.e., particularly in the range of 2 to ~ 6 kPa) has significant influence on the behaviour of shallow foundations under both static and dynamic (i.e., seismic) loading conditions.

1.5 Novelty of the Research Study

There are several novel aspects related to the research program undertaken in this thesis. Special equipment was designed and constructed for determining the bearing capacity and settlement behaviour of model footings under static loading taking account of the influence of capillary stresses. An extensive experimental work was carried out using model footings in sand under both saturated and unsaturated conditions. Based on the experimental results, a framework has been put forward to both interpret and predict the bearing capacity of shallow foundations in unsaturated sandy soil was proposed. The semi-empirical model that is proposed requires the information of the saturated shear strength parameters (i.e., c' and ϕ') and the soil-water characteristic curve (SWCC) for predicting the variation of bearing capacity with respect to suction.

A cone penetrometer was designed and several series of CPTs were carried out in a controlled laboratory environment in saturated and unsaturated sand. In addition to these tests, SPTs and PLTs were also conducted in-situ sand deposit at Carp region in Ottawa under both saturated and unsaturated conditions. The test results from the SPTs and PLTs

at Carp were used along with other data from the literature for developing simple and easy to use correlations for estimating the in-situ bearing capacity and settlement behavior of both saturated and unsaturated sands.

A Flexible Laminar Shear Box (FLSB) was specially designed and constructed for the undertaken research in this thesis at the University of Ottawa Machine Shop. The FLSB was used to simulate the realistic behaviour of model footings in saturated and unsaturated sand under seismic loading conditions. Such equipment is first of its kind in the literature to the best of the knowledge of the author.

1.6 Layout of the Thesis

The thesis is summarized in seven chapters, which includes this Chapter, “Introduction”, and Chapter 7 “Summary and Conclusions”. Four of the chapters (i.e., Chapter’s 2, 3, 4 and 5) were developed extending papers that were published in conferences and journals. Chapter 6 is presented in a conventional format. A separate chapter on the “Literature Review” is not presented in the thesis separately as an independent chapter because each of the chapter’s has a separate section that provides background information regarding the topic. A flow-chart illustrates the research undertaken in the thesis is shown in Figure 1.1.

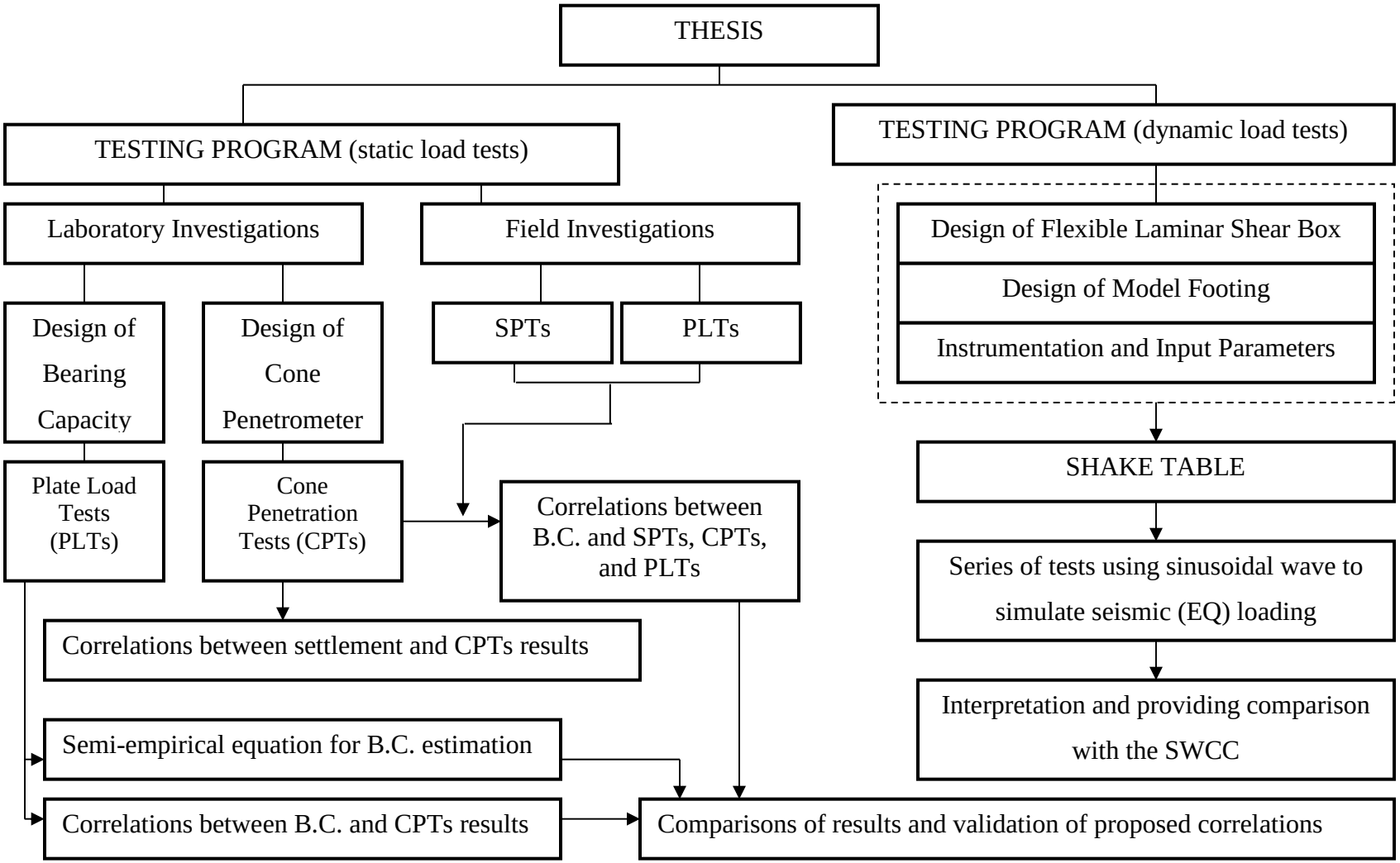

Figure 1. 1 Research Program Summary in the form of Flow-Chart

Second Chapter summarizes design and construction of the University of Ottawa Bearing Capacity Equipment (UOBCE-2011). Results of several plate load tests in saturated and unsaturated sand are presented and discussed. Based on these studies, a general equation is proposed for interpreting bearing capacity of coarse-grained unsaturated soils. In addition, a semi-empirical equation is proposed for predicting the variation of the bearing capacity of unsaturated sands with respect to suction. This chapter is developed based on the studies presented at the 14th Pan-American Conference on Soil Mechanics and Geotechnical Engineering and the 64th Canadian Geotechnical Conference held in 2011 in Toronto, Canada. This paper was awarded the 2011-CGS Graduate Student Award by the Canadian Geotechnical Society (Mohamed, Vanapalli and Saatcioglu 2011). More analysis and details were added to this paper and published in the International Journal of GEOMATE (Vanapalli and Mohamed 2013).

In the Third Chapter, an extensive experimental investigation of the bearing capacity of unsaturated sand using cone penetration tests (CPTs) was carried out. This chapter is developed by extending two papers summarized from this research program; the first paper was published in the proceedings of the 62nd Canadian Geotechnical Conference, 2009 in Halifax, Canada (Mohamed and Vanapalli 2009); and the second paper (Mohamed, Vanapalli and Saatcioglu 2010) was published in the proceedings of the 5th International Conference on Unsaturated Soils in Barcelona, Spain, 6-8 September 2010, published by the CRC Press/Balkema.

The Fourth Chapter provides details and comparisons between estimated settlement values from proposed simple relationships and measured settlement values of several footings constructed in saturated and unsaturated sands. This chapter is developed from a journal paper summarized based on the research undertaken for the present research. This paper was published in the International Journal of Geomechanics and Engineering (Mohamed, Vanapalli and Saatcioglu 2013).

The Fifth Chapter presents a series of standard penetration tests (SPTs) and plate load tests (PLTs) are conducted in-situ at Carp in Ottawa. This chapter is developed by extending a technical paper that was published in the Proceedings of the 2012 World

Congress on Advances in Civil, Environmental, and Materials Research (ACEM'12). Edited by Chang-Koon Choi. 26-29 August 2012, Seoul, Korea (Mohamed and Vanapalli 2012).

In the Sixth Chapter; design, construction, and use of a Flexible Laminar Shear Box (FLSB) on a 1-*g* shake table to study the behaviour of model footing on unsaturated sand is presented.

The Seventh Chapter, includes the "Summary and Conclusions" from the studies undertaken in this research program and also provides recommendations for proposed future studies with respect to implementing the mechanics of unsaturated soils in engineering practice.

1.7 List of Published Papers from the Research Undertaken in This Thesis

Mohamed, F. M. O. and Vanapalli, S. K. (2009). An experimental investigation of the bearing capacity of an unsaturated sand using cone penetration tests. Proceedings of 62nd Canadian Geotechnical Conference, 20-23 September, Halifax, NS: 205-213.

Mohamed, F. M. O., Vanapalli, S. K., and Saatcioglu, M. (2010). Comparison of bearing capacity of unsaturated sand using cone penetration tests (CPT) and plate load tests (PLT). In the Proceedings of the 5th International Conference on Unsaturated Soils, 6-8 September 2010, Barcelona, Spain: 1183–1188.

Mohamed, F. M. O., Vanapalli, S. K., and Saatcioglu, M. (2011). "Settlement estimation of shallow footings in saturated and unsaturated sands using cone penetration test (CPT) results." In the Proceedings of the CSCE General Meeting and Annual Conference – Engineers Advocates for Future Policy, 14-17 June 2011, Ottawa, ON, Canada.

Mohamed, F. M. O., Vanapalli, S. K. and Saatcioglu, M. (2011). "Bearing capacity and settlement behaviour of footings in an unsaturated sand." Proceedings of the 14th Pan-American on Soil Mechanics and Geotechnical Engineering, and the 64th Canadian Geotechnical Conference, 2-6 October 2011, Toronto, ON, Canada: Paper # 173.

Mohamed, F. M. O., Vanapalli, S. K. and Saatcioglu, M. (2012). Settlement estimation of shallow footings of saturated and unsaturated sands. Proceedings of GeoCongress 2012: State of the art and practice in geotechnical engineering, ASCE 2012, ISBN: 978-0-7844-1212-1, Oakland, California, USA: 2552-2561.

Mohamed, F. M. O., and Vanapalli, S. K. (2012). "Bearing capacity of shallow foundations in saturated and unsaturated sands SPT-CPT correlations." In the Proceedings of the 2012 International Conference on Geomechanics and Engineering, 26-30 August 2012 in Seoul, South Korea.

Vanapalli, S. K., and Mohamed, F. M. O. (2012). Bearing capacity and settlement of footings in an unsaturated sand. Keynote Paper in the proceedings of GEOMATE 2012 Conference, 14 – 16 November 2012 in KL, Malaysia: 12-21.

Vanapalli, S. K., and Mohamed, F. M. O. (2013). "Bearing capacity and settlement of footings in an unsaturated sand." International Journal of GEOMATE-2013 (Geotechnique, Construction Materials and Environment), ISSN: 2186-2982(P), 2186-2990(O), Japan, Vol. 5, No. 1 (Sl. No. 9): 595-604.

Mohamed, F. M. O., Vanapalli, S. K., and Saatcioglu, M. (2013). "Generalized Schmertmann equation for settlement estimation of shallow footings in saturated and unsaturated Sands." Geomechanics and Engineering, An International Journal, 2013 Techno-Press Ltd., Vol. 5, No. 4 (2013): 343-362.

1.8 References

Alonso EE, Gens A, Josa A. (1990). "A constitutive model for partially saturated soils." Geotechnique, 40 (3), 405 – 430.

Bishop, A. (1959). The principle of effective stress. Teknisk Ukeblad 106, 859–863.

Bishop, A. W., Blight, G. E. (1963). "Some aspects of effective stress in saturated and partly saturated soils." Geotechnique, (13), 177 – 197.

Broms, B. B. (1964). "The effect of degree of saturation on the bearing capacity of flexible pavements." Highway Research Record, (71), 1 – 14.

Charlie, W., Martin, J. P., Shinn, J., Blouin, S., and Melzer S. (1980). "Blast Induced Soil Liquefaction: Phenomena and Evaluation." Proceedings of the International Symposium on Soils under Cyclic and Transient Loading, Swansea, Balkema, Leiden, The Netherlands, 533 – 542.

Costa, Y. D, Cintra, J. C and Zornberg, J. G. (2003). “Influence of matric suction on the results of plate load tests performed on a lateritic soil deposit.” Geotechnical Testing Journal, 26 (2), 219 – 226.

Eseller-Bayat, E. E. (2009). “Seismic Response and Liquefaction Prevention of Sands Partially Saturated through Introduction of Gas Bubbles”, Ph.D. Thesis, Northeastern University, Boston, MA.

Fredlund, D. G., and Morgenstern, N. R. (1977). “Stress state variables for unsaturated soils.” Journal of Geotechnical Engineering Division, ASCE, 103(GT5), 447-466.

Fredlund, D. G and Rahardjo, H. (1993). “Soil mechanics for unsaturated soils.” 1st Ed., Wiley, New York.

Fredlund, D. G. (1996). “The emergance of unsaturated soil mechanics.” The 4th Spencer. J. Buchanan Lecture, Collage Station. Texas, A&M University Press, P39.

Meyerhof, G. G. (1951). “The ultimate bearing capacity of foundations.” Géotechnique, (2), 301-332.

Miller, G. A. and Muraleetharan, K. K. (1998). “In situ testing in unsaturated soil.” In the Proceedings of the 2nd International Conference on Unsaturated Soils, Beijing, China, 1, 416 – 42.

Mohamed, F. M. O and Vanapalli, S. K. (2006). “Laboratory investigations for the measurement of the bearing capacity of an unsaturated coarse-grained soil.” In the Proceedings of the 59th Canadian Geotechnical Conference, Vancouver, BC, 219 – 226.

Oloo, S. Y., Fredlund, D. G. and Gan, J. (1997). “Bearing capacity of unpaved roads.” Canadian Geotechnical Journal, 34(3), 398 – 407.

Prandtl, L. (1921). “Über die Eindringungsfestigkeit (Härte) plastischer Baustoffe und die Festigkeit von Schneiden.” (On the penetrating strengths (hardness) of plastic

construction materials and the strength of cutting edges), Zeit. Angew. Math. Mech., 1(1), 15 – 20.

Reissner, H. (1924). "Zum erddruckproblem." Proceedings of the 1st International Congress of Applied Mechanics, Delft, The Netherlands, 295 – 311.

Terzaghi, (1943) Terzaghi K. (1943). "Theoretical Soil Mechanics." John Wiley and Sons. New York, NY, USA.

Rojas, J. C., Salinas, L. M. and Seja, C. (2007). "Plate-load tests on an unsaturated lean clay. Experimental Unsaturated Soil mechanics." Proceedings of the 2nd International Conference on Unsaturated Soils (Springer Proceedings in Physics), Weimar (Germany), 445 – 452.

Rollins, K. M., and Seed, H. B. (1990). "Influence of buildings on potential liquefaction damage." Journal of Geotechnical Engineering, 116 (2), 165–185.

Schiff, A. J., (1998). "The Loma Prieta, California, Earthquake of October 17, 1989-Lifelines." U.S. Geological Survey (USGS) Professional Paper 1552 – A.

Schmertmann, J., Hartman, J. and Brown, P. R. (1978). "Improved strain influence factor diagrams." Journal of Geotechnical Engineering Division, ASCE, 104 (8), 1131-1135.

Schnaid, F., Consoli, N. C., Cumdani, R. and Milititsky, J. (1995). "Load-settlement response of shallow foundations in structured unsaturated soils". Proceedings of the 1st International Conference on Unsaturated Soils, Paris, 999 – 1004.

Vanapalli, S. K, Fredlund, D. G, Pufahl, D. E. and Clifton, A. W. (1996). "Model for the prediction of shear strength with respect to soil suction." Canadian Geotechnical. Journal, 33 (3), 379 – 392.

Yongfu, Xu. (2004). "Bearing capacity of unsaturated expansive soils." Geotechnical and Geological Engineering, (22), 611 – 625.

CHAPTER 2

[1]GENERAL EQUATION FOR ESTIMATING THE BEARING CAPACITY FOR FOOTINGS IN UNSATURATED SAND

2.1 Introduction

The two key properties required in the design of shallow foundations are the bearing capacity (i.e., q_u) and settlement (i.e., δ) behaviour of soils. Structures such as silos, antenna towers, bridges, multistory buildings and other infrastructures can be constructed on shallow foundations in sandy soils (e.g., spread footings near the ground surface) assuring a safe and economical design. The shallow footings are typically designed to transfer the loads safely from the superstructure to the supporting soil such that the settlements are in acceptable limits as per the design and construction codes. The bearing capacity of shallow foundations is estimated using the approaches originally presented by Terzaghi (1943) or Meyerhof (1951) assuming the soil is in a state of saturation condition. The measured bearing capacity from field tests typically higher than the estimated or computed bearing capacity values using analytical and empirical methods (Terzaghi 1943, Meyerhof 1951 and Meyerhof 1956, Vesic 1973). Typically, shallow foundations of structures are placed above the ground water table and the variation of stress with respect to depth associated with the loads from the superstructure is distributed in the vadose zone (i.e., unsaturated condition) of sandy soils. Such a scenario is typical in semi-arid and arid regions. Fredlund (1996) commented that "the portion of

[1]This chapter is developed by extending a technical paper that was presented in the 14th Pan-American Conference on Soil Mechanics and Geotechnical Engineering & the 64th Canadian Geotechnical Conference, October 2011 in Toronto, ON, Canada. This paper developed to a journal paper and published in the International Journal of GEOMAT 2013.

the soil profile above the groundwater table called the vadose zone that can be subdivided into two portions. The portion immediately above the water table, called the capillary fringe, remains saturated even though the pore-water pressures are negative. The portion above the capillary fringe is unsaturated." It can be seen in Figure 2.1 that with evaporation the pore-water pressure will be negative and with infiltration will be positive.

A framework for interpreting the bearing capacity and settlement behaviour of sands from experimental and modelling studies for unsaturated soils is recently evolving (Vanapalli and Mohamed 2007, Vanapalli 2009, Oh and Vanapalli 2011a, Oh and Vanapalli 2011b, and Mohamed et al. 2011). Comprehensive data for interpreting the bearing capacity of footings in unsaturated sands taking account of influence of the capillary stresses, overburden stress (i.e., confinement) and dilation is however not available in the literature. Due to these reasons, an experimental program as summarized in Figure 2.2 is undertaken to study the bearing capacity of a sandy soil using model footings in specially designed equipment. Terzaghi (1943) and Meyerhof (1951) equations are modified in this research for proposing a semi-empirical equation for bearing capacity of shallow foundations in unsaturated sands. Comparisons are provided between the estimated and measured values of the bearing capacity of model footings in saturated and unsaturated sand. The study shows that there is a good comparison between the measured and estimated values of the bearing capacity using the proposed modified equation.

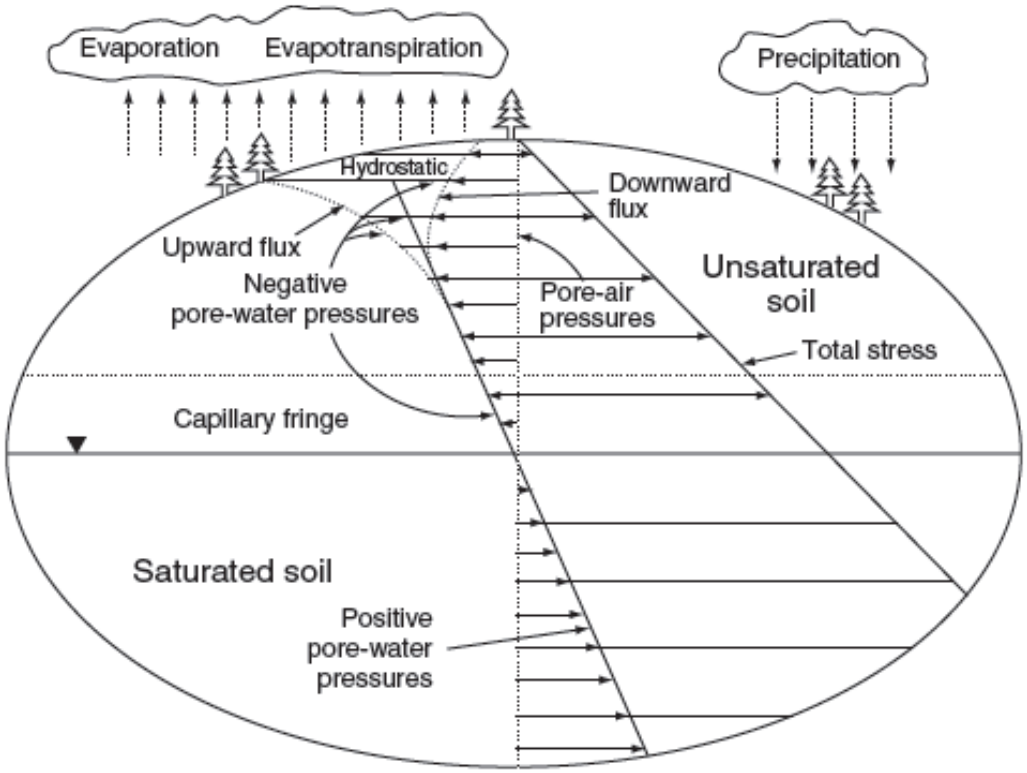

Figure 2. 1 Visualization of soil mechanics showing the role of surface flux boundary conditions (Fredlund 1996)

2.2 Background

2.2.1 Bearing Capacity of Soils

Prandtl (1921) and Reissner (1924) were the pioneers who considered a rigid loaded strip. Terzaghi (1943), Meyerhof (1951), and De Beer (1965) studies were directed towards understanding the bearing capacity of shallow foundations in saturated or dry conditions using the conventional soil mechanics. However, shallow foundations are found to be built close to the ground surface where the soils are unsaturated. Due to this reason, estimation of the bearing capacity of shallow foundations using conventional soil mechanics for which may underestimate the bearing capacity values and lead to conservative and costly foundation designs.

Comprehensive data for interpreting the bearing capacity of footings in unsaturated sands taking account of influence of the capillary stresses, overburden stress (i.e., confinement) and dilation is however not available in the literature. Due to these reasons, an experimental program as summarized in Figure 2.2 is undertaken to study the bearing capacity of a sandy soil using model footings in specially designed equipment. Terzaghi (1943) and Meyerhof (1951) equations are modified in this research for proposing a semi-empirical equation for bearing capacity of shallow foundations in unsaturated sands. Comparisons are provided between the estimated and measured values of the bearing capacity of model footings in saturated and unsaturated sand. The study shows that there is a good comparison between the measured and estimated values of the bearing capacity using the proposed modified equation.

Several researchers carried out investigations to study the bearing capacity of unsaturated soils (Broms 1963, Steensen-Bach et al. 1987, Fredlund and Rahardjo 1993, Schnaid et al. 1995, Oloo 1997, Miller and Muraleetharan 1998, Costa et al. 2003, Vanapalli and Mohamed 2007, Rojas et al. 2007, Vanapalli and Oh, 2010). Mohamed and Vanapalli (2006) designed special equipment (UOBCE-2006) and conducted studies to understand the bearing capacity of surface model footing in a sandy soil. These studies have shown that the matric suction values in the range of 2 to 6 kPa contribute to 5 to 7 times bearing capacity values in comparison to saturated condition. Vanapalli and Mohamed (2007) provided a framework to predict the variation of bearing capacity of a soil with respect to matric suction using the saturated shear strength parameters (c' and ϕ') and the Soil-Water Characteristic Curve (SWCC, which is a relationship between the gravimetric water content or volumetric water content and the matric suction).

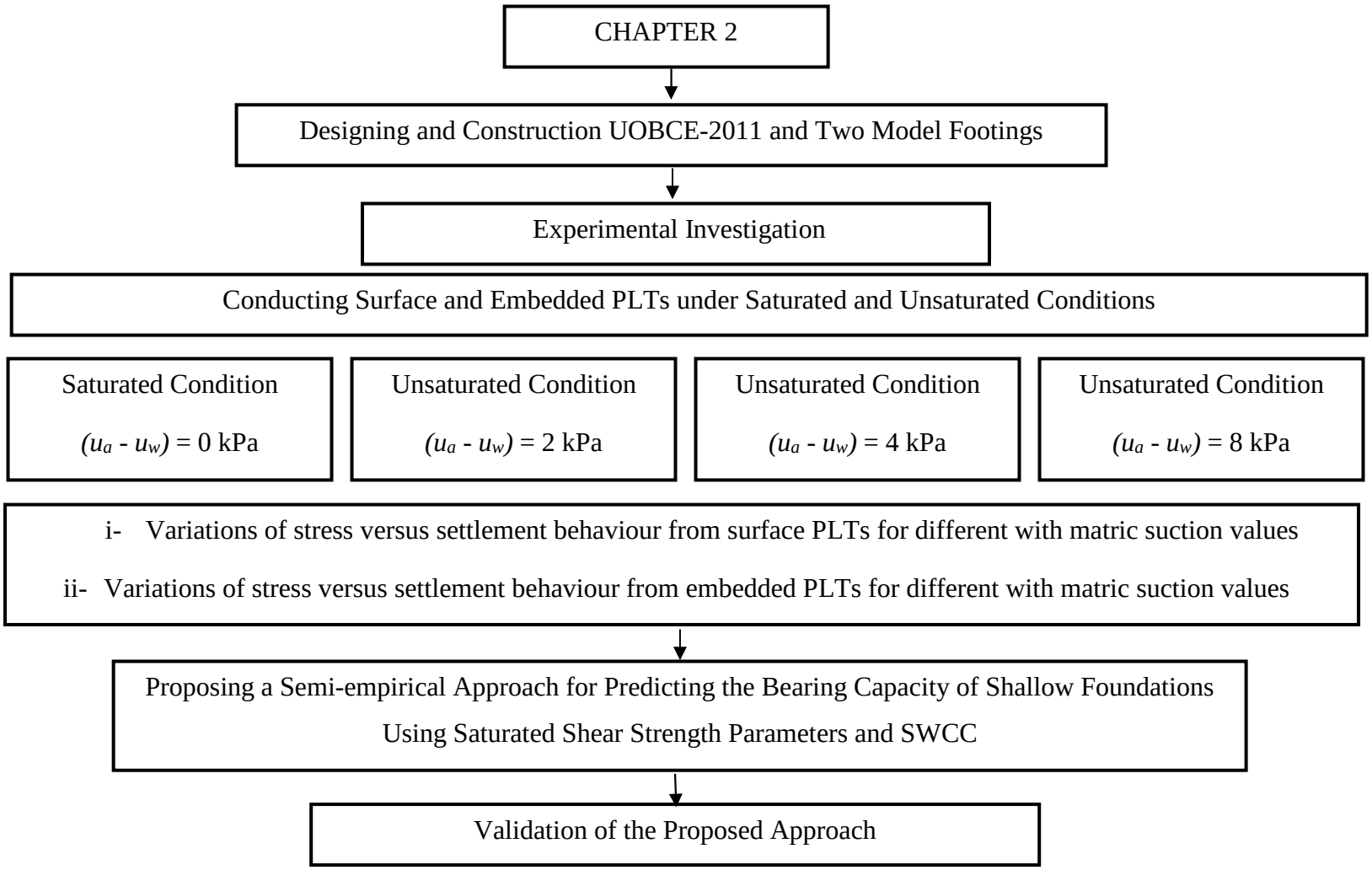

Figure 2.2 Flow-chart to illustrate the research program presented in this chapter

2.2.2 Dilation of Sandy Soils

Research studies related to dilation of sandy soils received great attention since 1960s because of its influence on the mechanical behaviour of soils. The term dilatancy is used to describe the increase in volume of a dense soil during shearing (Craig 2004). The conventional shear strength parameters (c' and ϕ') can only describe the full range of soil strength if both are allowed to change with density and stress (Bolton 1968). Hence, ignoring the influence of confinement and density particularly on the internal friction angle can lead to errors in determining the bearing capacity factors, N_c, N_q and N_γ needed for estimating the bearing capacity of shallow foundations.

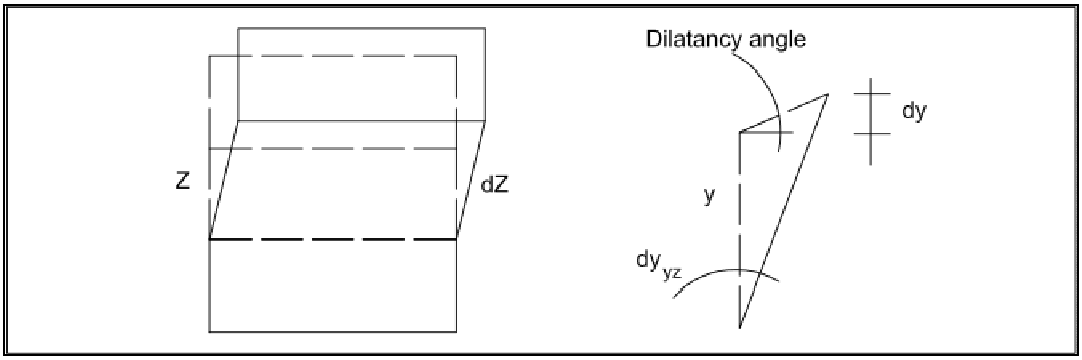

Figure 2.3 Angle of dilatancy for plane shear (Bolton 1986)

The change in shear stress and shear strain during shearing are shown in Eq. [2.1] and Eq. [2.2] respectively.

(Change in shear strain) $$d\gamma_{yz} = \frac{dz}{y} \qquad [2.1]$$

(Change in normal strain) $$d\varepsilon_y = -\frac{dy}{y} \qquad [2.2]$$

Hence: $$\tan\Psi = -\frac{d\varepsilon_y}{d\gamma_{yz}} = \frac{dy}{dz} \qquad [2.3]$$

The angle of dilation, Ψ as shown in Figure 2.3 and Figure 2.4 is equal to the instantaneous angle of motion of the sliding blocks relative to the rupture surface (see Eq. [2.3]). A great attention has been paid to the relationship between the internal friction angle, ϕ' and the dilation angle, Ψ and Eq. [2.4] was proposed by Rowe (1962), and Rowe (1969):

$$\phi' = \phi'_{Critical} + \Psi \qquad [2.4]$$

where:

ϕ' = effective angle of internal friction, °

$\phi'_{Critical}$ = effective angle of internal friction at critical state, °

Ψ = dilatancy angle, °

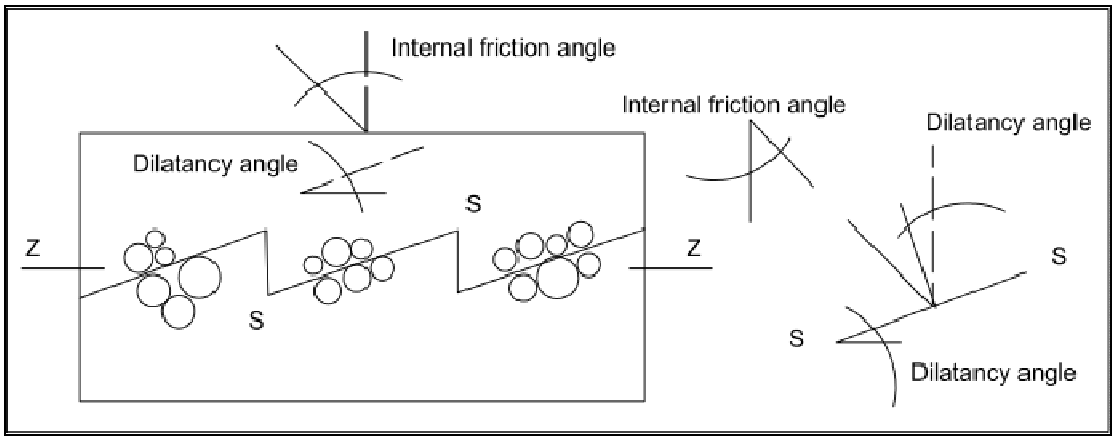

Figure 2.4 The saw blades model of dilatancy (after Bolton 1986)

Bolton (1986) found that Eq. [2.4] will overestimate $\phi' - \phi'_{Critical}$ by about 20 % (Figure 2.6). Based on experimental results on sandy soils, it was suggested that Eq. [2.4] can take the form as in Eq. [2.5]:

$$\phi' = \phi'_{Critical} + 0.8\Psi \qquad [2.5]$$

Effective internal friction angle, ϕ' obtained from the conventional laboratory tests (i.e. using triaxial shear or direct shear tests) need to be modified taking into account the difference between plane strain and axisymmetric conditions in the conventional triaxial compression tests as ϕ' from plane strain is typically higher than conventional triaxial compression (Marachi et al. 1981; Alshibli et al. 2003, and Wanatowski and Chu, 2007).

Several studies suggest that the overburden effective stress and density influence the dilatancy behaviour of sands (DeBeer 1965, Bolton 1986, and Sfriso 2009). The dilatancy angle, Ψ is always less than the effective friction angle, ϕ' based on the studies by Vemeer (1984).

Experiments (using steel shots that do not break down during shearing) conducted by Bishop (1972) have shown that an increase in confinement leads to decrease in the dilatancy angle, Ψ. More recent studies show that the dilation of sand decreases with an increase of the effective overburden stress (Chakraborty and Salgado 2010). Steensen-Batch (1987) found that good comparisons between the estimated and measured bearing capacity of model footing achieved when dilatancy angle of 10% of the effective internal friction angle was taken following the Danish Code of Practice (i.e., D.S. 415 1984). In this research program, the bearing capacity values were interpreted taking into account the influence of dilatancy angle, Ψ from direct shear test results of the tested sand.

From direct shear test results conducted on the tested sand, dilation angle, Ψ was estimated to be between 5 to 6° (i.e., approximately 15% of the effective internal friction angle) (see Figure 2.5). The Danish Code of Practice (DS 415-1984) recommends dilatancy angle of sands as 10% of the effective internal friction angle, ϕ'. More recently, Oh and Vanapalli (2011) have undertaken numerical modeling studies to predict the variation of bearing capacity with respect to matric suction for the same sand used in the present study. These modeling results also show good comparisons between the measured and modeled bearing capacity values using a dilatancy angle, Ψ which is equal to 10% of effective internal friction angle, ϕ'. Due to these reasons, in the present study, a dilatancy angle of approximately 3.53°, which is equal to 10% of the effective internal friction

angle, ϕ', has been used. Reasonably good comparisons were observed between the measured and predicted bearing capacity values extending this assumption in the present study.

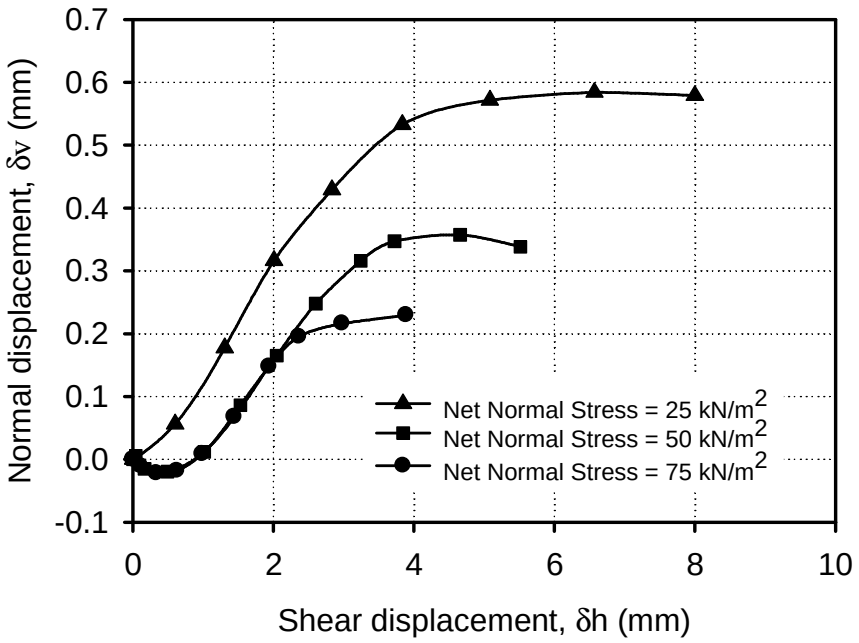

Figure 2.5 Normal displacement versus shear displacement for the tested sand

2.3 Routine Laboratory Tests and Properties of the Tested Soil

The soil used in this research was classified according to the Unified Soil Classification System (USCS) as poorly graded sand (fine sand) and has 5 % of silt. The average void ratio and the dry unit weight of the soil were 0.63 and 16.02 kN/m^3, respectively. The effective internal friction angle, ϕ' measured from direct shear test was 35.3 º (see Table 2.1). The routine laboratory tests that were conducted following ASTM D-3080 are presented in a form of flow-chart in Figure 2.6.

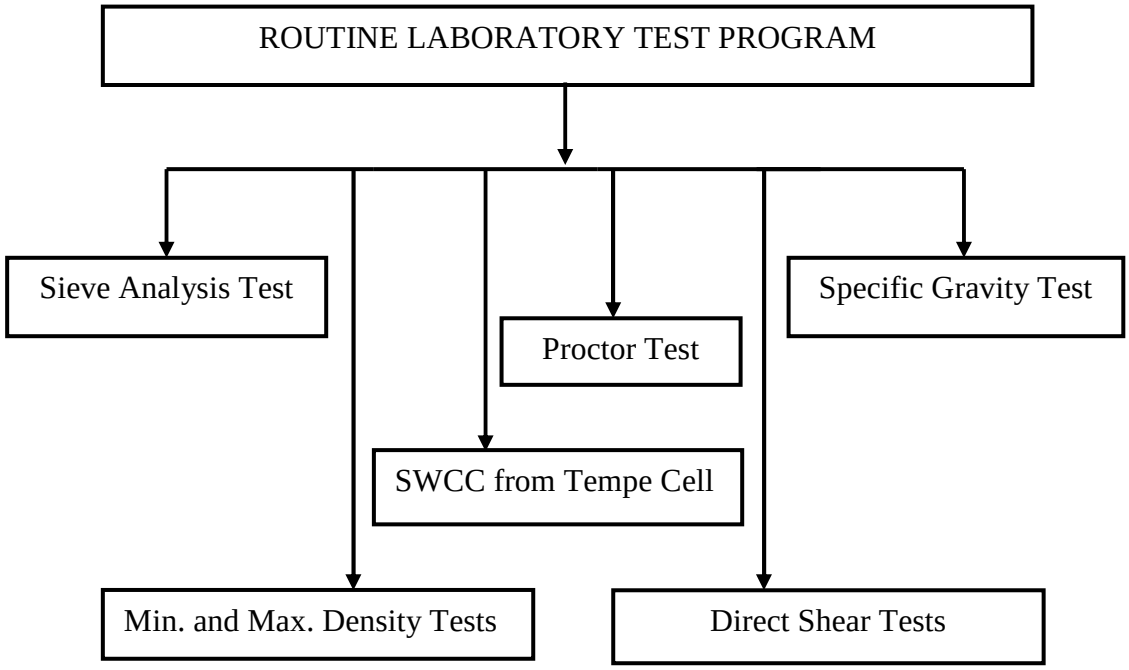

Figure 2.6 Routine laboratory tests conducted on the tested soil

Table 2. 1 Properties of the tested soil

Soil properties	**Value**
Coefficient of uniformity, C_u	1.83
Coefficient of curvature, C_c	1.23
Specific gravity, G_s	2.65
Average dry unit weight, γ_d , kN/m³	16.02
Min. dry unit weight, $\gamma_{d\,(min)}$, kN/m³	14.23
Max. dry unit weight, $\gamma_{d\,(max)}$, kN/m³	17.25
Average relative density, D_r %	65.0
Optimum water content, *o.w.c*, %	14.6
Void ratio, *e* (*after compaction*)	0.62 – 0.64
Effective cohesion, *c'*, kN/m^2 (*drained condition*)	0.6
Effective friction angle, ϕ' (^{o}) (*drained condition*)	35.3

2.4 Equipment and Methodology

Figure 2.7 shows the details of the modified University of Ottawa Bearing Capacity Equipment (modified UOBCE-2011). Schematic of a sectional view of the equipment is shown in Figure 2.8. The modified UOBCE-2011 is specially designed to determine the variation of bearing capacity and settlement of sands with respect to matric suction using model footings which are interpreted similar to plate load tests (i.e., PLTs). In the remainder of the thesis, model footing tests are referred to as model PLTs for brevity. The equipment setup consists of a rigid-steel frame made of rectangular hollow section with thickness of 6 mm and a box of 1500 mm (length) × 1200 mm (width) × 1060 mm

(depth). The test box can hold up to 3 tons of soil and the capacity of the loading machine (i.e., Model 244 MTS Hydraulic actuator with stroke length of 250 mm) is 28.5 kN. The ratio between the width of the test box and the width of the model footing was 1200/150 = 8.0 which is similar to ratios of test boxes reported in literature (see Table 2.2). The model PLTs were performed using different strain rates of 1.2 mm/min and 2.5 mm/min. The results suggest that the load carrying capacity of the sand is not influenced by the two different strain rates used in the present study.

The equipment used in the present study (UOBCE-2011, shown in Figure 2.7) in terms of test box size and its loading capacity is twice in comparison to the UOBCE-2006 used by Mohamed and Vanapalli (2006). The equipment in the present study has special provisions to achieve different degrees of saturation, *S* below the model footings similar to the original UOBCE-2006. The variation of matric suction with respect to depth in the unsaturated zone of the test box was measured using commercial Tensiometers. More details about the instrumentation and preparation for the testing are provided later in the chapter.

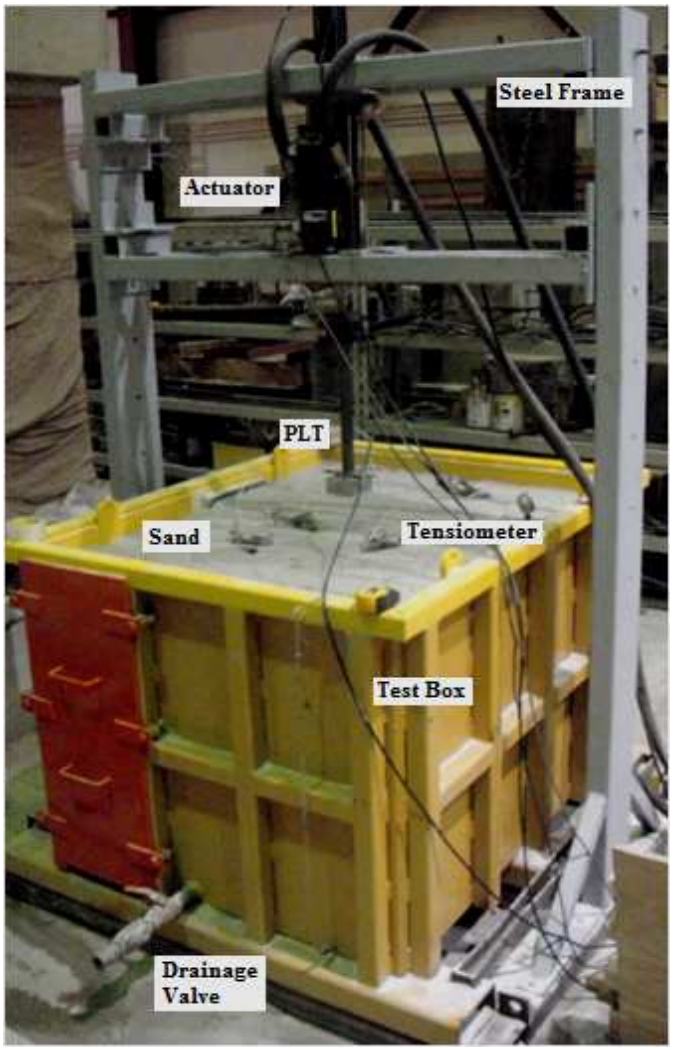

Figure 2.7 Photo: Modified University of Ottawa Bearing Capacity Equipment

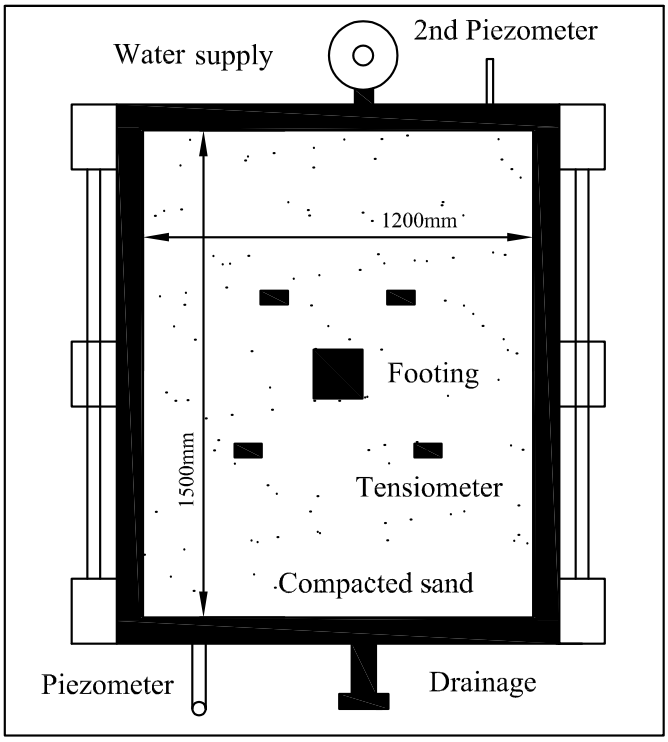

Figure 2.8 Schematic shows a top view of the test box

Table 2.2 Ratios between the widths of rigid test boxes and model footing sizes from previous studies

Test box size (mm) ($W \times H \times D$) [1]	Model Footing size (mm) ($B \times L$) or D_i	Ratio W/(B or D)	Reference
1270×1270×1780	102	12.4	Vesic (1973)
5400×6900×6000	910	5.93	Adams and Collin (1997)
1000×1000×1250	160	6.25	Hanna and Abdel-Rahman (1998)
2440×2440×1220 (test pit)	152×152, 305×305 and 457×457	16.05, 8 and 5.33	Cerato and Lutenegger (2006)
762×762×305	102×102 and 102 D_i	7.47	Cerato and Lutenegger (2006)
200 (D_i) ×120 (Depth)	22×22	9.10	Steensen-Bach et al. (1987)
900×900×600	150	6.00	Dash et al. (2003)
1200×3000×1400 (test pit)	310	3.87	Rojas et al. (2007)
600×600×400	100×100	6.00	Bera et al. (2007)
900×900×600	150×150	6.00	Latha and Somwanshi (2009)

[1] $W \times H \times D$ = Width × Height × Depth, and D_i = Diameter

2.5 Laboratory Plate Load Tests

Several tests were conducted to determine the bearing capacity of the sand with different values of matric suction using surface PLTs (i.e., model footing depth, D_f = 0 mm), and embedded PLTs (i.e., D_f = 150 mm). A minimum of three tests were conducted and average values are reported.

2.5.1 Surface Plate Load Test (PLTs)

Several surface PLTs (i.e., model footing depth, D_f = 0 mm), embedded PLTs (i.e., D_f = 150 mm) were conducted to determine the bearing capacity of the sand with different values of matric suction. Model PLTs of 150 mm × 150 mm (i.e., surface footings) were conducted using the UOBCE-2011. Applied stress versus settlement relationships for surface model footing of 150 mm × 150 mm are summarized in chapter 5.

Figure 2.9 shows the model footing at the soil surface and the MTS controller as well as the computer used to collect the measured results through the DAQS.

Figure 2.9 Model footing on the sand, control panel and computer

2.5.2 Embedded Plate Load Test (PLTs)

The model footings embedded in the modified UOBCE test box are analyzed considering the influence of average matric suction value in the proximity of the stress bulb zone which is equal to 1.5*B* (i.e., *B* = footing width). The depth 1.5*B* is the zone in which stresses are predominant due to the loading of square shallow footings with $D_f/B \leq 1.0$ (Polous and Davis 1974, Vanapalli and Mohamed 2007, and Oh and Vanapalli 2011). Figure 2.10 provides details used in the estimation of the average matric suction, $(u_a - u_w)_{AVR}$ value in the vicinity of the footing base as in Eq. [2.6].

$$(u_a - u_w)_{AVR} = \left(\frac{(u_a - u_w)_1 + (u_a - u_w)_2}{2} \right) \quad [2.6]$$

In this series of tests, a model footing of 150 mm × 150 mm is placed at a depth of 150 mm below the sand surface to investigate the effect of the overburden stress. The tests were conducted with different matric suction values below the footing (i.e., 0 kPa, 2 kPa and 6 kPa). Equilibrium conditions with respect to matric suction in the test box were typically achieved in a period of 48 hours in the test box (see Figure 2.10).

Table 2.3 summarizes a typical set of results in which the average matric suction in the vicinity of the footing base is 6 kPa (see Figure 2.10). The measured water content, *w.c.* and the matric suction, $(u_a - u_w)$ values from the test box of the modified UOBCE are similar to the corresponding water content and matric suction values in both measured and predicted SWCC of the tested sand. These results provide additional credence to the measurements of suction using the Tensiometers.

The SWCC for the tested sand was measured using Tempe Cell apparatus and the air-entry value (AEV) for the sand was found to be between 2.5 kPa and 3 kPa.

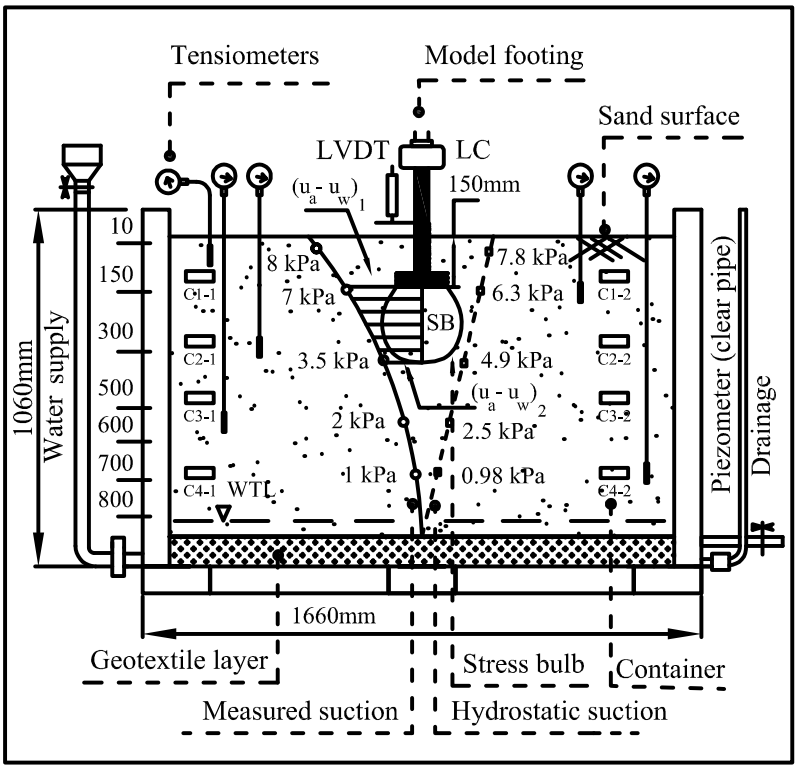

Figure 2.10 Schematic to illustrate the test setup and the procedure used for estimating the AVR matric suction of 6 kPa in the stress bulb zone of the embedded model footing in the modified UOBCE

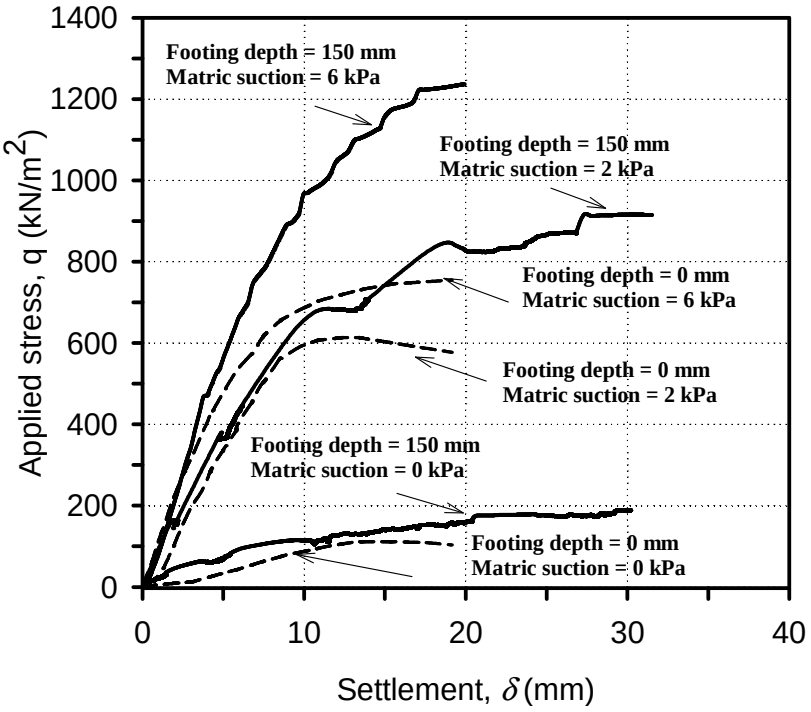

Figure 2.11 Relationship between the applied stress versus settlement behaviour of surface and embedded model footing tests of 150 mm × 150 mm in the UOBCE and modified UOBCE

The measured bearing capacity of the compacted unsaturated sand for both surface and embedded footings were in the range of 5 to 7 times higher than the saturated bearing capacity values as shown in Figure 2.11.

Table 2.3 Typical data from the test box for AVE matric suction of 6 kPa in the stress bulb zone

D* (mm)	γ_t (kN/m^3)	γ_d (kN/m^3)	*w.c.* (%)	S (%)	$(u_a - u_w)$ (kPa)
12	18.16	16.20	12.10	53	8.0
150	19.00	16.24	17.00	75	7.0
355	19.20	16.13	19.00	82	5.0
500	19.50	16.12	21.00	91	2.0
700	19.74	16.03	23.11	98	1.0
800	19.75	15.95	23.81	100	0.0

* Depth of Tensiometer from the soil surface

2.6 A Semi-empirical Equation for Predicting the Bearing Capacity of Unsaturated Soils (Surface Footings)

The bearing capacity equation for soils in terms of saturated shear strength parameters by Terzaghi (1943) was suggested based on Prandtl (1921) failure mechanism for a strip footing as given below.

$$q_u = c' N_c + \gamma D N_q + 0.5 \gamma B N_\gamma \qquad [2.7]$$

where:

q_u = ultimate bearing capacity, *kPa*

c' = effective cohesion, *kPa*

N_c, N_q, N_γ = bearing capacity factors due to cohesion, surcharge and unit weight

γ = soil unit weight, kN/m^3

B = footing width, m

The contribution of surcharge, N_q can be neglected for estimating the bearing capacity of shallow foundations placed directly on the soil surface. In other words, Eq. [2.7] takes the form:

$$q_u = c' N_c + 0.5\gamma B N_\gamma \quad [2.8]$$

Equation [2.8] can be written as given below by introducing Vesic (1973) shape factors:

$$q_u = c' N_c \zeta_c + 0.5\gamma B N_\gamma \zeta_\gamma \quad [2.9]$$

where:

ζ_c = shape factor due to cohesion (proposed by Vesic 1973)

ζ_γ = shape factor due to unit weight (proposed by Vesic 1973)

The shear strength contribution due to capillary stresses (i.e., matric suction) can be added to the effective cohesion term to estimate the bearing capacity of unsaturated soils extending the philosophy presented by Oloo (1994).

$$q_u = [c' + (u_a - u_w)_b (\tan\phi' - \tan\phi^b) + (u_a - u_w)\tan\phi^b] N_c \zeta_c + 0.5\gamma B N \gamma \zeta_\gamma \quad [2.10]$$

where:

$(u_a - u_w)_b$ = air-entry value, *kPa*

$(u_a - u_w)$ = average matric suction in the depth of the stress bulb, *kPa*

ϕ^b = internal friction angle with respect to matric suction, °

ξ_c , ξ_γ = shape factors due to cohesion and unit weight (from Vesić 1973)

Eq. [2.10] can be used for interpreting the bearing capacity of unsaturated soils if all the data is available. This equation can also be modified for predicting the bearing capacity of unsaturated soils extending the philosophy proposed by Vanapalli et al. (1996) for predicting the shear strength of unsaturated soils.

Vanapalli et al. (1996) proposed a semi-empirical function for estimating the internal friction angle with respect to matric suction, tan ϕ^b using the SWCC and the saturated shear strength parameters as $\tan\phi^b = S^\kappa \tan\phi'$, where S = degree of saturation value from the SWCC. This form of the equation takes account of the non-linear variation of the shear strength of unsaturated soils. Extending these concepts, Eq. [2.10] can be modified to predict the bearing capacity of unsaturated soils for square footings as given below:

$$q_u = [c' + (u_a - u_w)_b (\tan\varphi' \quad S^{\psi_{BC}} \tan\varphi') + (u_a - u_w) S^{\psi_{BC}} \tan\varphi'] N_c \zeta_c + 0.5\gamma B N\gamma \zeta_\gamma \quad [2.11]$$

where:

S = degree of saturation

ψ_{BC} = fitting parameter in bearing capacity equation

$(u_a - u_w)_b$ = air-entry value, *kPa*

$(u_a - u_w)$ = average matric suction in the depth of the stress bulb, *kPa*

N_c = bearing capacity factor due to cohesion (proposed by Terzaghi 1948)

N_γ = bearing capacity due to unit weight (proposed by Kumbhokjar 1993)

ξ_c , ξ_γ = shape factors due to cohesion and unit weight (from Vesić 1973)

Eq. [2.11] can be used for providing comparisons between the measured and predicted bearing capacity values using a fitting parameter, ψ_{BC} . The parameter, ψ_{BC} is defined hereafter as a bearing capacity fitting parameter. In this equation, the bearing capacity contribution due to matric suction can be obtained from a part of Eq. [2.11], which is equal to $(u_a - u_w) S^{\psi_{BC}} \tan\phi'$ beyond the air-entry value, $(u_a - u_w)_b$. Up to the air-entry value, $(u_a - u_w)_b$, the contribution to bearing capacity will be equal to $(u_a - u_w)_b (\tan\phi' - S^{\psi_{BC}} \tan\phi')$. This technique is similar to the predicting the shear strength contribution due to matric suction, which is $[(u_a - u_w) S^\kappa \tan\phi']$ (Vanapalli et al. 1996).

The philosophy of using the fitting parameter, ψ_{BC} in the bearing capacity of unsaturated soils is similar to using the fitting parameter, κ for predicting the shear strength of unsaturated soils. The limitation of using Equation [2.10] for predicting the bearing capacity of unsaturated soils is similar to using the shear strength equation proposed by Vanapalli et al. (1996) of unsaturated soils. In other words, Eq. [2.10] can only be used for predicting the bearing capacity when the experimental results are available. To alleviate this limitation for the shear strength of unsaturated soils, Vanapalli and Fredlund (2000) provided a relationship between κ versus plasticity index, I_p for predicting the shear strength of unsaturated soils. Based on more recent studies Garven and Vanapalli (2006) provided a relationship as given below:

$$\kappa = 1 + 0.0975 I_p - 0.0016 I_p^2 \qquad [2.12]$$

This relationship can be used for the prediction of the shear strength of unsaturated soils.

Mohamed (2006), followed the same philosophy to propose a relationship between the bearing capacity fitting parameter, ψ_{BC} versus plasticity index, I_P such that the Eq. [2.11] can be used for predicting the bearing capacity of unsaturated soils using the saturated shear strength parameters, c' and ϕ' and the SWCC. The bearing capacity fitting parameter, ψ_{BC} along with the effective shear strength parameters (c' and ϕ') and the SWCC are required for predicting the variation of bearing capacity with respect to matric suction assuming drained loading conditions. The bearing capacity fitting parameter, ψ_{BC} can be estimated from relationship provided in Eq. [2.13] as given below:

$$\psi_{BC} = 1.0 + 0.34 (I_p) - 0.0031 (I_p^2) \qquad [2.13]$$

where:

I_p = plasticity index

Eq. [2.11] will take the form as given below for predicting the bearing capacity if a square model footing is used:

$$q_u = [c' + (u_a - u_w)_b (\tan\phi' - S^{\psi_{BC}} \tan\phi') + (u_a - u_w)_{AVR} S^{\psi} \tan\phi'] N_c \zeta_c + 0.5\gamma B N_\gamma \zeta_\gamma \quad [2.14]$$

where: $(u_a - u_w)_{AVR} = \left(\frac{(u_a - u_w)_1 + (u_a - u_w)_2}{2} \right)$ as defined in Figure 2.10.

$(u_a - u_w)_b$ = air entry value, kPa

The following assumptions were required for the proposed bearing capacity equation:

- The soil is isotropic and homogeneous in nature.
- The ultimate bearing capacity is the maximum load per area at failure for dense soils where a well-defined failure load can be determined from the stress-settlement curve (i.e., GSF). Local shear failure conditions are assumed when it was difficult to define failure load from the stress-settlement curve extending Terzaghi (1943) approach.
- The proposed equation is valid for vertical static loads.
- The variation of measured matric suction (from experimental investigations) with respect to depth shows a slightly non-linear relationship with depth for the tested sand. However, this variation is close to linear nature (e,g., hydrostatic distribution). Due to this reason, the average matric suction was estimated assuming the variation of matric suction with respect to suction to be linear in the proposed equation.

2.7 Bearing Capacity of Unsaturated Soils (Embedded Footings)

Terzaghi (1943) suggested Eq. [2.7] to estimate the ultimate bearing capacity, q_u of saturated soils assuming general shear failure conditions.

A bearing capacity equation (i.e., Eq. [2.13]) was suggested by Vanapalli and Mohammed (2007) to predict the variation of bearing capacity for surface footings in unsaturated sandy soil. The general form of the equation that can be used to estimate the

bearing capacity of unsaturated soils is shown in Eq. [2.15]. This equation takes into account the influence of overburden stress and shape of the footing.

$$q_u = [c' + (u_a - u_w)_b (\tan \phi' - S^{\psi_{BC}} \tan \phi') + (u_a - u_w)_{AVR} S^{\psi_{BC}} \tan \phi'] N_c \zeta_c F_c + \gamma D_f N_q \zeta_q F_q + 0.5 \gamma B N_\gamma \zeta_\gamma F_\gamma \quad [2.15]$$

where:

ζ_q = shape factor

F_c, F_q, and F_γ = depth factors

Several investigators provided bearing capacity factors for cohesion, N_c; surcharge, N_q and unit weight, N_γ (Terzaghi 1943, Meyerhof (1951), Kumbhokjar (1993), and Kumbhokjar (1993)). The values for bearing capacity factors of N_c and N_q provided by various investigators are approximately the same. For this reason, the bearing capacity factors, N_c and N_q originally proposed by Terzaghi (1943) were used in the analysis. The N_γ values suggested by Kumbhokjar (1993) have been more widely used in recent years. For this reason, the bearing capacity factor, N_γ values proposed by Kumbhokjar (1993) are used in this study.

2.8 Comparison between Measured and Predicted Bearing Capacity Values

2.8.1 Measured and Predicted B.C. for the Surface Model Footings

The bearing capacity values of surface model footings of 150 mm × 150 mm were measured using the UOBCE-2011 under both saturated and unsaturated conditions. The bearing capacity under saturated and unsaturated conditions was interpreted taking into account of influence on the dilatancy angle, Ψ for sand.

Table 2.4 Bearing capacity factors, shape factors, and depth factors used for the analysis of the surface model footing tested in the laboratory

Effective friction angle, ϕ' = 35.3 º								
Estimated dilatancy angle, Ψ = 3.53 º								
Modified friction angle, $\phi'_m = (\phi' + \Psi) \approx 39$ º								
B.C. Factors[1]			Shape Factors[2]			Depth Factors[3]		
N_c	N_q	N_γ	ζ_c	ζ_q	ζ_γ	F_c	F_q	F_γ
86	70	95	1.8	1.8	0.6	1.0	1.0	1.0

[1] from Terzaghi (1943); [2] from Vesic (1973); [3] from Hansen (1970)

In Figure 2.12, comparison between measured and predicted bearing capacity values of 150 mm × 150 mm model footing. It can be seen that the bearing capacity linearly increases with matric suction up to the air-entry value (AEV ~ 3 kPa). Beyond this value bearing capacity increases non-linearly up to the matric suction at the residual zone of the SWCC.

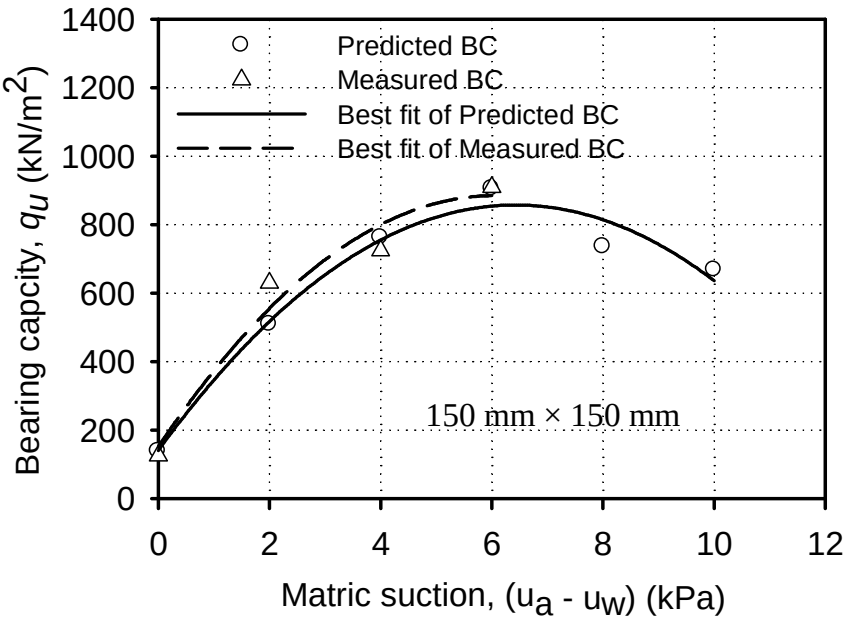

Figure 2.12 Typical results of the estimated BC using the proposed equations and the measured BC from surface 150 mm × 150 mm PLTs with respect to matric suction

2.8.2 Measured and Predicted B.C. for the Embedded Model Footings

The bearing capacity of 150 mm × 150 mm embedded model footing (tested in a sandy soil in both saturated and unsaturated conditions) was measured using the modified UOBCE (see Figures 2.7). The model footing of 150 mm × 150 mm was located at a depth, D_f of 150 mm below the soil surface simulating an overburden stress which also acts as a confinement all around the footing. There was a good comparison between the measured and estimated bearing capacity values for interpreting the embedded model footing results without taking account of the influence of dilatancy angle, Ψ. Such a behaviour can be attributed to the influence of the confinement with a depth which is equal to the width, B of the foundation (D_f = 150 mm; as illustrated earlier in Figure 2.9).

The obtained results using 150 mm × 150 mm model footing were consistent with the studies of several investigators who have shown that the influence of dilation in the sand

decreases with an increase in overburden effective stress or confinement (Bolton 1986, Chakraborty and Salgado 2010, and Liao and Hsu 2003).

Table 2.5 Bearing capacity factors, shape factors, and depth factors used for the analysis of the embedded model footing tested in the laboratory

Effective friction angle, ϕ' = 35.3 º								
Estimated dilatancy angle, Ψ = 0 º (Confined PLTs)								
B.C. Factors[1]			Shape Factors[2]			Depth Factors[3]		
N_c	N_q	N_γ	ζ_c	ζ_q	ζ_γ	F_c	F_q	F_γ
58	41	45	1.7	1.7	0.6	1.4	1.2	1

[1] from Terzaghi (1943); [2] from Vesic (1973); [3] from Hansen (1970)

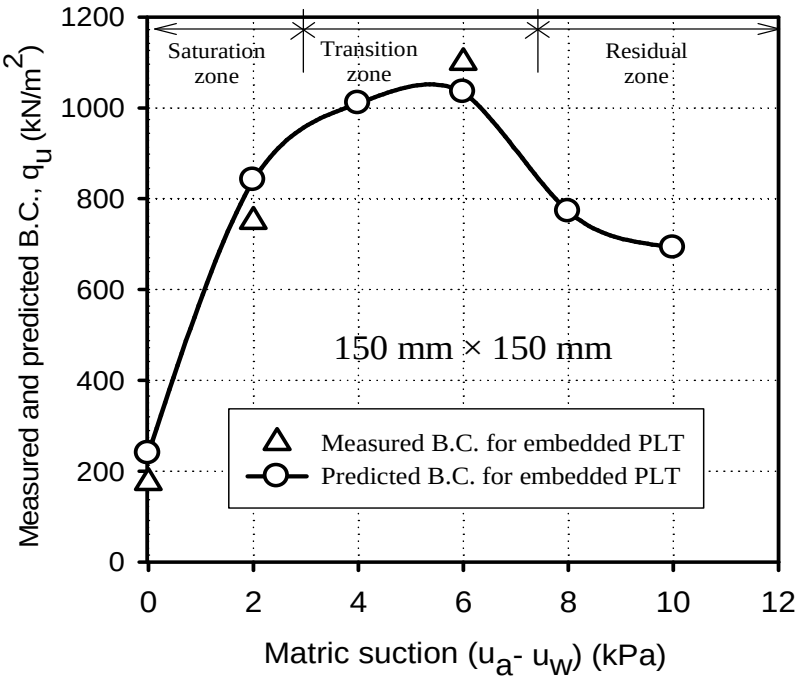

Figure 2.13 Measured and predicted bearing capacity of embedded model footing of 150 mm × 150 mm tested in the modified UOBCE

Because of the limited depth of the test box of both the UOBCE-2006 and the modified UOBCE-2011 in the laboratory, the maximum average matric suction value (i.e., $(u_a - u_w)_{AVR}$) simulated in the tank was 6 kPa. The proposed technique was developed based on test results using average matric suction values ≤ 6 kPa. In Figure 2.13, it can be seen that the bearing capacity linearly increases with matric suction up to the air-entry value (AEV ~ 3 kPa, which represents the differential air pressure minus water pressure that is required to cause desaturation of the largest pores) then increases non-linearly up to the matric suction at the residual zone of the SWCC. The reduction of the bearing capacity for matric suction values within the residual zone can be attributed to the discontinuous water phase surrounding the soil leading to stress state and inter-particle contact changes. Labedeff (1927) concluded that the increase of matric suction for a sandy soils below a certain water content (residual water content) has low effect on the water content of the soil.

2.9 Summary and Conclusions

The bearing capacity of a sandy soil under saturated and unsaturated conditions using surface and embedded model footings tests was studied in this research program. The bearing capacity of unsaturated sands increases with matric suction in a linear fashion up to the air-entry value (saturation zone). There is a non-linear increase in the bearing capacity in the transition zone (i.e., from air-entry to the residual suction value).

The bearing capacity values are underestimated for surface model footings (i.e., the depth of the model footing is equal to zero) when calculations are based on effective friction angle, ϕ' = 35.3 º for the tested sand both in saturated and unsaturated conditions. Typical value of dilatancy angle for sands was in the range of 10 % of effective friction angle, ϕ' (see Table 2.2). Reasonably good comparisons were observed between measured bearing capacity and predicted values for the surface model footings using Eq. [2.13] particularly when the influence of the dilatancy angle, Ψ was taken into account. There was no need to increase the effective friction angle, ϕ' by 10 % for embedded

footings using Eq. [2.14] (see Table 2.3). In other words, the overburden stress eliminates the influence of dilation for the case of the embedded model footing tests. These observations are consistent with the conclusions drawn in (Bolton 1986, Chakraborty and Salgado 2010 and Vesić and Clough 1968) with respect to dilation effects in sandy soils.

The observations of the bearing capacity results of the tested unsaturated sand are consistent with the shear strength behaviour of unsaturated sands (Vanapalli et al. 1996, and Vanapalli and Lacasse 2009). Hence, the modified Terzaghi equation for estimating the bearing capacity of sandy soils for both saturated and unsaturated conditions can be used by practicing engineers.

2.10 References

Adams, M. T. and Collin, J. C., 1997, “Large Model Spread Footing Load Tests on Geosynthetic Reinforced Soil Foundations”, Journal of Geotechnical and Geoenvironmental Engineering, 123, (1), 66 – 72.

Alshibli, A. K., Batiste, S. N. and Sture, S. (2003). "Strain localization in sand: plane strain versus triaxial compression". Journal of Geotechnical and Geoenvironmental Engineering, ASCE, 129 (6), 484 – 494.

Bolton, M. D. (1986). “The strength and dilatancy of sands,” Géotechnique, 36 (1), 65–78.

Broms, B. B. (1963). “The effect of degree of saturation on the bearing capacity of flexible pavements.” Highway Research Record, 71, 1 – 14.

Bishop, A. W. (1972). “Shear strength parameters for undisturbed and remoulded soils specimens,” In stress strain behaviour of soils. Foulis, London, 3 – 58.

Chakraborty, T. and Salgado, R. (2010). “Dilatancy and shear strength of sand at low confining pressure.” Journal of Geotechnical and Geoenvironmental. Engineering, (136), 527 – 32.

Cerato, A. B. and Lutenegger, A. J. (2006). “Specimen Size and Scale Effects of Direct Shear Box Tests of Sands.” Geotechnical Testing Journal, ASTM, 29 (6), 1 – 10.

Cerato, A. B. and Lutenegger, A. J. (2006). “Bearing capacity of square and circular shallow foundations on a finite layer of granular soil underlain by a rigid base.” Journal of Geotechnical and Geoenvironmental Engineering, ASCE, 132 (11), 1496 – 1501.

Costa, Y. D, Cintra J. C. and Zornberg, J. G. (2003). “Influence of matric suction on the results of plate load tests performed on a lateritic soil deposit.” Geotechnical Testing Journal, 26 (2), 219 – 226.

Craig, R. F. (2004). Craig’s Soil Mechanics. 7th edition. Published in the Taylor & Francis. 11 New Fetter Lane, London EC4P 4EE.

Das, B. and Sivakugan, N. (2007). “Settlement of shallow foundations on granular soil – an Overview,” International Journal of Geotechnical Engineering, (1), 19 – 29.

DeBeer, E. (1965). “Bearing capacity and settlement of shallow foundations on sand.” In the Proceedings of Symposium on Bearing Capacity and Settlement of Foundations, Durham, NC, 15 – 33.

D. S. 415. (1984). “The Danish code of practice for foundation engineering.” Danish Society of Civil Engineering.

Fredlund, D. G. and Rahardjo, H. (1993). “Soil mechanics for unsaturated soils.” 1st Ed., Wiley, New York.

Fredlund, D. G. (1996). “The emergance of unsaturated soil mechanics.” The 4th Spencer. J. Buchanan Lecture, Collage Station. Texas, A&M University Press, P39.

Hanna, A. and Abdel-Rahman, M. (1998), “Experimental investigation of shell foundation on dry sand.” Journal of Canadian Geotechnical, (35), 847 – 857.

Hansen, B. J. (1970). "A revised and extended formula for bearing capacity." Bulletin No. 28, Danish Geotechnical Institute, Copenhagen, Denmark, 5 – 11.

Kumbhokjar, A. S. (1993). "Numerical evaluation of Terzaghi's N_γ." Journal of Geotechnical Engineering, ASCE, (3), 598 – 607.

Lee, J. and Salgado, R. (2002). "Estimation of footing settlement in sand." The International Journal of Geomechnics, 1 (2), 1 – 28.

Labedeff, A. F. (1927). "The movement of ground and soil waters." Proceedings of the 1st International Congress of Soil Science, (1), 459 – 494.

Liao, H. J. and Hsu, S. T. (2003). "Uplift behaviour of blade-underreamed anchors in silty sand," Journal of Geotechnical and Geo-environmental Engineering: 560 – 568.

Madhavi, L. G. and Somwanshi, A. (2009). "Effect of reinforcement form on the performance of square footings on sand." Geotextiles and Geomembranes, (27), 409 – 422.

Marachi, N. D., Duncan, J. M., Chan, C.K. and Seed, H.B. (1981). "Plane-strain testing of sand. Laboratory Shear Strength of Soils." ASTMSTP740, R.N. Yong and F.C. Townsend (Ed.), 294 – 302 (ASTM: Philadelphia, PA).

Meyerhof, G. G. (1951). "The ultimate bearing capacity of foundations." Géotechnique, (2): 301 – 332.

Meyerhof, G. G. (1956)."Penetration tests and bearing capacity of cohesionless soils." Journal of Soil Mechanics and Foundation Division, ASCE, 82 (1), 1 – 19.

Mohamed, F. M. O. and Vanapalli, S. K. (2009). "An experimental investigation of the bearing capacity of an unsaturated sand using cone penetration tests." Proceedings of the 62nd Canadian Geotechnical Conference, Halifax, NS, 205 – 213.

Mohamed, F. M. O. (2006). “A semi-empirical approach for the interpretation of the bearing capacity of unsaturated soils.” Master’s Thesis, University of Ottawa, Ottawa, ON, Canada.

Mohamed, F. M. O., Vanapalli, S. K. and Saatcioglu, M. (2011). Bearing capacity and settlement behaviour of footings in an unsaturated sand. Proceedings of 2011 Pan-Am CGS Conference, Toronto, ON, Paper # 173.

Mohamed, F. M. O. and Vanapalli, S. K. (2006). “Laboratory investigations for the measurement of the bearing capacity of an unsaturated coarse-grained soil.” In the Proceedings of the 59th Canadian Geotechnical Conference, Vancouver, BC: 219 – 226.

Oh, W. T. and Vanapalli, S. K. (2011). “Modeling the stress versus settlement behaviour of model footings in saturated and unsaturated sandy soils.” Canadian Geotechnical Journal, (48), 425 – 438.

Oh, W. T. and Vanapalli, S. K. (2012). “Modelling the settlement behaviour of shallow foundations in unsaturated sands,” In the Proceedings of the GeoCongress2012, Oakland, 2542 – 2551.

Oloo, S. Y., Fredlund, D. G. and Gan, J. K M. (1997). “Bearing capacity of unpaved roads.” Canadian Geotechnical Journal, (34), 398 – 407.

Poulos, H. and Davis, E. (1974). “Elastic solutions for soil and rock mechanics.” John Wiley and Sons, NY, USA.

Prandtl, L. (1921). “Über die Eindringungsfestigkeit (Härte) plastischer Baustoffe und die Festigkeit von Schneiden.” (On the penetrating strengths (hardness) of plastic construction materials and the strength of cutting edges), Zeit. Angew. Math. Mech., 1(1), 15-20.

Reissner, H. (1924). “Zum erddruckproblem.” Proc., 1st Int. Congress of Applied Mechanics, Delft, The Netherlands, pp. 295–311.

Rojas, J. C., Salinas, L.M. and Seja, C. (2007). "Plate-load tests on an unsaturated lean clay. Experimental Unsaturated Soil mechanics." Proceedings of the 2nd International Conference on Unsaturated Soils (Springer Proceedings in Physics), Weimar (Germany), 445 – 452.

Sfriso, A. (2009). "The friction angle and critical state void ratio of sands." Proceedings of the 17th International Conference of Soil Mechanics and Geotechnical Engineering, ICSMGE, Alexandria, Egypt, 433 – 435.

Steensen-Bach, J. O., Foged, N. and Steenfelt, J. S. (1987). "Capillary induced stresses – fact or fiction?." In the Proceedings of the 9th ECSMFE, Groundwater Effects in Geotechnical Engineering, Dublin: 83 – 89.

Terzaghi, K. (1943). "Theoretical Soil Mechanics." John Wiley and Sons. New York, NY, USA.

Vanapalli, S. K. and Oh, W. T. (2010). "Mechanics of unsaturated soils for the design of foundation structures." Plenary Address. Proc. 3rd WSEAS International Conference on Engineering Mechanics, Structures, Engineering Geology, Corfu Island, Greece, 363 – 377.

Vanapalli, S. K, Fredlund, D. G, Pufahl, D. E. and Clifton, A. W. (1996). "Model for the prediction of shear strength with respect to soil suction." Canadian Geotechnical. Journal, 33 (3), 379 – 392.

Vanapalli, S. K. and Mohamed, F. M. O. (2007). "Bearing capacity of model footings in unsaturated soils." In Experimental Unsaturated Soil Mechanics, Springer Proc. in Physics. Springer-Verlag Berlin Heidelberg, (112), 483 – 493.

Vanapalli, S. K. (2009). "Shear strength of unsaturated soils and its applications in geotechnical engineering practice," Keynote Address. In the Proceedings of the 4th Asia-Pacific Conf. on Unsaturated Soils, New Castle, Australia, 579 – 598.

Vanapalli, S. K and Lacasse, F. (2009). “Comparison between the measured and predicted shear strength behaviour of four unsaturated sands.” In the Proceedings of the 4th Asia-Pacific Conference on Unsaturated Soils. New Castle, Australia, 121 – 127.

Vermeer, P. A. and DeBorst, R. (1984). “Non-associated plastic for soils, concrete and rock.” Heron, 5 – 64.

Vesić, A. S. and Clough, G. W. (1968). “Behaviour of granular materials under high stresses.” Journal of Soil Mechanics and Foundation Divison. ASCE, (SM3): 661 – 688.

Vesić, A. S. (1973). “Analysis of ultimate loads of shallow foundations.” Journal of the Soil Mechanics and Foundation Division, ASCE, (SM1), 45 – 7.

Wanatowski, D. and Chu, J. (2007). “Drained behaviour of Changi sand in triaxial and plane-strain compression.” Geomechanics and Geoengineering, 2(1), 29 – 39.

CHAPTER 3

[2]THE BEARING CAPACITY OF UNSATURATED SANDY SOIL FROM CONE PENETRATION TESTS AND PLATE LOAD TESTS

3.1 Introduction

A semi-empirical model was proposed earlier in chapter 2 (i.e., Eq. 2.14) for predicting the variation of bearing capacity with respect to suction. The saturated shear strength parameters and the soil-water characteristic curve (SWCC) are required for using the proposed model. This method is useful for estimation the bearing capacity of shallow foundations, however, in practice the bearing capacity of sandy soils is often determined from the cone penetration test (CPT) results. The CPTs are preferred because they are simple and less expensive in comparison to the field bearing capacity tests such as the plate load tests. Due to this reason, a simple cone was specially manufactured and used in a laboratory environment to investigate the influence of matric suction on the bearing capacity of a sandy soil. CPTs were conducted in a specially designed box (University of Ottawa Bearing Capacity Equipment, UOBCE) to experimentally investigate the variation of bearing capacity of sand with respect to matric suction. Figure 3.1 shows flow-chart which illustrates the experimental program presented in this chapter. The test results of the CPTs are used to propose correlations between CPTs data and the bearing

[2]This chapter is summarized from the research work that presented at the 62nd Canadian Geotechnical Conference, September 2009 in Halifax, NS, Canada. Along with another technical paper that was published in the 5th International Conference on Unsaturated Soils, Sep. 2010, Barcelona, Spain.

capacity of shallow foundations in saturated or unsaturated sands. There is a good agreement between the estimated and measured bearing capacity values using the proposed model.

The results of this research study were encouraging towards extending the mechanics of unsaturated soils into engineering practice using the CPT results.

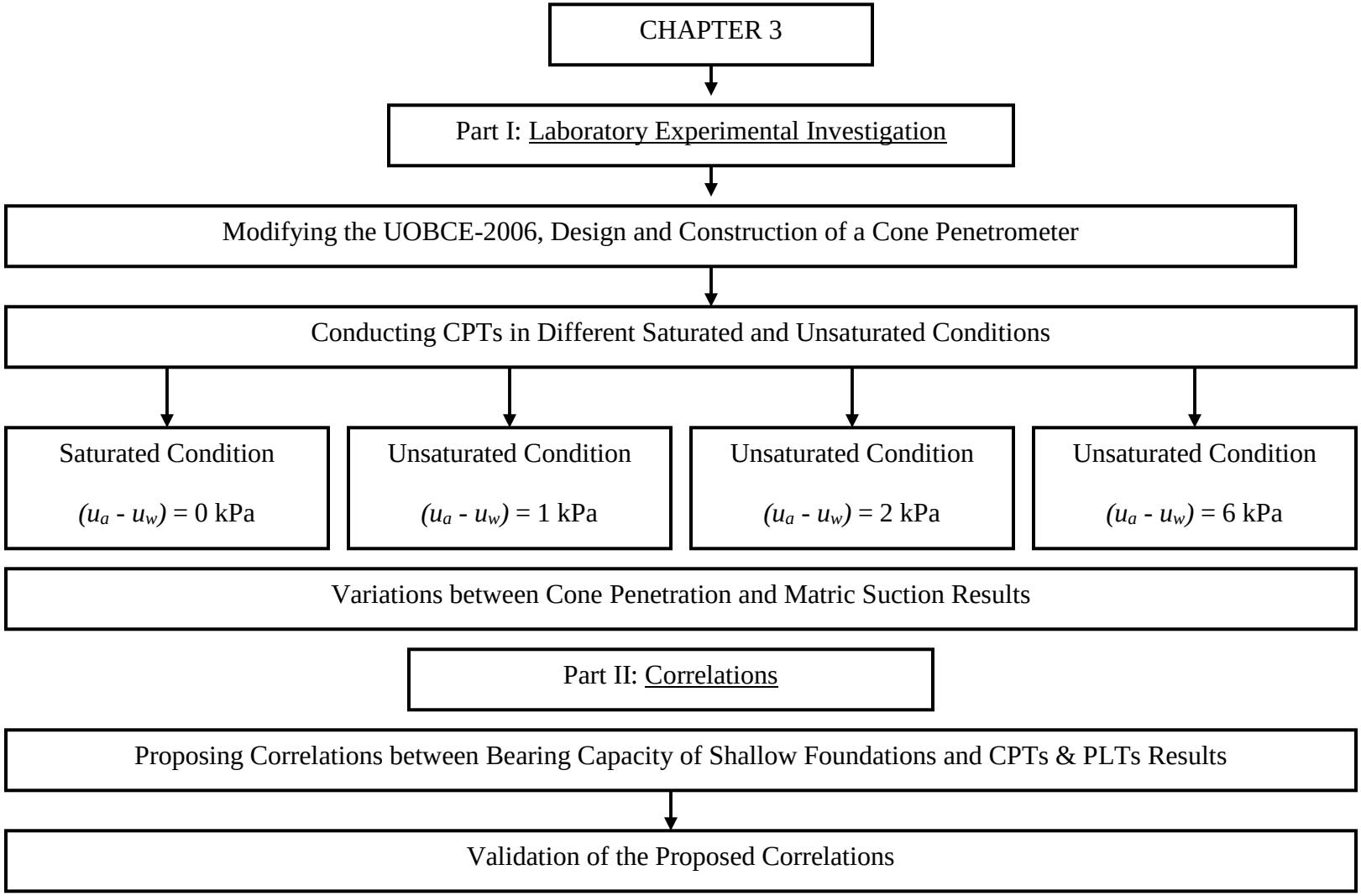

Figure 3.1 Flow-chart to illustrate the research program presented in this chapter

3.2 Background

Mohamed and Vanapalli (2006) have undertaken an extensive experimental investigation program to determine the bearing capacity of model footings (i.e., plate load tests, PLTs) in both saturated and unsaturated sand. These tests were conducted in specially designed equipment which is referred as the University of Ottawa Bearing Capacity Equipment (UOBCE-2006) (chapter 2 provides details of the equipment).

The bearing capacity of soils can be determined using the PLTs. However, these tests are elaborate, need extensive equipment and hence are expensive in comparison to cone penetration tests (CPTs). The CPT-based methods are conventionally used for determination of the bearing capacity of soils (Campanella et al. 1983, Hryciw and Dowding 1987, Puppala et al. 1993, Salgado et al. 1997, Huang et al. 1999 and Eslami 2006). The soil resistance is estimated from the CPTs relationships to calculate the bearing capacity of both coarse and fine-grained soils (Yu and Mitchell 1998, Lee and Salgado 2005 and Russell and Khalili 2006). A series of CPTs were carried out recently by Lehane et al. (2004) in the field where the soil was quartz sand with fines less than 5 % in two different periods (i.e., wet season and dry season). The results of their study suggest that the matric suction has a significant influence on the cone resistance in unsaturated soils. Some CPT studies were carried out on two different sands under unsaturated conditions by Russell and Khalili (2006). They concluded that the matric suction contribution approximately doubles the cone penetration resistance, q_c. In addition, results of CPTs conducted by Shaqour (2007) in calcareous sand under saturated, wet (unsaturated conditions) and dry conditions confirmed that the penetration resistance was relatively high in wet conditions (i.e., unsaturated conditions). More recently, Muszynski (2008) carried out CPTs in a sandy soil with capillary tension (i.e. matric suction) and observed greater cone penetration resistance in comparison to CPTs in saturated sand. While these studies provide evidence of the influence of matric suction on the bearing capacity of unsaturated soils, in the literature no interpretation techniques are available.

In the present research study, a lab-manufactured cone which was attached to a sleeve (penetrometer) and used to determine the variation of the cone resistance, q_c with respect to matric suction, $(u_a - u_w)$ during penetration. The obtained experimental results along with discussions (comparisons between cone resistance from the CPTs and bearing capacity from the PLTs) are provided. Based on these studies, simple correlations between the CPTs data and the bearing capacity of unsaturated sands are developed. The ease of determining the bearing capacity of unsaturated soils from the CPTs is highlighted.

3.3 Equipment and Methodology

3.3.1 Test Setup

The test setup which referred to as the University of Ottawa Bearing Capacity Equipment (i.e., UOBCE) was used to determine the variation of bearing capacity of sands with respect to matric suction using model plate load tests (PLTs) in a controlled laboratory environment. Several modifications were introduced to the UOBCE for determining the bearing capacity using the CPTs for the present study (Figure 3.2). The setup consists of a rigid-steel tank of 900 mm-length × 900 mm-width × 750 mm-depth. The test box can hold 1000 kg of soil and the capacity of the loading machine is 15 kN. Different loading rates can be applied by gears manipulation such that the cone connected to the loading rod can be advanced at a constant rate of strain into the compacted soil in the UOBCE to determine the cone resistance, q_c. The water table in the UOBCE can be controlled in the test box by adding or removing water from the system using water-supply valve and water-drainage valves. Tensiometers were located at different depths above the water table to measure the matric suction. The loading rod passes through a shaft and two horizontal aluminum channel sections to guide the vertical movement and prevent bending or deformation of the rod (see Figure 3.2).

The strain rate of the cone used for testing in the present research program was equal to 1.2 mm/min which is the same rate used for conducting model PLTs in the UOBCE for determining the bearing capacity of the same soil and to assure a drained condition. More details about the equipment design and construction of the test setup are available in Mohamed and Vanapalli (2006).

3.4 Design and Manufacture of the Cone Penetrometer

A simple cone with base diameter, D_c of 40 mm, cone tip angle, 60 ^{o} and cone point of radius of 0.1 mm was specially designed for conducting the experimental investigations reported in this chapter. The base projected area, A_c (i.e., cross-sectional area) of the cone used in this study was 1275 mm^2.

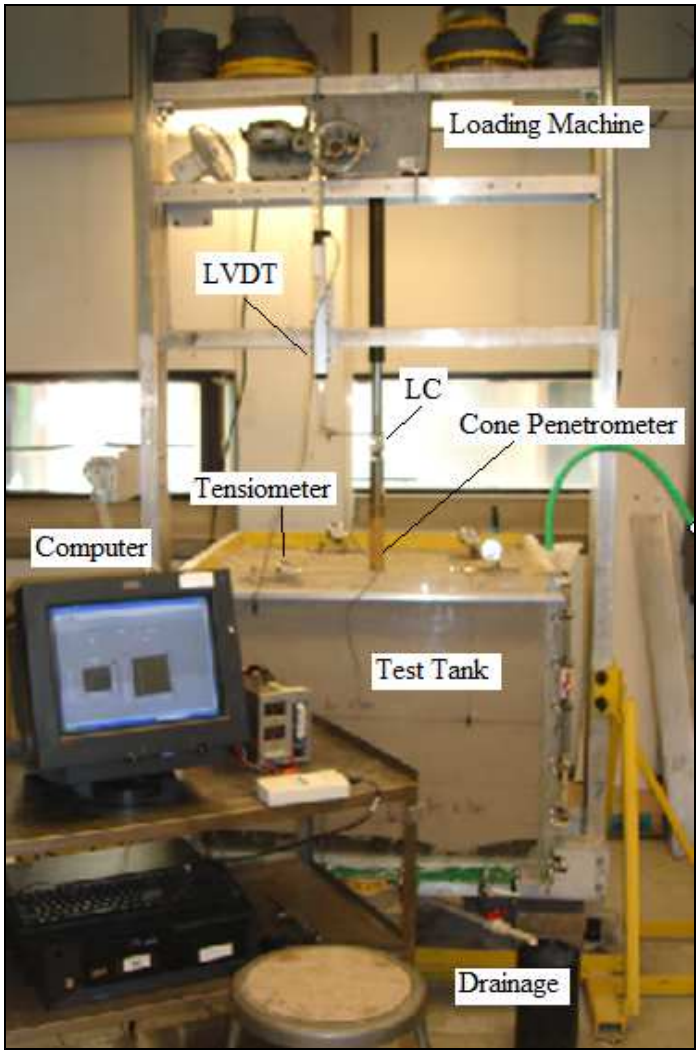

Figure 3.2 The University of Ottawa Bearing Capacity Equipment

The cone was securely connected to a penetrometer then a steel push rod with a screw connection to form a continuous axis sleeve of 360 mm length and 40 mm diameter. The cone diameter of 40 mm was chosen such that it represents an average value between the minimum and maximum standard cone diameters recommended by the ASTM D 5778-07 (i.e., 36 to 44 mm, see Figure 3.3). In addition, the diameter was chosen such that it would be greater than 20 × D_{50} size of the soil to eliminate the scale effect on the results for testing in typical sandy soils (Phillips and Valsangkar 1987 and Bolton et al. 1999 and Muszynski 2008). The cone was manufactured of hardened steel such that it is suitable to resist wear due to abrasion by soil. Figures 3.4 and 3.5 provide details of the experimental setup used for the present research program.

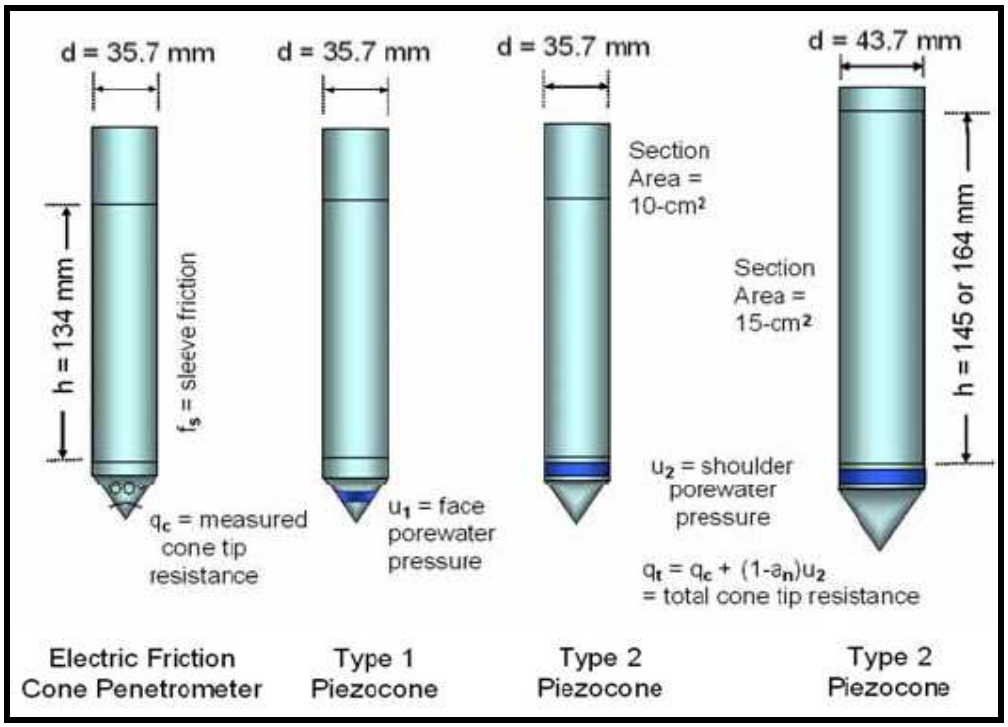

Figure 3.3 Different cone penetrometer sizes (ASTM)

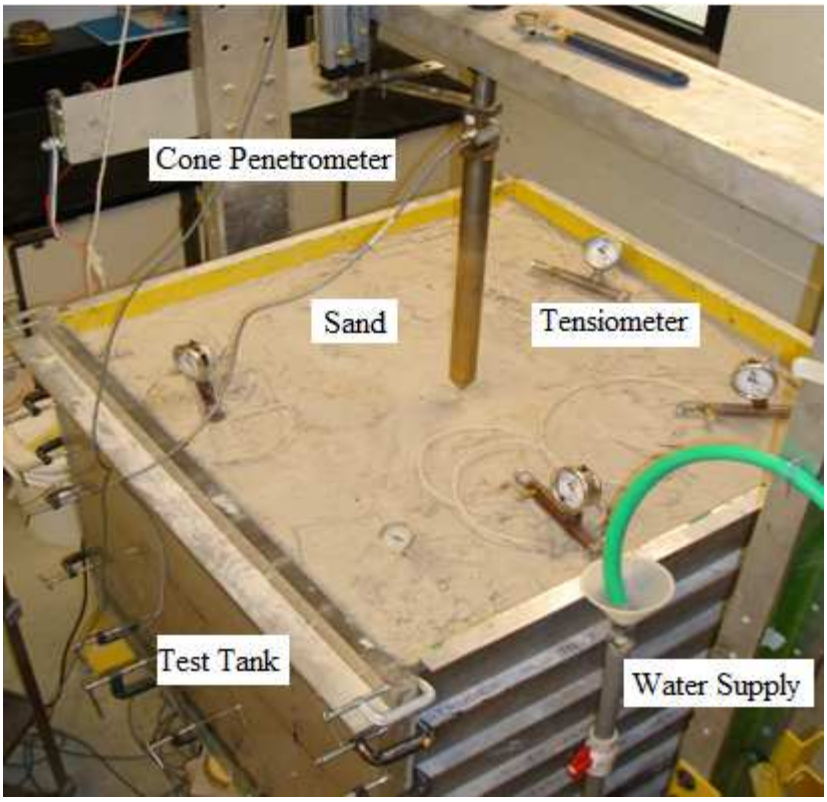

Figure 3.4 The test box of the UOBCE

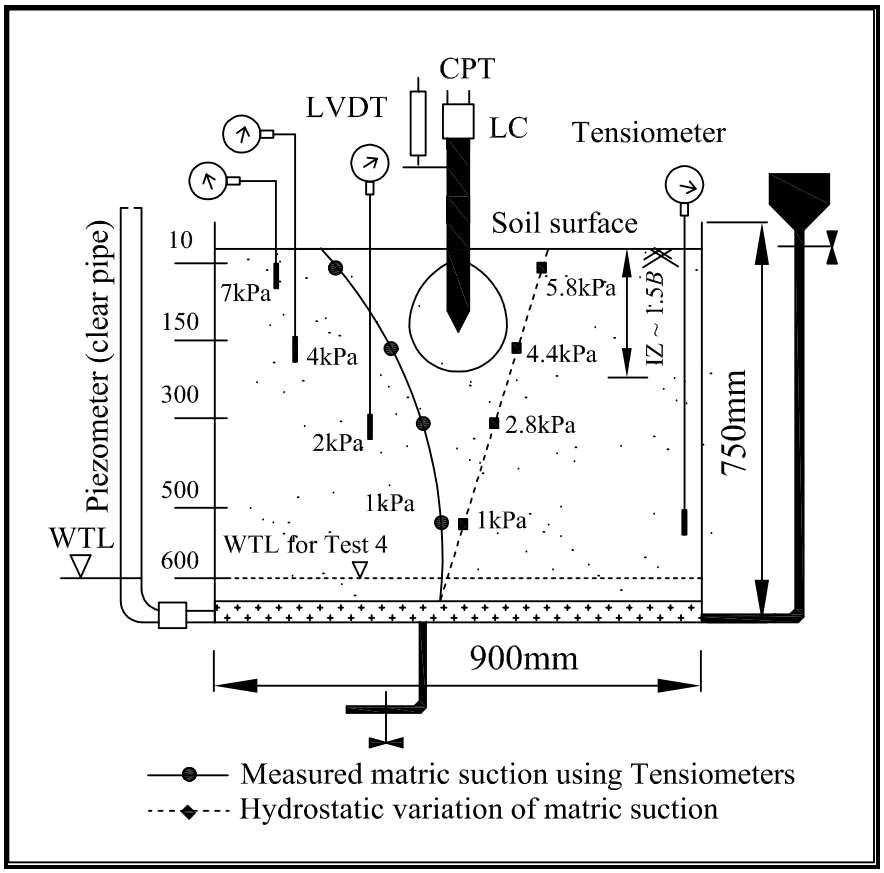

Figure 3.5 Schematic illustrates the procedure used for estimating the average matric suction within the influence zone, IZ

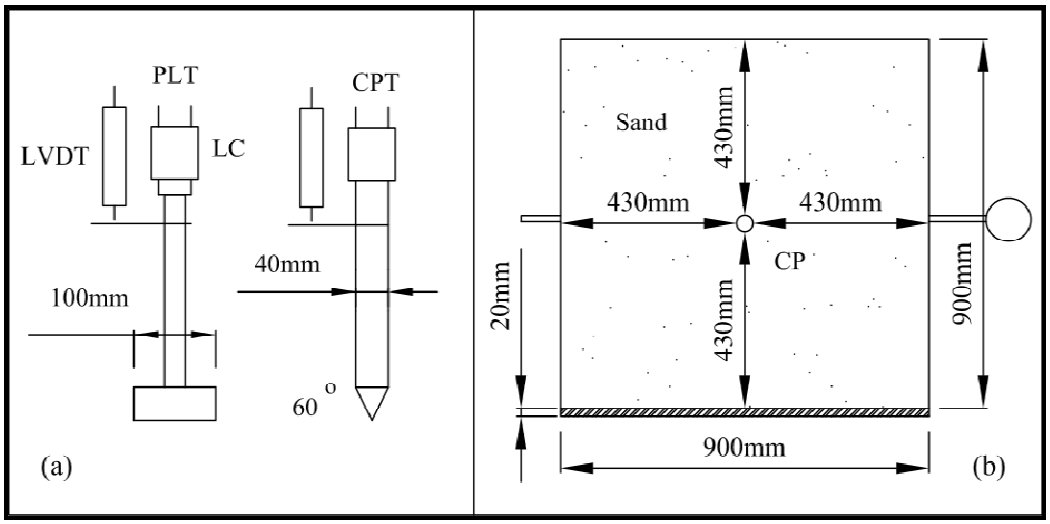

Figure 3.6 Schematic to illustrate; (a) section of the model plate load and cone penetrometer, and (b) top view of the UOBCE test box

3.5 Material Description

The soil was classified as poorly graded fine-sand, SP as per the Unified Soil Classification System (USCS). The properties of the sand are summarized earlier in chapter 2.

3.6 Test Program

3.6.1 General

The soil used in the present investigations (reported in this chapter) is the same sand used in an earlier study by Mohamed and Vanapalli (2006). The objective of the study was to determine the bearing capacity of the sand both in saturated and unsaturated conditions using model plate load tests in that study (see Figure 3.2). In the present study, a number of tests were conducted to determine the cone resistance, q_c of the compacted sand in the UOBCE under identical test conditions of saturated and unsaturated conditions reported in Mohamed and Vanapalli (2006). The first series of tests were carried out using sandy soil under saturated condition (i.e., matric suction = 0 kPa) and the later series of tests were conducted under three different unsaturated conditions (i.e., matric suction = 1 kPa, 2 kPa and 6 kPa).

The ultimate tip resistance typically mobilized at the cone tip by penetrating the cone in to a depth of 10 times the cone diameter was measured (Meyerhof 1956 and Eslami 2006). Studies by Salgado (2008) have shown that a pile tip mobilizes maximum resistance when the base penetrates into the compacted sand layer by at least 2 × the diameter, D_c. The cone was penetrated to approximately a depth of 400 mm to satisfy the above criteria.

3.7 CPTs Results under Saturated Condition

The compacted sand in the UOBCE box was saturated by raising the water table by opening the water supply valve gradually. The compacted sand was saturated from the bottom aggregate layer such that water advances in the upwards direction. This technique allowed the air in the compacted sand to be expelled from the top surface of the sand. All the Tensiometers in the test box indicated zero readings when the water level reached the top surface confirming that the sand is saturated (i.e., $(u_a - u_w) = 0$ kPa). A number of CPTs were conducted after ensuring saturated conditions and average values of the results was used in the analyses.

3.8 CPTs Results under Unsaturated Conditions

The soil was saturated similar to the procedure followed in the previous section. The water table was then lowered down to different levels of depth (using the drainage valve located at the bottom of the test box) to achieve varying capillary stresses (i.e., matric suction) values above the water table. The series of the CPTs were conducted under different matric suction values after ensuring equilibrium condition. The three different series of CPTs were carried out under three scenarios of unsaturated (sand) conditions (i.e., 1 kPa, 2 kPa and 6 kPa).

The Tensiometers were used to measure the matric suctions in the soil above the water table. The principles, construction guidelines, operating procedures and use of commercial Tensiometers measurement are provided by Stannard (1992). The gravimetric water contents were also measured by collecting specimens using small containers with perforations. The small containers were embedded in the unsaturated zone close to ceramic tip of the Tensiometers. Figure 3.7 and Figure 3.8 show the cross-section of the test box and provide details of the placement and locations of Tensiometers. Collected data are presented in Table 3.1, Table 3.2 and Table 3.3.

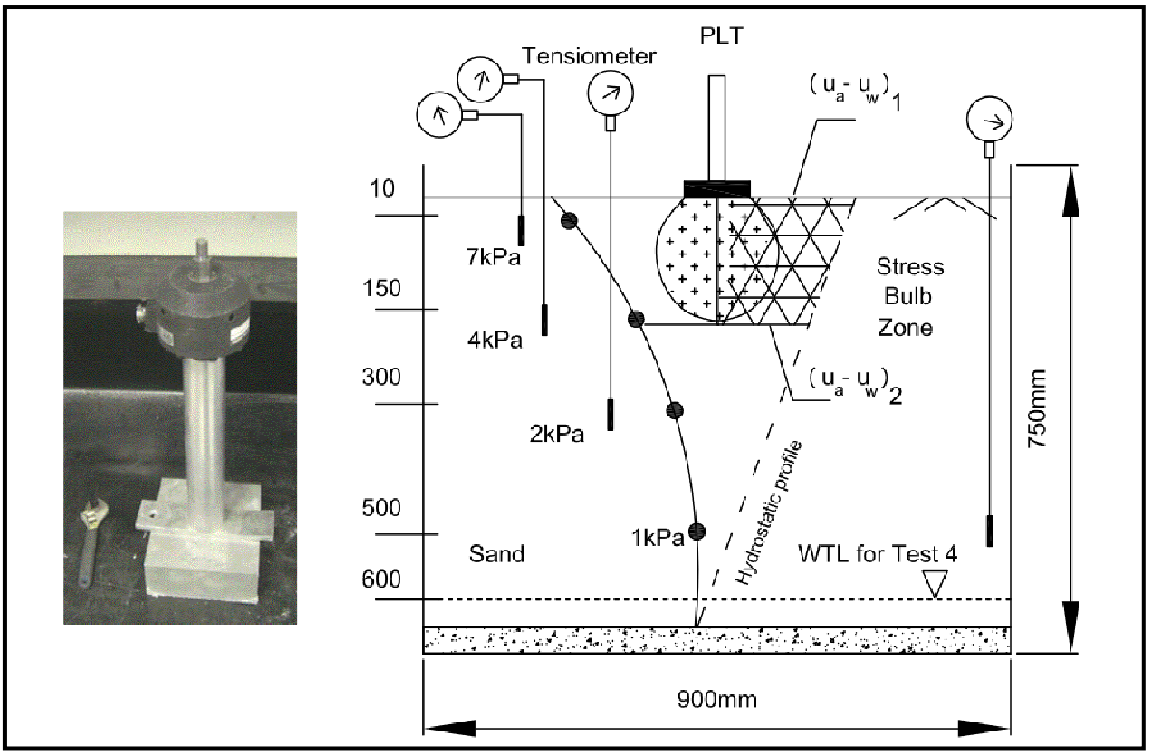

Figure 3.7 Schematic to illustrate the procedure used for determining AVR matric suction below the PLTs (after Mohamed and Vanapalli 2006)

The same average matric suction values (see Eq. 3.1) were achieved in the region of stress bulb (i.e.1.5*B*). Figure 3.7 shows a schematic of the procedure used for determining the average matric suction in the stress bulb of the PLTs and Figure 3.8 shows the procedure for estimating the influence zone for the CPTs.

$$(u_a - u_w)_{AVR} = \left[\frac{(u_a - u_w)_1 + (u_a - u_w)_2}{2}\right] \qquad [3.1]$$

where:

$(u_a - u_w)_{AVR}$ = Average matric suction in the influence zone (see Figure 3.7 and Figure 3.8)

$(u_a - u_w)$ = Measured matric suction by Tensiometers, kPa

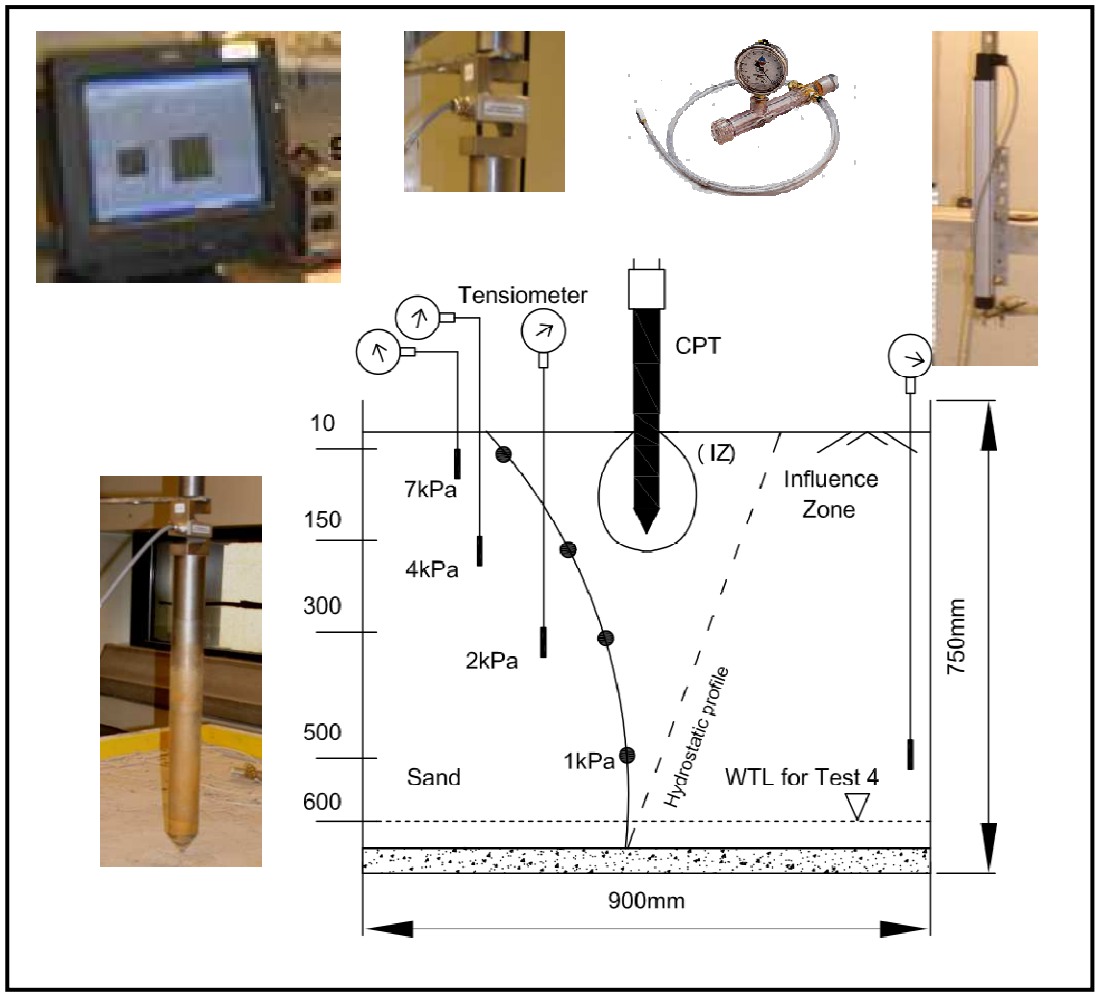

Figure 3.8 Schematic to illustrate the procedure used for determining AVR matric suction 6 kPa below the CPT

Table 3. 1 Data from the test tank for an average matric suction value of 1 kPa in the influence zone

D^* (mm)	γ_t (kN/m^3)	e	$w.c.$ (%)	S (%)	AVR[1] $(u_a - u_w)$ (kPa)
10	19.53	0.64	21.7	89.9	1.0
150	19.75	0.62	24	100.0	0.0
300	19.75	0.62	24	100.0	0.0

D^* = depth of Tensiometer, [1]AVR = average matric suction value; γ_t = total unit weight, kN/m³ ; e = void ratio; $w.c.$ = gravimetric water content, %; S = degree of saturation, %; $(u_a - u_w)$ = matric suction, kPa

Table 3. 2 Data from the test tank for an average matric suction value of 2 kPa in the influence zone

D^* (mm)	γ_t (kN/m^3)	e	$w.c.$ (%)	S (%)	AVR[1] $(u_a - u_w)$ (kPa)
10	19.54	0.64	21.5	89	2.0
150	19.72	0.625	23	98	1.0
300	19.74	0.63	24	100	0.0

D^* = depth of Tensiometer, [1]AVR = average matric suction value; γ_t = total unit weight, kN/m³ ; e = void ratio; $w.c.$ = gravimetric water content, %; S = degree of saturation, %; $(u_a - u_w)$ = matric suction, kPa

Table 3.3 Data from the test tank for an average matric suction value of 6 kPa in the influence zone

D^* (mm)	γ_t (kN/m^3)	e	$w.c.$ (%)	S (%)	AVR[1] $(u_a - u_w)$ (kPa)
10	18.17	0.63	14.00	58	6.0
150	18.76	0.64	18.33	76	4.0
300	19.20	0.62	19.48	83	2.0
500	19.30	0.64	22.38	93	1.0
600	19.74	0.63	23.76	100	0.0

[1]D = depth of Tensiometer, [1]AVR = average metric suction value; γ_t = total unit weight, kN/m³ ; e = void ratio; $w.c.$ = gravimetric water content, %; S = degree of saturation, %; $(u_a - u_w)$ = matric suction, kPa

3.9 Cone Resistance and Sleeve Friction from CPTs Results

The cone resistance, q_c can be determined using different methods proposed by researchers (Fleming and Thorburn 1983, and Eslami and Fellenius 1997). In this chapter, since the total applied loads (friction and tip resistance) were evaluated, the cone resistance for the tested soil was determined using the following equation (ASTM D 5778 - 07):

$$q_c = \frac{Q_c}{A_c} \qquad [3.2]$$

where:

q_c = the cone resistance, MPa

Q_c = load carried by the cone, kN

A_c = the cone base area, mm^2

The sleeve friction, f_s (due to sleeve soil interaction) can be directly measured using an electronic cone. However, the sleeve friction in the present testing program was estimated (following the ASTM D 5778-07 guidelines) using Eq. [3.3]:

$$f_c = \frac{Q_f}{A_s} \quad [3.3]$$

where:

f_c = the sleeve friction, kPa

Q_f = load carried by the sleeve in saturated condition, kN

A_s = surface area of the sleeve, mm^2

The friction ratio, R_f which is defined as the sleeve friction, f_s divided by the cone resistance, q_c was estimated (following the ASTM D 5778-07 guidelines) using Eq. [3.4]:

$$R_f = \frac{f_s}{q_c} \times 100 \quad [3.4]$$

The saturated coefficient of permeability of sand is relatively high and the penetration rate used (1.2 mm/min) is relatively slow enough for assuming the pore-water pressure increase to be negligible (i.e., two piezometers used for observations did not show any increase in the piezometer readings assuring drained condition; due this reason, it is assumed $q_c = q_t$). The penetration rate used is lower than Iwasaki et al. (1988) who performed CPT at 2 mm/sec to assure fully drained condition of Toyoura sand. These results were encouraging and hence a pressure transducer was not considered when the cone was designed. The 4th Edition of "Guide to Penetration Testing for Geotechnical Engineering" by Robertson and Cabal (2010) also suggests "the q_c may be assumed = to q_t for sandy soils".

The cone penetrometer and the equipment used by the authors designed and manufactured at the university machine shop without strain gauge load cells (sensors). Due to this reason, it was not possible to measure the sleeve friction. The sleeve friction was not measured in the present study as the cone resistance for cohesionless soils such as sands is negligible (Nes 2004). Vos (1982) and Bakker (2004) used an electronic cone

penetrometer and determined the friction ratio, R_f values and summarized empirical friction ratio values for various soil types as shown in Table 3.4.

Table 3.4 Soil type as function of friction ratio (from Vos 1982 and Bakker 2004)

Soil type	Friction ratio R_f (%) (from Vos 1982)	Friction ratio R_f (%) (from Bakker 2004)
Coarse sand and gravel	< 0.5	0.2 - 0.6
Fine sand	1.0 - 1.5	0.6 - 1.25
Silt or loam	1.5 - 3.0	1.2 - 4.0
Clay	3.0 - 7.0	3.0 - 5.0
Peat	> 5.0	5.0 - 10.0

Furthermore, Vanapalli et al. (2010) extended β – Method for the design of piles using the mechanics of unsaturated soils and proposed equation [3.5] taking account of matric suction for determining the shaft capacity (sleeve friction) of open-end pile (D = 65 mm) in sandy soil under moist (i.e., unsaturated) conditions.

$$Q_{f\,us} = Q_f + Q_{(u_a - u_w)} \qquad [3.5]$$

$$Q_{f_{us}} = \beta \frac{\gamma L_{sh.}}{2} (A_s) + [(u_a \quad u_w)\{(\Theta^k)(\tan\varphi')\}](A_s) \qquad [3.6]$$

where:

$Q_{f\,us}$ = total shaft capacity (sleeve friction), kN

$Q_{(u_a-u_w)}$ = shaft capacity (sleeve friction) due to unsaturated condition, kN

β = constant function of lateral earth pressure ratio

γ_d = dry unit weight, kN/m^3

$L_{sh.}$ = embedded length of the shaft, m

A_s = surface area of shaft or sleeve, mm^2

$(u_a - u_w)$ = matric suction, kPa

Θ = normalized water content (equivalent to degree of saturation)

κ = fitting parameter as function of plasticity index (1 for sandy soils) for shear strength

φ = soil / pile interface friction angle, ^{o}

$$Q_t = Q_c + Q_{fus} \quad [3.7]$$

where:

Q_t = total applied force (taken by sleeve and cone), kN

The friction ratio, R_f can be determined by substituting the values of sleeve friction, f_s and the cone resistance, q_c in Eq. [3.4]. The friction ratio was equal to 0.13 % at midpoint of the assumed influence zone length (IZ = 150 mm; refer to Appendix A for sample calculation). The results of the friction ratio, R_f are lower than the values summarized in Table 3.4. These results suggest that the load carrying capacity contribution from the sleeve friction is negligible. Such observations are consistent with the behavior of pile foundations in sandy soils in which the load carrying capacity is primarily carried at the tip of the pile. The results of the cone resistance, q_c for the tested soil under saturated and unsaturated conditions are plotted with respect to the depth in Figure 3.9.

3.10 Discussion of CPTs Results

In cone penetration tests (CPTs), as the cone is advanced into the soil it forms a mechanism of rupture which is comparable to single pile failure behavior (Salgado 2008). Similar pattern of failure mechanisms based on the bearing capacity theory was proposed by many researchers (Terzaghi 1943, Vesic 1963, and DeBeer 1965) to approximately visualize the failure load when conducting the CPTs. A method was proposed by Salgado (2008) to determine the end bearing capacity of a single pile which takes an average load over an influence zone length equal to the summation of pile diameter, D above the pile base and 1.5 × the pile diameter, D below the pile base. Assuming the behavior of the cone similar to a single pile, a representative value of cone resistance, q_c was required for

comparison of the estimated bearing capacity vales using the proposed procedure with the bearing capacity values from PLTs.

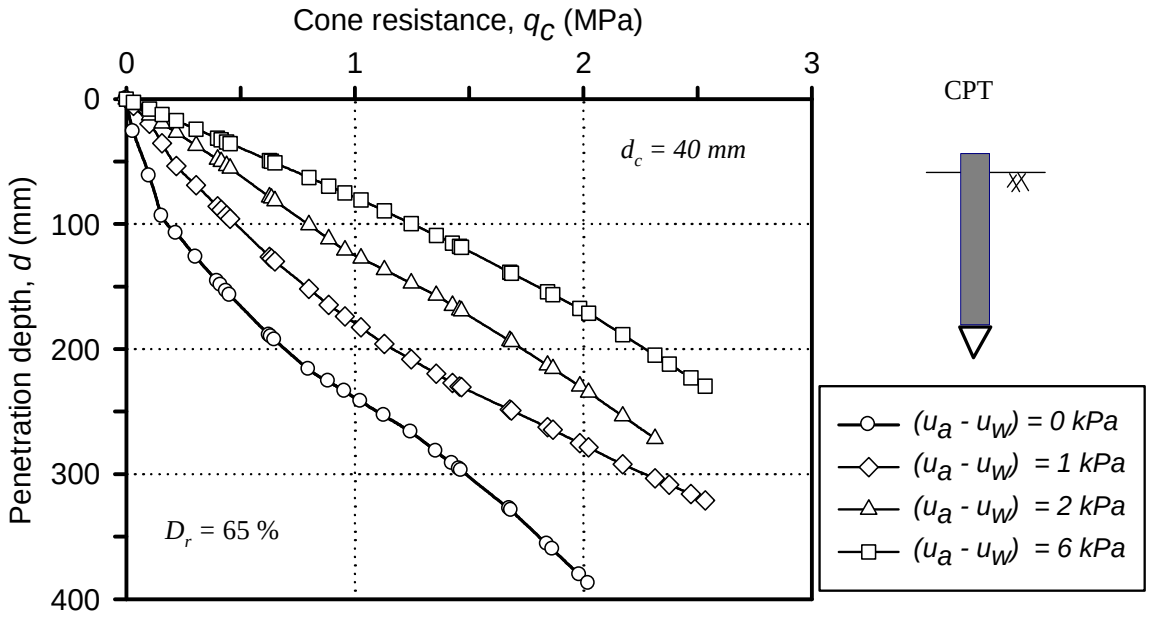

Figure 3.9 Variation of cone resistance (CPTs) with depth under saturated and unsaturated conditions

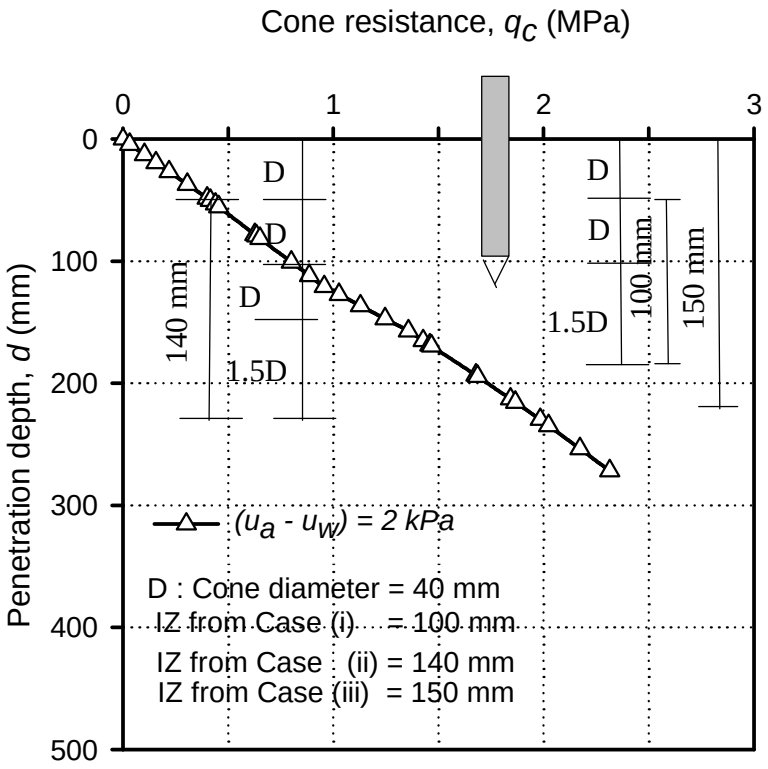

Figure 3.10 Schematic illustrates CPT results for three cases

(i.e., Case (i), Case (ii) and Case (iii))

Three influence zones were assumed below the CPT illustrated in Figure 3.10 and labeled as: Case (i) represents an influence zone length of 100 mm, Case (ii) represents an influence zone length of 140 mm and Case (iii) represents an influence zone length of 150 mm (Figure 3.10). It can also be noticed that the cone resistance increased as the soil condition changes from saturated (0 kPa) condition to unsaturated (1 kPa, 2 kPa and 6 kPa) conditions in the capillary zone as shown in Figure 3.9. These results are consistent with the observations from CPTs carried out by Russell and Khalili (2006). The increase in the cone resistance, q_c can be attributed to the contribution of the matric suction to the bearing capacity of the tested soil similar to the PLTs results (Mohamed and Vanapalli, 2006). Figure 3.11 presents the details of measured bearing capacity of the PLTs (100 mm × 100 mm) from Mohamed and Vanapalli (2006) and the cone resistance obtained

from this study. Both model PLTs and the cone resistance from the CPTs show similar contributions of matric suction (i.e., capillary tension) towards the bearing capacity.

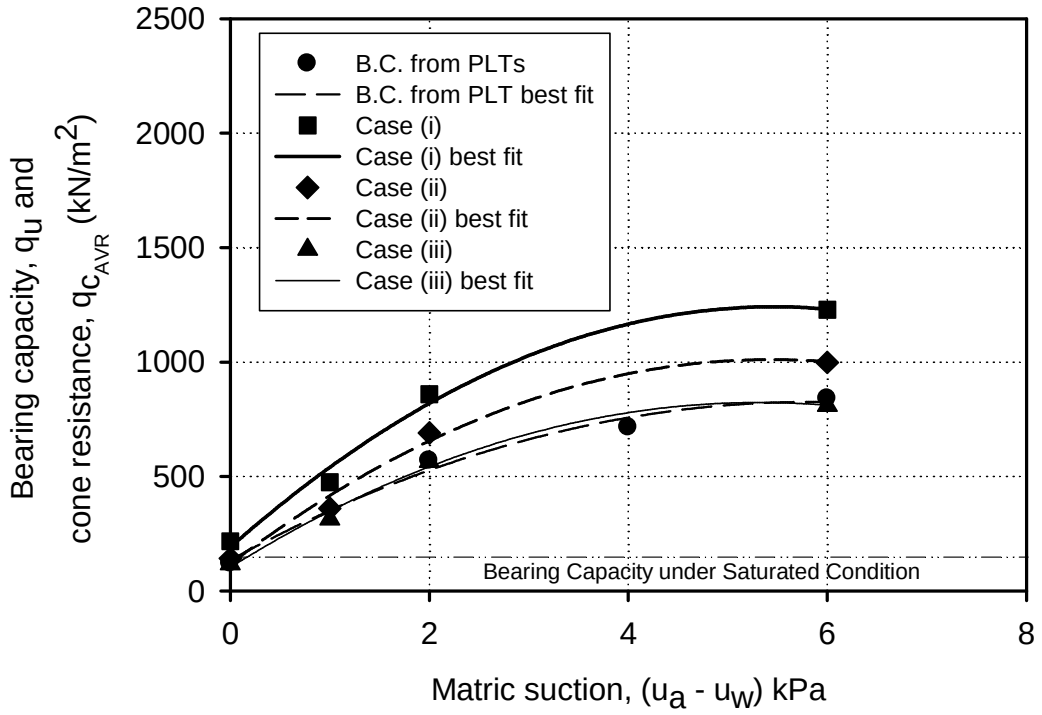

Figure 3.11 Comparison between the bearing capacity from PLTs tests and the cone resistance from CPTs with respect to matric suction

3.11 Correlations between the CPTs and the Bearing Capacity of Sands

The field or in situ bearing capacity of soils can be determined from the plate load tests (PLTs) or the cone penetration tests (CPTs). The PLTs are cumbersome and expensive and hence are not commonly used in geotechnical engineering practice. The CPTs are conventionally used in practice because of their reliability, simplicity and associated low costs. A number of studies are reported in the literature for evaluating the bearing capacity of saturated soils using CPTs-based empirical equations (Meyerhof 1956,

Eslaamizaad and Robertson 1996, Lee and Salgado 2005, Eslami and Gholami 2006, and the CFEM 2006). These methods however are not suitable for arid and semi-arid regions where the natural ground water table is relatively deep and soils are typically in a state of unsaturated condition (i.e., vadose zone).

The bearing capacity of unsaturated soils is significantly influenced by matric suction. Experimental studies show that even low matric suction values of 2 to 6 kPa can increase the bearing capacity of sands by 4 to 6 times in comparison to saturated conditions (Mohamed and Vanapalli 2006). Steensen-Bach et al. (1987) commented that ignoring the influence of capillary stresses in the bearing capacity of unsaturated soils would be equivalent to disregarding the influence of reinforcement in the design of reinforced concrete.

Simple relationships are proposed for estimating the bearing capacity of sands in both saturated and unsaturated conditions deriving correlations between the PLTs and CPTs using results from the present study and other studies published in the literature. The proposed approach is simple and consistent with the conventional techniques followed in engineering practice towards the estimation of the bearing capacity of sandy soils using CPTs.

3.12 Review of Available Bearing Capacity - CPT Correlations

Meyerhof (1956) proposed a correlation between the cone penetration resistance, q_c and bearing capacity of shallow foundations, q_u for saturated sands as follows:

$$q_u = (\frac{q_c}{12.2})(B)(1+\frac{Df}{B}) \qquad [3.8]$$

where:

q_u = ultimate bearing capacity; q_c = arithmetic average of cone resistance values in the influence zone equal to 1.5B; B = footing width; D_f = footing embedded depth.

Eslaamizaad and Robertson (1996) have proposed a relationship to estimate the ultimate bearing capacity of shallow foundations in sands from the CPTs data. The correlation between q_u and q_c was expressed as:

$$q_u = 0.1849(q_c)(\frac{B}{Df})^{-0.5093}(1 + F\frac{N\gamma}{Nq}\frac{B}{Df}) \quad [3.9]$$

where:

q_{ult} = ultimate bearing capacity at relative displacement of 10%; q_c = average cone resistance value over a depth of B; B and D_f = width and depth of footing respectively; F = shape factor.

More recently, Lee and Salgado (2005) have proposed another relationship to estimate the ultimate bearing capacity from CPTs data as shown below.

$$q_{bL} = \beta(q_{cAVR}) \quad [3.10]$$

where:

q_{bL} = limit unit bearing capacity, $q_{c\,AVR}$ = average of q_c values from the footing base to a depth from footing base equal to footing diameter B; and β = constant function of lateral earth pressure ratio, K and relative density, D_r.

3.13 Relationships for estimating B.C. of Sands under both Saturated and Unsaturated Conditions from CPTs

Empirical methods to correlate CPTs and the bearing capacity of shallow foundations valid for both saturated and unsaturated soils are valuable for practicing engineers. As a first step in this direction, Mohamed and Vanapalli (2009) carried out CPTs in a laboratory environment to propose such correlations providing comparison with the model PLTs results. As discussed in section 3.10, the different influence zone depths are considered in the analysis (i.e. referred to as Case (i), Case (ii) and Case (iii)) to provide comparisons between the cone penetration resistance, q_c and the measured bearing

capacity from the model PLTs (see Figure 3.12). A difference of 20 % to 50 % between the CPTs results and the PLTs results was observed when the sand was under unsaturated condition for the influence zone depths, IZ presented in Case (i) and Case (ii) respectively. However, better comparisons were possible between the cone resistance, q_c and the bearing capacity values from the model PLTs using the influence zone depth, IZ is 1.5*B* or slightly greater (see Case (iii)).

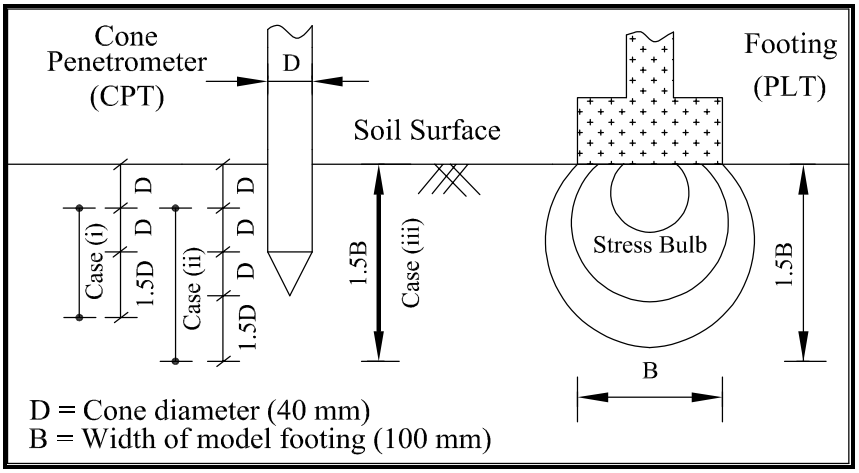

Figure 3.12 Schematic illustrates three different cases (i.e., Case (i), Case (ii) and Case (iii)) of influence zones (modified after Mohamed and Vanapalli 2009)

In the present study, a penetration depth (i.e. influence zone, IZ) for averaging q_c values is chosen to be equal to 1.5*B* after performing several trial studies on the sandy soil in saturated and unsaturated conditions. This depth corresponds to 150 mm in the present study (i.e. 1.5 × *B* = 150 mm; note *B* = 100 mm width, see Figure 3.12).

The average CPTs values over a depth IZ = 150 mm were used to develop correlations with the measured bearing capacity values from model PLTs including some field data from the literature. The depth of penetration of 1.5*B* is consistent with the depth zone in which the stresses are predominant (Poulos and Davis 1974, Chen 1999). The influence zone (i.e., a depth of 1.5*B* from the footing base) provides good correlations between

average cone resistance, $q_{c\ AVR}$ and the bearing capacity of sand in both saturated and unsaturated conditions. This depth (i.e., IZ) also provides requisite confinement to the shaft to which cone is connected. Similar influence zone depth of 1.5*B* was used by Meyerhof (1956) and Schmertmann et al. (1978) to relate the ultimate bearing capacity of shallow footings to an average of cone penetration resistance value.

Several investigators, for example, Meyerhof (1956) and Eslaamizaad and Robertson (1996) suggested forms of expressions with correlation factors range from 0.17 to 0.25 for estimating the bearing capacity of saturated sands using CPTs. A correlation factor value of 0.1 was recommended by the Canadian Foundation Engineering Manual (CFEM-2006) for the evaluation of allowable bearing capacity of a soil using CPTs results regardless of the condition of the soil.

Two different equations are proposed based on the PLTs and CPTs conducted in this research to estimate the bearing capacity of shallow foundations of surface footings on saturated and unsaturated homogenous sand respectively.

Eq. [3.11] is suggested using the database of the experimental results of both PLTs and CPTs presented in this chapter to estimate the bearing capacity for saturated sands (i.e., $(u_a - u_w)$ = 0 kPa):

$$q_{u\,(sat)} = \Theta(q_{c\,sat}) \qquad [3.11]$$

where:

$q_{u\ (sat)}$ = bearing capacity for saturated homogenous sand, $\Theta = s_1/B^{s_2}$ (i.e., correlation factor), s_1 = first fitting parameter for saturated condition, s_2 = second fitting parameter for saturated condition, $q_{c\ sat}$ = average cone resistance under saturated sand condition (e.g. within influence zone, IZ equal to 1.5*B* from the footing base level) and *B* = footing width in meter.

Eq. [3.12] is suggested to estimate the bearing capacity for unsaturated sands (i.e., $(u_a - u_w) > 0$ kPa):

$$q_{u\,(unsat)} = \Omega(q_{c\,unsat}) \qquad [3.12]$$

where:

$q_{u\ (unsat)}$ = bearing capacity for unsaturated homogenous sand, $\Omega = u_1/B^{u_2}$ (i.e., correlation factor), u_1 = first fitting parameter for unsaturated conditions, u_2 = second fitting parameter for unsaturated conditions, $q_{c\ unsat}$ = average cone resistance under unsaturated sand conditions (e.g., within influence zone, IZ equal to 1.5B from the footing base level), B = footing width in meter.

The fitting parameters (i.e., s_1 & s_2 for saturated condition and u_1 & u_2 for unsaturated conditions) were computed by iteration process as the PLTs and CPTs results were known for the tested saturated and unsaturated sand (Table 3.5 and Table 3.6 for saturated condition and unsaturated condition respectively).

Table 3. 5 Database used for proposing the fitting parameters, s_1 and s_2

Analysis for saturated condition $(u_a - u_w) = 0$ kPa

Data from PLTs of 100 mm × 100 mm, 150 mm × 150 mm and CPTs (conducted in the UOBCE)

B (mm)	$q_{c\ AVR}$ *(MPa) from CPTs*	*Matric suction kPa*	q_u *(kN/m²) from PLTs*	s_1	s_2	q_u *(kN/m²) estimated using* Θ *and* q_c	$\frac{q_{u\,sat}\,(estimated)}{q_{u\,sat}\,(measured)}$
[1]100	118	0	121	0.15	0.63	81	0.7
[1]150	270	0	125	0.15	0.63	133	1.0
[1]Surface square footing						AVR =	0.85

Thus, $\Theta = 0.15/B^{0.63}$ for saturated sands provides good estimation of the B.C. using CPT data.

Table 3. 6 Database used for proposing the fitting parameters, u_1 and u_2

Analysis for unsaturated conditions $(u_a - u_w) > 0$ kPa Data from PLTs of 100 mm × 100 mm, PLTs of 150 mm × 150 mm and CPTs (conducted in the UOBCE)							
B (mm)	$q_{c\ AVR}$ *(MPa) from CPTs*	*Matric suction kPa*	q_u *(kN/m²) from PLTs*	u_1	u_2	q_u *(kN/m²) estimated using* Ω *and* q_c	$\frac{q_{u\,unsat}[estimated]}{q_{u\,unsat}[measured]}$
[1]100	565	2	570	0.19	0.68	504	0.88
[1]100	805	6	840	0.19	0.68	769	0.90
[1]150	900	2	630	0.19	0.68	621	0.98
[1]150	1235	6	745	0.19	0.68	852	1.14
[1]Surface square footing						AVR	0.97
Thus, $\Omega = 0.19/B^{0.68}$ for saturated sands provides good estimation of the B.C. using CPT data.							

3.14 Validation of the Proposed Technique Using In-Situ Data from Literature

Studies undertaken through this research program show that a correlation factor, Θ value of 0.1 to 0.64 is required using Eq. [3.11] for estimating the bearing capacity of sands that are in a state of saturated condition.

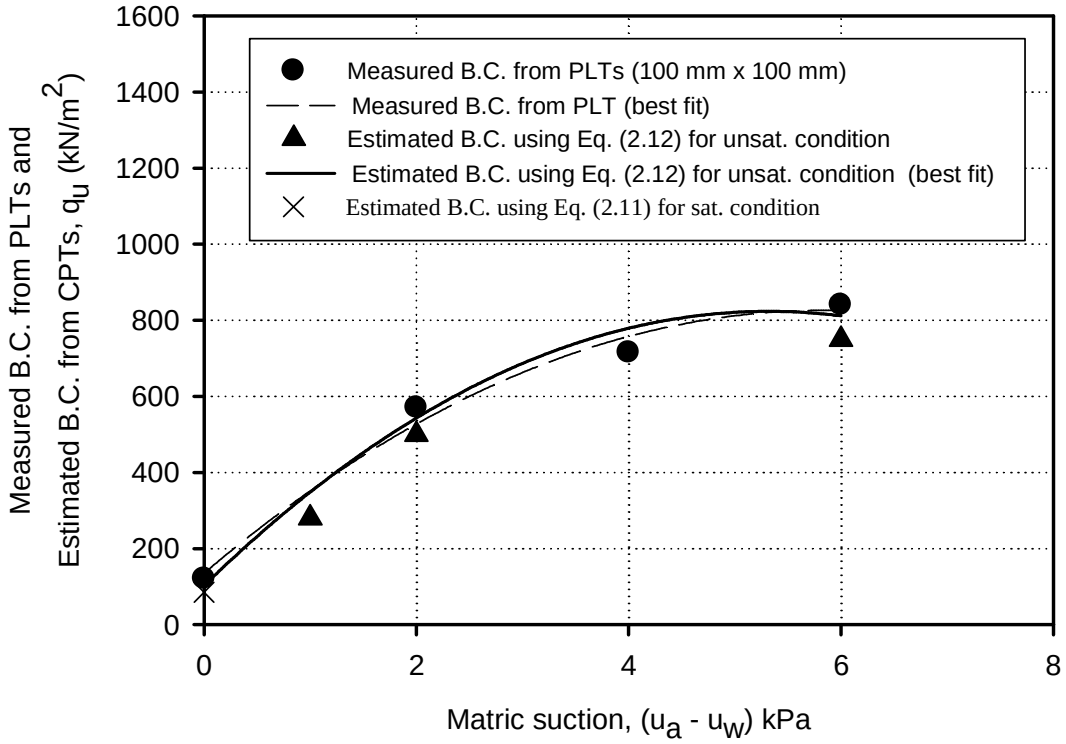

Figure 3.13 Typical results of the estimated BC using the proposed equations and the measured BC from 100 mm × 100 mm PLTs with respect to matric suction

The factor, Ω for reliable estimation of the bearing capacity of unsaturated sands using Eq. [3.11] lies between 0.1 and 0.9. The need for using a larger range of Ω values in comparison to Θ demonstrates the contribution of matric suction towards the bearing capacity of unsaturated sands. The factors, Θ and Ω for saturated and unsaturated sands

respectively are dependent on the footing width, *B*. In both the cases, the correlation factor increases as the footing width, *B* decreases.

Figure 3.13, shows the measured results from CPTs for both saturated and unsaturated conditions over an influence zone (IZ) of 1.5*B* depth. In addition, the bearing capacity values of sands calculated using Eq. [3.11] (AVR $q_{u\ \text{sat (estimated)}}/q_{u\ \text{sat (measured)}} = 0.85$ for sands in saturated condition) and Eq. [3.13] (AVR $q_{u\ \text{unsat (estimated)}}/q_{u\ \text{unsat (measured)}} = 0.97$ for sands in unsaturated conditions) using CPTs data are also plotted along with the model PLT results. There is good comparison between the estimated bearing capacity values (from CPTs) and the measured bearing capacity values (from PLTs) (see Figure 3.14). Table 3.7 provides comparison between the estimated bearing capacity values (e.g., using Eq. [3.11] for saturated sands and Eq. [3.12] for unsaturated sands) and the measured bearing capacity values from six model PLTs (from this study) and three footing test results reported in literature by Lee and Salgado (2005). The results (i.e., plotted in Figure 3.14) show reasonably a good comparison between the estimated and measured bearing capacity values for plate load tests (PLTs) and in-situ footing load tests (FLTs).

Table 3.7 Estimated BC using the proposed correlations based on the CPTs results and the measured BC of PLTs from this study and in-situ FLTs

Soil type	$(u_a - u_w)$ (kPa)	$q_{c\ AVR}$ (kPa)	B (m)	Measured BC (kPa)	Estimated BC (kPa)
SP	0	118	0.10	121	81 (Eq. [3.11])
SP	2	565	0.10	570	504 (Eq. [3.12])
SP	6	805	0.10	840	769 (Eq. [3.12])
SP	0	270	0.15	125	133 (Eq. [3.11])
SP	2	900	0.15	630	621 (Eq. [3.12])
SP	6	1235	0.15	745	852 (Eq. [3.12])
S [#]	33 [†]	2800	1.00	500	532 (Eq. [3.12])
S [#]	~25 [†]	3530	2.00	525	419 (Eq. [3.12])
S [#]	~20 [†]	10000	3.00	950	900 (Eq. [3.12])
S*	10[†]	5400	1.00	1000	1026 (Eq. [3.12])
S*	10[†]	6000	1.50	800	865 (Eq. [3.12])
S*	10[†]	6500	2.50	630	662 (Eq. [3.12])
S*	10[†]	7500	3.00	600	675 (Eq. [3.12])

[†]Estimated average suction (along an influence zone of 1.5B) values assuming hydrostatic profile. [#] Sand from Lee and Salgado (2005); [*] Sand from Giddens and Briaud (1994).

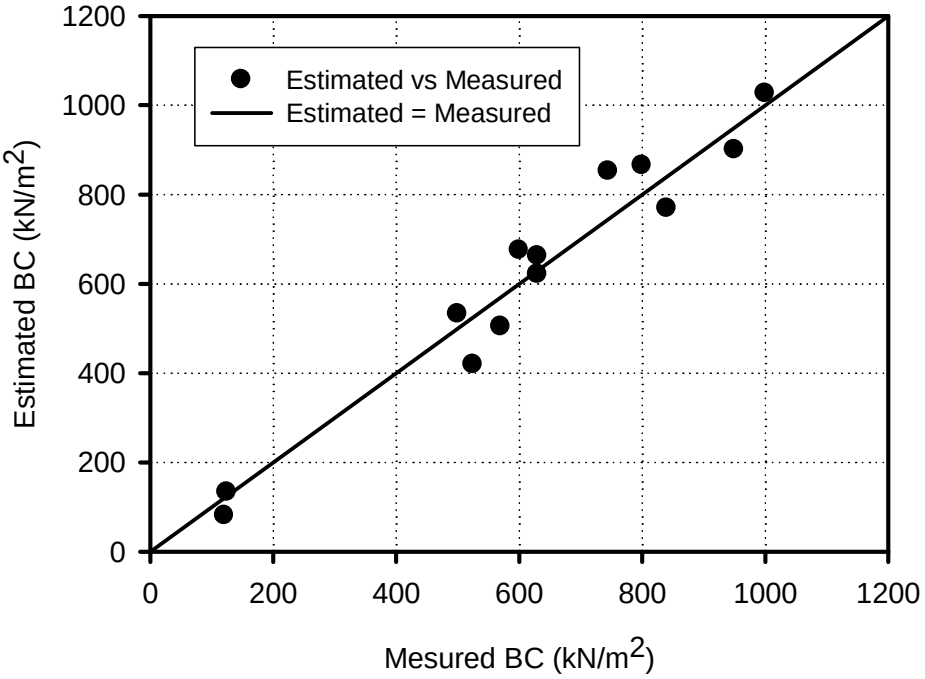

Figure 3.14 Comparison between estimated bearing capacity using the proposed equations and measured bearing capacity obtained from experimental laboratory PLTs laboratory and in-situ FLTs

3.15 Summary and Conclusions

The results presented in the chapter demonstrate significantly low sleeve friction contribution to the load carrying capacity but dramatic increase of the cone resistance when the CPTs were performed under unsaturated conditions. The increase of the cone resistance can be attributed to the contribution of matric suction.

The comparison between the cone resistance values obtained from the CPTs in this study and the bearing capacity results from the PLTs under similar conditions show approximately same values when the tests (CPTs) were conducted under saturated conditions. In contrast, there was a difference of 20 % to 50 % between the CPTs results and the PLTs results under unsaturated conditions. The differences may be attributed to the assumed influence zone length presented in Case (i) and Case (ii) respectively. In

addition, the cone resistance is also affected by the weight of the soil (i.e., overburden stress) above the cone which causes confinement around the tip and higher resistance than that of the surface PLTs. However, the cone resistance of CPTs and the bearing capacity values of PLTs were approximately the same (for both saturated and unsaturated conditions) using the influence zone length presented in Case (iii) (150 mm). This validates the procedure used for averaging the values of matric suction and cone resistance, q_c over an influence zone length of 150 mm which is equal to the depth of the stress bulb proposed for the PLTs. The trend of both the cone resistance values of the CPTs and the bearing capacity of the PLTs demonstrate a linear increase up to the air-entry value (AEV = 3 kPa) and then a nonlinear increase beyond that value.

Based on the results reported in this chapter, it appears that the influence zone length over which the average cone resistance should be considered plays a significant role in deciding the appropriate and representative cone resistance value for the proposed correlations.

In this chapter, simple relationships were proposed between the average cone resistance, q_c and the bearing capacity, q_u of sandy soil in saturated and unsaturated conditions. The proposed relationships provide reasonable comparisons between the estimated and measured bearing capacity values for sands in both saturated and unsaturated conditions. Further research work is however necessary to be conducted to check the validity of the proposed relationships using different types of sands both in the laboratory and in field.

3.16 References

ASTM, D3441-2007. “Standard Test Method for Mechanical Cone Penetration Tests of Soils.” ASTM Book of standards.

ASTM, D 5778 -2007. “Standard Test Method for Electronic Friction Cone and Piezocone Penetration Testing of Soils.” ASTM Book of standards.

Bakker, M. A. J. (2004). “The internal structure of Pleistocene push moraines.” A multidisciplinary approach with emphasis on groundpenetrating radar. PhD thesis, Queen Mary, University of London.

Bolton, M. D., Gui, M. W., Garnier, J., Corte, J. F., Bagge, G., Laue, J. and Renzi, R. (1999). “Centrifuge cone penetration tests in sand.” Geotechnique, 49 (4), 543 – 552.

Broms, B. B. (1964). “The effect of degree of saturation on the bearing capacity of flexible pavements.” Highway Research Record, (71), 1 – 14.

Campanella, R. G., Robertson, P. K. and Gillespie, D. (1983). “Cone penetration testing in deltaic soils.” Canadian Geotechnical. Journal, 20(1), 23 – 35.

Costa, Y. D, Cintra J. C. and Zornberg J. G. (2003). “Influence of matric suction on the results of plate load tests performed on a lateritic soil deposit.” Geotechnical Testing Journal, 26(2), 219 – 226.

De Beer, E. E. (1965). “Bearing capacity and settlement of shallow foundations on sand.” Proceedings of a Symposium on Bearing Capacity and Settlement of Foundations, Duck University, Durham, 15 – 32.

Eslami, A. and Fellenius, B. H. (1997). “Pile capacity by direct CPT and CPTu methods applied to 102 case histories.” Canadian Geotechnical Journal, 34(6): 880 – 898.

Eslami, A. (2006). “Bearing capacity of shallow and deep foundations from cone point resistance - A scale effect approach.” GeoCongress Geotechnical Engineering in the Information Technology Age, 1 – 6.

Fleming, W. and Thorburn, S. (1983). “Recent piling advances.” State of the Art Report in the Proceeding Conference on Advances of Piling and Ground Treatment for Foundations, ICE, London.

Hryciw, R. D and Dowding, C.H. (1987). “Cone penetration of partially saturated sands.” Geotechnical Testing Journal 10(3), 135 – 141.

Huai-Houh, H. and An-Bin H. (1999). “Calibration of cone penetration test in sand.” In the Proceeding of Natural Science Council, 23(5), 579 – 590.

Lee, J. and Salgado, R. (2005). “Estimation of bearing capacity of circular footings on sands based on cone penetration test.” Journal of Geotechnical and Geoenvironmental Engineering, 131(4), 442 – 452.

Lehane, B. M., Ismail, M. A. and Fahey, M. (2004). “Seasonal dependence of in situ test parameters in sand above the water table.” Geotechnique, 54(3), 215 – 218.

Meyerhof, G. G. (1956). “Penetration tests and bearing capacity of cohesionless soils.” Journal of the Soil Mechanics and Foundations Division, ASCE, 82 (SM1) Paper 866.

Mohamed, F. M. O. and Vanapalli, S. K. (2006). “Laboratory investigations for the measurement of the bearing capacity of an unsaturated coarse-grained soil.” In the Proceeding of the 59th Canadian Geotechnical Conference, Vancouver, BC, 1, 219 – 227.

Miller, G. A. and Muraleetharan, K. K. (1998). “In situ testing in unsaturated soil.” In the Proceedings of the 2nd International Conference on Unsaturated Soils, Beijing, China, 1, 416 – 42.

Muszynski, M. R. (2008). “Effect of particle shape and gradation on the results of miniature DCP tests in sand.” Geotechnical Testing Journal, 31(6), 1 – 9.

Nes, J. H. G. (2004). “Application of computerized tomography to investigate strain fields caused by cone penetration in sand.” M.Sc., Thesis, Delft University of Technology, Faculty of Civil Engineering and Geosciences Department of Applied Earth Sciences.

Oloo, S. Y. and Fredlund, D. G. Gan, J. K. M. (1997). “Bearing capacity of unpaved roads.” Canadian Geotechnical Journal, 34, 398 – 407.

Phillips, R. and Valsangkar, A. J. (1987). “An experimental investigation of factors affecting penetration resistance in granular soil in centrifuge modeling.” CUDE/D TR 210.

Puppala, A. J., Acar, Y. B. and Senneset, K. (1993). “Cone penetration in cemented sands: bearing capacity interpretation.” Journal of Geotechnical Engineering, 119(12), 1990 – 2001.

Russell, A. R. and Khalili, N. (2006). “Cavity expansion theory and the cone penetration test in unsaturated sand.” Unsaturated Soils, 2456 – 2556.

Salgado, R. Mitchell, J. K. and Jamiolkowski, M. (1997). “Cavity expansion and penetration resistance in sand.” Journal of Geotechnical and Geoenvironmental Engineering, 123(4), 344 – 354.

Salgado, R. (2008). “The engineering of foundations.” McGraw – Hill, New York, NY, USA.

Shaqour, F. M. (2007). “Cone penetration resistance of calcareous sand.” Bulletin Engineering Geology, (66), 59 – 70.

Skempton, A. W. (1951). “The bearing capacity of clays.” Building research congress, London, (1), 180 – 189.

Terzaghi, K. and Peck, R. B. (1948). “Soil mechanics in engineering practice.” Asia Publishing House.

Vanapalli, S. K. and Mohamed, F. M. O. (2007). “Bearing capacity of model footings in unsaturated soils.” Experimental Unsaturated Soil mechanics, Springer, New York, 483 – 493.

Vanapalli, S.K. and Oh, W. T. (2007). "Determination of the bearing capacity of unsaturated soils under undrained loading conditions." Proceedings of the 60th Canadian Geotechnical Conference, Ottawa, Ontario, Canada.

Vanapalli, S. and Eigenbrod, E. (2009). "A technique for estimating shaft resistance of test pile in unsaturated soils." Revised version in preparation for submission to the Canadian Geotechnical Journal.

Vesić, A. S. (1963). "Bearing capacity of deep foundations in sand." Highway Research Record, (39), 112 – 153.

Vos, D. J. (1982). "The practical use of CPT in soil profiling." Proceedings of the 2nd European symposium on Penetration Testing, ESOPT-2, 2, Amesterdam, 933 – 939.

Yu, H. S. and Mitchell, J. K. (1998). "Analysis of cone resistance: review of methods." Journal of Geotechnical and Geoenvironmental Engineering, 124(2), 140 – 14.

Campanella, R. G., Robertson, P. K. and Gillespie, D. (1983). "Cone penetration testing in deltaic soils." Canadian Geotechnical Journal 20(1), 23-35.

Canadian Foundation Engineering Manual, CFEM (4th Ed.). (2006). Canadian Geotechnical Society. Vancouver, Bitech Publisher, P 512.

Chen, F. H. (1999). "Soil Engineering, Testing, Design and Remediation." Florida, USA: CRC Press LLC.

Eslaamizaad, S. and Robertson, P. K. (1996). "Cone penetration test to evaluate bearing capacity of foundations in sands." In the Proceedings of the 49th Canadian Geotechnical Conference, St, John's, NF, 429 – 438.

Eslami, A. and Gholami, M. (2006). "Bearing capacity analysis of shallow foundations from CPT data." Scientia Iranica, 13(3), 223 – 233.

Lee, J. and Salgado, R. (2005). “Estimation of bearing capacity of circular footings on sands based on cone penetration test.” Journal of Geotechnical and Geoenvironmental Engineering, 131(4), 442 – 452.

Meyerhof, G. G. (1956). “Penetration tests and bearing capacity of cohesionless soils.” Journal of the Soil Mechanics and Foundations Division, ASCE 82 (SM1), 1 – 19.

Mohamed, F. M. O. and Vanapalli, S. K. (2006). “Laboratory investigations for the measurement of the bearing capacity of an unsaturated coarse-grained soil.” Proceedings of 59th Canadian Geotechnical Conference, Vancouver, BC, 219 – 227.

Mohamed, F. M. O. and Vanapalli, S. K. (2009). “An experimental investigation of the bearing capacity of an unsaturated sand using cone penetration tests.” In the Proceedings of the 62nd Canadian Geotechnical Conference, Halifax, NS, 205 – 213.

Poulos, H. D. and Davis, E. H. (1974). “Elastic solutions for soil and rock mechanics.” New York, John Wiley and Sons.

Russell, A. R. and Khalili, N. (2006). “Cavity expansion theory and the cone penetration test in unsaturated sand.” Geotechnical Special Publication, ASCE 147 (2), 2456-2556.

Schmertmann, J. H. (1978). “Guidelines for cone penetration test, performance and design.” Report No. FHWA-TS-78-209, US Department of Transportation, Washington, D.C., P. 145.

Stannard, D. I. (1992). ‘‘Tensiometers – theory, construction, and use.’’ Geotechnical Testing Journal, 15 (1), 48–58.

Steensen-Bach, J. O., Foged, N. and Steenfelt, J. S. (1987). “Capillary induced stresses-fact or fiction?.” In the Proceedings of the 9th ECSMFE, Groundwater Effects in Geotechnical Engineering, Dublin, 83-89.

Terzaghi, K. (1943). “Theoretical soil mechanics.” New York, USA: John Wiley and Sons.

Vanapalli, S. K. and Mohamed, F. M. O. (2007). “Bearing capacity of model footings in unsaturated soils.” In the Proceedings of the 2nd International Conference on Unsaturated Soils, 7-9 March, Weimar, Germany, 483 – 493.

Vanapalli, S. K., Oh, W. T. and Puppala, A. J. (2007). “Determination of bearing capacity of unsaturated soils under undrained conditions.” In the Proceedings of the 60th Geotechnical Conference, Ottawa, ON, 1002 – 1009.

CHAPTER 4

[3]BEARING CAPACITY OF SHALLOW FOUNDATIONS IN SATURATED AND UNSATURATED SAND FROM SPT-CPT CORRELATIONS

4.1 Introduction

The bearing capacity is one of the key parameters required in the design of shallow foundations in sandy soils. The plate load tests (PLTs); standard penetration tests (SPTs) and cone penetration tests (CPTs) are used in geotechnical engineering practice for the determination or estimation of the bearing capacity of sands. The SPTs however are more widely used to estimate the bearing capacity of sands. There are several well-established SPT-based design techniques available in the literature for estimating the bearing capacity and settlements of shallow foundations in sands (for example, Meyerhof 1956, Peck and Bazaraa 1967, Parry 1971, Burland and Burbidge 1985 and Bowles 1996). Nevertheless, the influence of capillary stresses (i.e., matric suction) above the ground water table (GWT) is ignored in the estimation of the bearing capacity of sands in conventional engineering practice. Ignoring the contribution of matric suction towards the bearing capacity leads to conservative design of shallow footings in sands, particularly in semi-arid and arid regions, where the natural GWT is typically at a greater depth. Steensen-Batch et al. (1987) commented that ignoring the influence of capillary

[3]This chapter is developed by extending a technical paper that was presented at the 2012 International Conference on Geomechanics and Engineering, 26-30 August 2012 in Seoul, South Korea.

stresses in the bearing capacity of unsaturated sands would be equivalent to disregarding the influence of reinforcement in the design of reinforced concrete.

In the research presented in this chapter, in-situ PLTs and SPTs were conducted in sand under both saturated (i.e., matric suction, $(u_a - u_w) = 0$ kPa) and unsaturated (i.e., $(u_a - u_w) > 0$ kPa) conditions at Carp, Ottawa, to highlight the differences in the bearing capacity results. Series of PLTs were conducted to measure the bearing capacity of sand in the field in both saturated and unsaturated sand (i.e., 0 kPa, 2 kPa and 8 kPa). The bearing capacity of the sand at a matric suction value of 8 kPa was found to be approximately 3.5 times greater in comparison to the bearing capacity of the same soil under saturated condition (i.e., 0 kPa). The N_{SPT} values from the SPTs that conducted in sand under unsaturated condition (with no rain for more than 3 continuous days from 21 to 23 May 2012, see Figure 4.1) was 3 times higher than the N_{SPT} values obtained from the SPT conducted in saturated condition at the same site. Relationships are derived from the field investigation studies along with other studies in the literature to estimate the bearing capacity of sands under both saturated and unsaturated conditions from the conventional SPT results. The results of the study suggest that the proposed relationships can be used in the estimation of the bearing capacity.

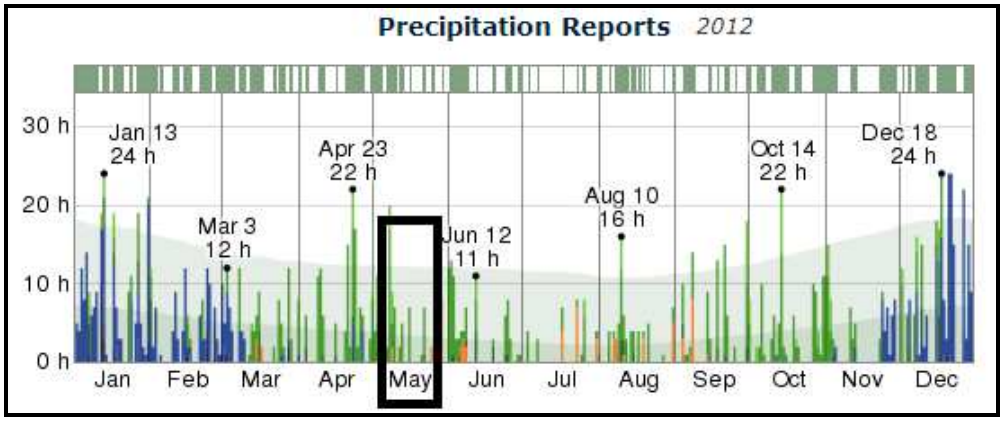

Figure 4.1 The daily number of hourly observed precipitation reports during 2012, color coded according to precipitation type, and stacked in order of severity. Dark to light green: light rain; Lightest green: drizzle (WeatherSpark.com)

4.2 Background

The bearing capacity of shallow foundations has received the attention of several investigators over the last century. Prandtl (1921) and Reissner (1924) were one of the earliest investigators who studied the bearing capacity of soils by loading a strip rigid footing. The applied stress at which stability failure occurs was defined as the ultimate bearing capacity of the soil. Several techniques and empirical procedures that followed Prandtl's research were valuable to provide a comprehensive understanding of the bearing capacity of soils (Terzaghi 1943, Terzaghi and Peck 1948, Meyerhof 1951, Meyerhof 1956, Lawrence 1968, Vesić 1973, and Bolton and Lau 1993). These studies are widely used in the estimation of the bearing capacity of saturated soils using the saturated shear strength parameters, footing dimensions, shape, depth and inclination factors and the GWT depth. The focus of bearing capacity studies were mainly directed towards understanding the behaviour of saturated soils using PLTs, CPTs and SPTs. The influence of capillary stress above the GWT (i.e., matric suction) on the in-situ bearing capacity of soils has not received the attention it deserve in the geotechnical literature. Limited studies are reported in literature on understanding the influence of bearing capacity using PLTs or CPTs (Schnaid et al. 1995, Costa et al. 2003, Mohamed and Vanapalli 2006, Rojas et al. 2007, Russell and Khalili 2006 and Pournaghiazar et al. 2011).

In-situ bearing capacity of soils can be determined using field tests such as the PLTs, CPTs and the SPTs. These tests also have some limitations and hence the results have to be carefully interpreted. PLTs are difficult, time consuming and expensive and their results are influenced by many parameters such as the plate size and its influence on the stress bulb zone (Oh and Vanapalli 2013). A number of studies are also reported in the literature for evaluating the bearing capacity of soils from the CPTs results using empirical equations (for example, Meyerhof 1956, Robertson et al. 1983, Eslaamizaad and Robertson 1996, Lee and Salgado 2006, Eslami and Gholami 2006, CFEM 2006).

SPT-based methods are more widely used to estimate the variation of bearing capacity with respect to depth (Meyerhof 1956, Burland and Burbidge 1985, Bowles 1996, and McGregor and Duncan 1998). Some investigators highlighted the possible uncertainties associated with the N_{SPT} values obtained from the SPTs as they are operator dependent (for example, Seed et al. 1985). The reliability of interpreting the bearing capacity of sandy soils from in-situ SPTs has significantly increased over a period of time due to the developments in the SPT equipment and the standards used in conducting them (Mitchell, 2000). In other words, the presently used the SPTs are quick and reliable in addition to providing access to collecting the soil samples along the depth of investigation (Arman et al. 1997). Correlations between soil properties and SPTs results are also available in the geotechnical literature (Carter and Bentley 1991). ASTM D6066-96 and ASTM D1586-11 provide details of the SPT that can be followed for sandy soils. These procedures are widely used in practice in many regions of the world. All the field tests (i.e., PLTs, CPTs and SPTs) that are presently used in conventional engineering practice are used for estimating the bearing capacity of saturated soils. The contribution of matric suction in the capillary zone is not considered. There is a need to conduct more field studies to better understand the behaviour of foundations in sands both in saturated and unsaturated conditions. Based on such studies, empirical relationships should be developed not only to understand the influence of matric suction but also to contribute to the design of shallow foundations reliably. These studies form the focus of the research summarized in this chapter.

4.3 Details of the Site and Soil Properties

4.3.1 Description of the Test Site

The test site is located at Carp Region in Ottawa, Ontario, Canada as shown in the map in Figure 4.2. The GWT level was found at - 2.8 m below the natural ground level. The site was also surveyed and the level of the water table at the lower level (where a small lake was found) confirmed that the GWT was approximately at -2.8 m.

The site has a sloping terrain with two different levels which are referred to hereafter as the upper level of the site (± 0.0 m) and the lower level (- 2.4 m) in the remainder of the chapter (refer to Figure 4.3 and Figure 4.4). Photos from the site are shown in Figures 4.3 and 4.5.

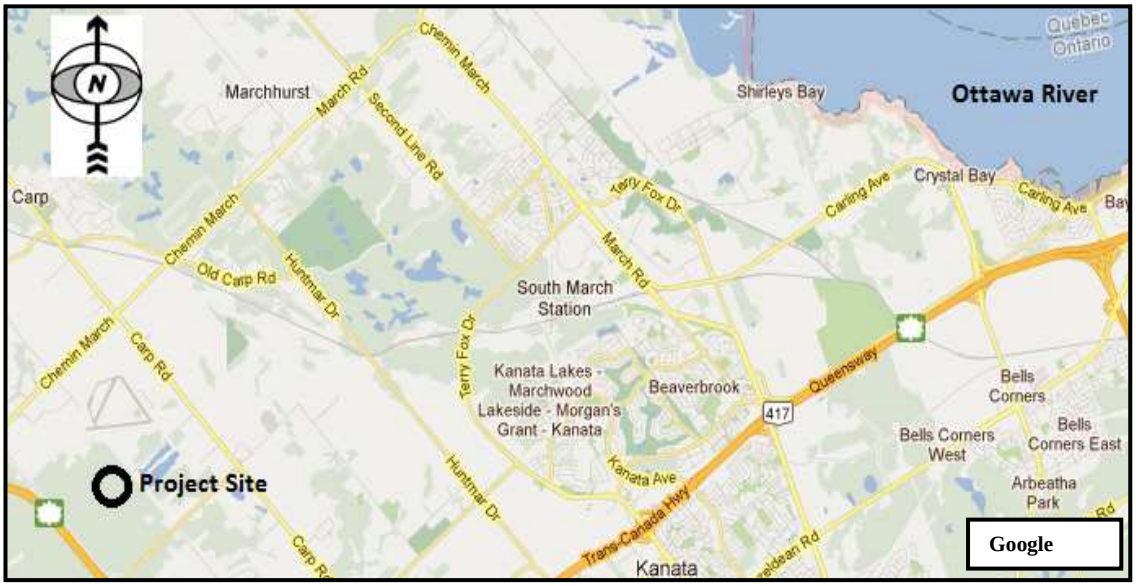

Figure 4.2 Location of the test site, Carp Region of Ottawa in Canada

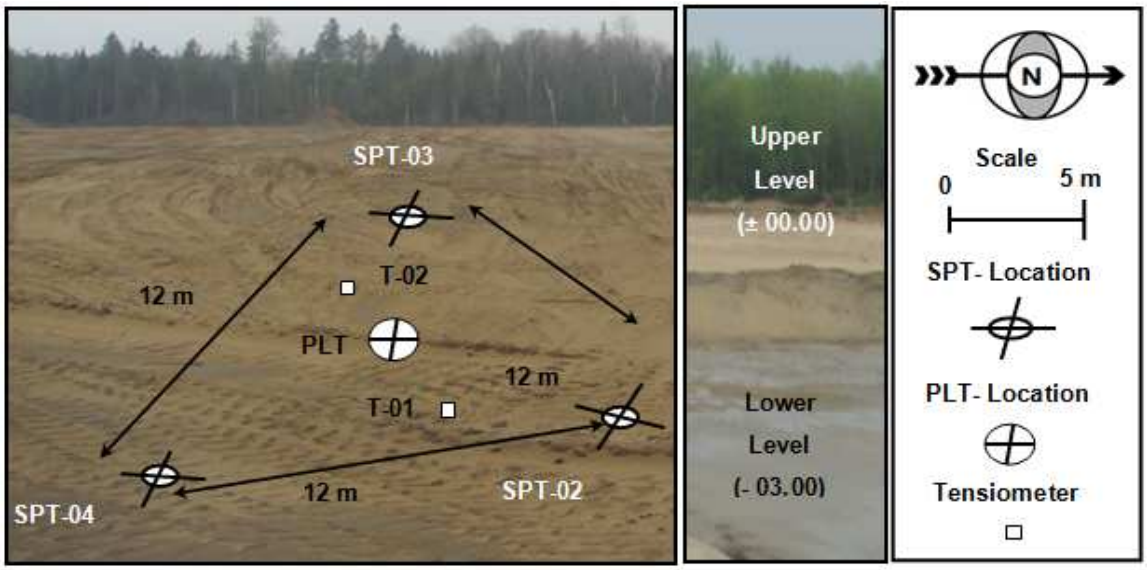

Figure 4. 3 Location of the SPTs, PLTs and Tensiometers on the test site

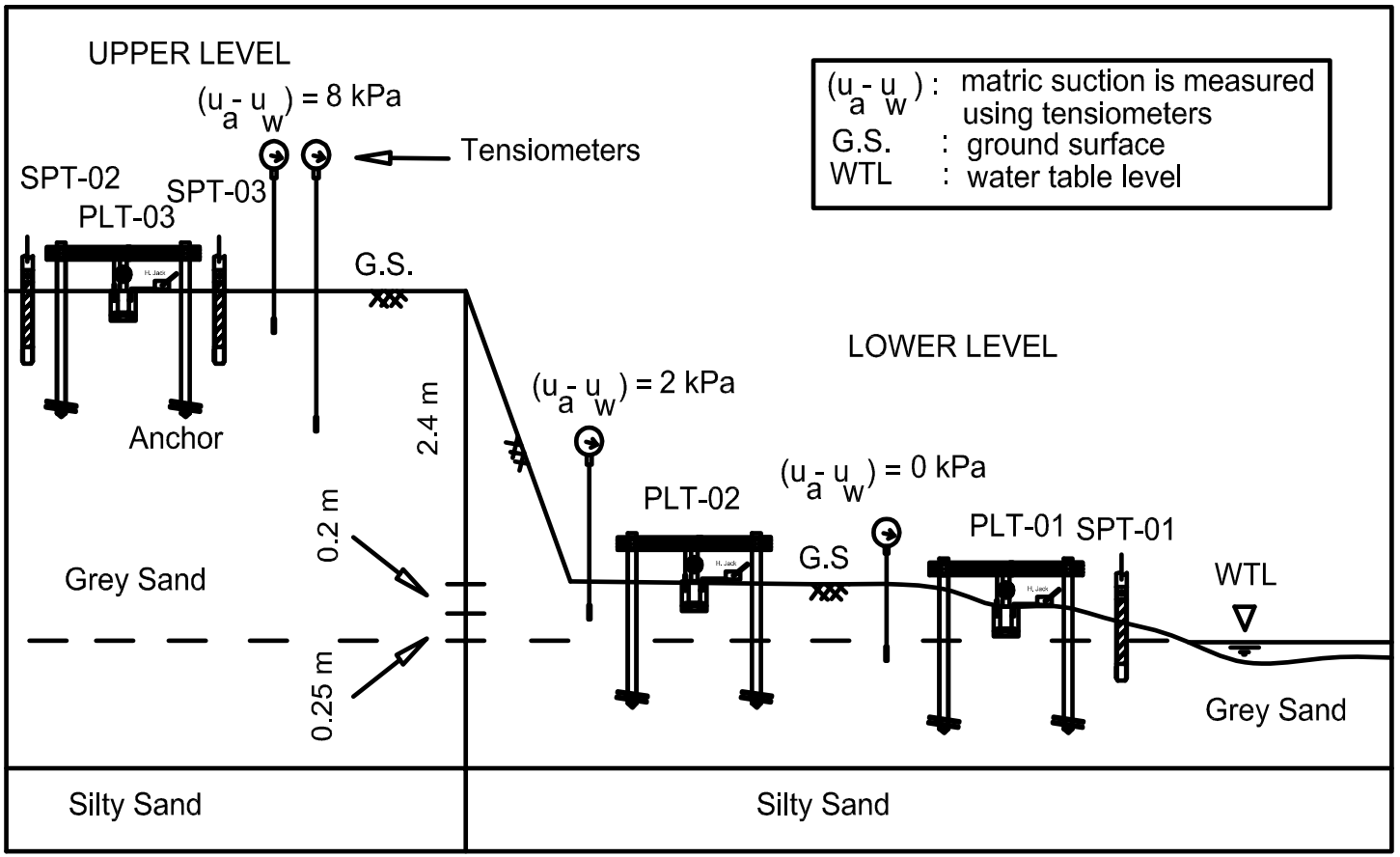

Figure 4.4 Sectional view of the test site with details of SPTs and PLTs locations

Figure 4.5 Photos of the PLT setup and a Tensiometer used at the site

4.3.2 The Properties of the Tested Soil at Carp Region

Soil samples were collected using the split spoon-sampler of the SPT from different depths where the SPTs conducted to determine the soil properties and the soil-water characteristic curve, SWCC. Flow-chart in Figure 4.6 shows the tests conducted using the collected soil samples.

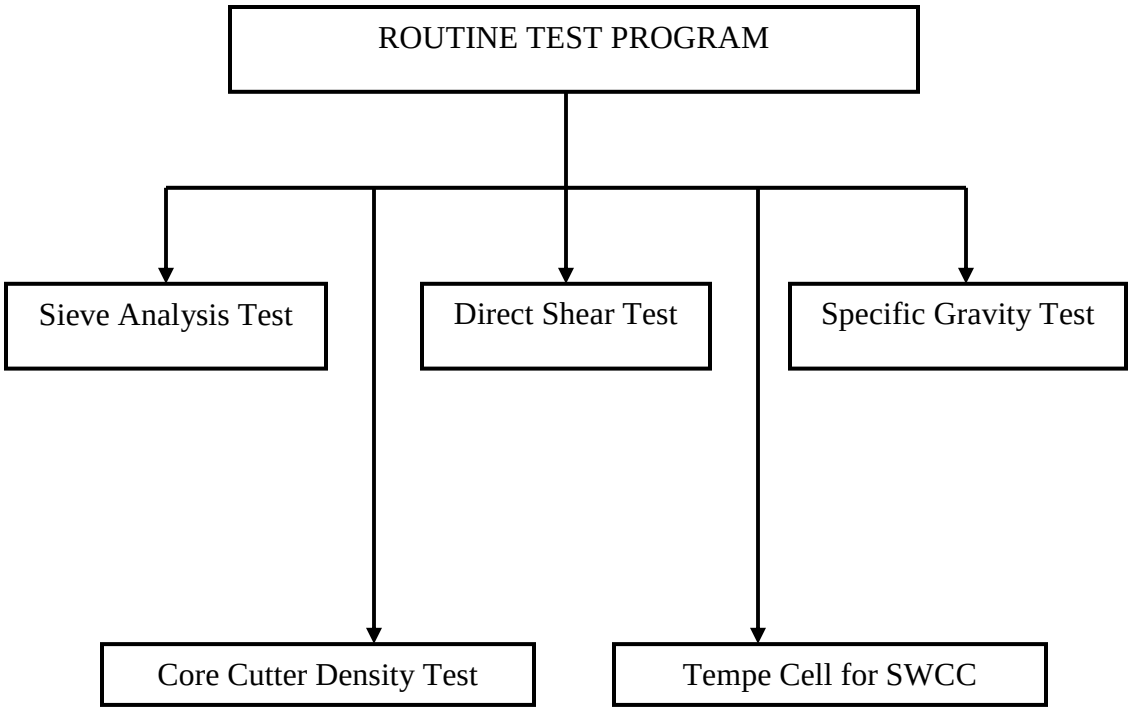

Figure 4.6 Flow-chart illustrates the routine tests conducted on the soil

Grey sandy soil with some dark silt (i.e., known locally as septic sand) was available up to a depth of - 4.7 m below the ground surface (from the upper level). Dark-grey silty sand was located underneath the septic sand. The soil at this site (i.e., Carp area) was described at late to post-glacial sediments (see Figure 4.7 from Motazedian et al. 2010) indicating that the soil is relatively new. Hence, the soil at the site can be described as a normally consolidated soil.

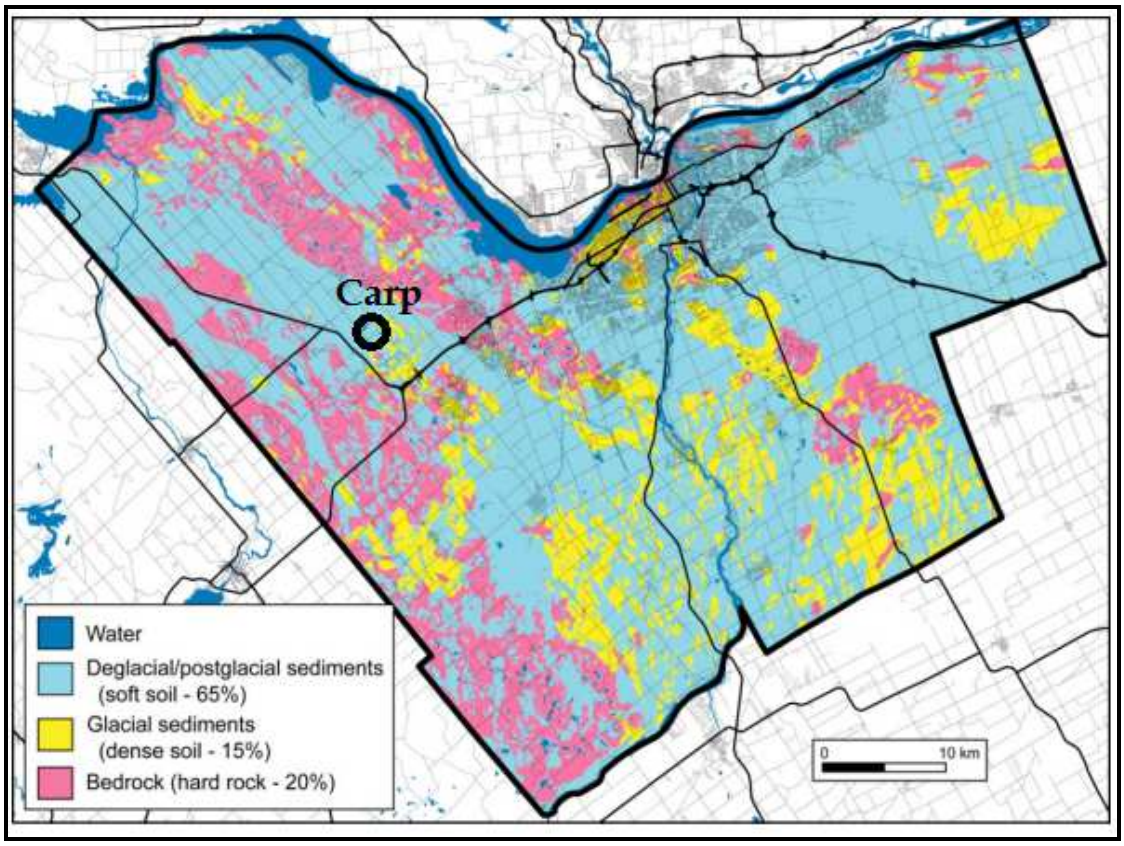

Figure 4. 7 Microzonation map with surficial geology of Ottawa

(from Motazedian et al 2010)

The grain-size distribution of the soil at the site is shown in Figure 4.8. Properties of the tested soil are presented in Table 4.1. The soil can be classified as poorly-graded sand, *SP* according to the USCS. The average dry unit weight and the specific gravity of the sand were 17.75 kN/m^3 and 2.65, respectively. The effective cohesion, *c'* and the angle of internal friction, ϕ' were determined using direct shear test (i.e., DST) apparatus (i.e, consolidated drained condition) to be 0.4 kN/m^2 and 36.5 ° respectively. Results from the DST are shown in Figures 4.9 to 4.10. It has been observed from the vertical displacement (i.e., normal displacement) versus the horizontal displacement (i.e., shear displacement) curves (see Figure 4.11) which obtained from the DST that there was a slight increase in the normal direction of the soil in the shear box (i.e., 60 mm × 60 mm)

while the specimen was being sheared (snap shot is in Figure 4.11). This phenomenon indicates that the sand specimen was dilating.

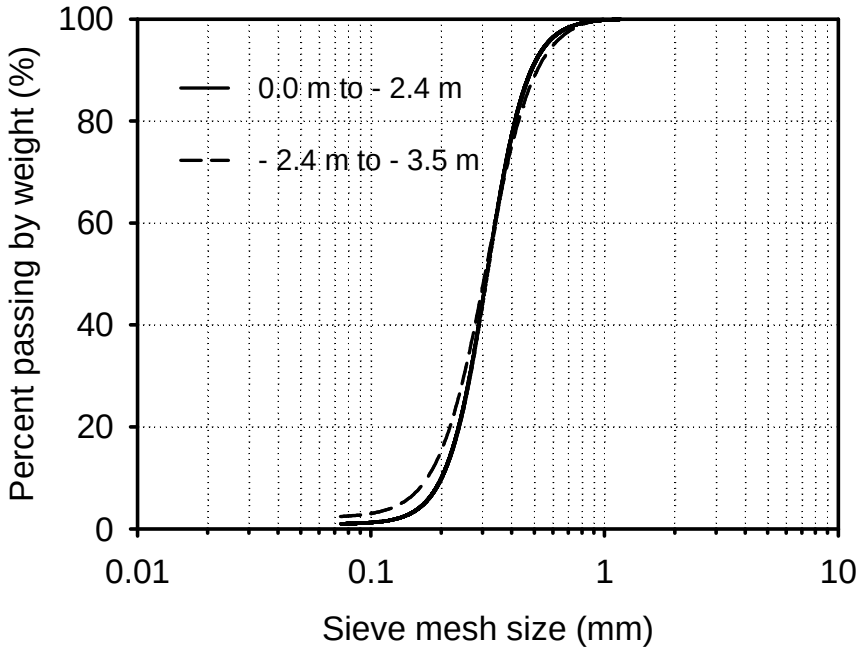

Figure 4. 8 Grain size distribution of the tested Carp sand

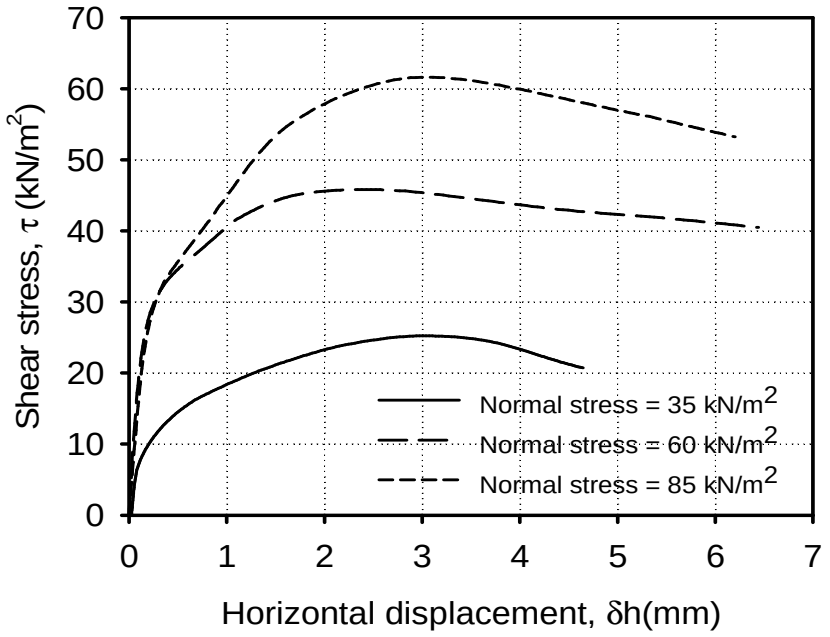

Figure 4.9 Shear stress versus horizontal displacement for the tested sand

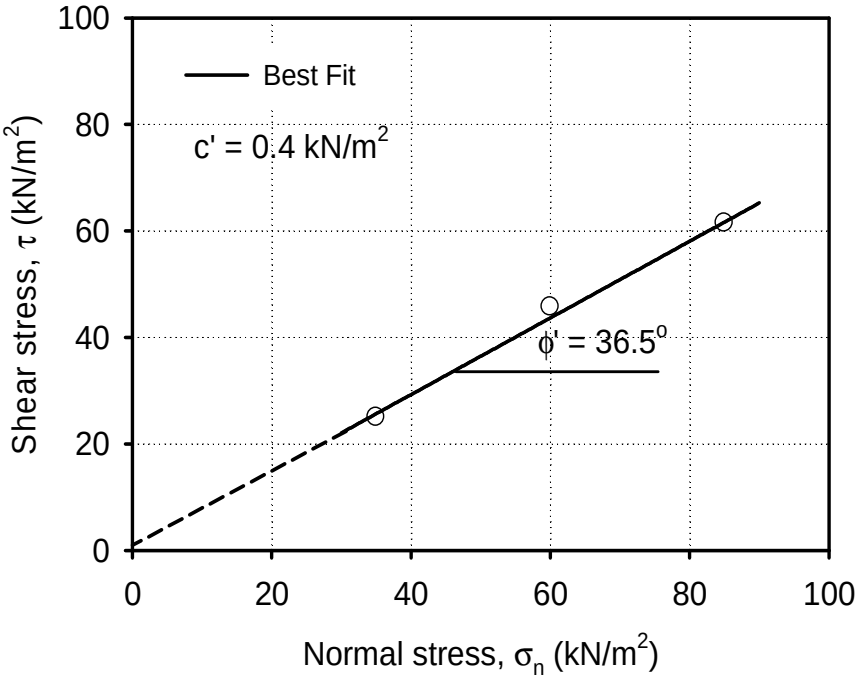

Figure 4.10 Shear stress versus normal stress for the tested sand

Table 4. 1 Properties of the tested soil at Carp site in Ottawa

Property	Soil at depth from 0.0 m to - 2.4 m	Soil at depth from - 2.4 m to - 3.5 m
Specific Gravity, G_s	2.65	2.65
D_{60} (mm)	0.33	0.33
D_{30} (mm)	0.266	0.260
D_{10} (mm)	0.198	0.169
Coefficient of uniformity, C_u	1.67	1.96
Coefficient of curvature, C_c	1.08	1.21
Dry unit weight, γ_t (kN/m^3)	17.5 to 18.0	17.5 to 18.0
Soil friction angle, ϕ' (°)	36.5	36.5
Effective cohesion, c' (kN/m^2)	0.4	0.4

4.3.3 The Soil-Water Characteristic Curve (SWCC) of the tested sand at Carp Region

The SWCC is known as the relationship between the matric suction, $(u_a - u_w)$ and the gravimetric water content, w. Tempe Cell apparatus was used for measuring the SWCC in the laboratory (see Figure 4.11). The measured SWCC using the Tempe Cell is plotted in Figure 4.12. Two measured matric suction values obtained from using the Tensiometers installed in-situ in the vicinity of the SPTs locations were also plotted on the SWCC. The measured matric suction values from the Tempe Cell apparatus and the matric suction from in-situ are consistent.

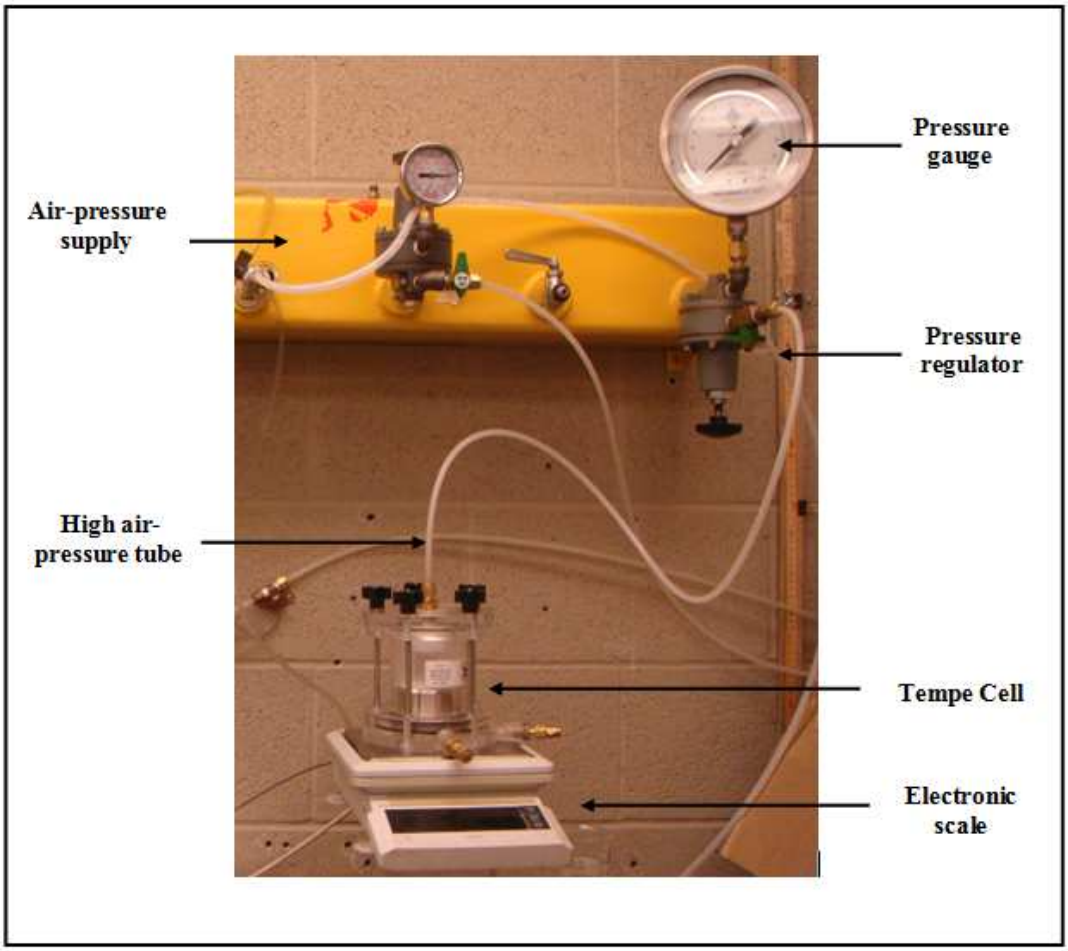

Figure 4.11 Equipment setup for measuring the SWCC using the Tempe Cell

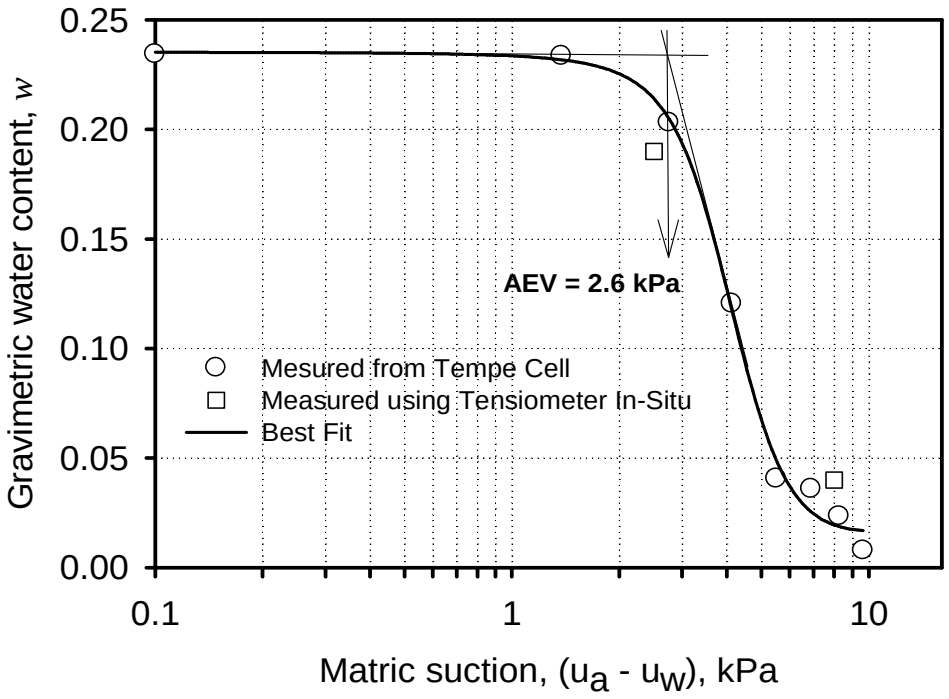

Figure 4.12 Soil Water Characteristic Curve (SWCC) for the tested sand in laboratory along with measured data at the site

4.4 In-Situ Standard Penetration Tests (SPTs)

4.4.1 Equipment Details

The SPTs were conducted at the test location under both saturated and unsaturated conditions following the ASTM D1586-11. The SPT equipment used in this research program is shown in Figure 4.13. A steel hammer (of weight 623 N) was used to drive the sampler vertically. The SPTs were conducted up to a depth - 3.5 m from the natural ground surface. The split-spoon sampler (with an inside and outside diameter of 34.93 mm and 50.8 mm, respectively) with a spring core catcher was used for collecting soil samples. After the split-spoon sampler was withdrawn, the soil sample from within was removed, stored in labelled zipped plastic bags and used for determining the water content, grain-size distribution, and specific gravity from laboratory tests.

Figure 4.13 SPT falling model truck mounted equipment used in-situ

2.4.2 Summary of the SPT and matric suction measurement results

The first SPT test which is referred to as SPT-01 was conducted at the lower level (for the saturated condition) which is close to natural GWT (at the water basin; see the lower level in Figure 4.3). The sand in the vicinity where the tested were conducted was in a state of saturated condition in the field. Three additional SPTs which are referred to as SPT-02, SPT-03, SPT-04 were conducted at the upper level where the sand was in a state of unsaturated condition. The SPTs were conducted in triangular-grid area separated by approximately 12 m spacing in the upper level of the site (see Figure 4.3). A number of soil samples were collected and kept in zipped plastic bags to determine the variation of water content with respect to depth of the soil. Some of those samples were used for the routine laboratory tests such as the sieve-analysis, direct shear test, and specific gravity.

The SPT tests were performed using a Falling Model Truck mounted with a rotary drilling rig. The length of each of the drill rods (i.e., standard N rods) is 3.0 m with 1.5 m length extension rods that were used as needed. The blow counts over 450 mm of penetration were recorded in three intervals (e.g., 150 mm per interval). The N_{SPT}-value for each interval is noted as the summation of the blows for the last two 150 mm penetrations. Gibbens and Briaud (1994) measured the SPT/W energy (i.e., the amount of energy delivered to the drill rods which is function of the type of hammer system (donut, safety, and automatic)) in a sandy soil (using a pair of Piezoresistive Accelerometers and foil resistive strain gauges) and reported that the blow counts were measured with an energy efficiency averaging 53 %. Field testing indicated that the energy delivered to the rods during an SPT test can vary from 30 to 90 % of the theoretical maximum, depending on the type of hammer system used as investigated by Aggour and Radding (2001). It was concluded by Aggour and Radding (2001) that for safety hammer which is similar to the hammer used in the present study have an AVR energy coefficient of 70.2 % as shown in Table 4.2.

Table 4.2 Transferred energy efficiency (Aggour and Radding 2001)

Hammer System	Donut	Safety	Automatic
AVR efficiency	63.5 %	70.2 %	81.4 %

In the present study, the SPT/W energy was not estimated or measured in the field; however, an energy efficiency of 60 % as recommended by Das (2007) was used in the present study for the SPT blow count interpretations.

The results of the SPTs (i.e., SPT-02, SPT-03 and SPT-04) conducted in the upper level of the site are summarized in Figure 4.14. The SPT-01 and SPT-05 results (blow counts of N_{SPT} with respect to the depth) conducted at the lower site are summarized in Figures 4.15 and Figure 4.16 respectively. The corrected N_{SPT} values for all the SPTs are summarized in Tables 4.3, 4.4 and 4.5. There is an increase in N_{SPT} values obtained from

SPTs conducted in the unsaturated sand due to the contribution of matric suction as shown in Figure 4.14.

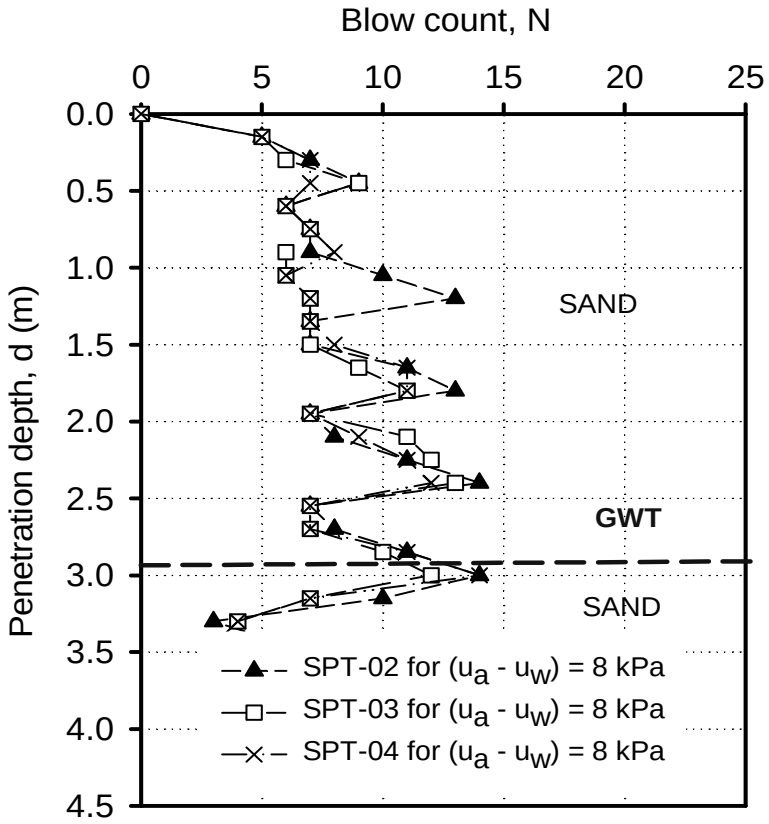

Figure 4.14 Blow count, N_{SPT} versus depth for the sand tested under unsaturated conditions (8 kPa in the upper level) with approximate depth of GWT at Carp, Ottawa

Table 4.3 Recorded and corrected SPT-N values from SPT conducted at ($u_a - u_w$) = 8 kPa

Depth (m)	0-0.45	0.45-0.90	0.90-1.35	1.35-1.8	1.8-2.25	2.25-0.2.7	2.7-3.15
N_{SPT}	6	8	10	8	9	5	6
Corrected N_{SPT}	4	5	6	5	6	3	4

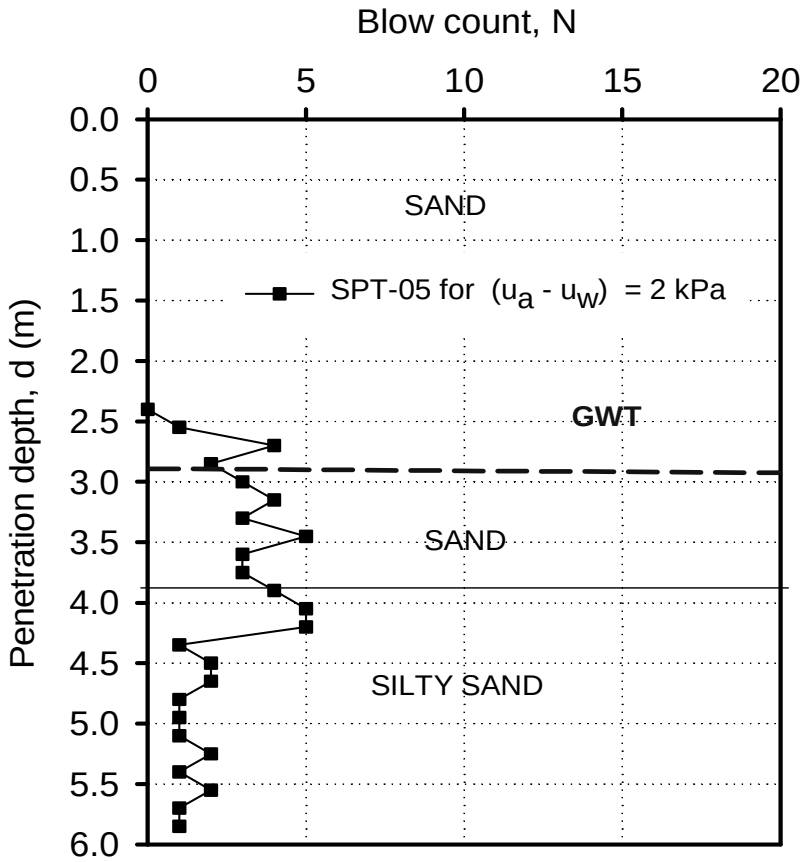

Figure 4.15 Blow count, N_{SPT} versus depth for the sand tested under unsaturated condition (2 kPa in the lower level) with approximate depth of GWT at Carp, Ottawa

Table 4.4 Recorded and corrected SPT-N values from SPT conducted at $(u_a - u_w)$ = 2 kPa

Depth (m)	0-0.45	0.45-0.90	0.90-1.35	1.35-1.8	1.8-2.25	2.25-0.2.7	2.7-3.15
N_{SPT}	6	8	10	8	9	5	6
Corrected N_{SPT}	4	5	6	5	6	3	4

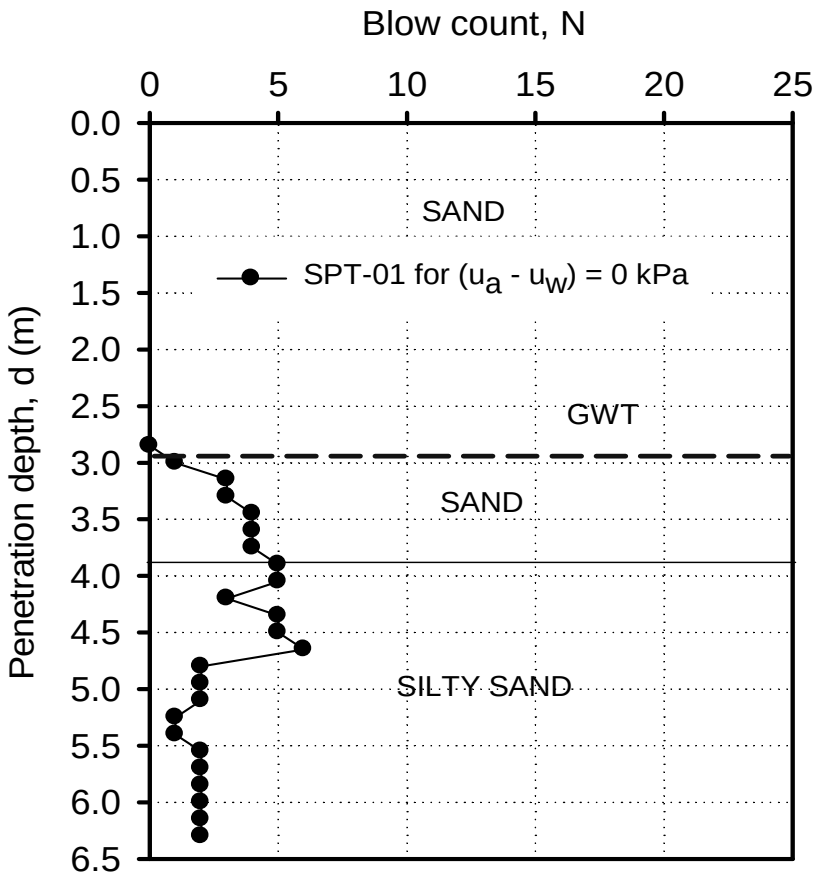

Figure 4.16 Variation of blow count, N_{SPT} versus depth for the sand tested under saturated condition (0 kPa in the lower level) with approximate depth of GWT at Carp, Ottawa

Table 4.5 Recorded and corrected SPT-N values from SPT conducted at ($u_a - u_w$) = 0 kPa

Depth (m)	0-0.45	0.45-0.90	0.90-1.35	1.35-1.8	1.8-2.25	2.25-0.2.7	2.7-3.15
N_{SPT}	4	12	7	8	4	6	6
*Corrected N_{SPT}	3	8	5	5	3	4	4

4.5 In-Situ Plate Load Tests (PLTs)

Three PLTs were conducted in this research program using a steel plate of 0.2 m × 0.2 m. The first PLT (i.e., PLT-01) was conducted at the lower level close to the GWT level where the sand is in saturated condition as Tensiometer records zero matric suction. The second PLT (i.e., PLT-02) was also conducted at the lower level but at an elevation of + 0.25 m from the level where the PLT-01 was conducted. The Tensiometer at the PLT-02 recorded a matric suction of 2 kPa. The third PLT (i.e., PLT-03) was conducted at the upper level where the remaining two Tensiometers replaced at 0.15 m and 1.2 m depths and recorded 8 kPa confirming a uniform matric suction profile within that region. All the PLTs were conducted at a depth of 0.15 m. The matric suction values were measured at half-way of the depth of the stress bulb zone (i.e., 1.5*B*) using four Tensiometers.

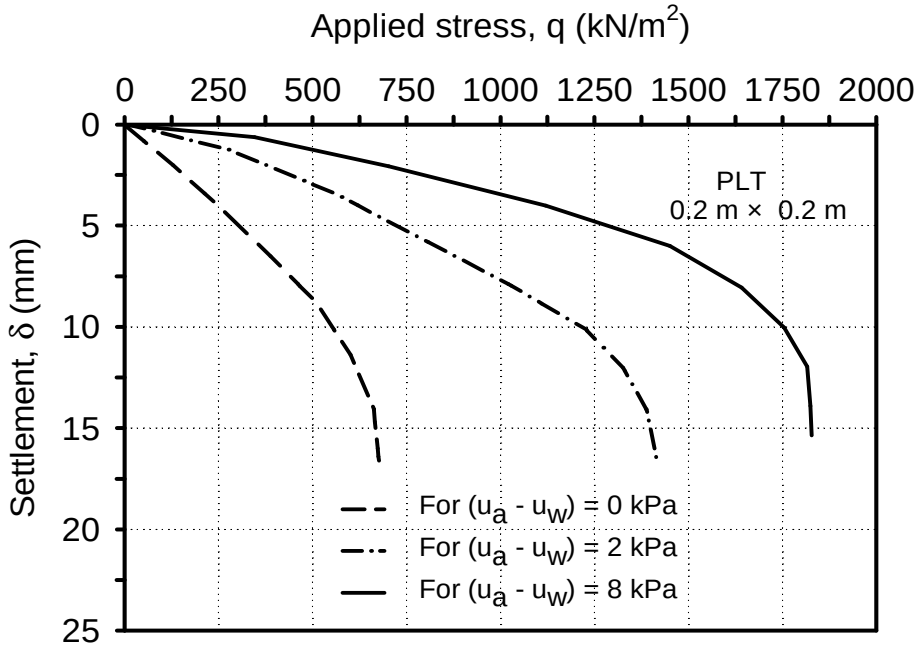

Figure 4.17 The relationship between the applied stress and the settlement of 0.2 m × 0.2 m square plate of the tested sand at Carp, Ottawa

The influence zone is the depth in which stresses are predominant for shallow square footings (Poulos and Davis 1974, Chen 1999). The relationship between the applied stress and the settlement of the in-situ PLTs conducted in this research program is shown in Figure 4.17. These relationships demonstrate that there is a significant increase in the applied stress (i.e., bearing capacity) of the PLTs due to the contribution of the matric suction in the tested sand.

Terzaghi and Peck (1948) proposed a relationship for estimating the settlement of a footing from PLTs using a plate of dimensions 0.3 m × 0.3 m as given below:

$$\delta_{B_1} = \delta_{B_2}\left[\frac{B_1(B_2+0.3)}{B_2(B_1+0.3)}\right]^2 \qquad [4.1]$$

where: δ_{B1} = the settlement of a footing with width B_1; δ_{B2} = the settlement of a footing with width B_2.

Terzaghi and Peck (1948) suggested the permissible settlement for large footing sizes of 2.0 m width as 25.4 mm. Several foundation codes from various regions of the world recommend a permissible settlement value for shallow foundations in coarse grained soils as 25 mm (CFEM-2006). However, lower values of settlement values are also used by investigators for estimating the allowable bearing capacity for smaller size footings. Nabil (1985) carried out PLTs (using plate size of 0.5 m × 0.5 m) and estimated the allowable bearing capacity as a value occurring at a settlement of 13 mm. The allowable bearing capacity in the present study was estimated for the tested sand under saturated and unsaturated conditions at a settlement value of 6 mm from the PLTs conducted on 0.2 m × 0.2 m plate. Estimated values of the bearing capacity using the proposed relationships in this study are compared with the allowable bearing capacity values for the PLTs.

4.6 Relationships Using the SPTs and CPTs for the Estimation of the Bearing Capacity of Sands

Meyerhof (1956) investigated the relationship between *N* value and static cone resistance q_c for fine and silty sands and suggested that:

$$q_c = 4.4\ N \qquad [4.2]$$

where: q_c is the cone resistance in kN/m^2 and *N* is the blow count.

Schmertmman (1970) suggested another relationship between the cone resistance of the CPT and the N-value from SPTs based on the results of several fine to medium sands and silty sands. Several other researchers also proposed different relationships to correlate the SPTs results to cone resistance, q_c values (De Alencar Velloso 1959, Meigh and Nixon 1961, Robertson et al. 1983, and Danziger and de Valleso 1998). More recently, Kara and Gündüz (2010) proposed a simple relationship between the *N*-value from SPTs and the cone resistance, q_c to be used for determining the bearing capacity of sand as in Eq. [4.3].

$$q_c = 0.533\ N^{0.8019} \qquad [4.3]$$

where:

q_c is in MPa and N is the corrected blow count ($(N_1)_{60}$).

2.6.1 Proposed Relationships

Mohamed et al. (2010) proposed relationships to estimate the bearing capacity of both saturated and unsaturated sands. Two equations were proposed based on the CPTs results to estimate the bearing capacity of shallow foundations of surface footings placed on saturated and unsaturated homogenous sand respectively. Details are summarized in Chapter 3. Eq. [4.4] (referred to as Eq. [3.11] in chapter 3) was suggested to estimate the bearing capacity for saturated sands (i.e., $(u_a - u_w) = 0$ kPa) from CPT results:

$$q_{ult\ (sat)} = \Theta(q_{c\ sat}) \qquad [4.4]$$

where: $q_{u\ (sat)}$ = bearing capacity for saturated homogenous sand, $\Theta = 0.15/B^{0.63}$ (i.e., correlation factor), $q_{c\ (sat)}$ = average cone resistance under saturated sand condition (e.g., within influence zone, IZ equal to 1.5*B* from the footing base level as illustrated in Figure 4.16) and *B* = footing width (in meter) as shown in Figure 4.18.

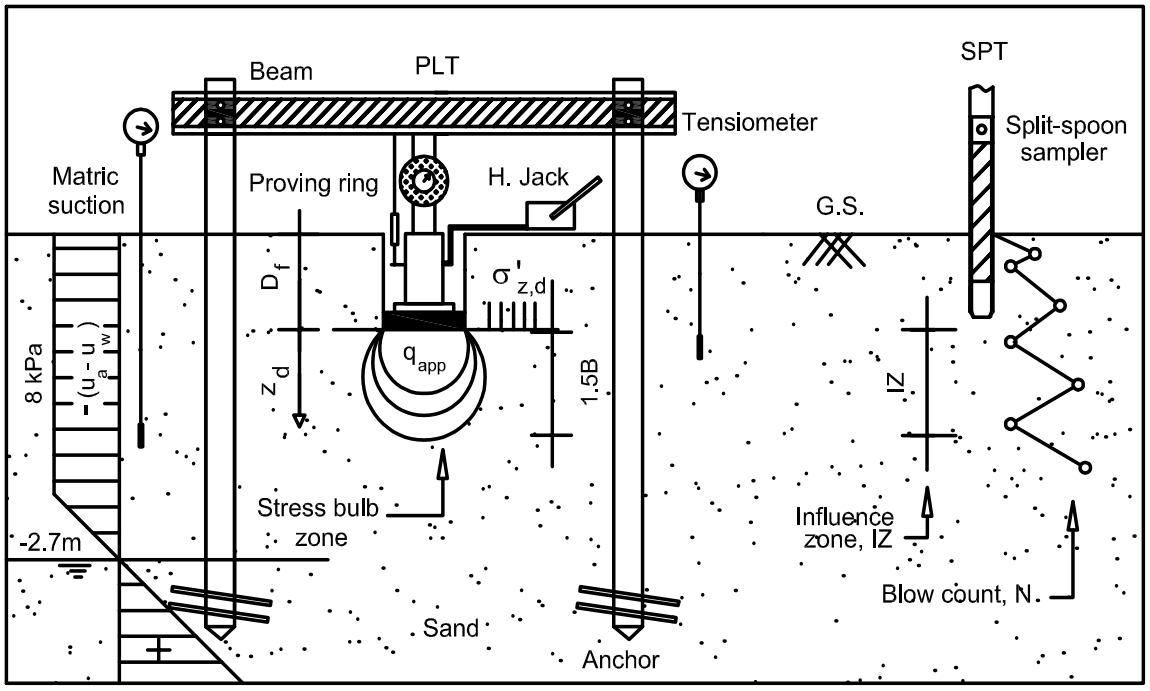

Figure 4.18 Schematic showing details of the in-situ PLT and the influence zone, IZ (for the upper level where SPTs and PLTs were conducted in unsaturated sand)

Eq. [4.5] (which referred to as Eq. [3.12] in chapter 3) was suggested to estimate the bearing capacity for unsaturated sands (i.e., $(u_a - u_w) > 0$ kPa):

$$q_{ult\ (unsat)} = \Omega(q_{c\ unsat}) \qquad [4.5]$$

where: $q_{u\ (unsat)}$ = bearing capacity for unsaturated homogenous sand, $\Omega = 0.19/B^{0.68}$ (i.e., correlation factor), $q_{c\ (unsat)}$ = average cone resistance under unsaturated conditions (e.g., within influence zone, IZ equal to 1.5B from the footing base level), B = footing width (in meter).

The two correlation factors, Θ and Ω presented in Eq. [4.4] and Eq. [4.5] respectively were derived from regression analysis of the experimental results obtained from model PLTs (Mohamed and Vanapalli 2006) and CPTs for sand under saturated and unsaturated sand conditions (Mohamed et al., 2010). Tables 4.3, 4.4 and 4.5 summarize the results of the estimated bearing capacity values taking into account the corrected N_{SPT}-value is N_{60} instead of $(N_1)_{60}$ (that was proposed by Kara and Gündüz 2010) as presented in Eq. [4.6] and Eq. [4.7] combination with Eq. [4.4] and Eq. [4.5] for sands in saturated and unsaturated conditions, respectively. Cone resistance, q_c values and the ratios between the estimated and the measured allowable bearing capacity values for the tested sand were in the range of 96 to 116 %.

Table 4.6 Summary of the database used for proposing the correlations (Eq. [4.6] and Eq. [4.7])

Sand condition	Saturated $(u_a - u_w)$ = 0 *kPa*	Unsaturated $(u_a - u_w)$ = 2 *kPa*	Unsaturated $(u_a - u_w)$ = 8 *kPa*
Footing width, *B* (*m*)	0.2	0.2	0.2
[1]Corrected N_{SPT}-value	3	5	8
[2]q_{all} (kN/m^2) (measured from in-situ PLTs)	357	834	1498
The general model: $q_c = C_{1spt}\ N^{C2spt}$			
*C_{1spt}	0.37	0.45	0.45
**c_{2spt}	0.73	0.83	0.83
[4]q_c (kN/m^2) (estimated)	825	1711	2528

For saturated sands:

$$q_{all\ (sat.)} = \frac{0.19}{B^{0.63}}\left[0.37\ (N_{SPT(sat.)})^{0.73}\right] \times 1000 \qquad [4.6]$$

For unsaturated sands:

$$q_{all\ (unsat.)} = \frac{0.19}{B^{0.68}}\left[0.45\ (N_{SPT(unsat.)})^{0.83}\right] \times 1000 \qquad [4.7]$$

[3]q_{all} (kN/m^2) (estimated)	341 (Eq.[4.6])	971 (Eq.[4.7])	1435 (Eq.[4.7])
Estimated/Measured	0.96	1.16	0.96

[1]Average corrected N_{SPT}-value (i.e., N_{60}) in the influence zone of 1.5*B*; [2]Measured bearing capacity from PLTs (i.e., allowable bearing capacity taken at settlement, δ = 6 mm of the 200 mm × 200 PLT conducted in Carp sand); [3]Estimated allowable bearing capacity using the proposed relationships; [4]Cone resistance from corrected N_{SPT}-value, * C_{1spt} = First fitting parameters; **c_{2spt} = Second fitting parameter.

The two empirical relationships Eq. [4.6] and Eq. [4.7] were derived extending Kara and Gündüz (2010) model based on the analyses of the obtained results of SPTs from the present research program. The two fitting parameters were computed by iteration process as the in-situ PLTs and SPTs results were known for the tested sand under both saturated and unsaturated conditions. The details are summarized in Table 4.6. These relationships can be used to estimate the allowable bearing capacity of shallow foundations in saturated and unsaturated sands. Figure 4.19 provides the measured and estimated allowable bearing capacity values of the tested sand in both saturated and unsaturated conditions.

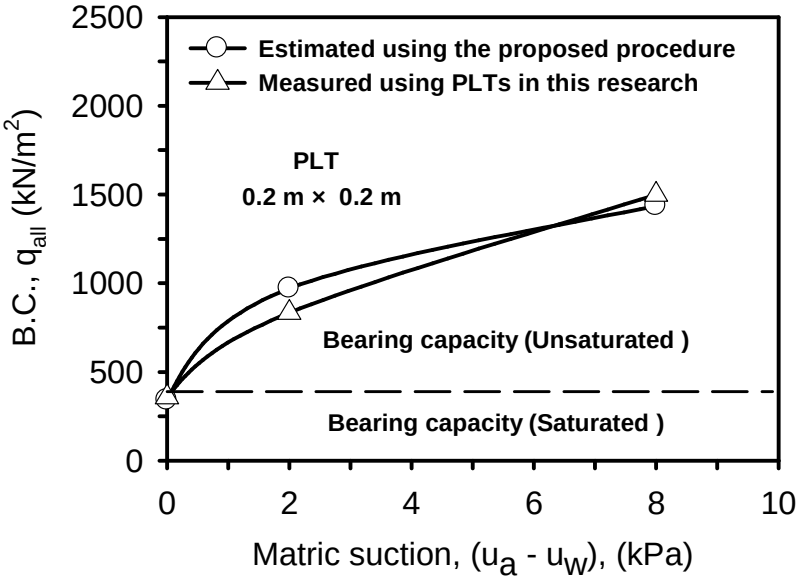

Figure 4.19 Comparison between the estimated and the measured bearing capacity values using 0.2 m × 0.2 m square plate

The obtained N_{SPT}-values which plotted in Figures 4.16, 4.15 and 4.16 were corrected for the recorded blow count values within the stress bulb zone depth of 1.5*B* from the base of footing base and used in the analyses of the data (see Tables 4.3, 4.4 and 4.5). Details of in-situ footing load tests, FLTs results along with the SPTs conducted in their vicinity published by Giddens and Briaud (1994) and Nabil (1985) are summarized and presented in the next section. These in-situ results (from Giddens and Briaud 1994, and Nabil 1985)

are used to check the validity of the proposed relationships (based on SPTs) for estimating the allowable bearing capacity values of other saturated and unsaturated sands.

4.7 Validation of the Proposed Technique Using In-Situ Data from Literature

Four large-scale footing load tests (FLTs) results (in a sandy soil with some silt) conducted in-situ by Giddens and Briaud (1994) were used to validate the proposed relationships in the present study. The footings were loaded in sand at the Texas A&M University National Geotechnical Experimentation site (i.e., data summarized in Table 4.7).

Table 4.7 Typical results of the estimated allowable bearing capacity using SPTs and measured allowable bearing capacity of FLTs at a settlement, δ of 25 mm conducted on sand in Texas, USA (from Giddens and Briaud 1994)

Sand condition	Unsat. $(u_a - u_w)$ = ~10 kPa	Unsat. $(u_a - u_w)$ = ~10 kPa	Unsat. $(u_a - u_w)$ = ~10 kPa	Unsat. $(u_a - u_w)$ = ~10 kPa
Footing width, B (m)	1.0	1.5	2.5	3.0
[1]Corrected N_{SPT}-value	18	14	18	21
[2]q_c (kN/m^2)	4955	4022	4955	5632
[3]q_{all} (kN/m^2) (estimated)	941	580	504	506
[4]q_{all} (kN/m^2) (measured)	1000	800	630	600
Estimated/Measured	0.94	0.73	0.80	0.84

[1]Average corrected N_{SPT}-value (i.e., N_{60}) in the influence zone of 1.5B; [2]Cone resistance; [3]Estimated allowable bearing capacity using the proposed relationships; [4]Measured

bearing allowable capacity from FLTs

In addition to these tests, two more footing load tests, FLTs results (performed in a sandy soil at different locations in Kuwait) reported by Nabil (1985) are also analyzed and used in the validation in this study (refer to Table 4.8).

Table 4.8 Typical results of the estimated allowable bearing capacity using SPTs and measured allowable bearing capacity of FLTs at a settlement, δ of 25 mm from Nabil (1985) conducted on sand in Kuwait

Sand condition	Unsat. $(u_a - u_w)$ = ~7 *kPa*	Unsat. $(u_a - u_w)$ = ~8 *kPa*	Unsat. $(u_a - u_w)$ = ~9 *kPa*	Unsat. $(u_a - u_w)$ = ~9 *kPa*
Footing width, *B* (*m*)	0.5	0.5	0.5	1.0
[1]Corrected N_{SPT}-value	7.5	7.5	15	15
[2]q_c (kN/m^2)	2396	2396	4259	4259
[3]q_{all} (kN/m^2) (estimated)	729	729	1296	809
[4]q_{all} (kN/m^2) (measured)	900	800	1200	1100
Estimated/Measured	0.81	0.91	1.08	0.74

[1]Average corrected N_{SPT}-value (i.e., N_{60}) in the influence zone of 1.5*B*; [2]Cone resistance; [3]Estimated allowable bearing capacity using the proposed relationships; [4]Measured bearing allowable capacity from PLTs

The average matric suction $(u_a - u_w)_{AVR}$ value for the sand at the Texas site was determined assuming constant matric suction distribution as water content throughout the depth of - 4.9 m was approximately uniform. The grain-size distribution of the sand at Texas site was found to be similar to that of the Sollerod Sand tested by Steensen-Bach et al. (1987). The matric suction value of 10 kPa corresponds to the gravimetric water

content, *w* value of 5% from the soil water characteristic curve (SWCC) of the Sollerod sand was estimated as 10 kPa and used in the present study.

The GWT level at the Kuwait site varied from - 2 *m* to - 10 *m* depth depending on the location where the PLT conducted; however the gravimetric water content values reported in the narrow range of 3 % to 6 %. The matric suction values for these water contents were approximately in the range 7 kPa to 10 kPa.

It can be observed that the average N_{SPT}-value required for the proposed relationships are functions of the width, *B* of the footing. The larger the footing width, *B* the larger would be the influence zone, IZ (see Figure 4.18). This relationship leads to the elimination of the scale effect in the estimated allowable bearing capacity values. Table 4.7 and Table 4.8 summarize the corrected N_{SPT}-values (i.e., N_{60}), the cone resistance, q_c and the estimated as well as the measured allowable bearing capacity values for Texas and Kuwait sites respectively.

Comparisons are provided in Figure 4.20 between the estimated allowable bearing capacity, q_{all} values using the proposed procedure and the measured allowable bearing capacity values for seven different footings (as summarized in Table 4.6, Table 4.7 and Table 4.8) in sandy soils under both saturated and unsaturated conditions.

4.8 Discussion of Results

The Eq. [4.6] and Eq. [4.7] provide good comparisons between the estimated cone resistance, q_c values and the measured values as presented in Table 4.7 and Table 4.8. The ratio between the estimated and measured bearing capacity of the six different footings at different sites is 92 %. In some cases, the estimated bearing capacity values are slightly lower than the measured bearing capacity values.

The contribution of matric suction to the bearing capacity of the tested sand can be clearly seen in the trends shown in Figure 4.18. The bearing capacity obtained from in-situ from PLTs of 0.2 m × 0.2 m (i.e., conducted for this research) increased linearly in

the low matric suction range. The rate of increase is non-linear for matric suction values greater than 2.5 kPa (which is approximately the value of the air-entry value of the sand as shown in Figure 4.12). This observation is consistent with the behaviour of unsaturated sands as well as the conclusions drawn by Vanapalli et al. (1996) with respect to the shear strength behaviour of unsaturated soils. Surface and embedded model footings of 0.1 m × 0.1 m and 0.15 m × 0.15 m tested by Mohamed and Vanapalli (2006) in saturated and unsaturated compacted sand in a controlled laboratory environment have shown similar trends in the bearing capacity behaviour.

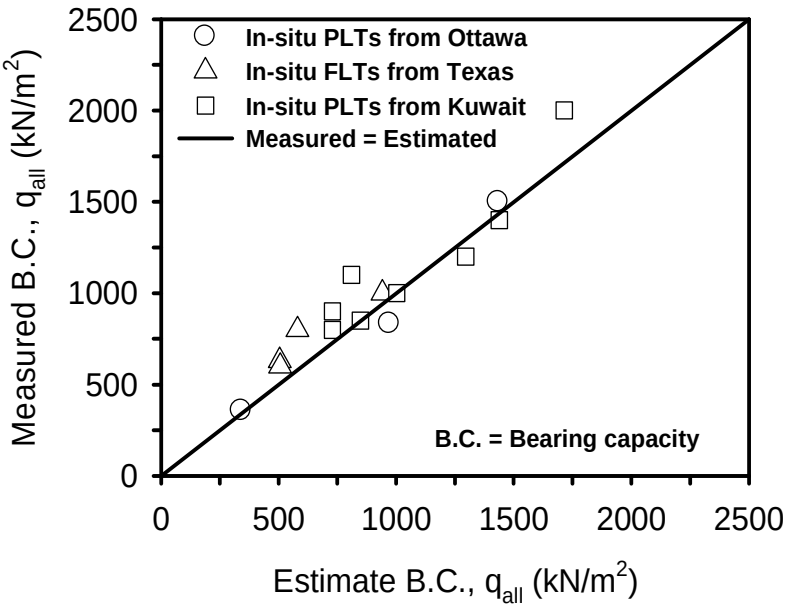

Figure 4.20 Comparison between the estimated and the measured allowable bearing capacity values in both saturated and unsaturated sands for seven different footings from both laboratory and field

Figure 4.20 provides comparisons between the estimated allowable bearing capacity from the proposed relationships and the measured values from in-situ PLTs and FLTs tested using Eq. [4.6] for saturated sands and Eq. [4.7] for unsaturated sand conditions. These two empirical equations are function of the footing, *B* and the average corrected N_{SPT}-value (i.e., N_{60}) in the influence zone of 1.5*B* from the footing base level. It is observed

that the larger the width, *B* the larger would be the influence zone, IZ which leads to the elimination of the scale effect on the estimated bearing capacity values. The results (i.e., plotted in Figure 4.20) show reasonably good comparison between the estimated and measured allowable bearing capacity values.

4.9 Summary and Conclusions

The bearing capacity of shallow foundations can be estimated from in-situ PLTs, CPTs or SPTs. The influence of matric suction on the bearing capacity of sands is usually ignored in conventional geotechnical engineering practice. Several SPTs and PLTs were conducted at Carp region in Ottawa, Canada to demonstrate the influence of matric suction on the bearing capacity of sand. Based on the analyses of the field and laboratory results, simple relationships are proposed to estimate the allowable bearing capacity of footings in both saturated and unsaturated sands.

The proposed relationships were tested for their validity using the in-situ SPTs, PLTs and FLTs data available in the literature (Giddens and Briaud 1994, and Nabil 1985). Reasonable comparisons were observed between the estimated and measured bearing capacity values. The study presented in this chapter is of interest for the practicing engineers to extend our understanding of the mechanics of unsaturated soils in the design of shallow foundations, which is more applicable for arid and semi-arid regions.

4.10 References

Aggour, M. S. and Radding, W. R. (2001). "Standard Penetration Test (SPT) Correction." Research report (Contract No: SP007B48), Maryland Department of Transportation State Highway Administration, 1.1 - 7.1.

Arman, A., Samtani, N., Castelli, R. and Munfakh, G. (1997). "Geotechnical and Foundation Engineering Module 1 – Subsurface Investigations." FHWA-HI-97-021, 305.

ASTM, D1586-11. “Standard test method for standard penetration test (SPT) and split-barrel sampling of soils.” In Annual Book of ASTM Standards, American Society of Testing Material.

ASTM, D6066-96. “Standard practice for determination the normalized penetration resistance of sands for evaluation of liquefaction potential.” In Annual Book of ASTM Standards, American Society of Testing Material.

ASTM, D2216-98. “Standard test method for laboratory determination of water (moisture) content of soil and rock by mass.” In Annual Book of ASTM Standards, American Society of Testing Material.

Bolton, M. D. and Lau, C. K. (1993). “Vertical bearing capacity factors for circular footings on Mohr-Coulomb soil.” Canadian Geotechnical Journal, (30), 1024-1033.

Bowles, J. E. (1996). “Foundation analysis and design.” 5th Edition, The McGraw-Hill Companies, Inc., New York.

Burland, J. B. and Burbidge, M. C. (1985). “Settlement of foundations on sand and gravel.” Proceedings of the Institution of Civil Engineers, Part I, 78(6): 1325-1381.

Canadian Foundation Engineering Manual, CFEM (4th Edition). (2006). Canadian Geotechnical Society.

Carter M. and Bentley, S. P. (1991). “Correlations of Soil Properties.” London, Pentech Press Publishers, London, 130.

Chen, F. H. (1999). “Soil engineering, testing, design and remediation.” CRC Press, LCC. N.W. Boca Baton, Florida, USA.

Costa, Y. D., Cintra, J. C. and Zornberg, J. C. (2003). “Influence of matric suction on the results of plate load tests performed on a lateritic soil deposit.” Geotechnical Testing Journal, 2(2): 219-226.

Danziger, F. A. B., Politano, C. F. and Danziger, B. R. (1998). “CPT-SPT correlations for

some Brazilian residual soils." In Robertson and Mayne (eds), Geotechnical Site Characterization, Rotterdam: Balkema: 907-912.

Das, B. M. (2007). "Principles of foundation engineering." 6th Edition, Publisher, Chris Carson, USA.

De Alencar, V. D. (1959). "O ensaio de diepsondeering e a determinacao da capacidade de cargo do solo." Rodovia, 29.

Eslaamizaad, S., and Robertson, P. K. (1996). "Cone penetration test to evaluate bearing capacity of foundation in sands." Proceedings of the 49th Canadian Geotechnical Conference. St. John's, Newfoundland. September, 429-438.

Eslami, A. and Gholami, M. (2006). "Analytical model for the ultimate bearing capacity of foundations from cone resistance." Scientia Iranica (13), 223-233.

Giddens, R. and Briaud, J. (1994). "Load tests on five large spread footings on sand and evaluation of prediction methods." Federal Highway Administration Department of Civil Engineering, A&M University, TX., USA.

Hatanaka, M. and Uchida, A. (1996). "Empirical correlation between cone resistance and internal friction angle of sandy soils." Soils and Foundations, 36(4), 1-10.

Kara, A. and Gündüz (2010). "Correlation between CPT and SPT in Adapazari, Turkey." 2nd International Symposium on Cone Penetration Testing, Huntington Beach, Carlifonia, USA.

Lawrence, A. L. (1968). "Theoretical bearing capacity of very shallow footings." Journal of the Soil Mechanics and Foundations Division, ASCE, 94(SM6), 1347-1357.

Lee, J. H. and Salgado, R. (2006). "Application of CPT cone resistance for footing bearing capacity estimation." Proceedings of the Geo-Shanghai International Conference, Shanghai, China.

McGregor, J. A. and Duncan, J. M. (1998). Performance and Use of the Standard Penetration Test in Geotechnical Engineering Practice. Center for Geotechnical Practice and Research, Virginia Tech.

Meigh, A. C. and Nixon, I. K. (1961). "Comparison of in-situ tests of granular soils." Proceedings of 5th International Conference on Soil Mechanics and Foundation Engineering. Paris, France, 1, pp., 499.

Meyerhof, G. G. (1951). "The ultimate bearing capacity of foundations." Géotechnique, (2), 301-332.

Meyerhof, G. G. (1956). "Penetration tests and bearing capacity of cohesionless soils." Proceedings of ASCE, 82(SM1), 1-19.

Mitchell, J. K. (2000). "Education in geotechnical engineering: Its evolution, current status and challenges for the 21st century", XI PCSMGE, Foz do Iguacu, Brazil, 4, 167-174.

Mohamed, F. M. O. and Vanapalli, S. K. (2006). "Laboratory investigations for the measurement of the bearing capacity of an unsaturated coarse-grained soil." In Proceedings of the 59th Canadian Geotechnical Conference, Vancouver, B.C., 1 - 4 October 2006. Canadian Geotechnical Society, Richmond, BC, 219-216.

Mohamed, F. M. O., Vanapalli, S. K. and Saatcioglu, M. (2010). "Comparison of bearing capacity of unsaturated sands using cone penetration tests (CPT) and plate load tests (PLT)", Unsaturated Soils, Edited by Antonio Gens, CRS Press 2010, 1183-1188.

Motazedian, D., Hunter, J.A., Belvaux, M., Sivathayalan, S., Pugin, A., Chouinard, L., Khaheshi Banab, K., Crow, H. L., Tremblay, M., Perret, D. and Rosset, Ph. (2010). "Seismic Microzonation of Montreal and Ottawa, Canada, In proceedings 10th Canadian AND 9th US National Conference of Earthquake Engineering, Toronto.

Nabil, I. F. (1985). "Allowable pressure from loading tests on Kuwaiti soils." Canadian Geotechnical Journal, (22), 151-157.

Oh, W. T. and Vanapalli, S. K. (2013). “Scale effects of plate load tests in unsaturated soils. International Journal of GEOMAT, Vol. 4, No. 2 (Sl. No. 8): 585-594.

Parry, R. H. G. (1971). “A Direct Method of Estimating Settlements in Sands from SPT Values”, Symposium on Interaction of Structure and Foundation, Foundation Engineering Society, Birmingham.

Peck, R. B., and Bazaraa, A.R.S. (1967). “Settlement of Spread Footings from SPT Values”, Proceedings, Symposium on Interaction of Structure and Foundation, Foundation Engineering Society, Birmingham, 905-909.

Poulos, H. G., and Davis, E. H. (1974). Elastic solutions for soil and rock mechanics, John Wiley and Sons, New York.

Prandtl, L. (1921). “Über die Eindringungsfestigkeit (Härte) plastischer Baustoffe und die Festigkeit von Schneiden.” (On the penetrating strengths (hardness) of plastic construction materials and the strength of cutting edges), Zeit. Angew. Math. Mech., 1(1), 15-20.

Reissner, H. (1924). “Zum erddruckproblem.” Proceeding of the 1st International Congress of Applied Mechanics, Delft, The Netherlands, 295–311.

Robertson, P. K., Campanella, R. G. and Wightman, A. (1983). “SPT-CPT correlation.” Journal of Geotechnical Engineering, 109(11), 1449-1459.

Rojas, J. C., Salinas, L. M. and Seja, C. (2007). “Plate-load tests on an unsaturated lean clay.” In Proceedings of the 2nd International Conference on Unsaturated Soils, Weimar, 445-452.

Schmertmann, J. H. (1970). “Static cone to compute static settlement over sand”, In ASCE, Journal of the Soil Mechanics and Foundations Division, 96(3), 1011-1043.

Schnaid, F., Consoli, N. C., Cumdani, R. and Milititsky, J. (1995). “Load-settlement response of shallow foundations in structured unsaturated soils”. Proceedings of the

1st International Conference on Unsaturated Soils, Paris, 999-1004.

Seed, H. B., Tokimatsu, K., Harder, L. F. and Chung, R. M. (1985). "Influence of SPT procedures in soil liquefaction resistance evaluations." Journal of the Geotechnical Engineering Division, ASCE, 111(12), 1425-1445.

Steensen-Bach, J. O., Foged, N., and Steenfelt, J. S. (1987). "Capillary induced stresses – fact or fiction?." In Proceedings of the 9th European Conference on Soil Mechanics and Foundation Engineering, Dublin, Ireland, A.A. Balkema, Rotterdam, the Netherlands, 83-89.

Terzaghi, K. (1943). "Theoretical soil mechanics." John Wiley and Sons, New York.

Terzaghi, K. and Peck, R. B. (1948). "Soil Mechanics in Engineering Practice." Asia Publishing House.

Vanapalli, S. K., and Mohamed, F. M. O. (2007). "Bearing capacity of model footings in unsaturated soils." In Experimental Unsaturated Soil Mechanics, Springer-Verlag, Berlin Heidelberg, Germany, 483-493.

Vanapalli, S. K., Fredlund, D. G., Pufahl, D. E. and Clifton, A. W. (1996). "Model for the prediction of shear strength with respect to soil suction." Canadian Geotechnical Journal, 33(3), 379-392.

Vesic, A. B. 1973. Analysis of ultimate loads of shallow foundations. Journal of the Soil Mechanics and Foundations Division, ASCE, 99(1), 45 – 73.

CHAPTER 5

[4]GENERALIZED SCHMERTMANN EQUATION FOR SETTLEMENT ESTIMATION OF SHALLOW FOOTINGS IN SATURATED AND UNSATURATED SANDS

5.1 Introduction

Shallow foundations such as isolated footings are preferred for light and low-rise buildings in comparison to deep foundations where relatively favourable soils are available. The performance of the shallow foundations is generally satisfactory in sandy soils and is less expensive in comparison to deep foundations (Briaud 1992). In the case of bridges where the cost of the foundation is often high, it is possible to save 50 % of the foundation cost, if spread footings are used instead of conventional deep foundations such as piles (Briaud 2007). The main function of the shallow foundations is to transfer the loads from the superstructure to the supporting soil with an adequate factor of safety against bearing capacity failure. In addition, the footings settlement should be lower than an allowable value, which is typically recommended as 25 mm for sands (Terzaghi and Peck 1967).

In most cases of shallow foundations design, it is the settlement that is the governing parameter rather than the bearing capacity, particularly for sands. The settlements of footings in sands are typically estimated from in-situ tests such as plate load tests (PLTs),

[4]This chapter is developed by extending a paper that was published in the International Journal of Geomechanics and Engineering 2013.

standard penetration tests (SPTs), or cone penetration tests (CPTs) without considering the influence of matric suction (i.e., capillary stresses) in the soil. The empirical correlations using the CPT results are more commonly used as a tool in the estimation of settlement of shallow footings in sands in engineering practice (Robertson 2009). A number of empirical equations are available in the literature that can be used for the estimation of the settlement of footings in sands using the CPTs results (for example, Meyerhof 1956, DeBeer 1965, Schmertmann et al. 1978, and Mayne and Illingworth 2010). Schmertmann et al. 1978 method used the same correlation factor to relate the cone resistance, q_c to the modulus of elasticity, E_s of soils. The settlement 1994 prediction session held in Texas clearly demonstrated the deficiencies in the present settlement prediction or estimation methods which generally overestimate the settlements making the foundation designs excessively conservative (Das and Sivakugan 2007).

The conventional methods are particularly conservative for unsaturated sands as they do not take account of the influence of matric suction while estimating settlements of shallow footings. Several researchers have used calibration chambers with flexible walls using either dry or saturated soils (Schmertmann 1976, Bellotti et al. 1982, Houlsby and Hitchman 1988, Iwasaki et al. 1988, Parkin 1988, Schnaid and Houlsby 1991, Tan 2005 and Others). A calibration chamber with rigid walls has also been used by Salgado et al. (1998) using saturated sand. Hryciw and Dowding (1987) conducted a series of CPTs in partially saturated sands and found that the capillary tensions (i.e., matric suction) significantly increase the penetration resistance higher than in that of saturated or dry condition. Miller et al. (2002), more recently Pournaghiazar et al. (2011) and Pournaghiazar et al. (2012) used a new calibration chamber to perform CPTs in unsaturated soils where matric suction values are controlled and demonstrated that the measured penetration resistances were influenced by the capillary stresses. They also suggested that the measured cone penetration values obtained in the chamber can be related to the equivalent field values to be used in practice. In addition, several researchers carried out investigations on the bearing capacity of unsaturated soils (Broms 1963, Steensen-Bach et al. 1987, Schnaid et al. 1995, Oloo et al. 1997, Miller and Muraleetharan 1998, Costa et al. 2003, Mohamed and Vanapalli 2006, and Rojas et al.

2007). All these investigations have shown a significant contribution of matric suction to increase of the bearing capacity of unsaturated soils. Recent studies also show that matric suction within the stress bulb region of a footing significantly influences the settlement behaviour of footings that are located above the groundwater level (Vanapalli 2009, and Oh and Vanapalli 2011).

Simple relationships are proposed in this chapter by modifying the Schmertmann's equation for settlement estimations of footings (i.e., $B/L \approx 1$) carrying vertical loads in saturated and unsaturated sandy soils. The modified method is developed using model plate load tests (PLTs) and cone penetration tests (CPTs) results conducted in a controlled laboratory environment. Seven in-situ full-scale footings tested under both saturated and unsaturated conditions in sands were used to validate the proposed technique. The results of the study are encouraging as they provide reliable estimates of the settlement of shallow footings in both saturated and unsaturated sands using the conventional CPT results.

5.2 Properties of the Tested Material

The properties of the sand used in the present study are summarized in Table 5.1. The grain-size distribution and the SWCC of the sand are shown in Figure 5.1. The tested soil is classified according to Unified Soil Classification System, *USCS* as poorly graded sand (fine sand).

Table 5. 1 Parameters and properties of the tested soil

Parameter or soil properties	Value
Specific gravity, G_s	2.64
Average dry unit weight, γ_d , kN/m³	16.02
Min. dry unit weight, $\gamma_{d\,(min)}$, kN/m³	14.23
Max. dry unit weight, $\gamma_{d\,(max)}$, kN/m³	17.25
Average relative density, D_r %	65.0
Optimum water content, *o.w.c*, % (*Standard Proctor Test*)	14.6
Void ratio, *e* (*after compaction*)	0.62 – 0.64
Effective cohesion, *c'* , kN/m^2 (*Drained Condition*)	0.6
Effective peak internal friction angle, ϕ' (°) (*Drained Condition*)	35.3

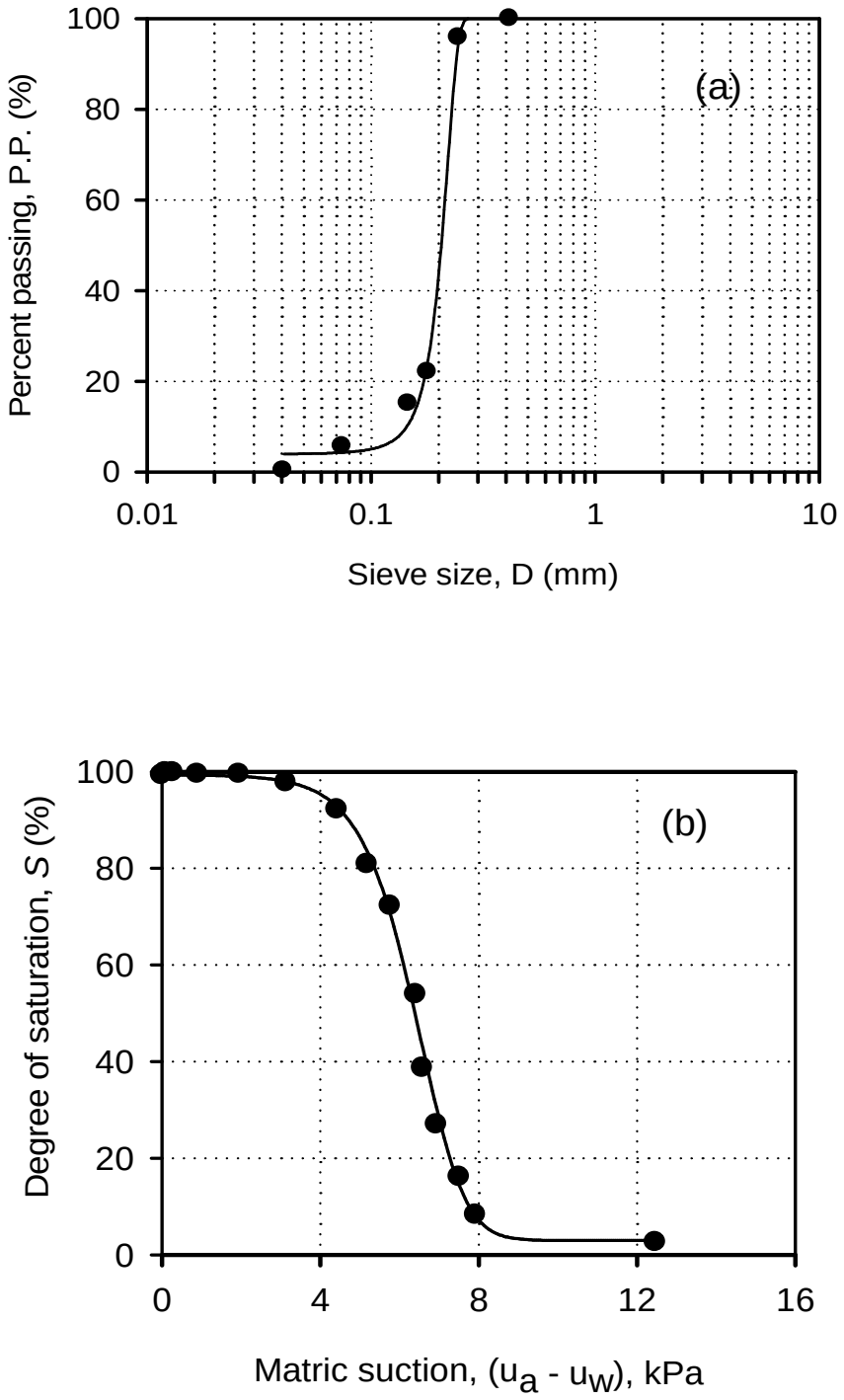

Figure 5.1 (a) The grain-size distribution of the tested sand; (b) The soil-water characteristic curve (SWCC) of the tested sand

5.3 Test Equipment

5.3.1 Test Tank (UOBCE-2006)

Mohamed and Vanapalli (2006) designed equipment (UOBCE-2006; the University of Ottawa Bearing Capacity Equipment) as illustrated in Figure 5.2. Two model footing of 100 mm × 100 mm and 150 mm × 150 mm (i.e., footings on sand) to determine the applied stress versus settlement response in a controlled laboratory environment. The test of the UOBCE-2006 was used to provide confinement to the compacted sand. It also has a system for saturating and de-saturating the soil as desired. These provisions allow conducting different test scenarios of saturated (matric suction = 0 kPa) and unsaturated (matric suction = 1 to 6 kPa) conditions in the test tank. The equipment consists of a rigid-steel tank of 900 mm (length) × 900 mm (width) × 750 mm (depth). The test tank can hold up to 1.2 tons of a compacted sandy soil. The sand in the test tank was compacted manually using a 5-kg flat steel-plate. The optimum water content value of 14.6 % determined from Standard Proctor test was simulated in the test tank to achieve an average dry density of 16 kN/m^3 approximately. Linear Variable Displacement Transducer (LVDT) was attached to the vertical loading arm and the tip of the LVDT was placed directly on the surface of the model footing to measure the settlement, δ as the load is being applied. A load cell (LC) capable of measuring 15 kN was mounted on the loading arm to measure the load being applied. Both the LVDT and the LC were connected to a data acquisition system (DAQS) to monitor and record data during testing (i.e., the DAQS is compatible with LabView software) and a computer. The model footing tests were carried out under different average matric suction values in the stress bulb region (i.e., 1.5*B*) of each model footing (i.e., 0 kPa, 2 kPa, 4 kPa and 6 kPa where the water table was located at 150 mm, 200 mm, 350 mm and 600 mm respectively).

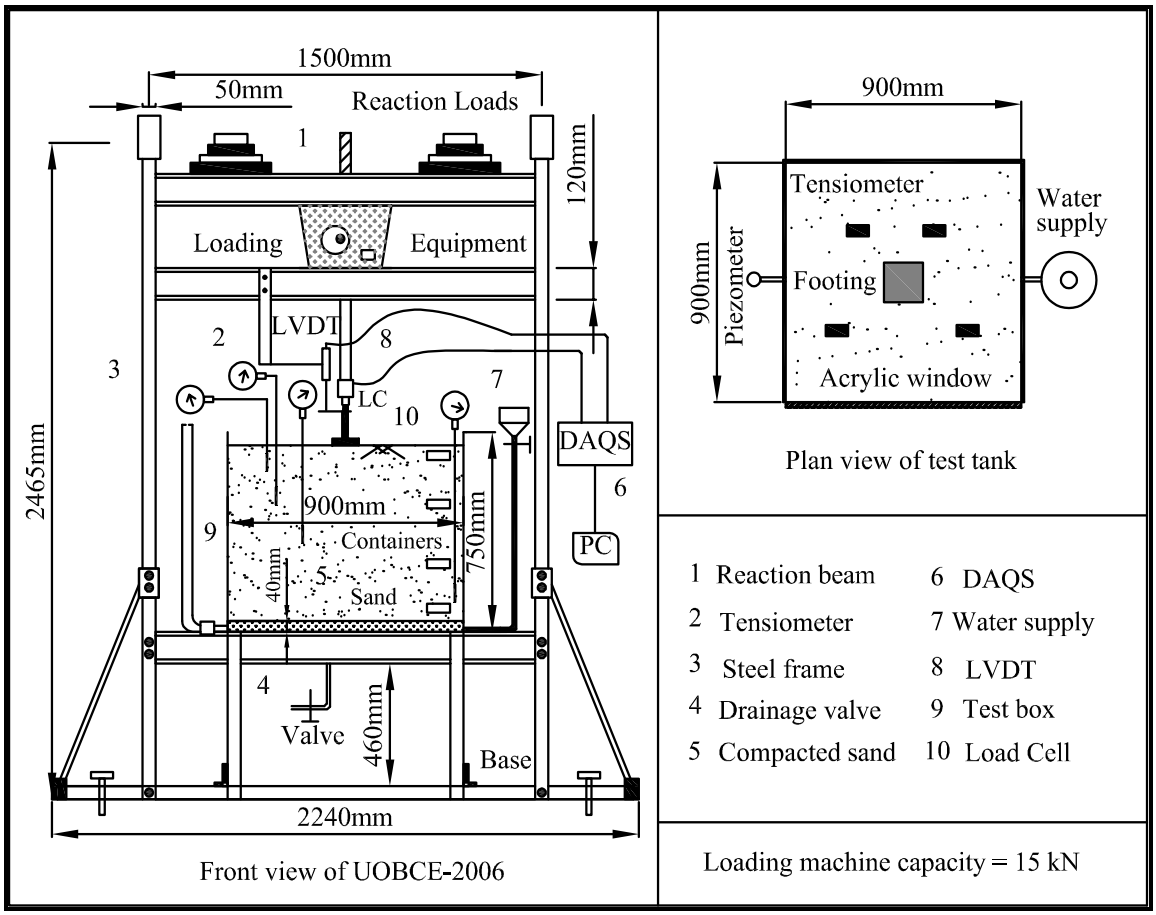

Figure 5.2 Schematic to illustrate the details of the UOBCE-2006

5.3.2 Test Tank (UOBCE-2011)

This equipment has twice the loading capacity of the UOBCE-2006 described in section 5.2. The equipment (i.e., UOBCE-2011; a schematic of the equipment is shown in Figure 5.3) consists of a rigid-steel frame made of rectangular sections with a thickness of 6 mm and a test tank of 1500 mm (length) × 1200 mm (width) × 1060 mm (depth). The test tank can hold up to 3 tons of a compacted sand. The sand in the test tank was compacted to achieve similar compaction properties as in the UOBCE-2006 test tank (i.e., optimum water content ~ 14.6 % and an average dry density of 16.02 kN/m3). The capacity of the loading machine (i.e., Model 244-Hydraulic Actuator with a maximum stroke length of 270 mm connected to MTS controller) is 28.5 kN. The built-in Linear Variable

Displacement Transducer (LVDT) and the load cell (LC) were directly connected to the data acquisition system (DAQS) and a computer. The sectional view of the UOBCE-2011 test tank is shown in Figure 5.4.

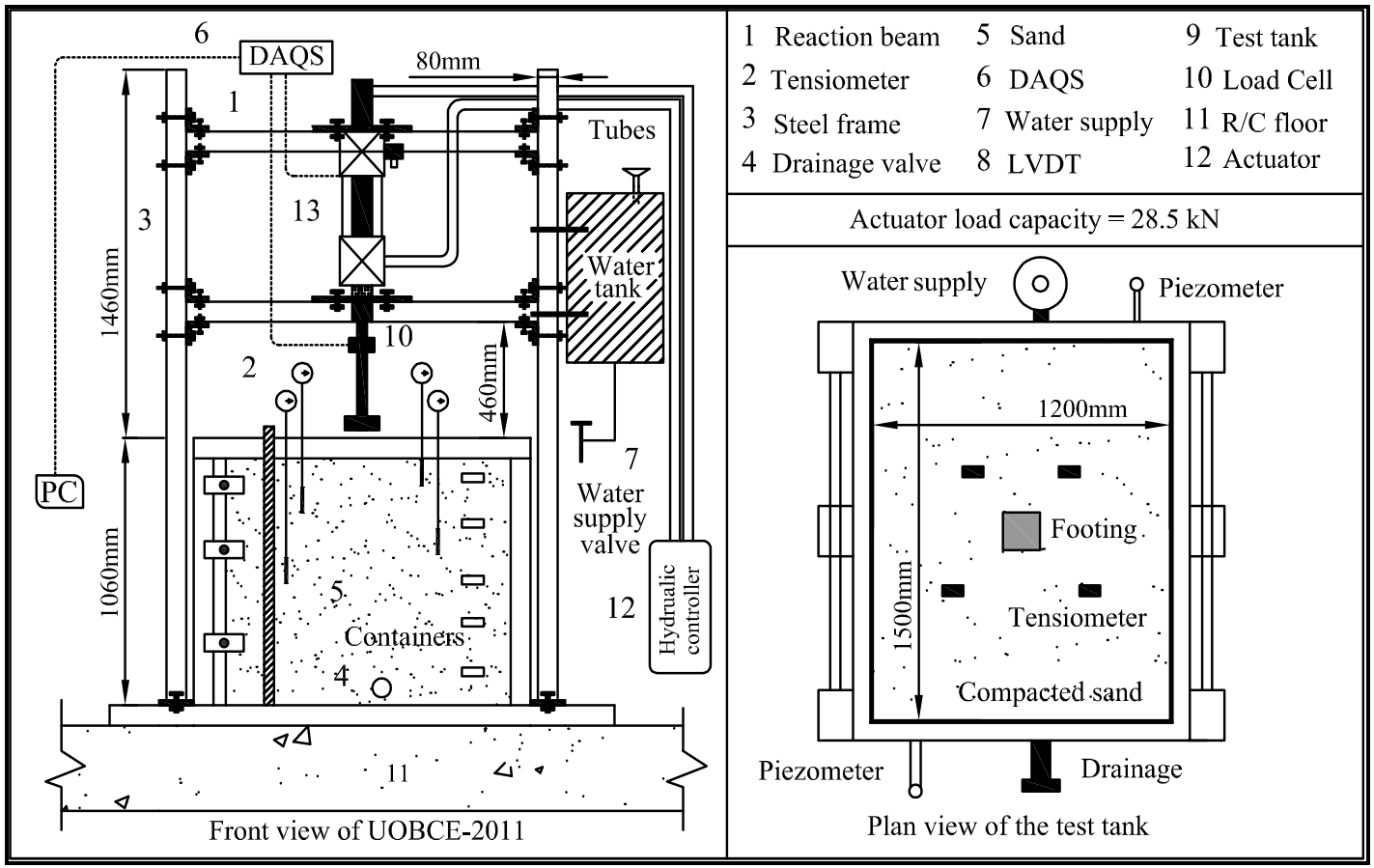

Figure 5.3 Schematic to illustrate the details of the UOBCE-2011

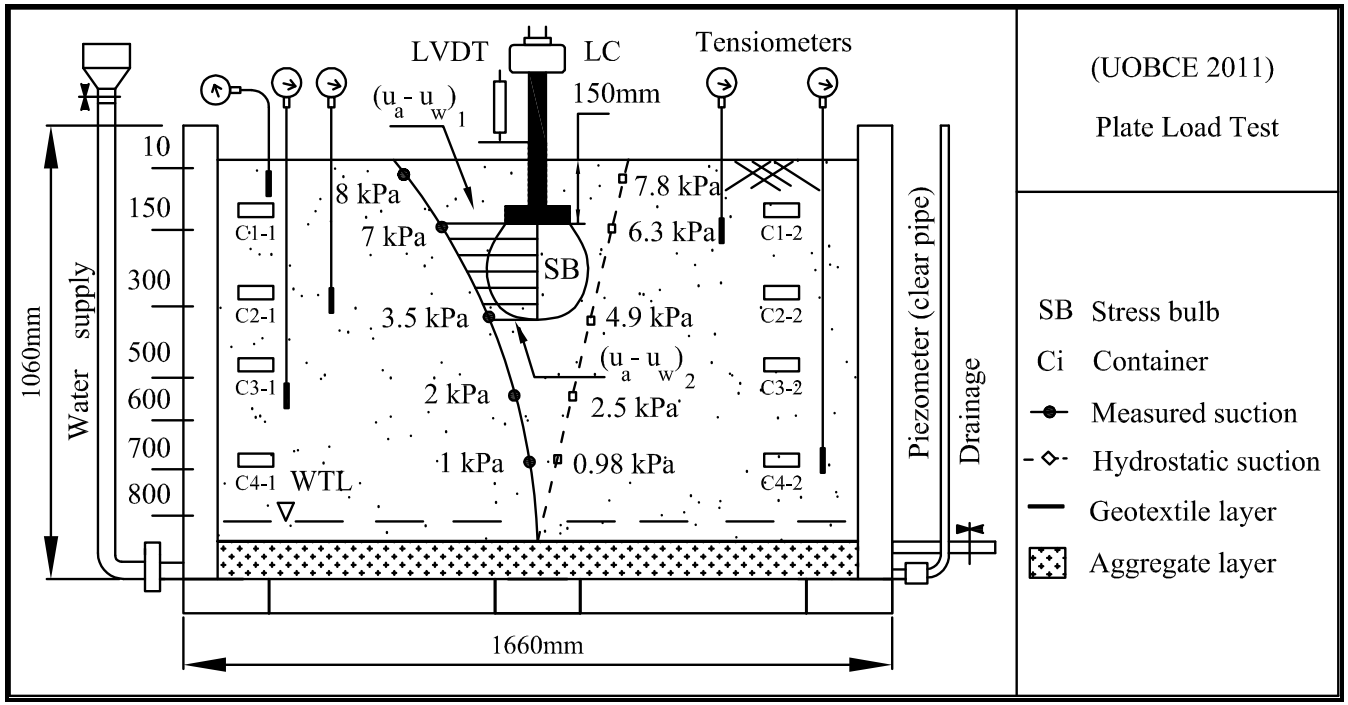

Figure 5.4 Sectional view of the test tank of the UOBCE-2011 illustrating the variation of average suction of 6 kPa in the stress bulb zone of embedded PLTs

5.4 Laboratory Model Footing Tests

5.4.1 Surface and Embedded PLTs under Saturated Condition

The water table was slowly raised from the base of the test tank (UOBCE-2006 and UOBCE-2011) through a 50 mm aggregate layer that was covered by a thin layer of a geotextile to prevent the sand from being washed out through the aggregate during desaturation process (see Figure 5.5). This technique ensured escape of air from bottom to the surface layers of the soil in the test tank to ensure saturated condition (i.e., $(u_a - u_w)$ = 0 kPa). The adjustments of the water level in the test tank were inspected periodically using the piezometers (i.e., transparent plastic tubes attached to the test tank as in Figs. 2, 3 and 4). The water supply valve was closed once the water level reached the soil surface in the test tank. The applied stress and the settlement of the saturated soil were measured (for 100 mm × 100 mm and 150 mm × 150 mm PLTs) during the gradually loading process of the model footings at a constant rate of 1.2 mm/min assuming drained condition. All Tensiometers in the test tank (as shown in Figures 5.5 and 5.6) indicated zero matric suction values after saturation and during the testing period.

5.4.2 Surface and Embedded PLTs under Unsaturated Condition

The soil in the tank was first saturated as detailed in the previous section. The water table was then lowered down slowly (using drainage valves shown in Figures 5.4 and 5.5) to different levels of depth from the soil surface to achieve different suction values as desired. Equilibrium conditions with respect to matric suction value in the stress bulb zone (i.e., depth of 1.5*B*) were typically achieved in a time period of 24 to 48 hours.

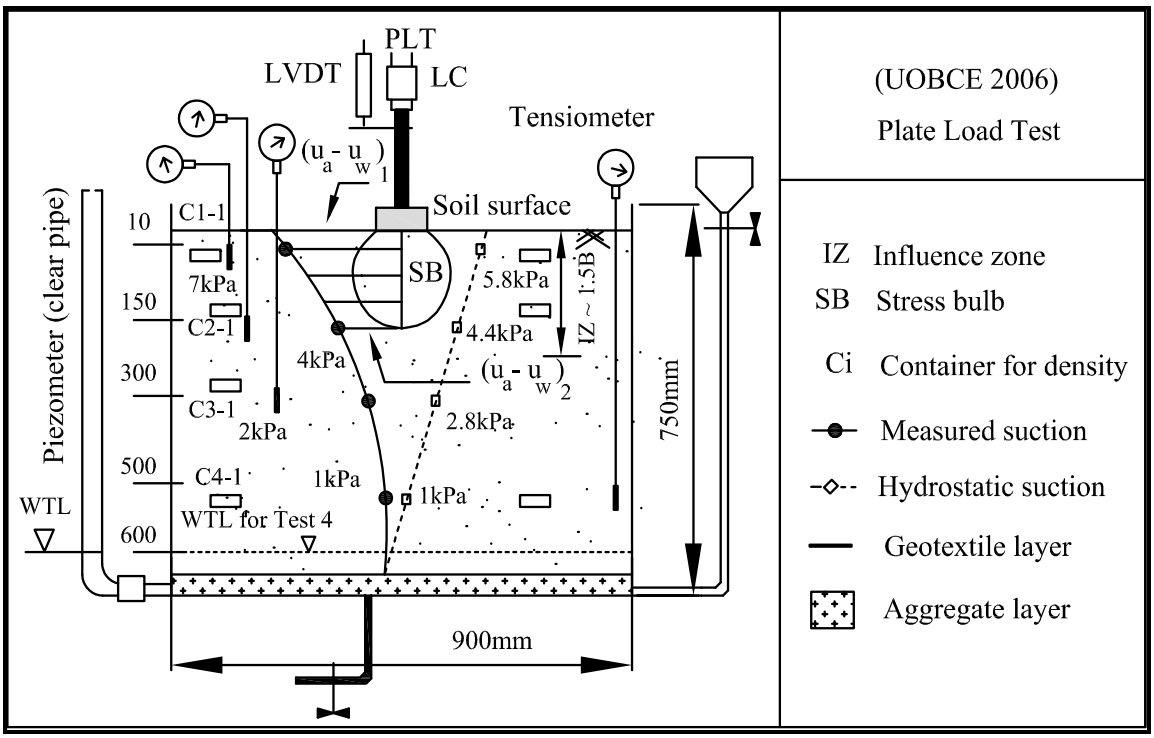

Figure 5.5 Sectional view of the test tank of the UOBCE-2006 illustrating the variation of average suction of 6 kPa in the stress bulb zone of a surface PLTs

As reported by Poulos and Davis (1974), Steensen-Bach (1987), and Agarwal & Rana (1987) the zone of depth in which the stresses due to loading are predominant is 1.5*B*. The applied stress and the settlement were measured during the tests under different average matric suction values (i.e., 2 kPa, 4 kPa and 6 kPa in the 1.5*B* region). While the matric suction values were measured using the Tensiometers, the gravimetric water contents at equilibrium conditions were determined approximately at the same levels where soil specimens were collected in small aluminum cups with perforations that were embedded inside the compacted sand prior to conducting the tests. These cups were placed within the proximity of the model footing (PLT). Figures 5.4 and 5.5 show the cross-section of the test tank in a schematic form and provides the details of the placement of Tensiometers and the aluminum cups of 15 mm (height) × 40 mm (diameter) at different depths (labeled as C1-1, C2-1, C3-1 and C4-1 …etc). Figure 5.5 also shows the variation of suction (i.e., measured and hydrostatic matric suction profiles) with respect to depth in the test tank. Table 5.2 summarizes the data set of results in which the average matric suction value in the stress bulb zone was 6 kPa (achieved by placing the water table at a depth of 600 mm).

Table 5.2 Typical data from the test tank for an average matric suction of 6 kPa in the stress bulb zone (i.e., 1.5*B*) (100 mm × 100 mm) surface model footing using UOBCE-2006

Parameter or Property					
[1]D (mm)	[2]γ_t	[3]γ_d (kN/m^3)	[4]w (%)	[5]S (%)	[6]$(u_a - u_w)_{AVR}$ (kPa)
10	18.17	15.94	14.0	58	6.0
150	18.75	15.85	18.3	76	4.0
300	19.27	16.07	20.0	86	2.0
500	19.40	15.77	23.0	94	1.0
600	19.74	15.95	23.8	100	0

[1]Depth of a Tensiometer from the soil surface; [2]total unit weight; [3]dry unit weight; [4]water content; [5]degree of saturation, [6]average matric suction in the stress bulb zone

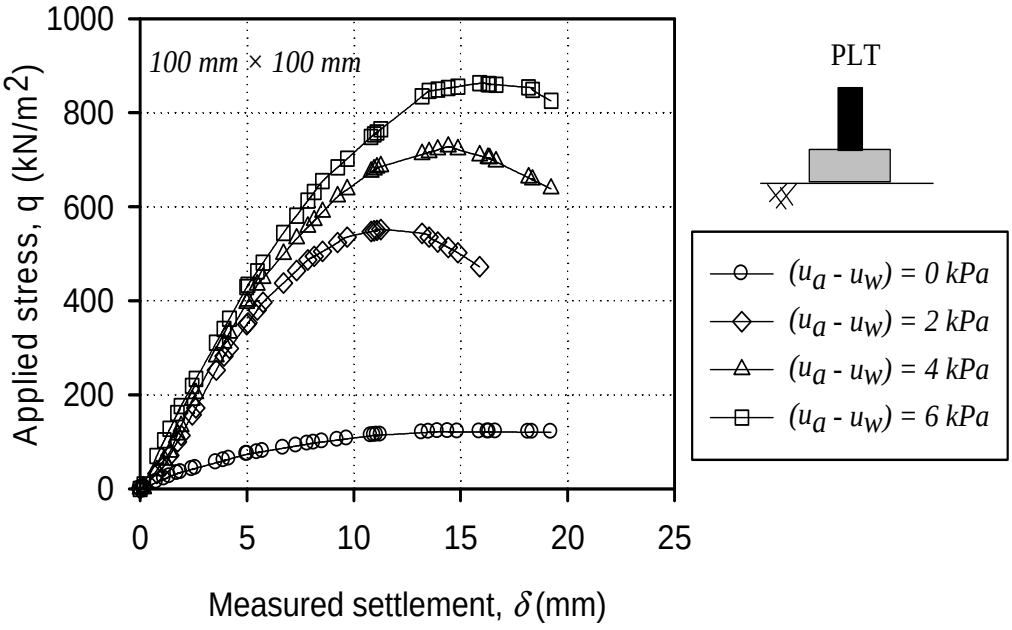

Figure 5.6 Applied stress versus settlement behaviour of surface model footing tests (PLTs) of 100 mm × 100 mm

The results of the experimental work conducted using two different model footings (i.e., surface PLTs) of 100 mm × 100 mm and 150 mm × 150 mm in the laboratory are plotted in Figure 5.6 and Figure 5.7 respectively. The stress versus settlement relationships show a dramatically increase of the applied stress, q and a decrease of the measured settlement, with an increase in the matric suction.

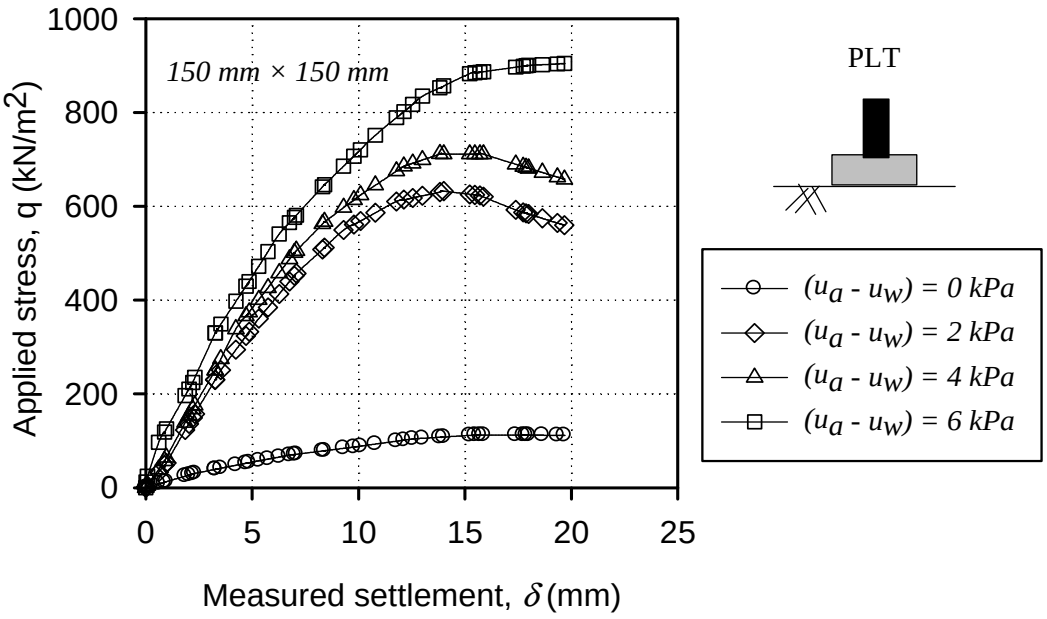

Figure 5.7 Applied stress versus settlement behaviour of surface model footing tests (PLTs) of 150 mm × 150 mm

Embedded model footing tests (PLTs) of 150 mm × 150 mm were also conducted by placing the model footing at a depth of 150 mm below the soil surface in the bearing capacity equipment, which is referred to as UOBCE-2011. Table 5.3 summarizes the data set of results in which the average matric suction value in the stress bulb zone was 6 kPa (achieved by placing the water table at a depth of 800 mm).

Table 5.3 Typical data from the test tank for an average matric suction of 6 kPa in the stress bulb zone (i.e., 1.5*B*) (150 mm × 150 mm) embedded model footing using UOBCE-2011

Parameter or Property					
[1]D (mm)	[2]γ_t	[3]γ_d (kN/m^3)	[4]w (%)	[5]S (%)	[6]$(u_a - u_w)_{AVR}$ (kPa)
12	18.16	16.20	12.1	53	8.0
150	19.00	16.24	17.0	75	7.0
355	19.20	16.13	19.0	82	5.0
500	19.50	16.12	21.0	91	2.0
700	19.74	16.03	23.1	98	1.0

[1]Depth of a Tensiometer from the soil surface; [2]total unit weight; [3]dry unit weight; [4]water content; [5]degree of saturation, [6]average matric suction in the stress bulb zone

These tests were conducted to investigate the influence of matric suction on the applied stress and settlement behaviour of footings in sands. Figure 5.8 presents the applied stress versus settlement behaviour for different tests using 150 mm × 150 mm model footing. The matric suction values (i.e., 0 kPa, 2 kPa, 4 kPa and 6 kPa) for each test represent an average value of capillary stress in the proximity of the stress bulb (i.e., 1.5*B*) of the model footing as shown in Figure 5.5.

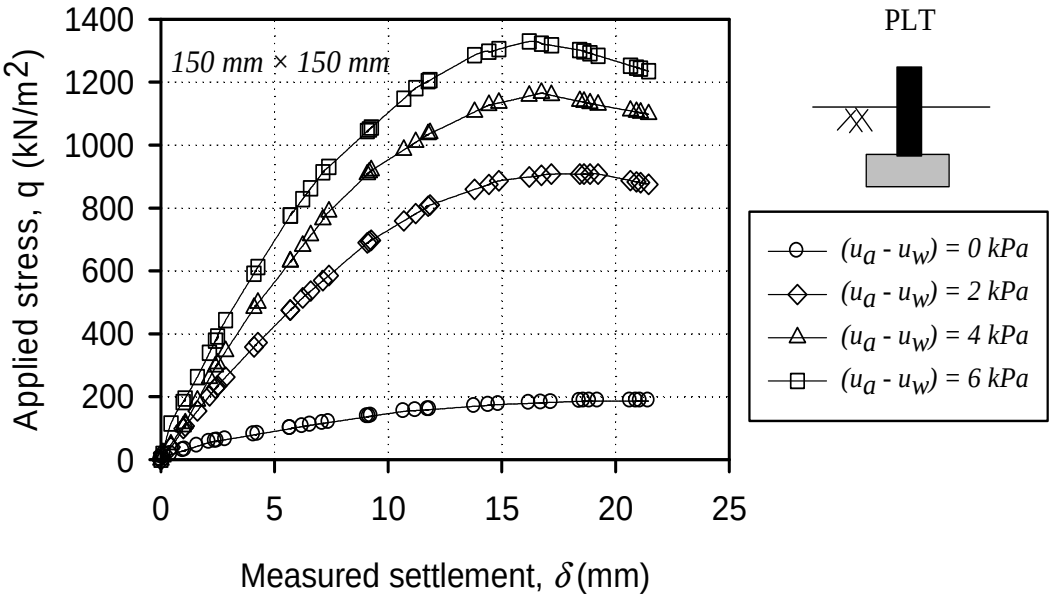

Figure 5.8 Applied stress versus settlement behaviour embedded model footing tests (PLTs) of 150 mm × 150 mm

The applied stress versus settlement relationships in Figures 5.6, 5.7, and 5.8 show that the maximum applied stress (i.e., bearing capacity) increases with an increase in matric suction of the tested sand in the range of 0 to 6 kPa. As the matric suction increases, it contributes to the component of the apparent cohesion in the shear strength of the unsaturated sand (Vanapalli et al. 1996).

5.5 Laboratory Cone Penetration Tests

In addition to the PLTs, cone penetration tests (CPTs) were also conducted in the same sand previously used for PLTs (more details of CPTs are presented in chapter 3). The UOBCE-2006 was modified (see Figure 5.9) and a cone penetrometer was designed. The cone penetrometer has a diameter of 40 mm and apex angle of the cone was 60 °. The projected area of the cone was 1256 mm^2. A smooth shaft of 600 mm was connected to

the cone along with the loading machine. Commercial manufacturing typically use cone diameter, d_c = 35.7 mm for penetrometers. The cone resistance, q_c results (form q_c vs d profile) can be used for the estimation of settlements of different footing sizes (e.g., ~ 150 mm × 150 mm to ~ 3000 mm × 3000 mm). Lunne et al. (1997) stated that "cone penetrometers with diameters differing from the standard 35.7 mm are quite frequently used". The ASTM-D 5778 standard suggests using cone penetrometer sizes in the range of 35.7 mm to 43.7 mm. These guidelines satisfying the researchers and 40 mm diameter cone is used in the present study. The size of the test tank was large enough for conducting the CPTs using a cone penetrometer of 40 mm in diameter with negligible size effects (width of test tank/diameter of cone ≈ 23).

A long stroke Linear Variable Displacement Transducer (LVDT) which can measure up to 500 mm was connected with the cone penetrometer to measure the penetration depth. A series of CPTs conducted on the compacted sand (i.e., the same sand used for the PLTs with D_r of 65 %) in the UOBCE-2006 under saturated and unsaturated sand conditions as shown in Figure 5.9.

The cone penetrometer was pushed through the sand at a constant rate of 1.2 mm/min. The saturated coefficient of permeability of sand is relatively high and the penetration rate used (1.2 mm/min) is relatively slow enough to assure no increase in exces pore-water pressure (in other words $q_t = q_c$). Iwasaki et al. (1988) performed CPT at 2 mm/sec to assure fully drained condition of Toyoura sand. Robertson and Cabal (2010) suggest that q_c may be assumed to be equal to q_t for sandy soils.

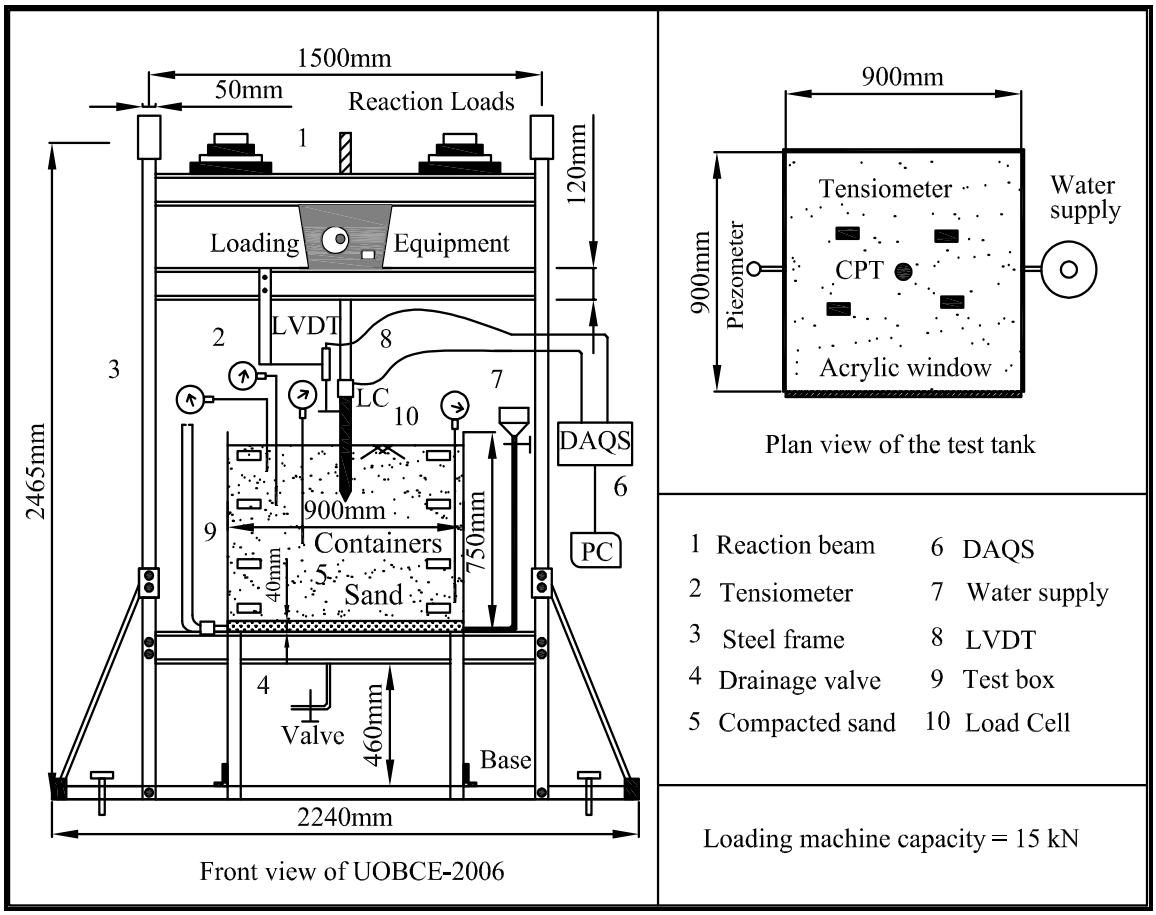

Figure 5.9 Schematic to illustrate the details of the UOBCE-2006 used for conducting CPTs

The sand in the test tank was manually compacted prior to testing as discussed earlier in section 5.3. The first series of tests (i.e., CPTs) was carried out under saturated condition (i.e., water level in the test tank was at the soil surface and the matric suction = 0 kPa) and the second series of tests was conducted under unsaturated conditions. Poulos and Davis (1974), Steensen-Bach et al. (1987), and Agarwal and Rana (1987) reported that the zone of depth in which the stresses due to loading are predominant is 1.5*B*. A representative value of cone resistance, q_c of each of the series of the CPTs results is taken as the average of the cone resistance in a depth of 1.5*B*.

Table 5.4 Typical data from the test tank for an average matric suction of 6 kPa in the influence zone (i.e., 1.5*B; B* = footing width) of the cone penetrometer

Parameter or Property					
[1]D (mm)	[2]γ_t	[3]γ_d (kN/m^3)	[4]w (%)	[5]S (%)	[6]$(u_a - u_w)_{AVR}$ (kPa)
10	18.17	15.94	14.0	59	6.0
150	18.76	15.85	18.3	76	4.0
300	19.20	16.07	19.5	83	2.0
500	19.30	15.77	22.5	93	1.0
600	19.74	15.95	23.8	100	0

[1]Depth of a Tensiometer from the soil surface; [2]total unit weight; [3]dry unit weight; [4]water content; [5]degree of saturation, [6]average matric suction in the stress bulb zone

Typical set of results of the CPT tests with an average matric suction of 6 kPa is summarized in Table 5.4. The experimental results of the variation of the cone resistance, q_c with penetration depth are plotted in Figure 5.10. From the measured CPTs results, the cone resistance, q_c under unsaturated conditions (average matric suction values of 1 kPa, 2 kPa and 6 kPa) found to be two to three times higher than the cone resistance of CPTs conducted in saturated condition. These results are consistent with the observations of Russell and Khalili (2006) and Pournaghiazar et al. (2011). The increase in the CPT values can be attributed to the contribution of the matric suction. The cone resistance increased as the soil condition changes from saturated (0 kPa) condition to unsaturated (1 kPa, 2 kPa and 6 kPa) conditions in the capillary zone. A summary of the sand properties along with the model plate footing tests (PLTs of 100 mm × 100 mm and 150 mm × 150 mm) and the cone penetration tests (CPTs) used in the development of the proposed technique (i.e., relationships) is presented in Tables 5.5, 5.6 and 5.7.

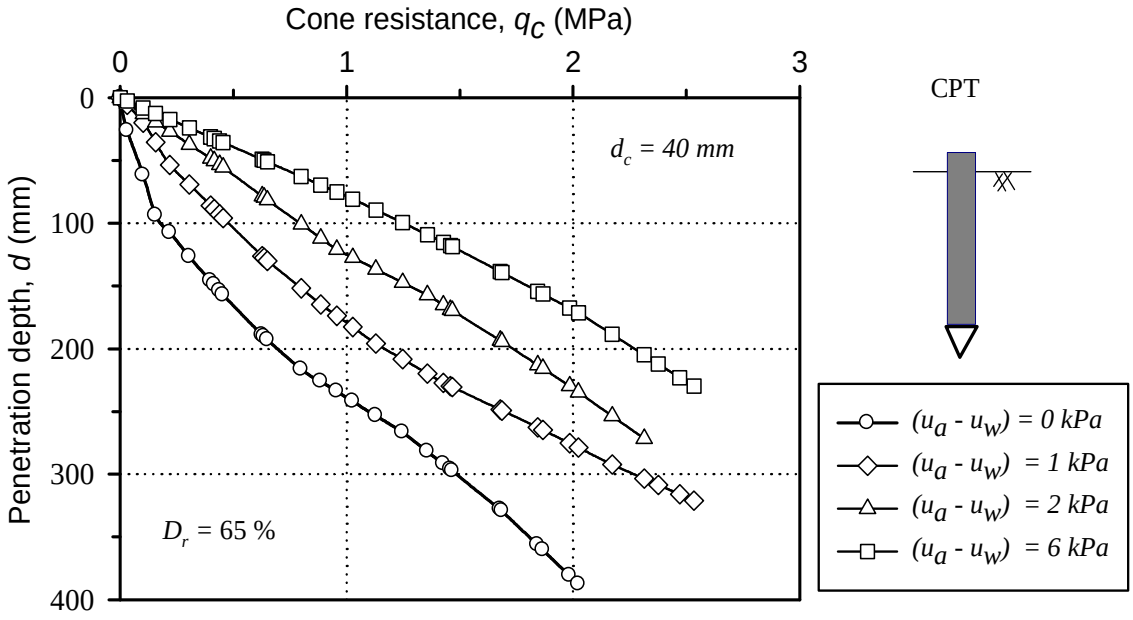

Figure 5.10 Variation of the cone resistance from CPTs with penetration depth under saturated and unsaturated sand conditions

Table 5.5 Data collected from PLTs and CPTs conducted in the laboratory using UOBCE-2006

Parameter or Property						
Soil	B (m)	[1]d (m)	Water level	[2]$(u_a - u_w)$	[3]D_r (%)	[4]$q_{c\ AVR}$
Surface model PLT from this research						
SP	0.1	0	0	0	65	118
SP	0.1	0	0.2	2.0	65	565
SP	0.1	0	0.6	6.0	65	805

[1]Depth of plate base from soil surface; [2]Measured matric suction in the test box; [3]Relative density; [4]Average cone penetration resistance (in kN/m^2) from laboratory CPTs

Table 5.6 Data collected from PLTs and CPTs conducted in the laboratory using UOBCE-2006

Parameter or Property						
Soil	B (m)	[1]d (m)	Water level	[2]$(u_a - u_w)$	[3]D_r (%)	[4]$q_{c\ AVR}$
Surface model PLT from this research						
SP	0.15	0	0	0	65	270
SP	0.15	0	0.2	2.0	65	900
SP	0.15	0	0.6	6.0	65	1235

[1]Depth of plate base from soil surface; [2]Measured matric suction in the test box; [3]Relative density; [4]Average cone penetration resistance (in kN/m^2) from laboratory CPTs

Table 5.7 Data collected from PLTs and CPTs conducted in the laboratory using UOBCE-2011

Parameter or Property						
Soil	B (m)	[1]d (m)	Water level	[2]$(u_a - u_w)$	[3]D_r (%)	[4]$q_{c\ AVR}$
Embedded model PLT from this research						
SP	0.15	0.15	0	0	65	550
SP	0.15	0.15	0.45	2.0	65	1200
SP	0.15	0.15	0.8	6.0	65	1600

[1]Depth of plate base from soil surface; [2]Measured matric suction in the test box; [3]Relative density; [4]Average cone penetration resistance (in kN/m^2) from laboratory CPTs

5.6 In-Situ Footing Load Tests and Cone Penetration Tests

5.6.1 In-Situ Footing Load Tests

Five full-scale footing load tests (FLTs of 1.0 m × 1.0 m, 1.5 m × 1.5 m, 2.5 m × 2.5 m, 3.0 m × 3.0 m (north) and 3.0 m × 3.0 m (south)) were (in a sandy soil with some silt) conducted in-situ by Giddens and Briaud (1994) were used to validate the proposed technique for estimating the settlement of footings in the present study. The footings were loaded in sand at the Texas A&M University National Geotechnical Experimentation site (see data in Table 5.8). The in-situ results of the CPT conducted close to the footing 3.0 m × 3.0 m (south), suggest the measured q_c is much lower compared to the q_c values of the other CPTs conducted close to 1.0 m × 1.0 m, 1.5 m × 1.5 m and 2.5 m × 2.5 m as well as the 3.0 m × 3.0 m at the north location of the site. Lee and Salgado (2002) also commented that the significant load underprediction resulting from the application of Schmertmann's method to the 3-m footing (south side) was due to the very low cone resistance at a depth equal to about 3 m observed in the CPT test used in the analysis. The researchers also speculated that these results may not be reflective of the true soil condition underneath the footing. Therefore, the 3.0 m × 3.0 m footing (south) and the CPT-07 in Giddens and Briaud (1994) results was not considered in this analysis. In addition to these tests, four footing load tests (0.55 m × 0.65 m, 1.1 m × 1.3 m, 1.60 m × 1.80 m, and 2.30 m × 2.50 m) results (in a sandy soil) conducted in Fittja site in Sweden by Bergdahl et al. (1985) were investigated in the present research (see data in Table 5.9). Nevertheless, the footing 1.10 m × 1.80 m was omitted in the present analysis as it showed a very low stress and large settlement because of the existence of clay lens underneath it as the focus of the present research is directed towards testing only sandy soils. The sands at both sites (i.e., National Geotechnical Experimentation site in Texas and Fittja site) are considered to be in unsaturated conditions as the groundwater table levels were at 4.9 m and 1.5 m deep respectively (from the ground surface). The sands at both sites (i.e., National Geotechnical Experimentation site in Texas and Fittja site in Sweden) are considered to be in unsaturated conditions as the groundwater table levels

were at 4.9 m and 1.5 m deep respectively (from the ground surface). The average matric suction value $(u_a - u_w)_{AVR}$ for the sand at the Texas site was assumed to be of uniform as the water content above the groundwater table was also uniform and equal to 5 %. The soil-water characteristic curve (SWCC) of Sollerod sand (Steensen-Bach et al. 1987) which has similar grain-size distribution of sand in Texas site was used to back calculate the matric suction value of the Texas site. A matric suction value of 10 kPa that corresponds to 5 % water content from the SWCC was used in the present study. The groundwater table at the Fittja site was at a shallow depth; therefore, a hydrostatic distribution was assumed and the average matric suction in the stress bulb zone was taken as 7 kPa.

5.6.2 In-Situ Cone Penetration Tests

Five cone penetration tests (CPTs) were conducted by Giddens and Briaud (1994) at Texas A&M University National Geotechnical Experimentation site near the locations of the spread footing load tests (FLTs) described earlier. The values of average cone resistance, q_c for the site was between 5400 kPa to 7500 kPa.

Table 5.8 FLTs and CPTs data summarized from the literature and used to validate the proposed technique from Giddens and Briaud (1994)

Parameter or Property						
Soil	B (m)	[1]d (m)	Water level	[2]$(u_a - u_w)$	[3]D_r (%)	[4]$q_{c\ AVR}$
Large-scale footings from Giddens and Briaud (1994)						
SP	1	0.5-1.5	4.9	~ 10	48	5400
SP	1.5	0.5-1.5	4.9	~ 10	46	6000
SP	2.5	0.5-1.5	4.9	~ 10	53	6500
SP	3	0.5-1.5	4.9	~ 10	57	7500

[1]Depth of footing from soil surface; [2]Estimated matric suction in-situ; [3]Relative density estimated from the CPT data; [4]Average measured cone penetration resistance (in kN/m^2) from in-situ CPTs

An average cone resistance, q_c from CPTs results for the Fittja site in Sweden was reported to be 2300 to 3300 kPa over an influence zone depth of 1.5*B*. These CPT results in combination with the FLTs described in the earlier section are used to validate the proposed relationships for the estimation of settlements of footings.

Table 5.9 FLTs and CPTs data summarized from the literature and used to validate the proposed technique from Bergdahl et al. (1985)

Parameter or Property						
Soil	B (m)	[1]d (m)	Water level	[2]$(u_a - u_w)$	[3]D_r (%)	[4]$q_{c\ AVR}$
Large-scale footings from Bergdahl et al. (1985)						
S	0.55	0.4-1.1	1.5	~ 7	30	2300
S	1.6	0.4-1.1	1.5	~ 7	30	3000
S	2.3	0.4-1.1	1.5	~ 7	30	3300

[1]Depth of footing from soil surface; [2]Estimated matric suction in-situ; [3]Relative density estimated from the CPT data; [4]Average measured cone penetration resistance (in kN/m^2) from in-situ CPTs.

5.7 Settlement Estimation Using Available CPT-Based Methods

One of the most commonly used CPT-based methods in practice for estimating the settlement of shallow footings in sand is the Schmertmann et al. (1978) method. This method assumes an influence zone, IZ for settlement computations that extends down to a depth of 2*B* for square footings. The modulus of elasticity, E_s typically increases with depth, and the stresses induced by the applied load decrease with depth and become negligible for depths greater than 1.5*B* (refer to Figure 5.5 in section 5.4). Schmertmann

et al. (1978) suggested an equation (i.e., Eq. 5.1) for the calculation of footing settlement in sands using average cone resistance over a depth of 2*B* from the base of the footing as in Table 5.10. Meyerhof (1974) also suggested an empirical equation (i.e., Eq. 5.2) for estimating settlements of footings on sandy soils using the CPTs results. More recently, Mayne and Illingworth (2010) analyzed a large database which consisted of full-scale footings and proposed an empirical equation (i.e., Eq. 5.3) for settlement estimation as well. Mayne and Illingworth (2010) more recently analyzed a large database which consisted of full-scale footings in the range of 0.5 m $\leq B \leq$ 6.0 m on different sands.

The key parameter required for the estimation of settlement of shallow footings is the modulus of elasticity (see Eq. 5.1). Stress history, natural cementation, apparent or total cohesion due to matric suction and over consolidation are other significant factors that influence the modulus of elasticity of cohesionless soils (e.g., sands). The measurement of the modulus of elasticity from field tests is complicated and also expensive. The measurement of modulus of elasticity using laboratory tests is not only time consuming but also difficult due to the problems associated with sampling disturbance for sands. Due to these reasons, the CPT has been widely used as a tool to estimate the modulus of elasticity from empirical correlations (DeBeer 1965, Meyerhof 1974, Schmertmann 1970, Schmertmann et al. 1978, and Robertson and Campanella 1986). The modulus of elasticity of sands can be estimated from the CPT results with a low degree of uncertainty in comparison to the SPT and PLT results. In practice, the soil modulus of elasticity is usually determined by multiplying the average cone resistance, q_c by a correlation factor such as f_i.

Table 5.10 CPTs-based equations reported in the literature for settlement estimations

Researcher	Equation	
Schmertmann et al. (1978)	$\delta = C_1 C_2 (q_a - \sigma'_{z,d}) \sum_{0}^{2B} [(I_{zi}\Delta_{zi})/(E_S)]$	Eq. [5.1]
Meyerhof (1974)	$\delta = (q_a)[B/(2q_C)]$	Eq. [5.2]
Mayne and Illingworth (2010)	$\delta = (q_a)^2[5B/(3q_C)]$	Eq. [5.3]

where: C_1 = depth factor (i.e., C_1 = 1 - 0.5[$\sigma'_{z,d}$ / (q_a - $\sigma'_{z,d}$), C_2 = time factor (i.e., C_2 = 1 - 0.21 log [t/0.1]), δ = settlement, (mm), q_a = footing pressure, (kN/m^2), $\sigma'_{z,d}$ = vertical effective stress at footing base level, (kN/m^2), E_s = elastic modulus of soil (i.e., E_s = f_i × q_{ci}), (kN/m^2), I_{zi} = influence factor, B = footing width, (mm), q_{ci} = resistance of each layer, (kN/m^2), f_i = correlation factor, t = time, (year), and Δ_{zi} = thickness of the soil layer, (mm), q_c = average cone resistance, (kN/m^2) over an influence depth in the range of B to 2B below the footing base.

Several researchers suggested correlation factors between the modulus of elasticity and cone resistance without considering the influence of density index or other initial conditions of the sand. Likewise, correlation factors between the modulus of elasticity and cone tip resistance for different sands were suggested by Schmertmann et al. (1978) and Robertson and Campanella (1986) as 2.5 - 3.5 for young normally consolidated sand, 3.5 - 6 for aged normally consolidated sands, and 6-10 for over-consolidated sands.

5.8 Proposed Correlations between Cone Resistance and Settlement of Footings in Saturated and Unsaturated Sands

The proposed relationships of f_1 and f_2 as functions of the relative density are to be used to correlate the cone tip resistance, q_c with the modulus of elasticity, E_s. Bowles (1996) suggested that the modulus of elasticity, E_s can be determined from CPT results using the

general form of $E_s = C_3 + C_4 (q_c)$; where, $C_3 = 0$ and $C_4 = 2.5 - 3.0$ for normally consolidated sand. Vesic (1970) suggested that E_s varies with relative density according to the relation $C_4 = 2 \times (1 + D_r^2)$ and used it to correlate q_c to E_s.

The two correlation factors, f_1 and f_2 were proposed using the database of the experimental results of both PLTs and CPTs presented in this study. The form which was proposed by Vesic (1970) was re-examined using the laboratory investigation results. The constant numbers (i.e., 2 and 1 which are referred to herein as X_1 and X_2) were back calculated to be used in the correlation relationships. The way the correlation factors, f_1 and f_2 were developed is presented in Tables 5.11 and 5.12 for saturated and unsaturated sand conditions, respectively. The general form of the proposed correlation factors can be as $f_1 = X_1 \times ((D_r/100)2 + X_2)$; where: D_r in (%); X_1 and X_2 are constants computed by iteration process as the measured E_s values from the PLTs were known.

Table 5.11 Database used for proposing the correlation factor, f_1

Analysis for saturated condition, $(u_s - u_w) = 0$ *kPa*							
B (mm)	E_s *(MPa) from PLTs*	q_c *(MPa) measured from CPTs*	D_r *(MPa) determined based on density from the test tank*	X_1	X_2	E_s *(MPa) estimated using* f_1	$\frac{E_s[estimated]}{E_s[measured]}$
[1]100	1.0	0.118	0.65	1.5	3.0	0.61	0.61
[1]150	1.45	0.27	0.65	1.5	3.0	1.39	0.96
[2]150	2.9	0.55	0.65	1.5	3.0	2.82	0.97
[1] Surface square footing (*matric suction = 0 kPa*) [2] Embedded square footing (*matric suction = 0 kPa*)						AVR	0.85
Thus, $f_1 = 1.5 \times ((D_r/100)^2 + 3)$ for saturated sands.							

Table 5.12 Database used for proposing the correlation factor, f_2

Analysis for unsaturated conditions, $(u_a - u_w) > 0$ *kPa*							
B (mm)	E_s *(MPa) from PLTs*	q_c *(MPa) measured from CPTs*	D_r *(MPa) determined based on density from the test tank*	X_1	X_2	E_s *(MPa) estimated using* f_1	$\frac{E_s[estimated]}{E_s[measured]}$
[1]100	5.5	0.565	0.65	1.7	3.75	4.01	0.73
[2]100	6.75	0.805	0.65	1.7	3.75	5.71	0.85
[3]150	7.75	0.9	0.65	1.7	3.75	6.38	0.82
[4]150	11.1	1.235	0.65	1.7	3.75	8.76	0.97
[5]150	10.5	1.2	0.65	1.7	3.75	8.51	0.81
[6]150	14.4	1.6	0.65	1.7	3.75	11.35	0.79
[1,3] Surface square footing (*matric suction = 2 kPa*) [2,4] Surface square footing (*matric suction = 6 kPa*) [5] Embedded square footing (*matric suction = 2 kPa*) [6] Embedded square footing (*matric suction = 6 kPa*)						AVR	0.85
Thus, $f_2 = 1.7 \times ((D_r/100)^2 + 3.75)$ for unsaturated sands with $D_r \geq 50$ %, and f_2 was also slightly reduced as $f_2 = 1.2 \times ((D_r/100)^2 + 3.75)$ for unsaturated sands with $D_r < 50$ %.							

The D_r for the case of unsaturated sand (i.e., to calculate f_2) categorized into two groups as follows: $D_r < 50$ % and $D_r \geq 50$ %. The D_r of sands studied in this research typically vary from 30 % to 65 % (see Figure 5.11).

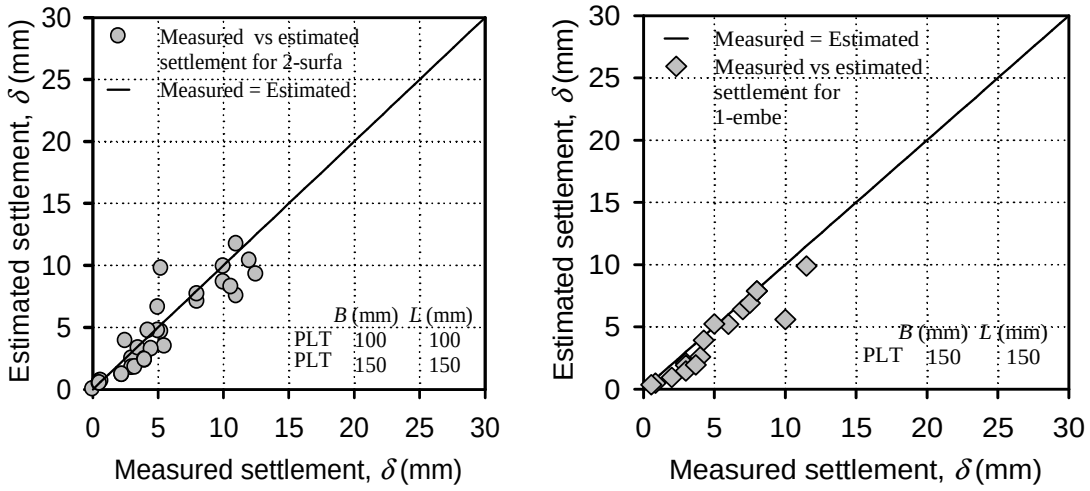

Figure 5.11 Comparison between estimated and measured settlement results of two model footings (PLTs) in both saturated and unsaturated sands corresponding to different applied stress values (proposed technique)

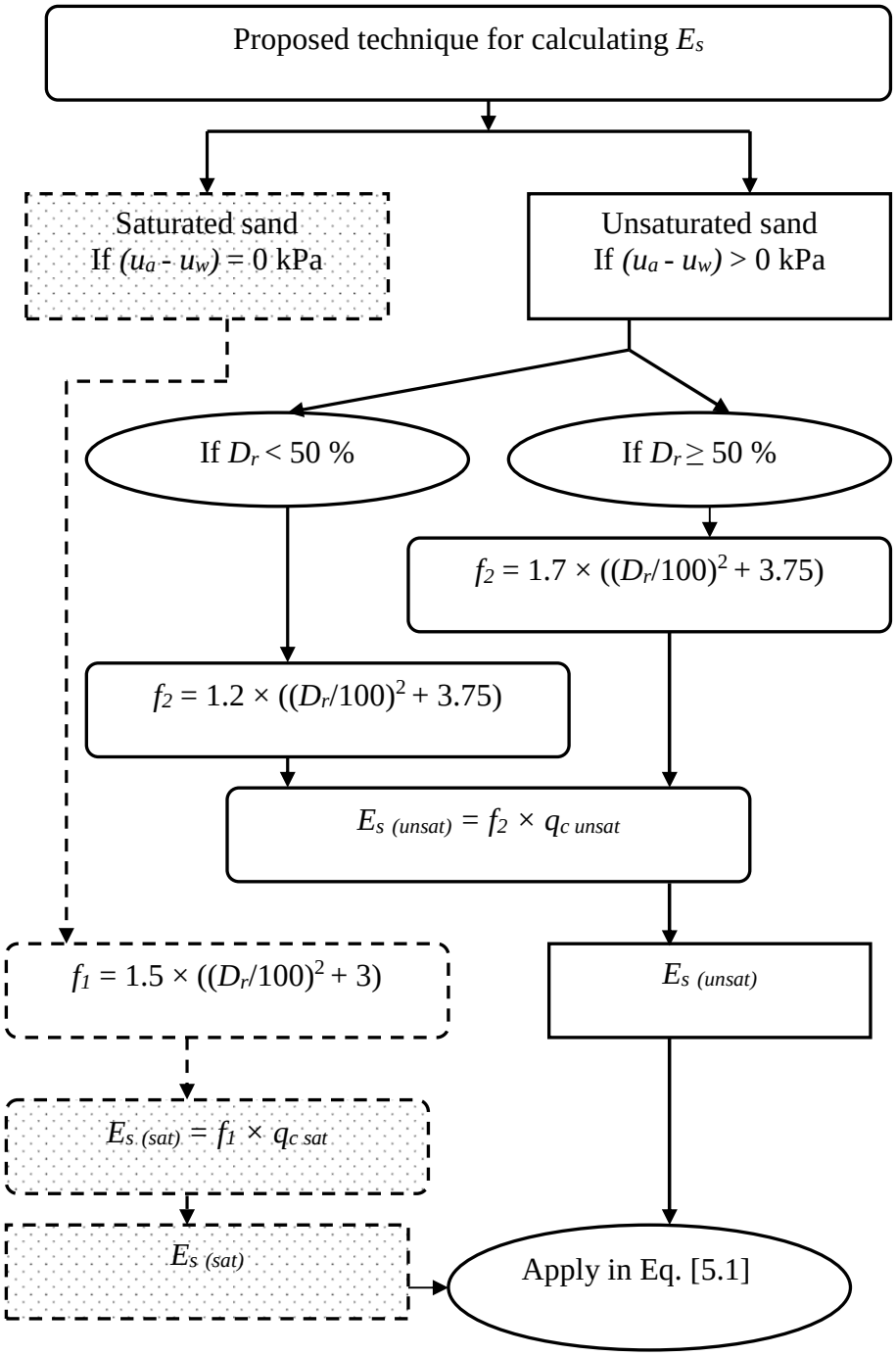

Figure 5.12 Flow-chart to illustrate the proposed technique used for calculating the modulus of elasticity of saturated and unsaturated sands

The proposed correlation factors were found to be valid for large-scale footings (seven large-scale footings) showing a good comparison between the estimated and measured settlement values. Robertson and Cabal (2010) concluded that the reliability of estimating the D_r from CPT is high to moderate; therefore, the measured q_c can be used with a greater degree of confidence to estimate the D_r which is required in the proposed relationships in this research. From Tables 5.9 and 5.10, it can be seen that the ratio between the estimated E_s from the proposed procedure and measured E_s from PLTs was in the range of 80 % to 85 % (underestimated) to account for any possible experimental errors or boundary effects on the cone penetrometer. The matric suction, $(u_a - u_w)$ was not included in the proposed correlations as its contribution is included in the measured q_c. Typically, the higher the matric suction the higher would be the cone resistance, q_c. The proposed correlation factors provide a good comparison between the estimated and measured settlement values for the two model footings tested in this research.

5.9 Validation of the Proposed Technique Using In-Situ Data from Literature

In the present study, an effective penetration depth (i.e., influence zone, IZ) is chosen to be equal to 1.5*B*. The average cone resistance, $q_{c\ \mathrm{AVR}}$ over the depth of 1.5*B* is used in the analysis of the results.

The influence zone (i.e., a depth of 1.5*B* from the footing base level) provides reasonable correlations between average cone resistance, q_c and the settlement of sand in both saturated and unsaturated conditions using the proposed relationships. Similar influence zone depth, IZ of 1.5*B* was used by Meyerhof (1956) and Schmertmann et al. (1978) to relate the settlement of spread shallow footings to estimate an average cone penetration resistance value. The results summarized in Figure 5.13 through Figure 5.15 show that the settlements estimated using the proposed relationships, provide goo correlations for both for model footings and full-scale in-situ footings. The proposed relationships in this

chapter provide better estimations in comparison to the other conventionally used methods from the literature.

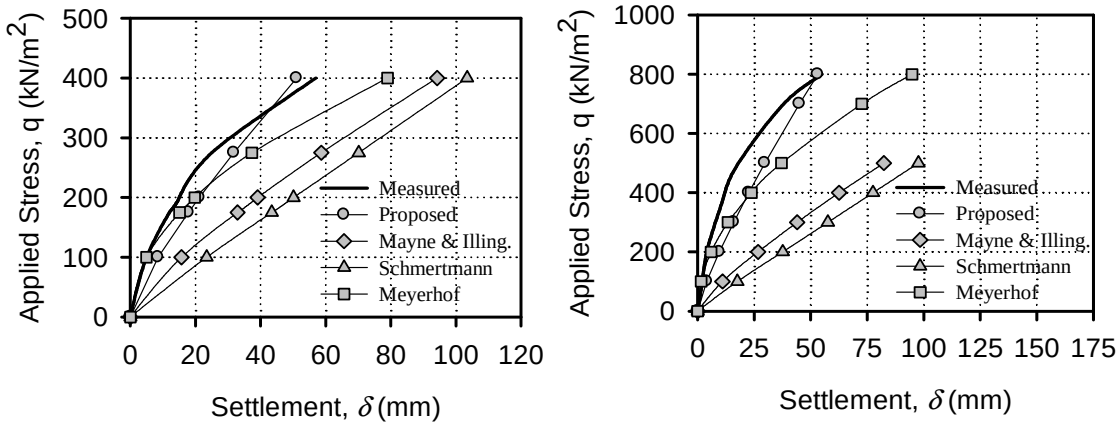

Figure 5.13 Typical results of a comparison between the estimated and measured settlements of two full-scale footing test using the studies of 1500 mm × 1500 mm and 3000 mm × 3000 mm by Giddens and Briaud (1994)

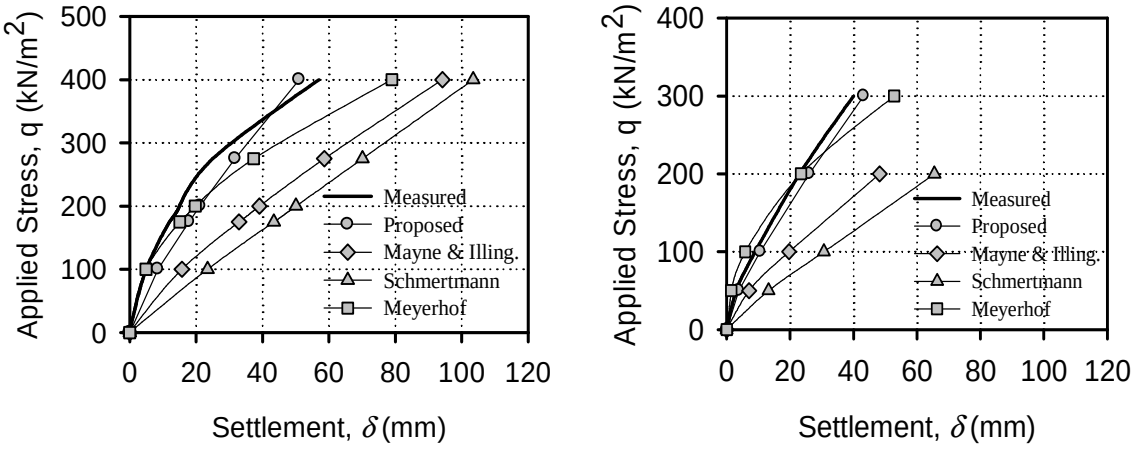

Figure 5.14 Typical results of a comparison between the estimated and measured settlements two full-scale footing test using the studies of 1600 mm × 1800 mm and 2300 mm × 2800 mm by Bergdahl et al. (1985)

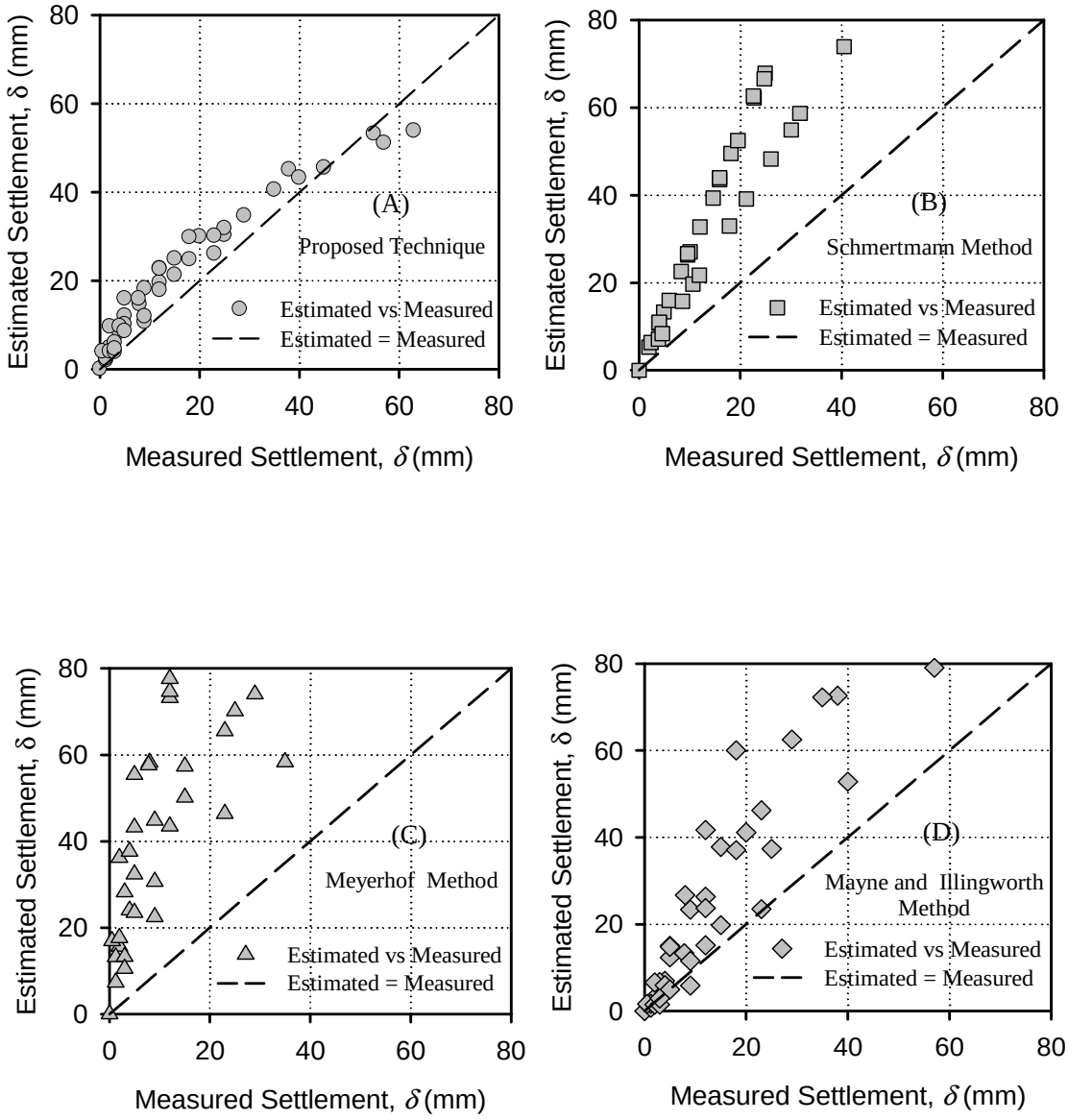

Figure 5.15 Comparison between the estimated and measured settlements of seven full-scale footings tested in unsaturated sands corresponding to different applied stress values (Bergdahl et al. 1985, and Giddens and Briaud 1994)

5.10 Results and Discussion

The correlation factor, f_1 value for estimating reliable settlement behaviour of shallow footings in sands under saturated condition is found to be in the range of 4.5 to 5.0 for the sands evaluated in this study. On the other hand, the correlation factor, f_2 value for estimating the settlement of unsaturated sands falls between 4.5 and 7.5 for the sands evaluated in this study. The need for using such a wide range of f_2 values (i.e., 4.5 to 7.5) can be attributed to the influence of matric suction on the cone resistance, q_c values which contributes to reducing the settlement, δ of sands under unsaturated conditions (i.e., $(u_a - u_w) > 0$ kPa).

It should be noted that the correlation factors, f_1 and f_2 values for saturated and unsaturated sand conditions respectively are dependent on the relative density, D_r. In both cases, the correlation factor increases proportionally with an increase in the relative density, D_r of the sand. These observations are consistent with the conclusions drawn by Lee and Salgado (2002).

Estimated and measured settlement values of both the model PLTs conducted in the laboratory (e.g., surface and embedded PLTs) and full-scale footings (FLTs) from the two summarized case studies in the geotechnical literature are compared in this research. The results of the research show that Schmertmann et al. (1978) method and Meyerhof (1974) method overestimate the measured settlements values by 3 times and 3 to 4 times, respectively (Figure 5.15(B) and Figure 5.15(C)). Mayne and Illingworth (2010) method provides settlement values of 1.25 to 2 times higher than the measured settlement values (Figure 5.15(D)). Comparisons are provided in Figure 5.15(A) between the estimated settlements, δ using the proposed technique and the other available methods for the in-situ FLTs showing that the error of the estimated settlement is in the range of ± 15 % of the measured settlement values. However, these results show reasonable comparison between the estimated and measured elastic settlements (i.e., for saturated and unsaturated sands conditions) particularly in the range of 0 to 25 mm.

5.11 Summary and Conclusions

The Schmertmann et al. (1978) method is conventionally used to estimate elastic settlements in sandy soils from the CPTs results using one correlation factor without regardless of the condition of the sand (saturated or unsaturated). Several studies reported in the geotechnical literature have shown that the estimated settlements using this method are typically two to three times higher than the measured settlement values. Two key reasons associated with the discrepancies may be due to not taking into account the influence of matric suction or relative density of sandy soils. The experimental investigation performed in this research using model PLTs showed that the settlement of shallow footings located above the groundwater table are less as the sand is in unsaturated condition. Simple relationships are proposed in to correlate the cone resistance to modulus of elasticity using the CPT results. These correlations considered by modifying the Schmertmann et al. (1978) equation. The modified equation using the proposed relationships provides reliable estimates of the settlement in the range of 0 to 25 mm (i.e., allowable settlement) for the full-scale in-situ shallow footings in sands both under saturated and unsaturated sand conditions. The proposed CPT-based technique is simple, reliable and consistent with methods used for estimation of the settlements of footings in sands by practicing engineers.

5.12 References

Agarwal, K. B. and Rana, M. K. (1987). "Effect of ground water on settlement of footing in sand." In the Proceedings of the 9th European Conference on Soil Mechanics and Foundation Engineering, Dublin, Ireland, Balkema, Rotterdam, the Netherlands, 751 – 754.

ASTM, D2487. (2006). "Standard practice for classification of soils for engineering purposes." (Unified Soil Classification System).

Bergdahl, U., Hult, G. and Ottosson, E. (1985). “Calculation of settlements of footings in sands.” In the Proceedings of the 11th International Conference on Soil Mechanics and Foundation Engineering, San Francisco, 4, 2167 – 2170.

Bellotti, R., Bizzi, G. and Ghionna, V. (1982). “Design, construction and use of calibration chamber.” In Proceeding of ESOPT II, Balkema, Amsterdam, The Netherlands, 2, 439 – 446.

Bowles, J. E. (1996). “Foundation analysis and design.” 5th Edition, The McGraw-Hill companies, Inc., N.Y., USA.

Briaud, J. L. (1992), “The Pressuremeter.” Balkema, Rotterdam.

Briaud, J. L. (2007). “Spread footings on sand: Load settlement curve approach.” Journal of Geotechnical and Geoenvironmental Engineering, 133, 8, 905 – 920.

Broms, B. B. (1963). “The effect of degree of saturation on the bearing capacity of flexible pavements.” Highway Research Record, 71, 1 – 14.

Costa, Y. D., Cintra, J. C. and Zornberg J. C. (2003). “Influence of matric suction on the results of plate load tests performed on a lateritic soil deposit.” Geotechnical Testing Journal, 26(2), 219 – 226.

Das, B. M. and Sivakugan, N. (2007). “Settlement of shallow foundations on granular soil - an overview.” International Journal of Geotechnical Engineering, 1(1), 19-29.

DeBeer, E. (1965). “Bearing capacity and settlement of shallow foundations on sand.” Proceedings of Symposium on Bearing Capacity and Settlement of Foundations, Durham, N.C., 15 – 33.

Giddens, R. and Briaud, J. L. (1994). “Load tests on five large spread footings on sand and evaluation of prediction methods.” Report to the Federal Highway Administration Department of Civil Engineering, A&M University, T.X., USA.

Houlsby, G. T. and Hitchman, R. (1988). “Calibration chamber tests of a cone penetrometer in sand.” Géotechnique, 38(1), 39 – 44.

Hryciw, R.D., and Dowding, C.H. (1987). “Cone penetration of partially saturated sands.” Geotechnical Testing Journal, GTJODJJ, 10(3), 135 – 141.

Iwasaki, K., Tanizawa, F., Zhou, I. and Tatsuoka, F. (1988). “Cone penetration and liquefaction strength of sand.” Penetration Testing, ISOPT-1, De Rutter (Ed.), Balkema, Rotterdam, 785 – 791.

Lee, J. and Salgado, R. (2002). “Estimation of footing settlement in sand.” International Journal of Geomechanics, 1(2), 1 – 28.

Lunne, T., Robertson, P. K. and Powell, J. M. (1997). “Cone penetration testing in geotechnical practice.” Blackie Academic and Professional, London, UK.

Mayne, P. and Illingworth, F. (2010). “Direct CPT method for footing response in sands using a database approach.” The 2nd International Symposium on Cone Penetration Testing, Huntington Beach, California.

Meyerhof, G. (1956). “Penetration tests and bearing capacity of cohesionless soils.” Journal of the Soil Mechanics and Foundation Division, ASCE, 82(1), 1 – 19.

Meyerhof, G. (1974). “Penetration testing in countries out-side Europe.” Proceedings of the European Symposium on Penetration Testing, 2.1, 40 – 48.

Miller, G. A., Muraleetharan, K. K., Tan, N. K. and Lauder, D.R. (2002). “A calibration chamber for unsaturated soil testing.” In the Proceedings of the 3rd International Conference on Unsaturated Soils, UNSAT 2002, Balkema, Lisse, 2, 453 – 457.

Mohamed, F. M. O. and Vanapalli, S. K. (2006). “Laboratory investigations for the measurement of the bearing capacity of an unsaturated coarse-grained soil.” In Proceedings of the 59th Canadian Geotechnical Conference, Vancouver, B.C., 1 – 4 October 2006. Canadian Geotechnical Society, Richmond, B.C., 1, 219 – 216.

Miller, G. A. and Muraleetharan K. K. (1998). “In situ testing in unsaturated soil.” Proceeding of the 2nd International Conference on Unsaturated Soils, Beijing, China, 1, 416 – 421

Oh, W. T. and Vanapalli, S. K. (2011). “Modeling the applied vertical stress and settlement relationship of shallow foundation in saturated and unsaturated sands.” Canadian Geotechnical Journal, 48, 425 – 438.

Oloo, S. Y., Fredlund, D. G. and Gan, J. (1997). “Bearing capacity of unpaved roads.” Canadian Geotechnical Journal, 34(3), 398 – 407.

Parkin, A. K. (1988). “The calibration of cone penetrometers.” In the Proceedings of the 1st International Symposium on Penetration Testing (ISOPT-1), Orland, FL, U.S.A.

Poulos, H.G. and Davis, E.H. (1974). “Elastic solutions for soil and rock mechanics.” John Wiley and Sons, New York.

Pournaghiazar, M., Russell, A. R. and Khalili, N. (2011). “Development of a new calibration chamber for conducting cone penetration tests in unsaturated soils.” Canadian Geotechnical Journal, 2, 314 – 321.

Pournaghiazar, M., Russell, A. R. and Khalili, N. (2012). “The cone penetration test in unsaturated sands.” Géotechnique, (Accepted: in press)

Robertson, P. K. (2009). “Interpretation of cone penetration tests - a unified approach.” Canadian Geotechnical Journal, 46, 1337 – 1355.

Robertson, P. K. and Campanella, R. G. (1983). “Interpretation of cone penetration resistance tests, Part I, sand.” Canadian Geotechnical Journal, 20(4), 718 – 733.

Robertson, P. K. and Campanella, R. G. (1986). “Liquefaction potential of sands using the CPT.” Journal of Geotechnical Engineering, ASCE, 3(3), 384 – 403.

Rojas, J. C., Salinas, L. M. and Seja, C. (2007). “Plate-load tests on an unsaturated lean clay.” Experimental Unsaturated Soil mechanics: In the Proceeding of the 2nd

International Conference on Unsaturated Soils, Springer Proceedings in Physics, Springer-Verlag Berlin Heidelberg, Weimar, Germany, 445 – 452.

Russell, A. R. and Khalili, N. (2006). "On the problem of cavity expansion in unsaturated soils." Computational Mechanics, 37(4), 311 – 330.

Salgado, R., Mitchell, J. K.. and Jamiolkowski, M. (1998). "Calibration chamber size effects on penetration resistance in sand." Journal of Geotechnical and Geoenvironmental Engineering, ASCE, 124(9), 878 – 888.

Steensen-Bach, J. O., Foged N. and Steenfelt J. S. (1987). "Capillary induced stresses – fact or fiction?." 9th ECSMFE, Groundwater Effects in Geotechnical Engineering, Dublin, 83-89.

Schmertmann, J. H. (1970). "Static cone to compute static settlement over sand." Journal of the Soil Mechanics and Foundation Division, 96, 1011 – 1043.

Schmertmann, J. H. (1976). "An updated correlation between relative density D_r and Fugro-Type electric friction cone bearing q_c." DACW 39-76 M6646, Waterways Experiment Station, USA.

Schmertmann, J., Hartman, J. and Brown, P. R. (1978). "Improved strain influence factor diagrams." Journal of Geotechnical Engineering Division, ASCE, 104(8), 1131 – 1135.

Schnaid, F. and Houlsby G. (1991). "An assessment of chamber size effects in the calibration of in-situ tests in sand." Géotechnique, London, England, 41(3), 437 – 445.

Schnaid, F, Consoli N. C., Cudmani R.O. and Militistsky J. (1995). "Load-settlement response of shallow foundations in structured unsaturated soils." In the Proceedings of the 1st International Conference of Unsaturated Soils, Paris, France, 999 – 1004

Tan, N. K. (2005). “Pressuremeter and cone penetrometer testing in a calibration chamber with unsaturated Minco silt.” Ph.D thesis. University of Oklahoma.

Terzaghi, K. and Peck, R. B. (1967). “Soil mechanics in engineering practice.” 2nd Edition, Wiley, New York.

Vanapalli, S. K. and Mohamed, F. M. O. (2007). “Bearing capacity of model footings in unsaturated soils.” In Experimental Unsaturated Soil Mechanics, Springer Proceedings in Physics. Springer-Verlag Berlin Heidelberg, 112, 483 – 493.

Vanapalli, S. K. (2009). “Shear strength of unsaturated soils and its applications in geotechnical engineering practice.” Keynote Address, Proceedings of the 4th Asia-Pacific Conference on Unsaturated Soils, N.C., Australia, 579 – 598.

Vesic, A. S. (1970). “Tests on instrumented piles, Ogeechee River site.” Journal of Soil Mechanics and Foundation Division, ASCE, 96(2), 561 – 584.

CHAPTER 6

[5]BEHAVIOUR OF A MODEL FOOTING SUBJECTED TO SEISMIC LOADING ON UNSATURATED SAND

6.1 Introduction

The response of shallow foundations of medium to low-rise buildings built on in unsaturated sand deposits during earthquakes is a topic which is of interest to many engineers in academia and practice. Several research projects were directed to study the performance of shallow foundations in sandy soils on seismically active areas since the 1964 Nigata earthquake (Seed and Silver 1972, Lee and Albaisa 1974, Finn and Byrne 1976, Tokimatsu and Seed 1987, Rollins and Seed 1990, Lui and Dobry 1997, and Rayhani and El-Naggar 2008).

Liquefaction of sandy soils occurs when the soil rapidly loses its shear strength due to increase in excess pore-water pressure and decrease in the effective stress. In many scenarios, large deformations of foundations of supporting structures and pavements are likely when sands are subjected to seismic loading. Liquefaction of soils has been a topic of significant research interest to several investigators (for instance, Terzaghi and Peck 1948, Casagrande 1975, and Vaid and Sivathayalan 1996). Typical example of failures due to liquefaction of saturated sands caused by EQ shaking from Niigata in 1964 is shown in Figure 6.1.

[5]This chapter is developed based on a paper in preparation for submission to the Canadian Geotechnical Journal in 2013.

Nigatta, Japan, 1964

Figure 6.1 Liquefaction example associated with an EQ

(National Geophysical Data Centre, USA)

6.2 Justification of Studying Liquefaction of Sandy Soils

Significant economic losses and human fatalities are associated with earthquakes, for example; 1985 Michoacán Earthquake in Mexico (magnitude of 8.1 and 9500 casualties), 1989 Loma Priata Earthquake in California (magnitude of 7.1 and 63 casualties), 1994 Northridge Earthquakes in California (magnitude of 6.8 and 61 casualties), 1995 Kobe Earthquake in Japan (magnitude of 6.9 and 5300 casualties), 1999 Izmit Earthquake in Turkey (magnitude 7.5 and 35000 casualties), and 2010 Earthquake in Haiti (magnitude of 7.0 and 316000 casualties), (Kramer 1997, NIST 1996, NEES 2004, and Kara and Gündüz 2010).

Approximately 150 lives were lost in the United States since 1975 as a result of earthquakes (Cutter 2001); the economic losses and social disruption associated with them were enormous (Mileti 1999). The cost of damages by EQs (e.g., Loma Prieta 1989 and Northridge 1999) in California for example was in the range of $30 billion. The damages to civil engineering structures and buildings due to the increased frequency of earthquakes (Figure 6.2 summarizes the earthquake prone regions of the world),

population growth, overcrowding of civil engineering facilities, and more importantly lack of understanding of the behaviour of supporting soils in general and soil structure interaction in particular are of concern. Table 6.1 and Figure 6.3 summarize the estimated economic costs and causative mechanisms of damages to houses by NEES (2004) and Asada (1998), respectively. Due to these reasons, research in earthquake geotechnical engineering has received significant attention during the last 5 decades.

Table 6.1 Economic cost of selected earthquakes in year of occurrence (NEES 2004)

Location	Year	Magnitude	*Cost	Reference
Nisqually, Washington	2001	6.8	$2.0	University of Washington
Taiwan	1999	7.7	$20.0 to $30.0	EERI (1999b)
Izmit, Turkey	1999	7.6	$5.0	EERI (1999a)
Kobe, Japan	1995	6.9	$200.0	NIST (1996)
Northridge, California	1994	6.7	$30.0	EQE (1994)
Loma Prieta, California	1989	6.9	$5.9	EQE (1989)

*Cost in billions US dollars.

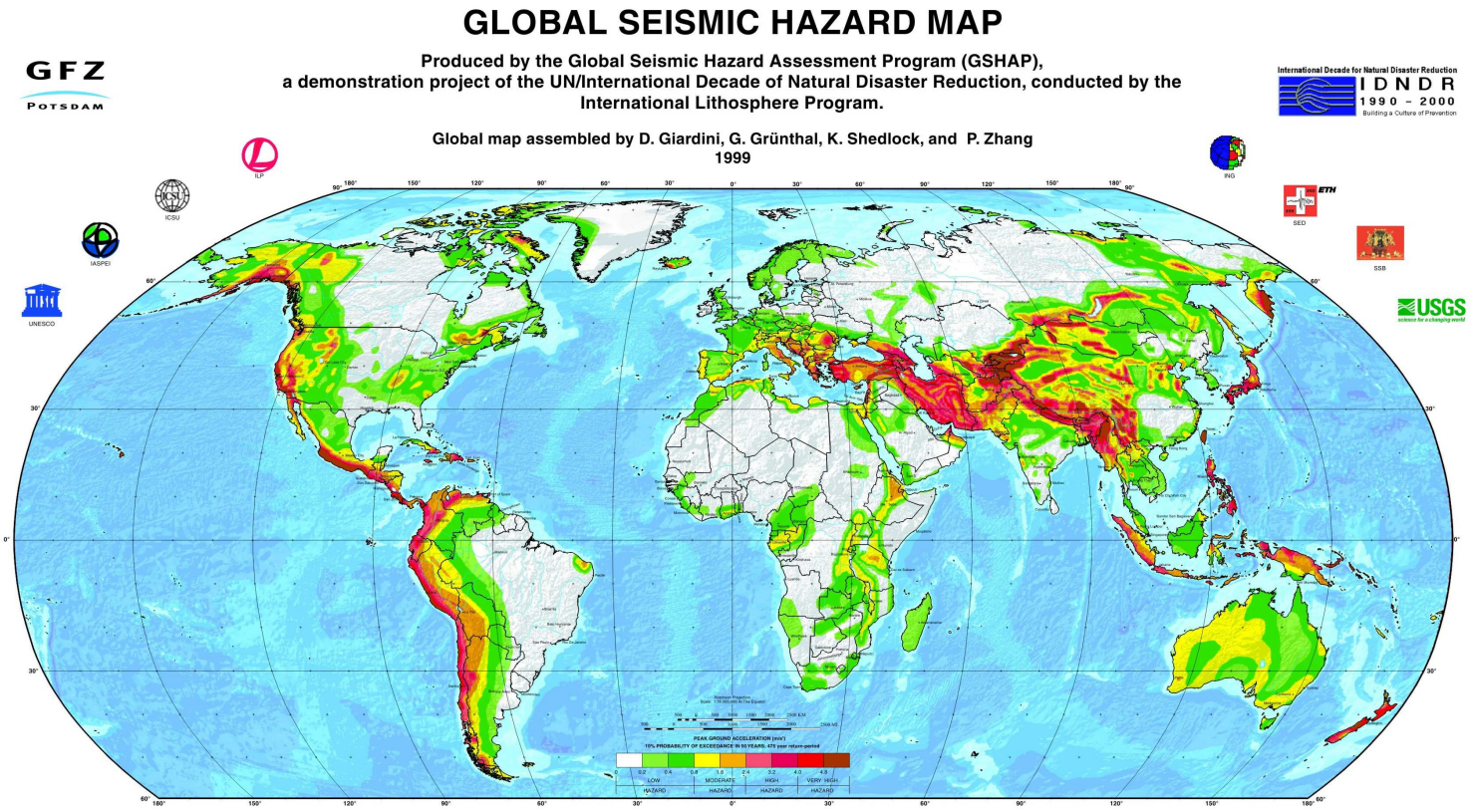

Figure 6. 2 Global Seismic Hazard Map (by Giardini et al. 1999)

Several researchers have studied seismically induced settlements of soils (e.g., sands) (Seed and Silver 1972, Lee and Albaisa 1974, Finn and Byrne 1976, Tokimatsu and Seed 1987, and Pradel 1998). Most of these early studies (i.e., ground shaking induced deformations of sand) were performed in dry conditions because it was assumed that the settlement of dry sand is caused by compression of void space and represents worst case scenario (D'Appolonia 1970, Youd 1970, Silver and Seed 1971, and Ghayoomi et al. 2013). Seed and Idress (1974) and Pradel (1998) suggested empirical relationships from their studies to estimate the settlement of dry sand under EQ loading conditions. On the other hand, Lee and Albaisa (1974), Ishihara and Yoshimine (1992), Wu and Seed (2004), Cetin et al. (2009) also studied saturated sands and correlated the measured volumetric strains after shaking with magnitude of accumulated pore-water pressures.

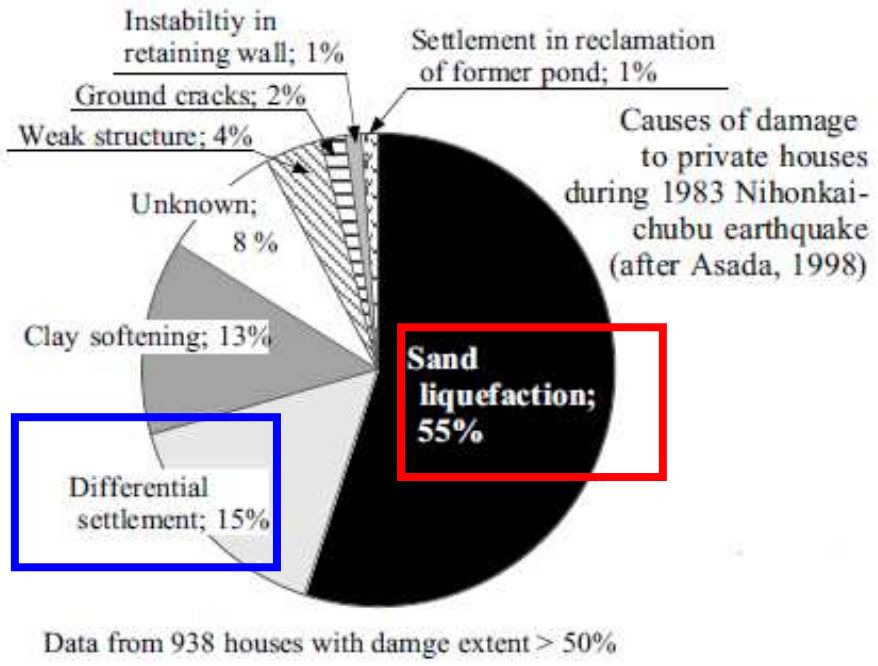

Figure 6. 3 Causative mechanisms of damage to houses during 1983 Nihonkai-Chubu EQ (from Towhata 2008 after Asada 1998)

Whang et al. (2005) and Sawada et al. (2006) tested unsaturated silty sand in a cyclic simple shear and a cyclic triaxial apparatus with seismic input motion, respectively. Their

studies show that the degree of saturation influenced the results. Relatively low shear strains were observed when the degree of saturation of the tested sand was between 30 to 75 %. Eseller-Bayat (2009) used a cyclic simple shear liquefaction box and tested partially saturated sand specimens with uniformly distributed gas bubbles. The results show that the number of cycles increased with an increase in gas bubbles to reach maximum excess pore-water pressure ratio; in other words this study supports the observation that the unsaturated sands have higher resistance to liquefaction comparison to saturated sands.

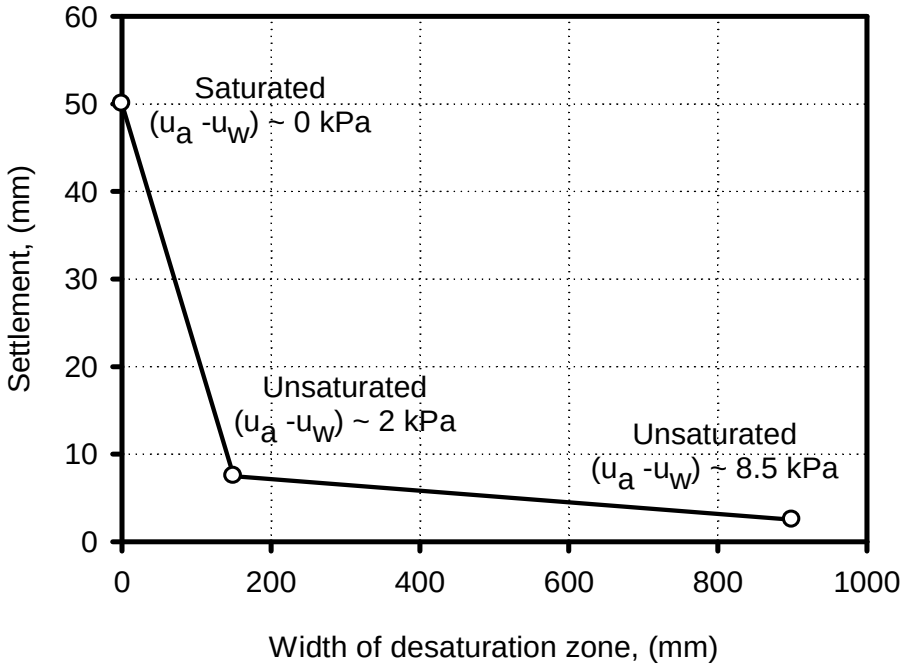

Figure 6. 4 Settlement of a model footing on sand at the end of shaking test with respect to degree of saturation (Okamura and Teraoka 2005)

Okamura and Teraoka (2005) carried out a series of tests using a rigid box of 900 mm × 300 mm × 600 mm on a shaking table to investigate the influence of initial degree of saturation of poorly-graded sand on soil liquefaction. Based on their studies, they suggested injecting air into the soil to keep it in unsaturated condition to reduce model

footing settlement by achieving degree of saturation, S < 90 % as shown in Figure 6.4. However, there is limited research with respect to the dynamic response of unsaturated sands supporting shallow foundations (i.e., footings) taking account of the influence of the stress state variable, matric suction (Unno 2008, Whang et al. 2005, and Sawada et al. 2006).

Physical models used in laboratories are valuable for understanding the seismic behaviour of unsaturated sands. Such studies are alternative to expensive field investigations and can be used to propose numerical methods. Model tests can also be used as benchmark studies or tools to better understand the influence of matric suction of the behaviour of unsaturated sands. In other words, small scale physical models using shaking tables along with numerical models can be invaluable both in understanding and predicting the response of unsaturated sands under seismic loading conditions.

The focus of the research work summarized in this chapter is directed to investigate the behaviour of shallow foundations using a model footing (150 mm × 150 mm) in unsaturated sand under EQ loading. The key objectives of this research are: (i) to design and construct a Flexible Laminar Shear Box (FLSB); (ii) to understand the behaviour of a model footing under EQ loading in both saturated and unsaturated conditions.

The design and construction of the FLSB, calibrations and performance of the shake table are described in this chapter. A small-scale model footing (150 mm × 150 mm) used to imitate a large-scale footing to study the seismic behaviour of shallow foundations built on unsaturated soils.

The experimental work consists of a series of tests carried out on sand under different saturated and unsaturated conditions. The tests performed using the FLSB and 1-g shaking table. The behaviour of a 40 kg-model footing of 150 mm × 150 mm on saturated and unsaturated sandy soil is investigated and analyzed. The sand response to a simple sinusoidal time-history is studied. The main purpose of the FLSB is to achieve similar behaviour as in the field without the interference of the boundary effects and also to overcome the limitation of the capacity of the available shake table. The obtained results

from different test scenarios of saturated and unsaturated sand are presented and analyzed in later sections of this chapter. The studies show that the model footing in sand performed well under EQ loading at matric suction value close to 6 kPa. The studies suggest that even low values of matric suction or capillary stresses (i.e., < 5 kPa) lead to decreased settlement of footings while offering resistance to liquefaction in sands.

6.3 Background

The response of medium to low-rise buildings with shallow foundations on unsaturated sand deposits during earthquakes is a topic of interest to researchers and engineers in practice. Earthquakes cause a displacement in bedrock due to vertically propagating shear-waves in the shallow layers soil that support buildings and other infrastructure. Depending on the properties of the soils overlying bedrock, the resultant ground motions caused by the vertically propagating shear-waves may be amplified at the ground surface where structures are typically built. During an earthquake, the overall response of structures on or embedded in soils may significantly be influenced by the soil conditions (i.e., saturated or unsaturated). A physical model was used in the current investigation to simulate the performance of shallow footings on saturated and unsaturated sand using the Flexible Laminar Shear Box (FLSB) and a shake table to study the problem described. The deformations (i.e., settlement and tilting) of the model footing were recorded through data acquisition system. The recorded data could be used to check the liquefaction potential of the tested sand during the time period of shaking. The FLSB was filled with a sandy soil used in this research program expecting *1-D* shear wave propagation throughout the soil as the base shear was applied by an MTS actuator. Similar studies using different FLSB setups and soils were also used by several investigators (Lin and Whang et al. 2012, Turan et al. 2008a, and Meymand 1998). However, the available data on seismically induced deformations and liquefaction are based on testing dry and saturated soils respectively. A rigid footing model (i.e., steel) was constructed at the University of Ottawa to be placed on top of sand under both saturated and unsaturated conditions along with instrumentation to determine the settlement response and

liquefaction resistance. Four different series of shaking tests were conducted in this research program under same EQ shaking. The response of the tested sand under saturated and unsaturated conditions were monitored and recorded using three accelerometers, six Cable Displacement Transducers (CDTs) connected to data acquisition system (DAQS) during the time period of shaking. Three Tensiometers wrer used to measure the matric suction. The vertical and horizontal deformations of the model footing, the accelerations on the table and at both top and bottom of the sand as well as the matric suction values were monitored and recorded during the shaking (the shaking was by a series of sinusoidal waves with a frequency of 3 Hz and a peak ground acceleration of 0.6*g* m/sec^2 for a duration of 30 to 40 seconds). In addition, samples of the tested sand were collected to check the water contents and the density values. The results are valuable for understanding the behaviour of shallow foundation in saturated and unsaturated sands. These results are used to understand the effect of capillary stresses (i.e., matric suction) on the liquefaction resistance of sands. The steps followed in the research program presented in the chapter is shown in Figure 6.4 in the form of flow-chart.

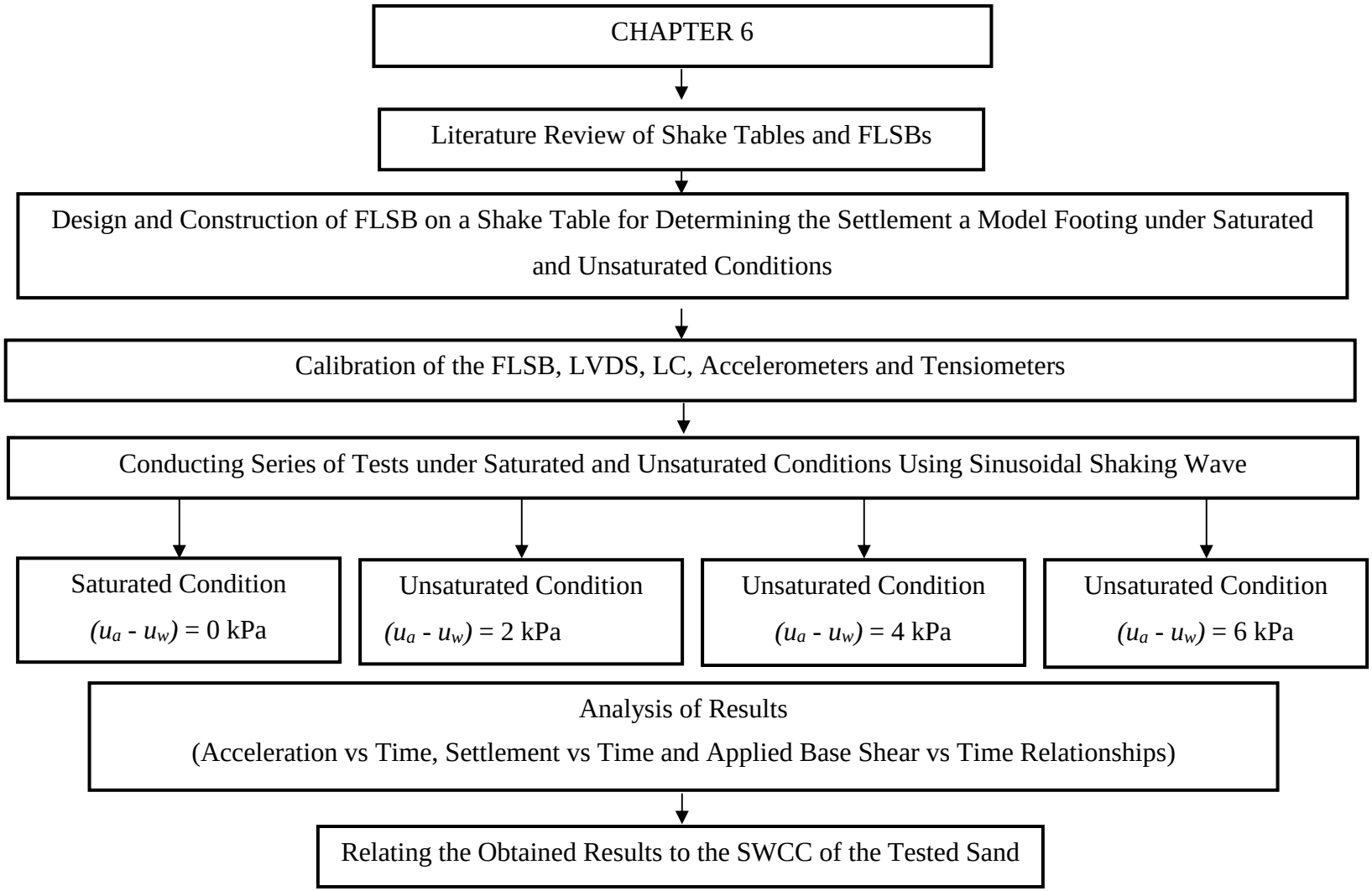

Figure 6.5 Flow-chart to illustrate the research program undertaken in this chapter

6.4 Literature Review of Shake Tables Studies

Small scale model tests studies using a 1-*g* shake table can be used as valuable tools to better understand the prototype behaviour taking account of the influence of different parameters (i.e., strength, deformation, liquefaction, matric suction and soil amplification) and the process leading to failure of prototype structures placed in soils in real time. Full scale studies however are complex, time consuming and difficult to conduct (Prasad et al. 2004). Figure 6.6 illustrates one of the pioneering works in which a big soil container moves back and forth along a track. The advantage of small scale 1-*g* shaking table test is that preparation of a model is easier and less time consuming compared to centrifugal models. Maintenance cost of shake table setups is lower as well. One of the limitations with case history studies (i.e., prototype) are that the subsurface deformation cannot be reliably measured (Towhata 2008). This problem is alleviated or addressed by conducting shaking table tests.

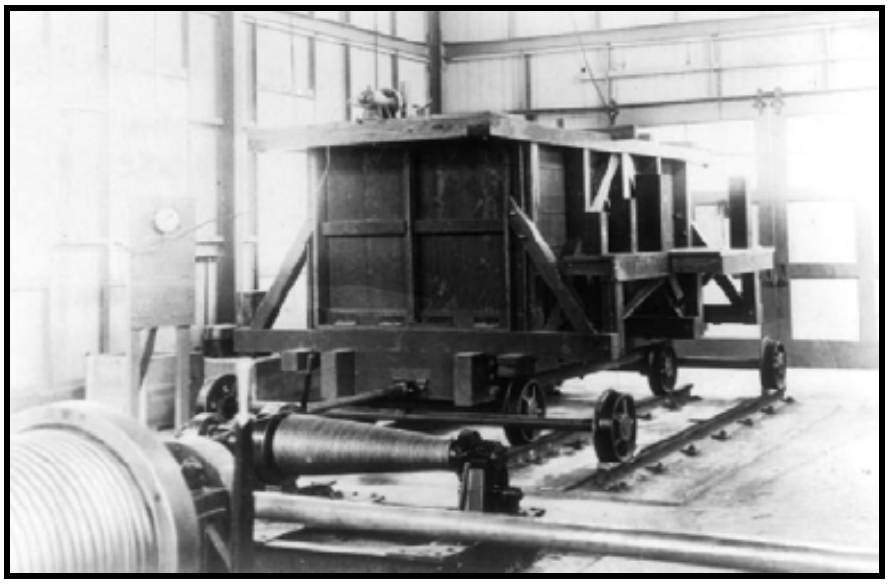

Figure 6.6 Early generation shake table device (Towhata 2008)

A large soil container shown in Figure 6.7 was used for conducting liquefaction tests by Motamed et al., (2009). This container measures 15 m in length and the soil deposit in the container has a 4.5 m height. The thickness others used was sufficient to claim that the facility reproduces the prototype stress level. Several researches used shake tables to understand the failure mechanisms and behaviour of saturated sands (Koga and Matsuo 1990, Kokusho 2003, and Orense 2003). Various types of shake tables used by several investigators are summarized in Table 6.2.

Table 6.2 Shake tables used in previous studies

Shape	Dimensions		Use in	Loading direction	Reported by
	Width (mm)	Length (mm)			
Square	3600	3600	1-*g*	2-D	Thevanayagam et al. (2009)
Rectangular	1000	1100	1-*g*	1-D	Kokusho (2003)
Rectangular	1940	2340	1-*g*	1-D	Ueng and Chen (2006)
Rectangular	2700	2700	1-*g*	1-D	Saman and Bathurst (2007)
Rectangular	600	1800	1-*g*	2-D	Prasad et al. (2004)
Rectangular	1220	1220	1-*g*	1-D	Turan et al. (2009)
Rectangular	1000	1000	1-*g*	1-D	University of Ottawa

g = 9.81 m/sec2; *D* = direction

6.4.1 Advantages of Shake Tables

The advantages of shaking tables can be summarized as follows:

- They can be uni-directional or multi-directional input motion.
- Relatively easier for experimental measurements.

- The experimental results can be used to validate numerical solutions.
- They are valuable to understand failure mechanisms.
- Amplitude and frequency can be well controlled and measured.
- Different real earthquake history records can be supplied to the model.
- Shaking table tests are inexpensive compared to centrifuge devices.
- Shake tables can be used to study behaviour of footings on or embedded in dry, saturated or unsaturated soils.

6.4.2 Disadvantages of Shake Tables

The disadvantages of shaking tables can be summarized as follows:

- High stresses that usually exists in the field cannot be simulated.
- Limited base shear capacity and needs expensive electro-hydraulic actuator.
- Limited soil mass capacity of small-scale shake tables.
- Cost is proportional with both the size of shake table and the amount of the soil.

Figure 6.7 E-Defense large shaking model test on lateral flow of liquefied sand induced by failure of sheet-pile quay wall (Motamed et al., 2009)

6.5 Review of Laminar Shear Boxes in Literature

Laminar Shear Boxes (i.e., flexible container) are designed such that they can be attached to shake tables for conducting tests at either 1-*g* or at N-*g* during centrifuge tests. In the following section, nine different laminar container designs are reviewed and their characteristics are summarized in Table 6.3. Gibson (1997) and Prasad et al. (2004) described single-axis flexible containers for 1-*g* seismic tests on shake tables. Single-axis flexible containers (i.e., 1-D loading) permit movement in a single axis only and typically comprise of either rigid guide walls that support laminae on bearings or laminae that are stacked on each other separated by bearings. In addition to the single-axis containers, Meymand (1998) and Ueng and Chen (2006) provide details of double-axis flexible containers for 1-*g* tests. Double axis containers permit horizontal movement of laminae in two principal directions.

The container designed by Meymand (1998) comprises of a ribbed membrane hanging from a top ring supported by a frame connected to the shaking table using universal joints. In contrast, Ueng and Chen (2006) describe a container with laminae supported by inner and outer frames connected to rigid guide walls.

6.6 Objectives

In Ottawa-Gatineau region, two recent earthquakes of magnitudes 5.0 and 5.2 in 2010 and 2013, respectively contributed to some damages in buildings and bridges as well as disruption in services. Such magnitude earthquakes did not occur during the last 65 years. These earthquakes serve as reminders of the importance for paying more attention towards the seismic damage potential in Eastern Ontario. Foundations may experience damages mainly due to the amplification of ground shaking which may lead to liquefaction particularly in sand deposits (e.g., Carp region, Ottawa) if they are not properly designed.

The primary focus of the research presented in this chapter is to understand the behaviour of seismically shaken model rigid footing placed on a sandy soil using both reduced scale

physical modeling techniques in 1-*g* environment mimicking an EQ magnitude that might occur in Ottawa region. In this research, the FLSB was designed and built to conduct four different scenarios of tests under EQ loading to study deformation of model footing and liquefaction phenomenon of poorly graded sand under saturated and unsaturated conditions.

The main objectives of the research program presented in this chapter are as follows:

- To design, construct and calibrate the Flexible Laminar Box (FLSB) with all its accessories.
- To utilize a small-scale shake table in order to simulate ground shaking during an earthquake using a model rigid footing on saturated and unsaturated sand under 1-g scaling model.
- To investigate both the influence of matric suction on the deformation of the model footing and to check the susceptibility of unsaturated sand to liquefaction during earthquake shaking.
- To analyze and discuss the results using the soil-water characteristic curve (SWCC) of the tested sand as a tool.

The gathered information and data will be valuable to understand liquefaction resistance of unsaturated sands and to suggest suitable procedures for shallow foundations designed and constructed in seismically active areas.

Table 6.3 Laminar shear boxes used in previous studies

Shape	Dimensions			Use in	Loading direction	Reported by
	Width (mm)	Length (mm)	Height (mm)			
Rectangular	350	900	470	1-*g*	1-D	Gibson (1997)
Rectangular	500	1000	1000	1-*g*	1-D	Prasad et al. (2004)
Circular	2280	2130	(D_i,H)	1-g	2-D	Meymand (1998)
Rectangular	1888	1888	1520	1-*g*	2 -D	Ueng and Chen (2006)
Rectangular	254	457	254	n-*g*	1- D	Van Laak et al. (1994)
Rectangular	355	710	355	n-*g*	1-D	Pamuk et al. (2007)
12-Sided Polygon	584	500	(D,H)	n-*g*	2-D	Shen et al. (1998)
Rectangular	200	450	325	n-*g*	1-D	Takahashi et al. (2001)
Rectangular	450	900	760	1-*g*	1-D	Turan et al. (2009)

6.7 Equipment, Methodology and Procedures Followed in the Research Program

6.7.1 General

The Flexible Laminar Shear Box (FLSB) was designed for this research program and built at the University of Ottawa machine shop is the first of its kind to test unsaturated sandy soil under seismic loading conditions to the best of the knowledge of the author.

Details are summarized in the following sections including the description and the key features of the FLSB and the external frame as well as the model footing. The methodology of using the FLSB and 1-*g* shake table is also presented. Other accessories and instrumentations which are used in the testing program, for example, Tensiometers, accelerometers, CDTs and data acquisition system are briefly described.

6.7.2 University of Ottawa Flexible Laminar Shear Box (FLSB)

The University of Ottawa FLSB was designed to reduce the influence of boundaries that are typically experienced in using a rigid shear box. The FLSB is to simulate conditions of the realistic behaviour of soils as the wave reflection from the side boundary is weakened greatly due to the relative horizontal deformation of the laminae.

The FLSB used in this research was constructed from aluminum frames, rectangular in plan, was stacked with a flexible plastic bag inside to create a hollow box that can be filled with the tested sand. The aluminum rings provide sufficient confinement and it is intended that the soil drives them not the other way around simulating realistic in-situ scenario of EQ. All the key features of the FLSB are summarized as below:

- The external steel frame for this equipment was constructed using a channel (50 mm × 50 mm section with 8 mm in thickness). The frame is shown in Figure 6.8. The purpose of the external frame is to carry the weight of the FLSB and the shaft rods, guide rods as well as the bearing brackets. The weight carried by the external frame is transferred to the large supporting beams (150 mm-flange and 200 mm-web) and then to the strong R/C floor. The other frame is made of steel channel (400 mm × 400 mm and 5 mm in thickness) fastened by bolts above the external frame and extended across the FLSB. This frame is to hold the wooden square plate used to hang the CDTs down to the footing to measure vertical deformations at the four corners of the footing (i.e., NE, NW, SE and SW). The frame is equipped with adjustable legs so that the FLSB can be levelled with 3 mm of clearance between the shaking table and the lowest lamina. Both the frames are adjustable and can be easily levelled as desired.

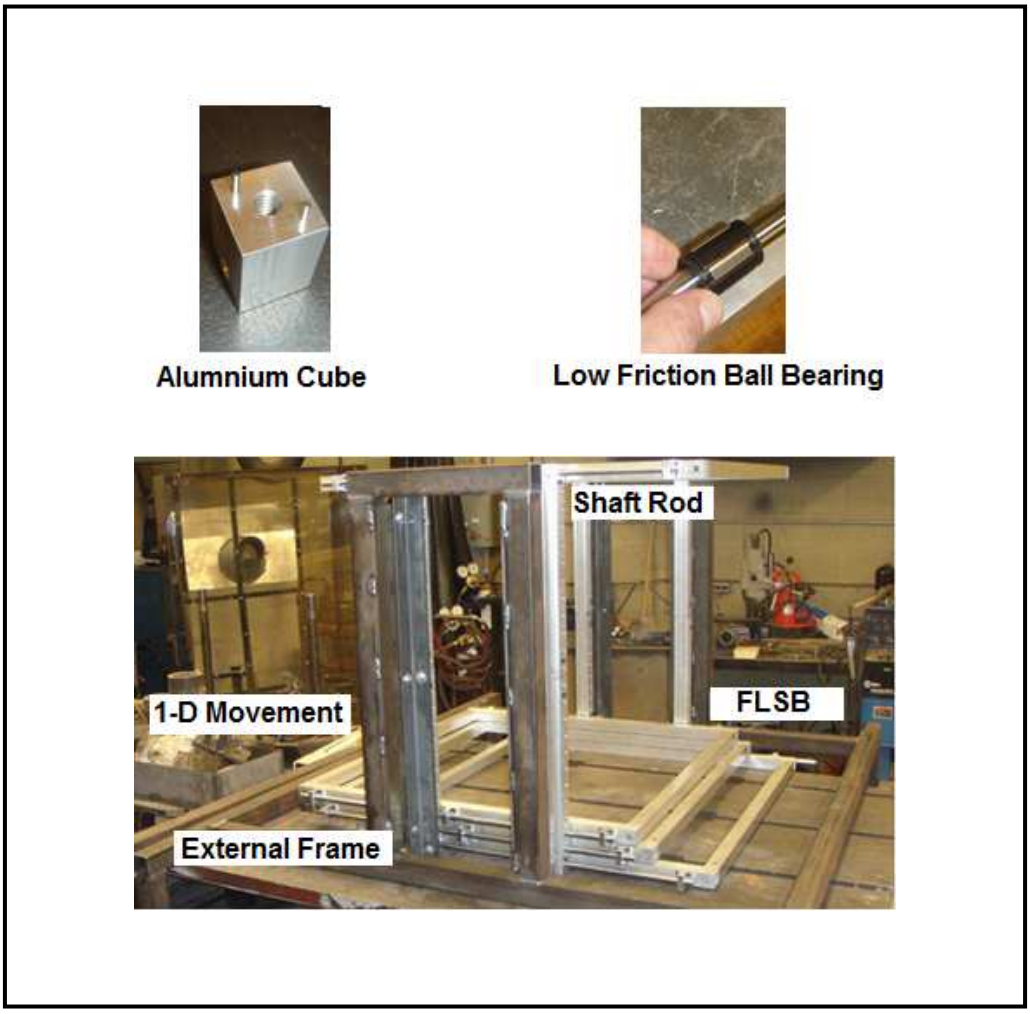

Figure 6.8 External frame of the University of Ottawa Flexible Laminar Shear Box (FLSB)

- A model footing of 150 mm × 150 mm in section and 300 mm in height is also placed on the soil surface. The bottom surface of the model footing was corrugated to introduce roughness in the footing. The mass of the model footing is 40 kg and the stress applied to the soil is 17.5 kN/m^2.
- The FLSB dimensions are 800 mm × 800 mm (in plan) and 800 mm (in depth) with provisions for collecting the required data that include; deformation, water level in the

box and matric suction below the surface footing. The FLSB described in this section (see Figure 6.8 through Figure 6.13), consists of 24 horizontal laminae supported individually by linear bearings and steel guide rods. The guide rods are connected to an external steel frame to transfer the load of the box into the ground and reducing the load applied on the shake table. The FLSB was designed to ensure that each laminae is sufficiently rigid during shaking tests. The laminae are comprised of solid high strength aluminum alloy box sections (31.65 mm × 31.65 mm) bolted together (using adjusting aluminum cubes installed as two per each lamina in the NS direction, see Figure 6.8) form rectangular laminae as shown in Figure 6.8 with plan dimensions of 800 mm × 800 mm. Each lamina is supported by two 15 mm diameter stainless steel guide rods connected to the outside edge of the lamina using stiff aluminum brackets (see Figure 6.8). The guide rods feed through six low-friction ball bearings per lamina which are housed in four vertical bearing brackets. The bearing brackets are in turn connected to the external support frame as shown in Figure 6.9 and Figure 6.10. The FLSB is formed by assembling the 24 lamina to form an 800 mm high, 800 mm long and 800 mm wide box with 2 mm of clearance between the lamina to ensure independent movement. The linear bearing system permits single-axis movement parallel to the longitudinal axis of the container (see Figure 6.10). Table 6.3 summarizes the physical properties of the flexible container and its components.

- Two L-channels are bolted to the four corners to align the lamina and to prevent shifting of the lamina during placement of the model sand layer in order to place soil into the flexible box.

- A thick wooden plate of 800 mm × 800 mm × 15 mm is bolted to the shaking table. The wooden plate was sprayed with sand on its surface in order to prevent sliding at the soil-base plate interface during shaking. The interior of the laminar shear box is then lined with thin flexible latex sheets, which prevent soil penetration into the gaps (i.e., 2 mm) between laminae and provide watertight confinement for cases where saturated soils are tested. Prior to compacting sand into the laminar container, the frictional resistance of each lamina was measured using a spring balance connected to the exterior face of each lamina. A flexible plastic bag of size of 800 mm × 800 mm ×

800 mm with 0.5 mm in thickness was used to prevent leakage of both the soil and water.

- The ratio between the width of the FLSB and the width of the model footing used in the study was 5.33 to alleviate the influence of boundary effects in the anticipated stress bulb zone (Poulos and Davis 1974). The depth of the FLSB was deeper than the expected depth of the stress bulb (i.e., 1.5*B* to 2*B*) below the model footing. Considerably larger depth was used such that the water table can be raised or lowered to vary the matric suction values in soil using the drainage valves.
- Cable Displacement Transducers (CDTs) were connected to the vertical frame and hanged down to the top of the model footing for measuring the vertical settlements of all the four corners of the model footing during testing. Another CDT was attached to the north side of the model footing and extended to the nearby wall of the laboratory to measure the horizontal deformation. An additional CDT was connected to measure horizontal movement of the shake table.
- An MTS actuator which has a loading capacity of 27 kN was used to apply the base shear to the shake table. A load cell capable of measuring 14 kN was mounted between the MTS actuator and the shake table too.
- Two transparent water supply plastic pipes of 15 mm in diameter were used to regulate the water supplied to the bottom layer of the soil in the plastic bag inside the FLSB. The main objective of supplying water is to gradually facilitate saturation of the soil. A 50 mm thick layer of clean coarse-sand was laid on the base area of the FLSB and a thin geotextile sheet that was placed on top of the coarse-sand to function as a porous barrier between the fine and coarse-grained sand. The objective of this layer is to facilitate free and gradual movement of water in the test tank in order to achieve uniform saturation or de-saturation conditions as desired by the testing requirements. Both saturation and de-saturation conditions were achieved successfully in the FLSB using this system.
- Three Tensiometers were installed after saturating the ceramic tips and located at different depths.

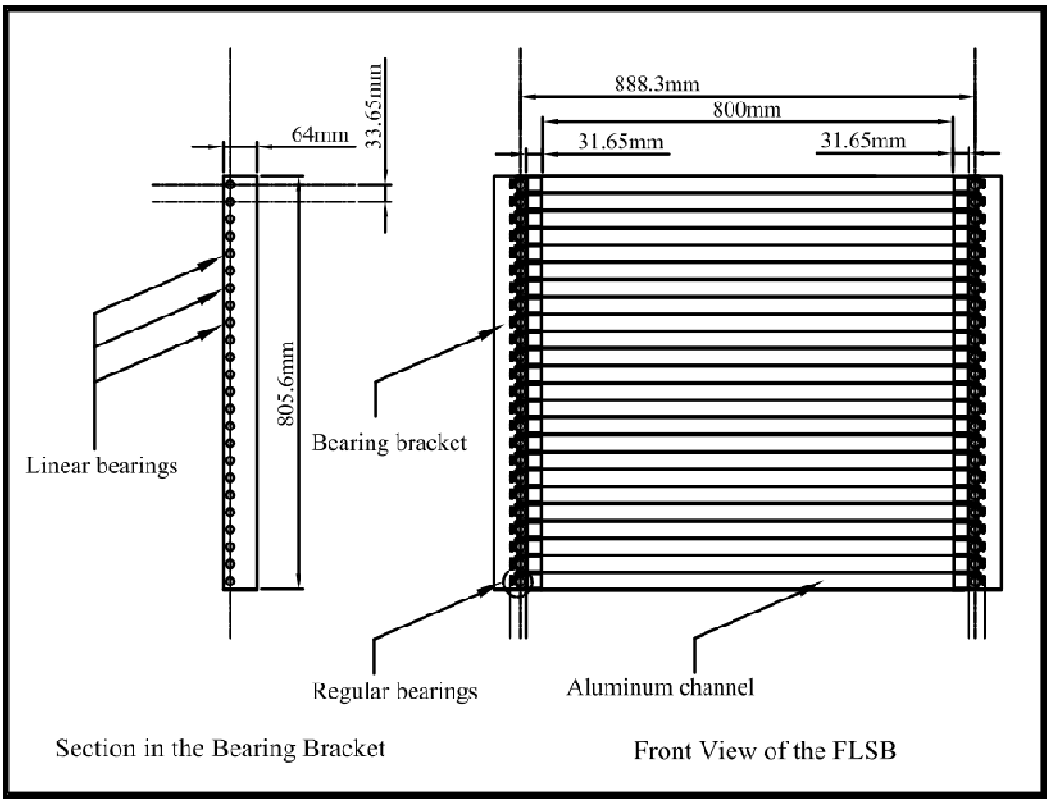

Figure 6.9 Section of the University of Ottawa Flexible Laminar Shear Box

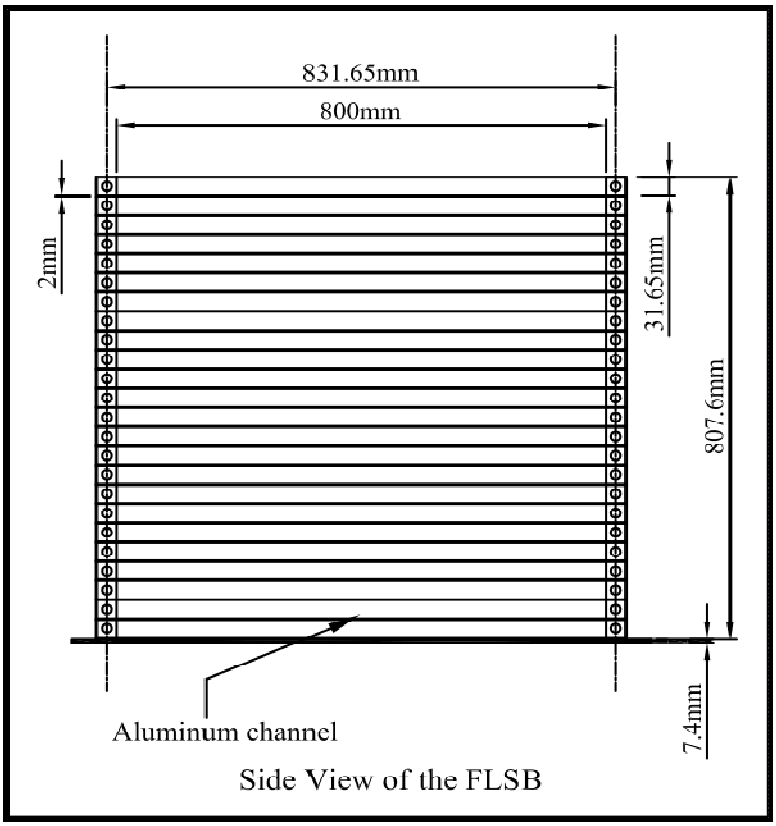

Figure 6.10 Side view of the University of Ottawa FLSB

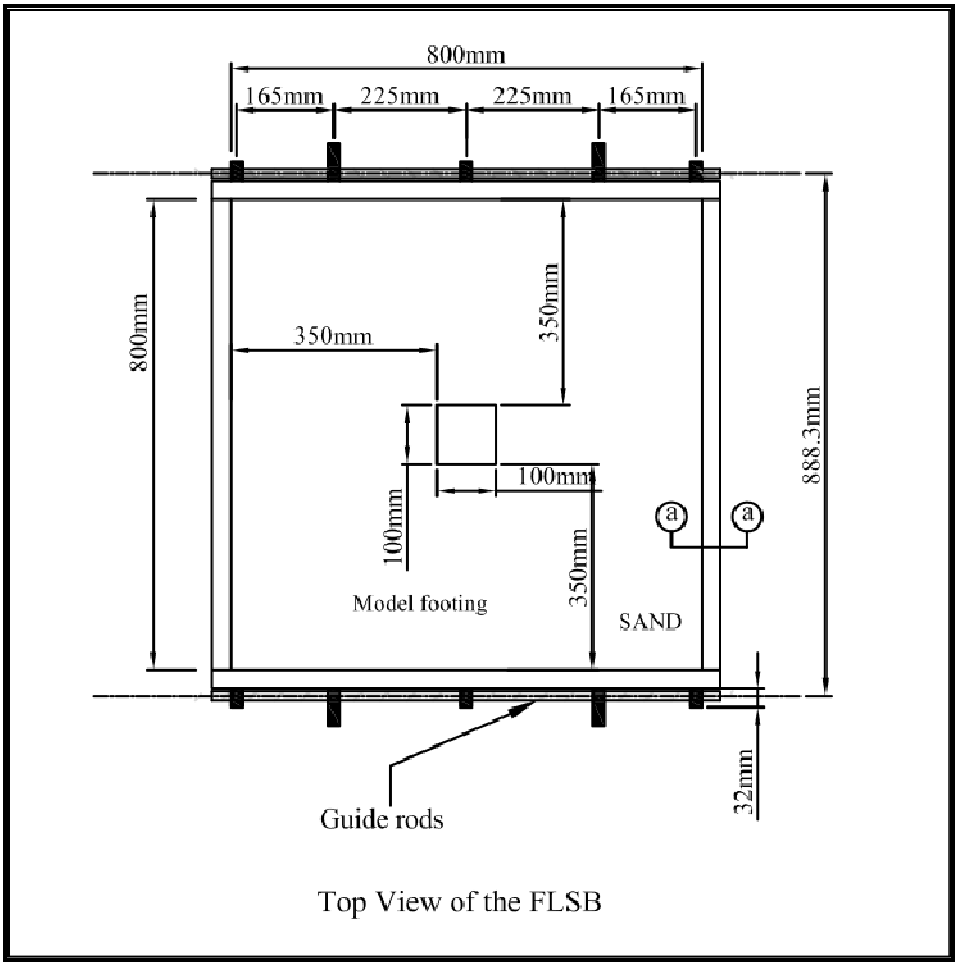

Figure 6.11 Plan view of the University of Ottawa FLSB

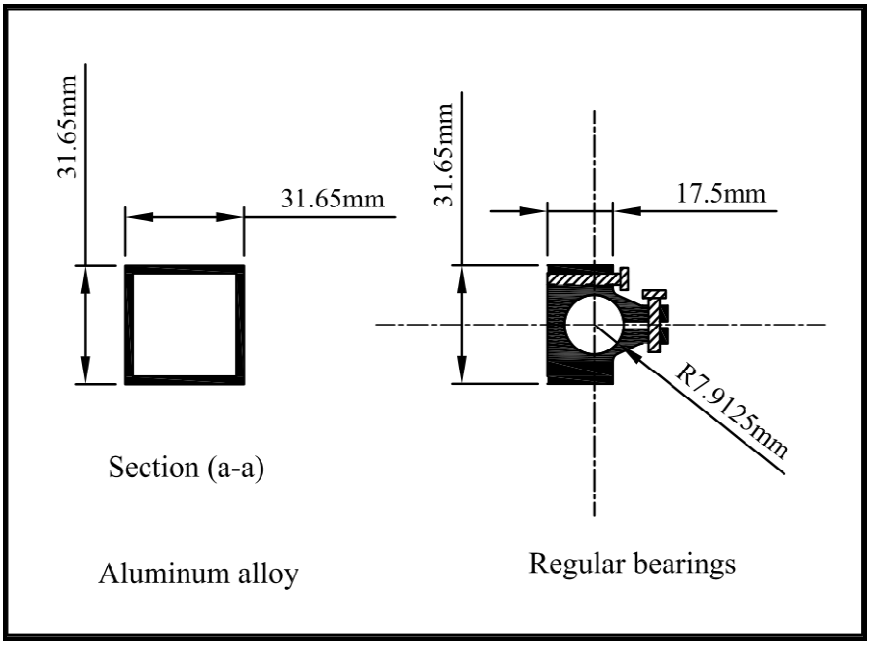

Figure 6.12 Sections of a lamina and the regular bearing of the University of Ottawa FLSB

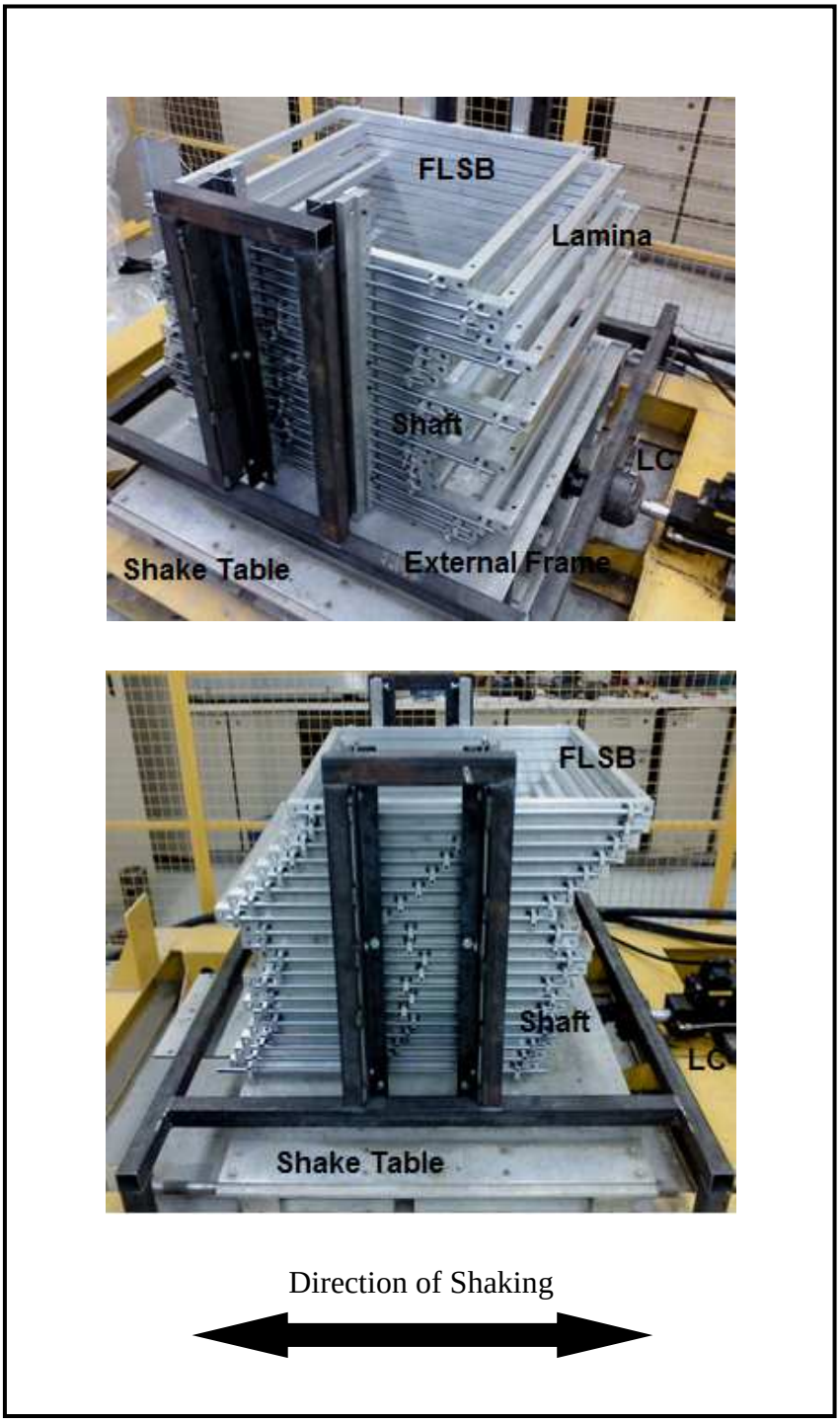

Figure 6.13 Two photos of the University of Ottawa Flexible Laminar Shear Box (FLSB)

Thompson bearings were used for the FLSB. The shafts were made of stainless steel bars of 850 mm long and 15 mm in diameter. The supporting blocks were custom designed in the University of Ottawa machine shop. Preliminarily tests on the FLSB were performed without the sand. It was expected that the mass of the FLSB and other connections will contribute to the inertia of the system. Due to this reason, a steel frame was designed in such a way to transfer the weight directly to the floor of the laboratory.

The FLSB was checked for friction resistance between the shaft rods and the bearings (while the FLSB is empty) by pulling each lamina individually using a spring scale. The test results show a small force of less than 0.005 N was required to move each of the lamina. The effect of the inertia due to the mass of the FLSB (~ 150 kg) was eliminated by transferring to the ground via external frames. The design of external frames used for the FLSB was consistent with Turan et al. (2009) as their actuator has a limited base shear capacity to apply on the shake table.

The flexible plastic bag (0.5 mm thickness; see Figure 6.14) which was used to hold the soil inside the FLSB has small stiffness in comparison to the tested sand and hence its effect on the movement of the FLSB was negligible.

Table 6.4 University of Ottawa FLSB components

Component	Property	Value	
Laminae	Number	24	
	Inside dimensions	31 mm × 31 mm	
	Mass	3.17 kg	
Bearing brackets	Number	4 External	2 Internal
	Dimensions	800 and 10 mm diameter	
	Mass	3.9 kg external	2.68 kg internal
Guide rods	Number	48	
	Mass	0.78 kg	
Linear bearings	Number	96	
	Length	20 mm	
	Diameter	10 mm	
	Mass	0.02 kg	
Membrane	Frictional force per lamina*	0.05 kg	
Bearings	Number	144	
	Mass	0.04 kg	
Adjusting aluminum cubes	Number	96	
	Mass	0.06 kg	
Total Mass of the Empty Test Box = 147.97 kg			
Model footing	Dimensions	150 mm × 150 mm × 300 mm	
	Mass	40 kg	
Soil mass	Mass	840 kg	

Figure 6.14 Photo showing the plastic bag in the University of Ottawa Flexible Laminar Shear Box (FLSB)

6.7.3 University of Ottawa Shake Table

The shaking table (i.e., earthquake simulator) at the University of Ottawa comprises of a 1-D 1000 mm × 1000 mm table that has features of lateral displacement (i.e., one degree of freedom as it moves back and forth to represent the soil motion during an earthquake). A hydraulic actuator controlled by a digital control module was used to drive the shake table. The shake table consists of two rigid steel panels (i.e., base and platform of 1000 mm × 1000 mm) with steel C-channels between them. It is designed to simulate ground excitations (i.e., sinusoidal or earthquake shaking) and vibrations to investigate the performance of shallow foundations in both saturated and unsaturated soils. A photograph of the shake table is shown in Figure 6.15.

The digital control module allows simulation of various types of dynamic displacement time-histories, including harmonic spectrum and pre-stored earthquake records. An amplifier is used to amplify the low voltages generated by the digital control module to high voltage signals suitable for driving the shake table. The shaking table can efficiently run in the range of 1 to 17 Hz, with 120 mm displacement limit in each directions and 27 kN base shear capacity.

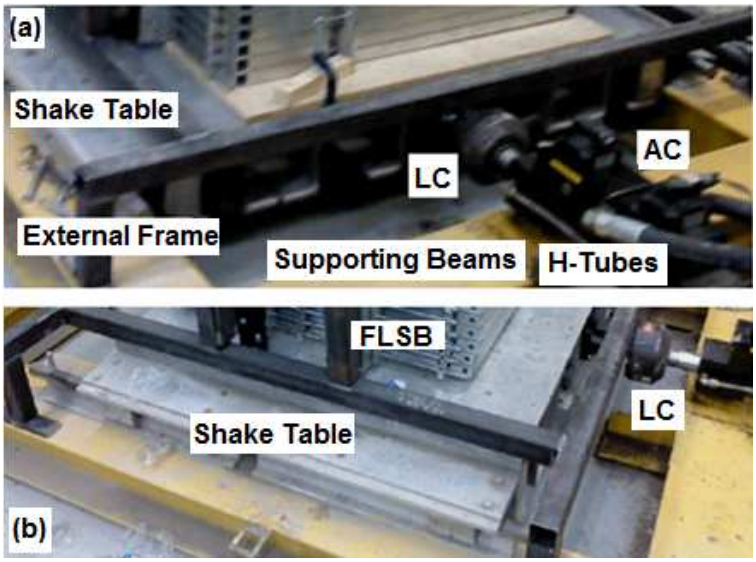

Figure 6.15 Photos (a) and (b) from different angles for the University of Ottawa shake table

6.7.4 Setup Preparation

Figure 6.16 shows the shake table setup used in the research program. Figures 6.17 through 6.20 show the instrumentation and the other components used in this research. The setup mainly consists of the following:

- Two computers
- Signal conditioning and data acquisition system Data Acquisition System (DAQS)
- Shake table
- Flexible Laminar Shear Box (FLSB)
- Hydraulic Actuator
- Hydraulic pump

- Load Cell (LC)
- Model footing (40 kg)
- Three accelerometers (2g)
- Tensiometers (0 to 90 kPa)
- Six cable displacement transducers (CDTs) (0 to 40 mm)
- Three small cups for soil sampling.
- Hand compactor (weight of 5 kg)
- Measuring tape, level and a ruler
- Camera

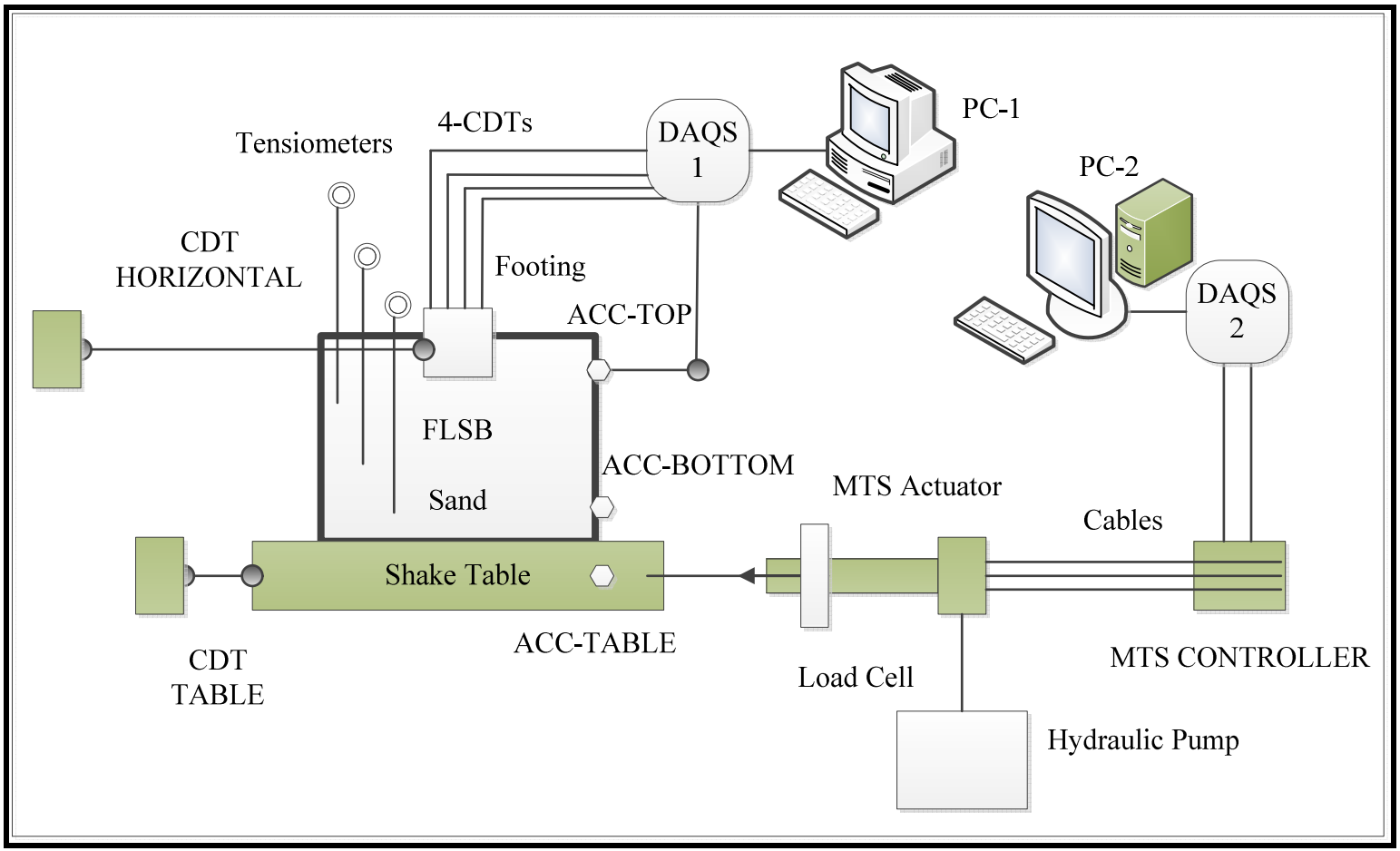

Figure 6.16 Schematic diagram of the test setup with different components

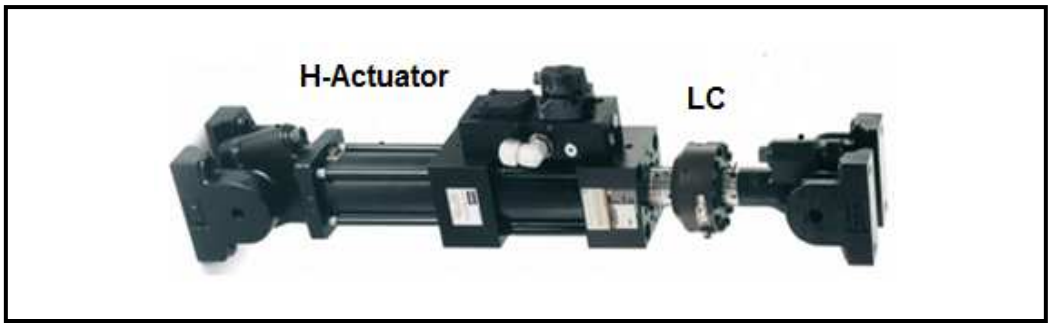

Figure 6.17 Photo of the MTS actuator (25 kN capacity)

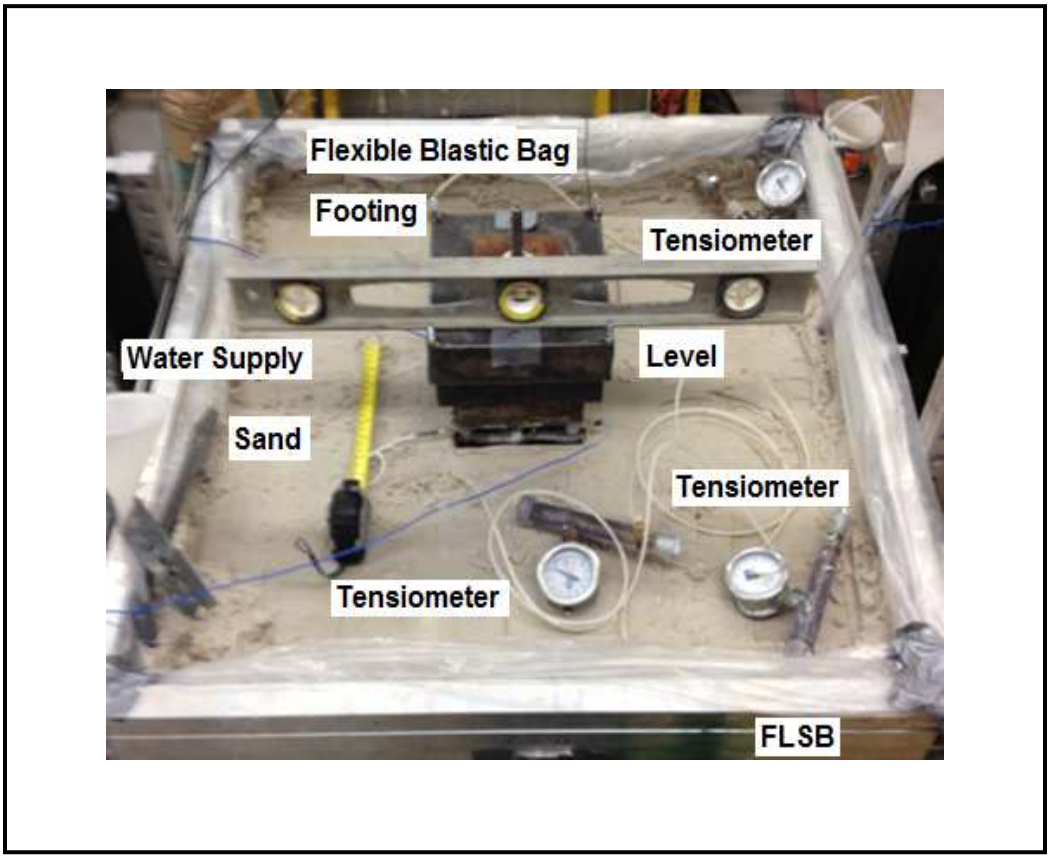

Figure 6.18 Photo showing the model footing and Tensiometers on the soil surface

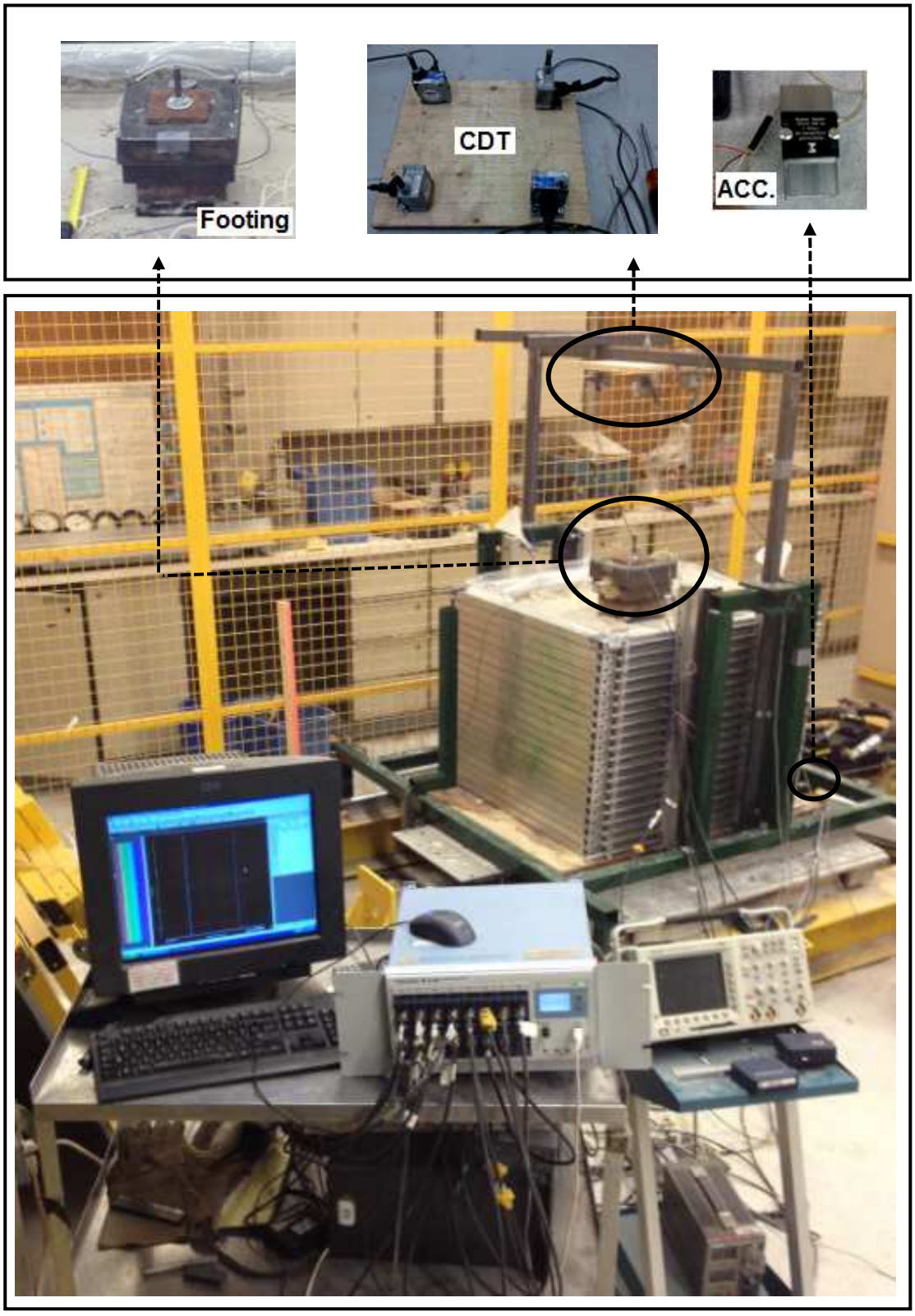

Figure 6.19 The shake table, LC and actuator

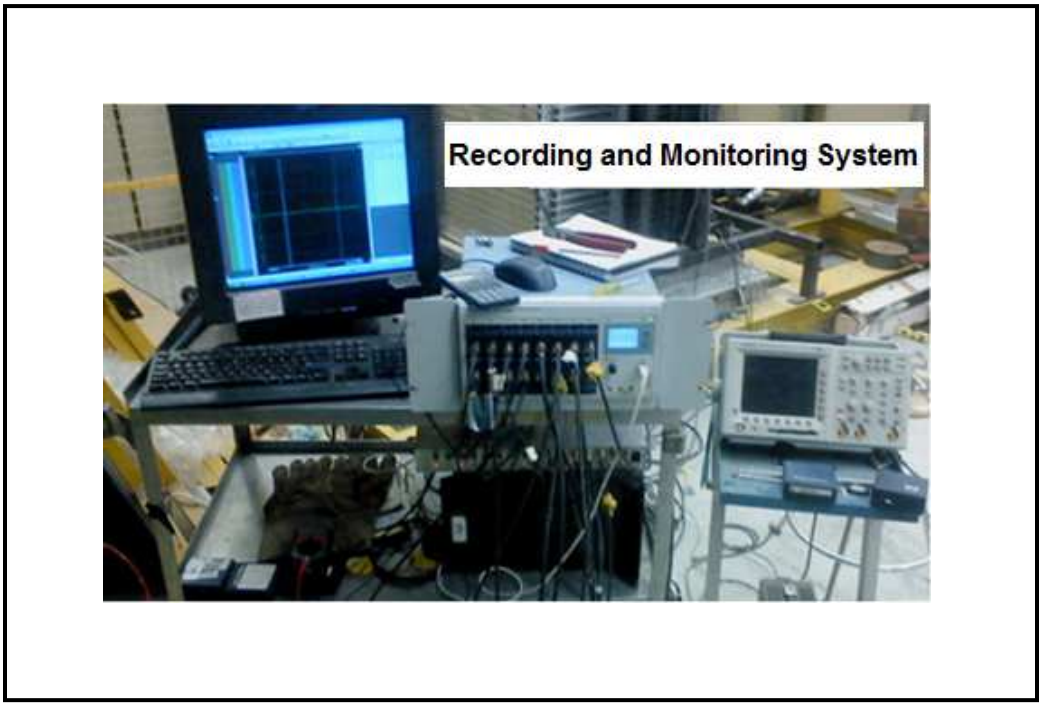

Figure 6.20 Computer and DAQS used for monitoring and recording deformations and accelerations

6.8 Tested Material

6.8.1 General

Classification of seismic response of soils is encouraged for all regions of Canada as per the National Building Code of Canada (NBCC-2010). Carleton University and the Geological Survey of Canada have applied different geophysical methods to carry out site classification measurements within the city of Ottawa. Figure 6.21 shows a map of the surficial geology of Ottawa region based on Motazedian et al. (2010) investigations. Coarse-grained soils (e.g., sands) are widely found in some regions of Ottawa. For example, sandy soils in Carp region are susceptible to liquefaction during EQ the ground shaking leading to damages in buildings and other infrastructure. Thus, understanding of

the behavior of sandy soils subjected to EQ loading condition valuable for improving design and construction procedures and guidelines. For this reason, a sandy soil was chosen for the study undertaken in the current investigations.

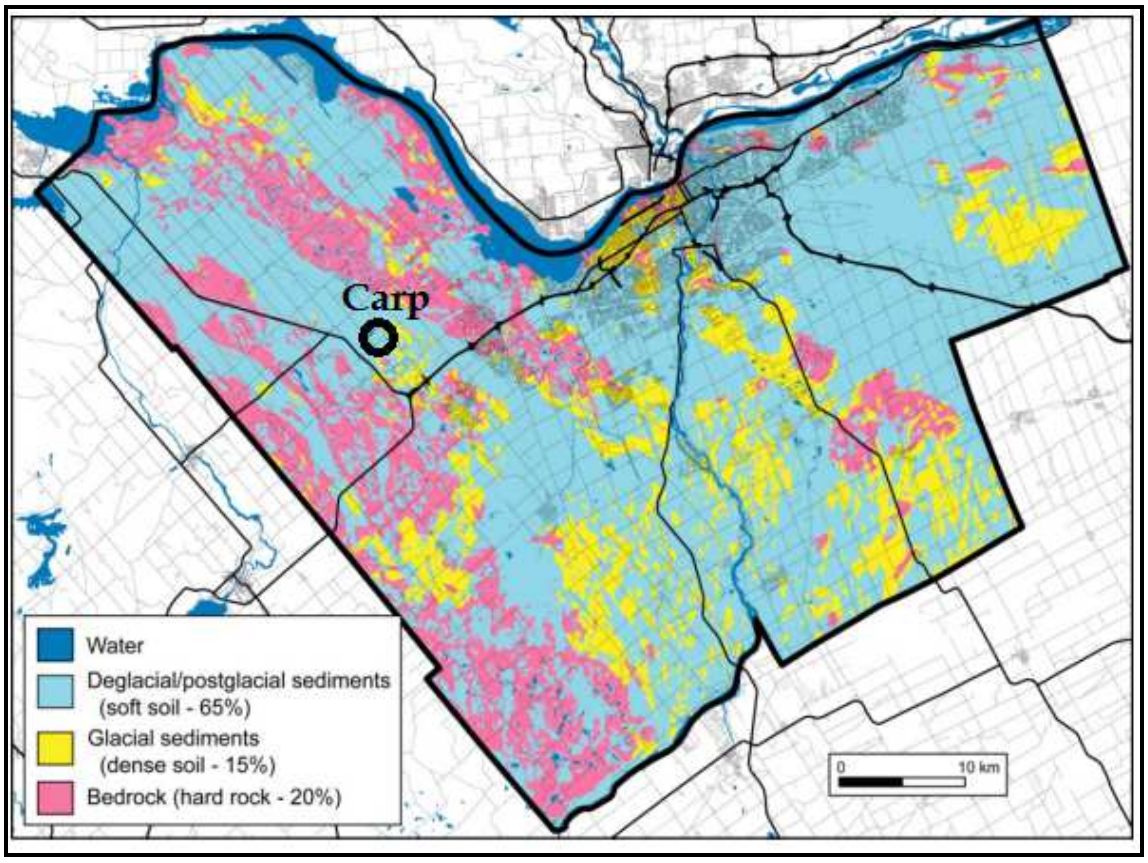

Figure 6.21 Microzonation map of the surficial geology of Ottawa (from Motazedian et al 2010)

6.8.2 Properties of Tested Material

The basic properties of the sand used for the testing program is summarized in Table 6.5. The tested soil is classified as per the USCS as poorly graded sand, *SP* (Figure 6.22)

which is more susceptible to liquefaction. In addition, the sand can be saturated or desaturated within a relatively short time period (i.e., 24 to 48 hrs).

Table 6.5 Summary of properties of the tested soil

Parameter or Soil Property	Value
Average dry unit weight, γ_d , kN/m³	16.02
Min. dry unit weight, $\gamma_{d\,(min)}$, kN/m³	14.23
Max. dry unit weight, $\gamma_{d\,(max)}$, kN/m³	17.25
Optimum water content, *o.w.c*, % (Standard Proctor Test)	14.6
Void ratio, *e* (after compaction)	0.62 – 0.64
Effective cohesion, *c'* , kN/m^2	0.6
Effective peak internal friction angle, ϕ' (^{o})	35.3

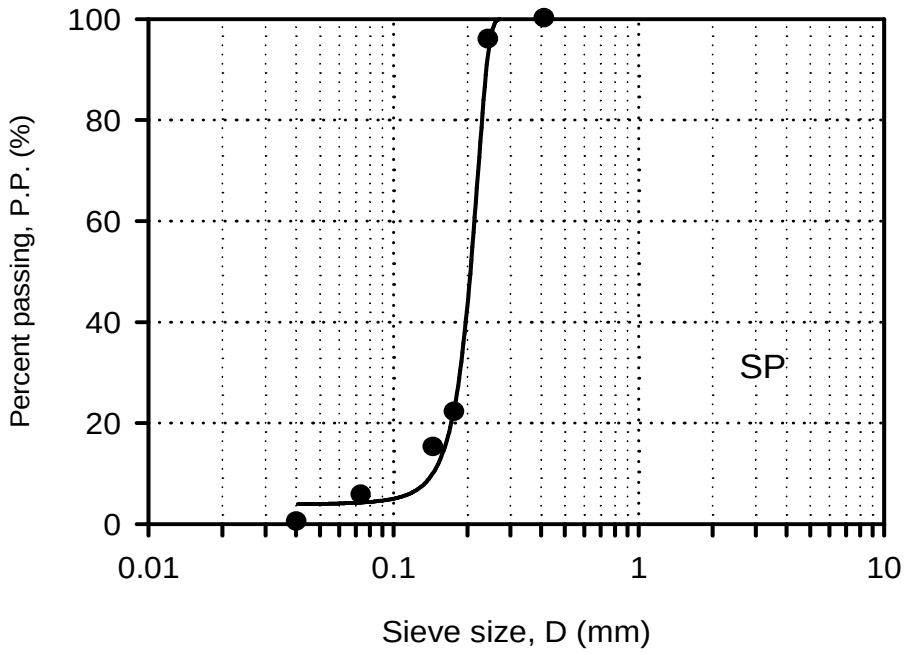

Figure 6.22 The grain-size distribution of the tested soil

6.9 Scale of the Model Footing

6.9.1 Scaling Factors from Previous Studies

Scaling relations are necessary to relate the small-scale studies to prototype (i.e., full-scale) using theories of small scale model similitude. The small scale models offer easy and economical approach for understanding the behaviour of soils under dynamic loading conditions as large scale or prototype studies are time consuming and expensive. Small scale models can be used to validate numerical models and to develop relationships to interpret or predict the results of full-scale geotechnical problems, both qualitatively and quantitatively. Table 6.6 presents the well-known scaling factors (i.e., geometric scaling) for single gravity dynamic models.

Table 6.6 Scaling factors for 1-*g* model simulated in a laboratory environment (Meymand 1998)

Description	Dimension	Prototype	Model
Stress	MLT^{-2}	1	$1/\lambda$
Length or displacement	L	1	$1/\lambda$
Acceleration	LT^{-2}	1	1
Mass	M	1	$1/\lambda^3$
Force	MLT^{-2}	1	$1/\lambda^3$
Time	T	1	$1/\lambda^{1/2}$
Frequency	T^{-2}	1	$\lambda^{1/2}$

6.9.2 Design of Model Footing

The results from shake table tests using small-scale model footings can be used for understanding the behaviour of large-scale footings. However, the interpretation of the results for field applications can be a difficult task (Al-Karani and Budhu 2001). Investigators such as Al-Karni and Budhu (2000) and Tsukamoto et al. (2012) have used model footings of 20.9 kg (applied stress of 20.5 kN/m^2) and 62.7 kg (applied stress of 61.5 kN/m^2), and 73 kg (applied stress of 8.7 kN/m^2) respectively for testing sandy soils under earthquake loading conditions. In this research program, a testing approach that was proposed by Iai (1989) and adopted by Al-Karani and Budhu (2001) for designing the model footing under seismic loading was followed. The relationship between the load carried by a large-footing on a cohesionless soil and the equivalent load that the model footing apply on the soil during shake table tests is shown in Eq. [6.1] as follows:

$$Q_m = Q_p/\lambda^3 \qquad [6.1]$$

where:

Q_m = equivalent load on the model footing, kg

Q_p = load on the large-scale (prototype) footing, kg

λ = scaling factor

A dead load of 1800 kN has to be applied on an in-situ footing (e.g., 1500 mm × 1500 mm) to reach an allowable settlement of 25 mm a sand under unsaturated conditions (Giddens and Briaud 1994). The section of the model footing used in the present study was 150 mm × 150 mm in order to provide stability and reduce the possibility of toppling during the early stages of each shaking test. Thus, a scaling factor, λ was equal to 10.

Using Eq. [6.1], the equivalent load on the model footing would be 180 kg. Due to the limitation of the size of the FLSB as well as the limited carrying capacity of the shake table available in the laboratory, a model footing of 40 kg-mass (applied stress of 17.5 kN/m^2) was designed. Three masses of steel (in square sections) were attached together as shown in Figure 6.23. A height of 350 mm for the model footing was also sufficient for the undertaken test program.

6.10 Testing Program

The primary goal of the testing program was to measure deformation behaviour at selected locations on the model footing (i.e., North-East, NE, North-West, NW, South-East, SE and South-West, SW, see Figure 6.23) using calibrated Cable Displacement Transducers, CDTs. Accelerations at three elevations on the setup (i.e., on the table, at the bottom of the soil and at the top of the soil) were measured using calibrated accelerometers. The FLSB and the shake table were used along with square model footings (i.e., 50 mm × 150 mm) to simulate earthquake ground shaking under both saturated and unsaturated conditions. The water table was raised to the top of the soil using tubes (made of flexible plastic, refer to Figure 6.14) inside the FLSB to achieve fully saturated conditions. Calibrated Tensiometers were used to measure the matric suction in the soil. After achieving desired saturated and unsaturated conditions, the tests were conducted to determine the relationship between the settlements, accelerations and

actuator force as function of time. Figure 6.24 shows the details of the experimental program as a flowchart. Table 6.7 provides summary of the tests conducted.

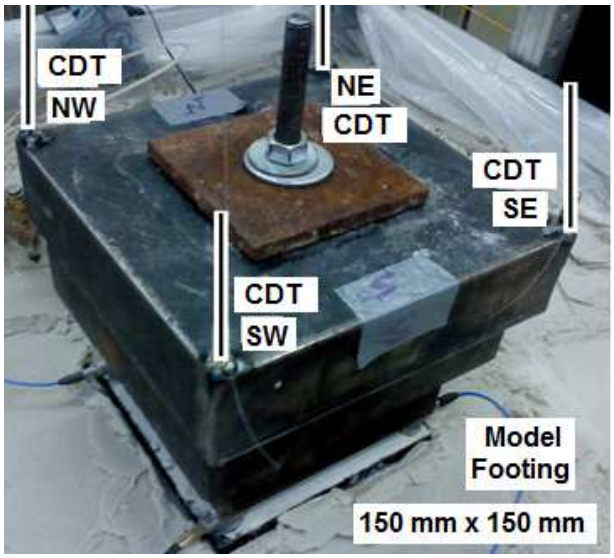

Figure 6.23 Measured settlement versus time of the model footing for saturated condition (Matric suction = 0 kPa)

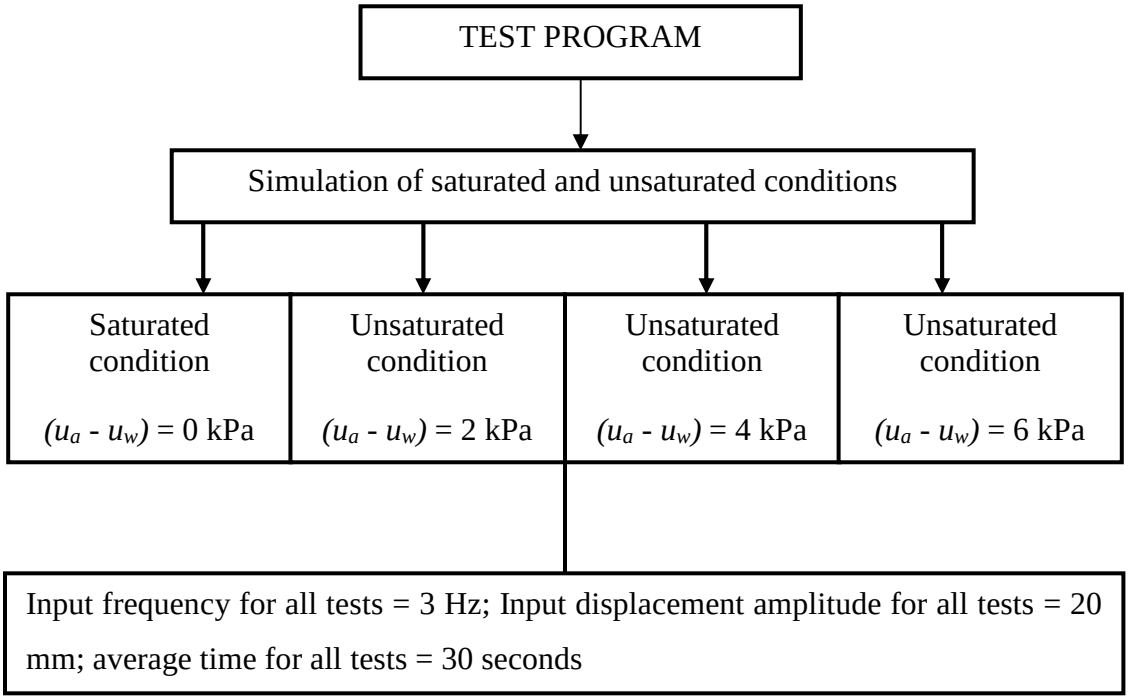

Figure 6.24 Flow-chart showing the simulated soil conditions in the FLSB

Table 6.7 Summary of the tests conducted

Test code	Objective	Type of loading	No. of tests
Test (I)	[1]to simulate saturated condition	Sine wave	1
*Test (II)	[2]to simulate unsaturated condition	Sine wave	2
*Test (III)	[3]to simulate unsaturated condition	Sine wave	2
Test (IV)	[4]to simulate unsaturated condition	Sine wave	2

[1]$(u_a - u_w)$ = 0 kPa; [2]$(u_a - u_w)$ = 2 kPa; [3]$(u_a - u_w)$ = 4 kPa; [4]$(u_a - u_w)$ = 6 kPa; *Test (II) and Test (III) are presented in Appendix (B)

6.10.1 Preparation of the Model Soil in the FLSB

All the tests were performed under identical initial conditions such that results are not influenced by changes in density. The relative density, D_r was carefully controlled for all the tests (D_r = 65 %). The density of the tested soil was verified by collecting soil samples in aluminum cups for all the tests (see Figure 6.25). The small cups used in the study had perforations which were placed at different levels in the box to determine the variation of water content with respect to the depth.

A number of experiments were performed in the tested sand by simulating earthquake loading under saturated and unsaturated conditions. The deformations (i.e., settlements) were recorded during each test. Accelerations at three different locations were monitored and recorded for comparison purposes. The first series of shake table tests performed under fully saturated condition (i.e., zero matric suction), and the second series of tests were conducted under unsaturated conditions for three different suction values (i.e., 2 kPa, 4 kPa and 6 kPa).

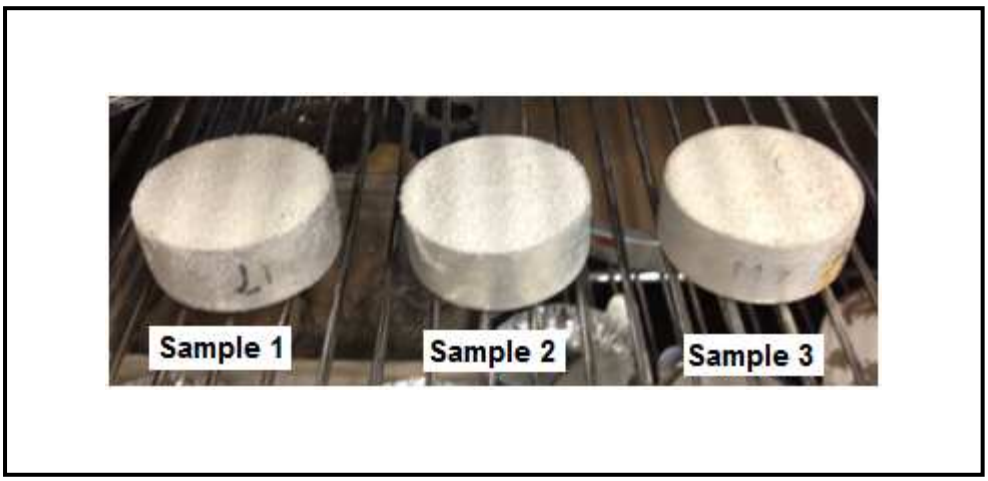

Figure 6.25 Aluminum cups for soil samples collection

6.10.2 Selection of Input Frequency and Amplitude

Three shake table tests were conducted at frequency values of 3 Hz, 4 Hz and 5 Hz for the same displacement amplitude of 20 mm (10 mm back and 10 mm forth). To simulate Ottawa region earthquake with ground acceleration of ~ 0.6*g* the following parameters were used as input into the system; the frequency, f = 3 Hz; amplitude = 20 mm; time, t = 30 seconds. Figure 6.26 summarizes the sinusoidal wave equation (i.e., $y(t) = A \times \sin(\omega \times t)$; where: A is the amplitude, $\omega = 2\pi \times f$ is the angular frequency, t is the elapsed time during shaking).

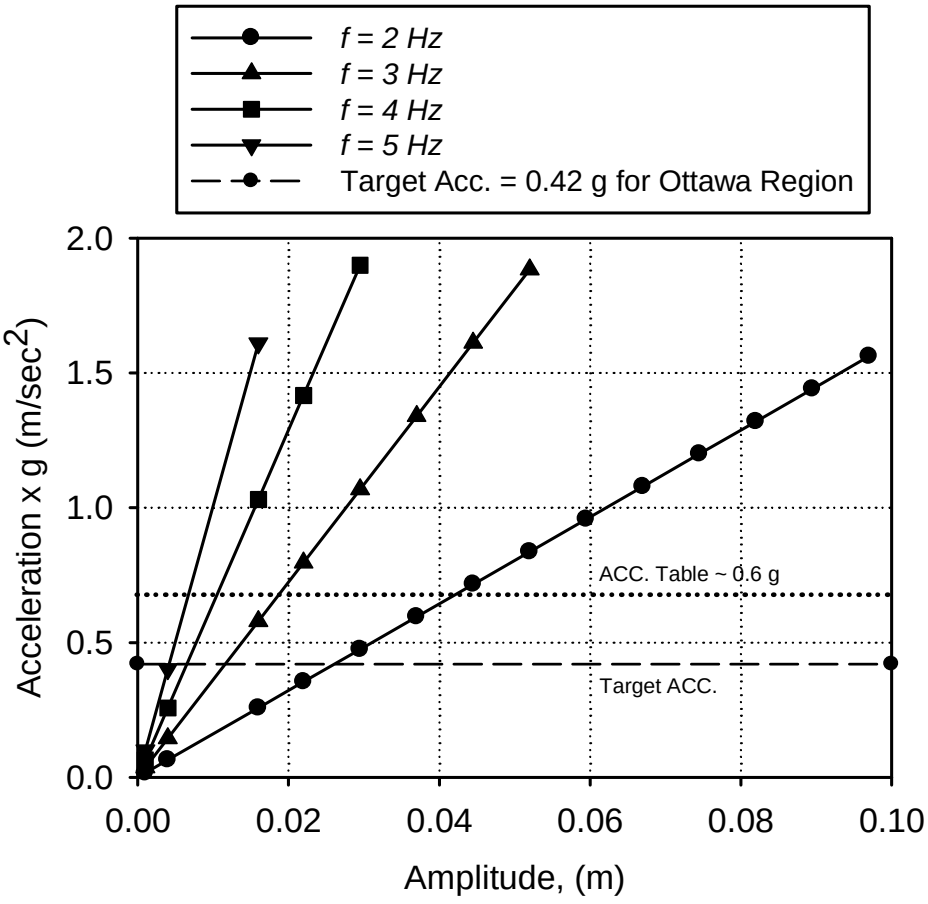

Figure 6.26 Acceleration versus amplitude of horizontal displacement for Ottawa region at different frequencies

From trial tests using the FLSB and the shake table and the tested sand, it was found that an acceleration level of 0.5*g* to 0.7*g* (at the base of the table) was enough to allow the movement of the FLSB as per the design specifications. It was noticed that a frequency value of 3 Hz provided smooth shaking in comparison to tests simulated with 4 Hz or 5 Hz which can be attributed to the difference between the input frequency and the natural frequency of the setup. In other words, a frequency of 3 Hz was used as an input in this research program (for all testes) to avoid approaching resonance state which might lead to damaging the instrumentation, if not the entire setup. The entire setup which consists of the FLSB and the shake table, was used to simulate worst case scenario of an

earthquake ground shaking (e.g., sinusoidal wave form) that might occur in Ottawa region with peak ground acceleration of ~ 0.42 m/sec^2.

For that reason, each shaking test was prepared to be conducted at an input frequency of 3 Hz, amplitude of 20 mm and 30 to 40 seconds applying a sinusoidal wave form. The different tests carried out in this testing program are discussed in a later section.

6.10.3 Shake Table Test (I) for Saturated Condition ($(u_a - u_w) = 0$ kPa)

The water table was slowly raised from the base of the FLSB for saturation through the bottom layer of the coarse sand (50 mm in thickness). This technique facilitated escape of air from bottom to the surface layers of the soil in the box gradually to ensure a fully saturated condition. The water supply was stopped once the water level reached the soil surface in the FLSB. All Tensiometers recorded zero suction values after saturation and during the testing period. The model footing 150 mm × 150 mm was gently placed on the soil surface and the test was conducted for 30 to 40 seconds. Samples of sand were collected before the test started and the results are shown in Table 6.8.

The data recorded on the computer was post-processed, organized and plotted using Xviewer and using SigmaPlot software, respectively. The measured acceleration at the top of the soil (i.e., ACC TOP, see Figure 6.27) was lower in comparison to the recorded acceleration (i.e., ACC TOP = 65 % of the ACC BOTTOM, see Figure 6.28) due to the occurrence of liquefaction of the saturated sand which was observed immediately after the shaking test was initiated.

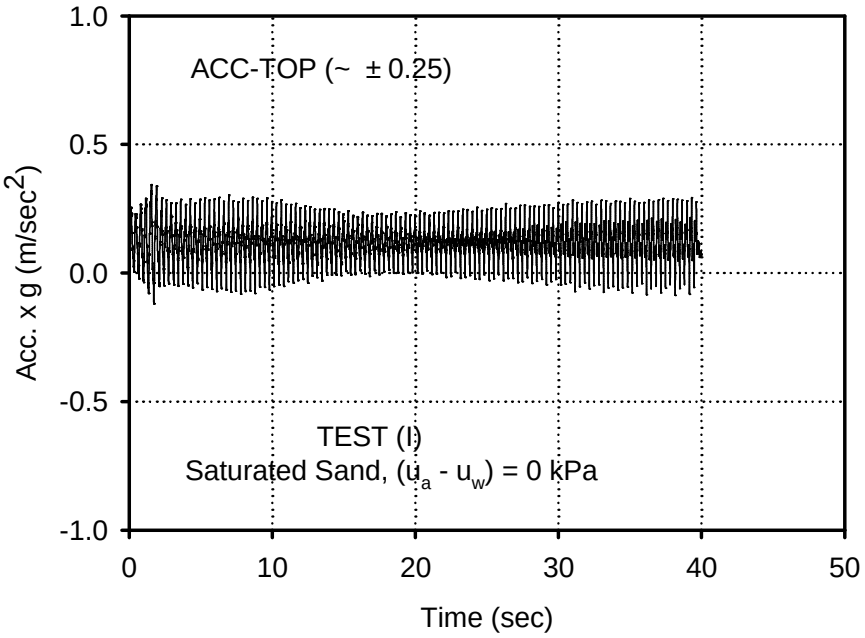

Figure 6.27 Measured accelerations time history at the top of the soil for the test conducted under saturated condition (Matric suction = 0 kPa)

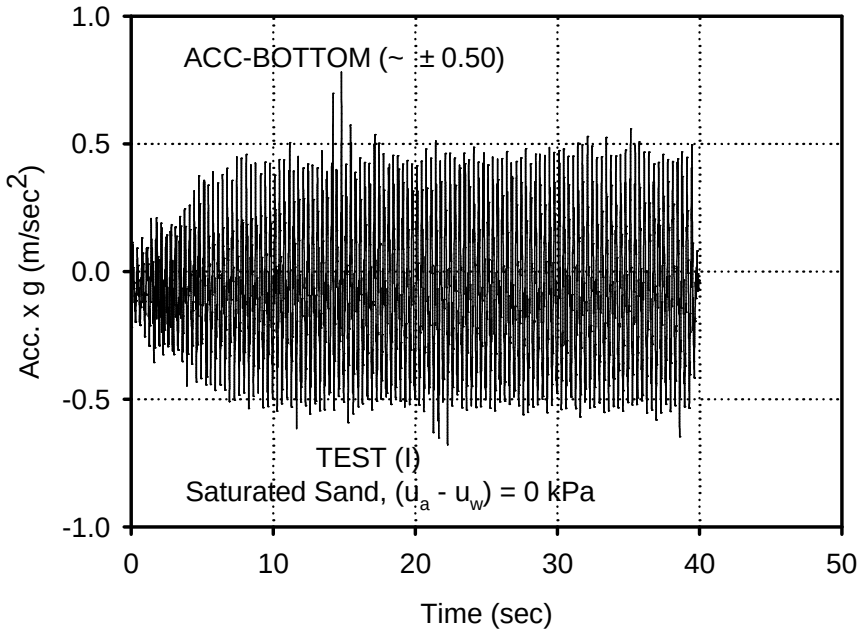

Figure 6.28 Measured accelerations time history at the bottom of the soil for the test conducted under saturated condition (Matric suction = 0 kPa)

Table 6.8 Data from the tested sand (prior to shaking) for AVR matric suction of 0 kPa in the stress bulb zone (i.e., 1.5*B*) surface model footing using FLSB on Shake Table

Parameter or Property (Test I)					
[1]D (mm)	[2]γ_t (kN/m^3)	[3]γ_d (kN/m^3)	[4]w (%)	[5]S (%)	[6]$(u_a - u_w)_{AVR}$ (kPa)
10	19.74	15.95	23.8	~100	0.0
225	19.74	15.95	23.8	~100	0.0

[1]Depth of a tensiometer from the soil surface; [2]total unit weight; [3]dry unit weight; [4]water content; [5]degree of saturation, [6]average matric suction in the stress bulb zone.

Figure 6.29 shows the measured force during shaking the table back and forth by the MTS actuator which was 1375 N within an input value of displacement amplitude of 20 mm.

Figure 6.30 shows the measured settlements at the four corners of the 150 mm × 150 mm model footing (i.e., NE, NW, SE, and SW). The settlement was increasing linearly with time during the shaking for this particular case (i.e., saturated condition). The increase in settlement can be attributed to the fact the sand started to liquefy soon after the shaking commenced. The model footing was observed to slowly sink into the saturated sand. This sinking of the footing can attenuate the seismic motion transfer from the soil surface. These observations were consistent with the conclusions drawn by Tutunchian et al. (2011) where excessive settlement was observed.

The model footing tested on saturated sand (i.e., Test I) had a 12 mm of settlement (i.e., static settlement) prior to shaking.

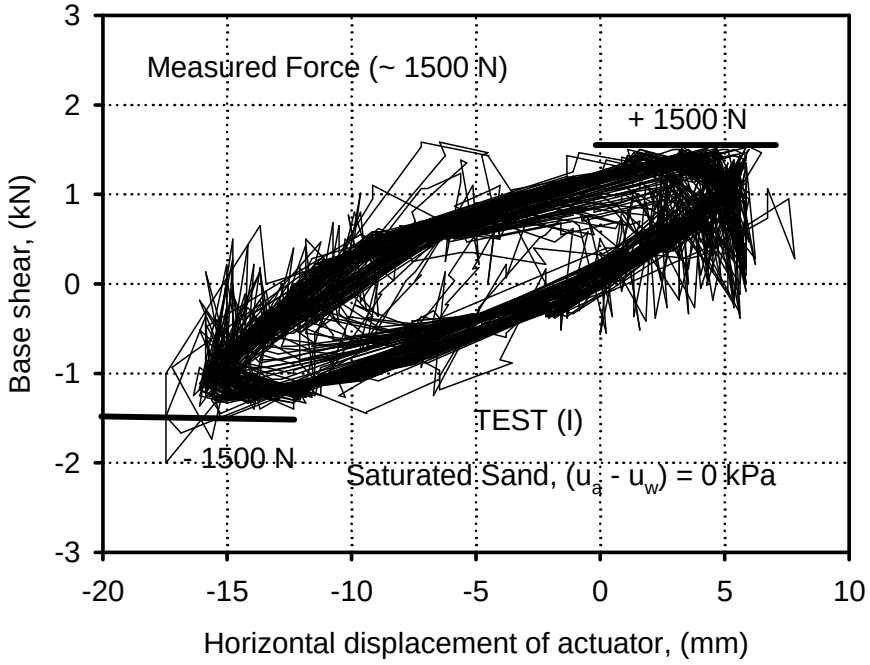

Figure 6.29 Measured base shear versus horizontal displacement for the test conducted under saturated condition (Matric suction = 0 kPa)

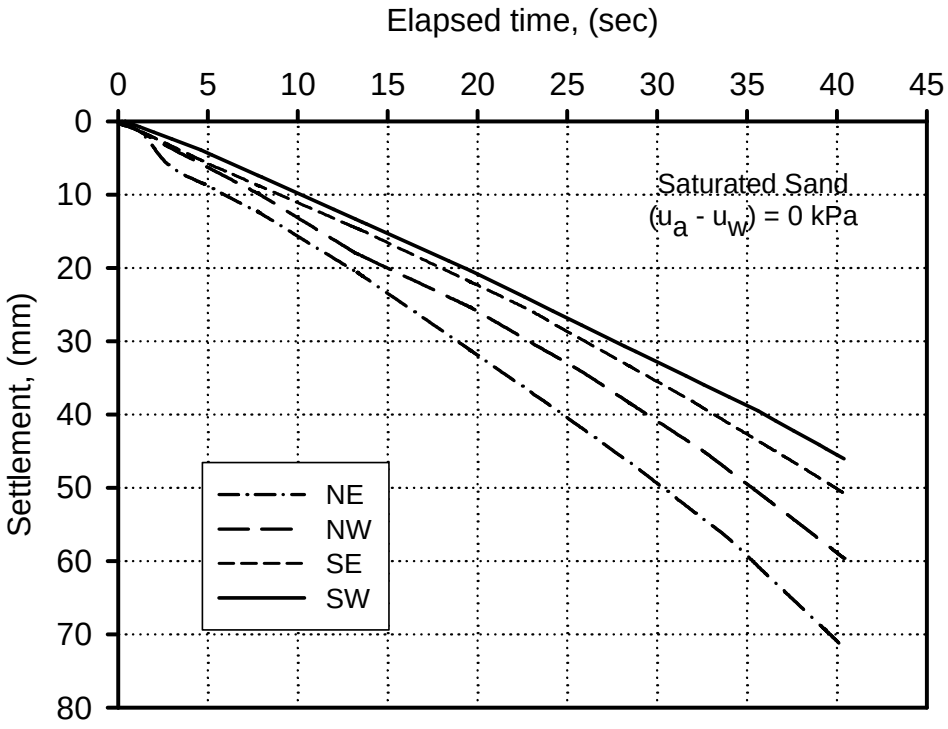

Figure 6.30 Measured settlement versus time of the model footing for the test conducted under saturated condition

6.10.4 Shake Table Test (IV) for Unsaturated Condition ($(u_a - u_w)$ = 6 kPa)

Table 6.9 summarizes the key test data collected during the tests. Matric suction value of 6 kPa was achieved in the stress bulb zone of the model footing.

The measured acceleration at the top of the soil (i.e., ACC TOP, see Figure 6.31) was close to the input acceleration recorded at the bottom of the sand (i.e., ACC TOP = 80 to 85 % ACC BOTTOM, see Figure 6.32) showing small amplitude spikes. These spikes can be attributed to dilative response of the sand as there was low confinement at the shallow depth of the soil. This observation is consistent with conclusions drawn by Wang et al. (2012). Liquefaction of the unsaturated sand (matric suction = 6 kPa) was not noticed. This may be attributed to the negligible increase in the pore-water pressure due to shaking as the water table was far below the stress bulb zone of the model footing.

Figure 6.33 shows the measured base shear during shaking the table back and forth by the MTS actuator. The maximum measured force was 2300 N; this value is within the required amplitude of 20 mm as measured from horizontal displacement data. Figure 6.34 shows lower settlement values measured in comparison to the previous tests (maximum ~ 2.5 mm) at the four corners of the model footing. No increase in settlement was observed during the shaking confirming that the sand was still in unsaturated condition (6 kPa) which has higher shear strength compared to the previous three cases (i.e., 0 kPa, 2 kPa and 4 kPa). The settlement of the footing on the sand (i.e., static settlement) prior to shaking was approximately 2 mm. In contrast to the other test results, it was noticed that the Tensiometers did not change after the test completed and no water was gushing from both the water supply pipes confirming that no excess pore water pressure was generated in the unsaturated sand for this particular case (6 kPa). More details about this behavior are discussed in a later section using the SWCC as a tool.

Table 6.9 Data from the tested sand (prior to shaking) for an average matric suction of 6 kPa in the stress bulb zone (i.e., 1.5*B*) surface model footing using FLSB on Shake Table

Parameter or Property (Test IV)					
[1]D (mm)	[2]γ_t (kN/m^3)	[3]γ_d (kN/m^3)	[4]w (%)	[5]S (%)	[6]$(u_a - u_w)_{AVR}$ (kPa)
10	18.17	15.94	14	58.2	6
220	19.27	16.07	20.0	86	4
600	19.74	15.95	23.8	100	0.0

[1]Depth of a Tensiometer from the soil surface; [2]total unit weight; [3]dry unit weight; [4]water content; [5]degree of saturation, [6]average matric suction in the stress bulb zone.

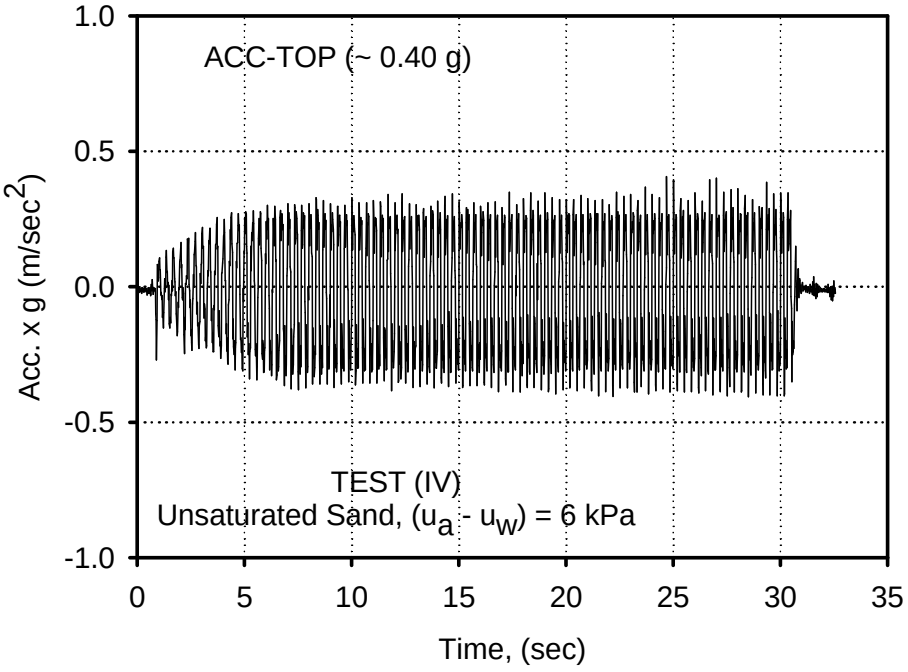

Figure 6.31 Measured accelerations time history at the top of the soil for the test conducted under unsaturated condition (Matric suction = 6 kPa)

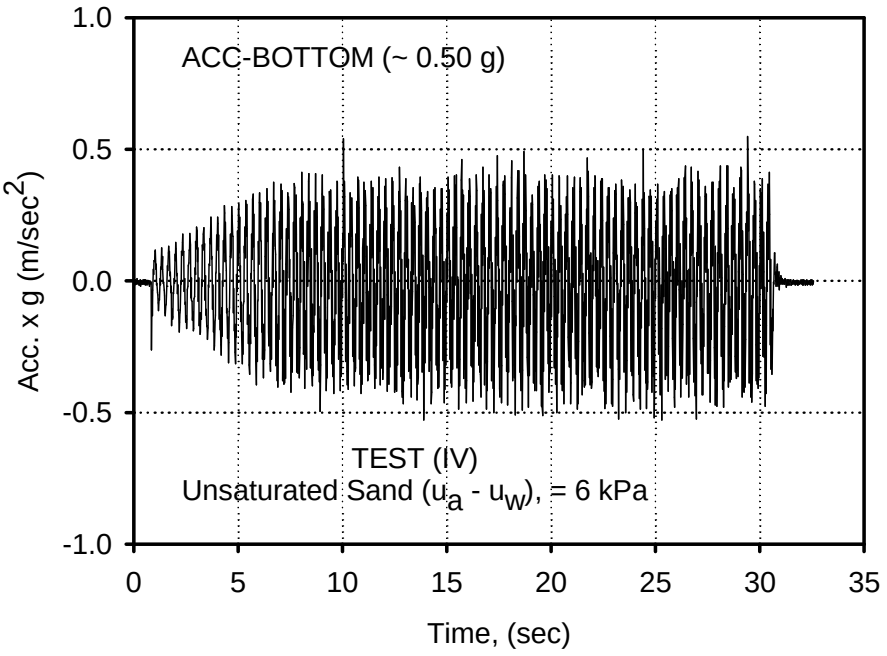

Figure 6.32 Measured accelerations time history at the bottom and of the soil for the test conducted under unsaturated condition (Matric suction = 6 kPa)

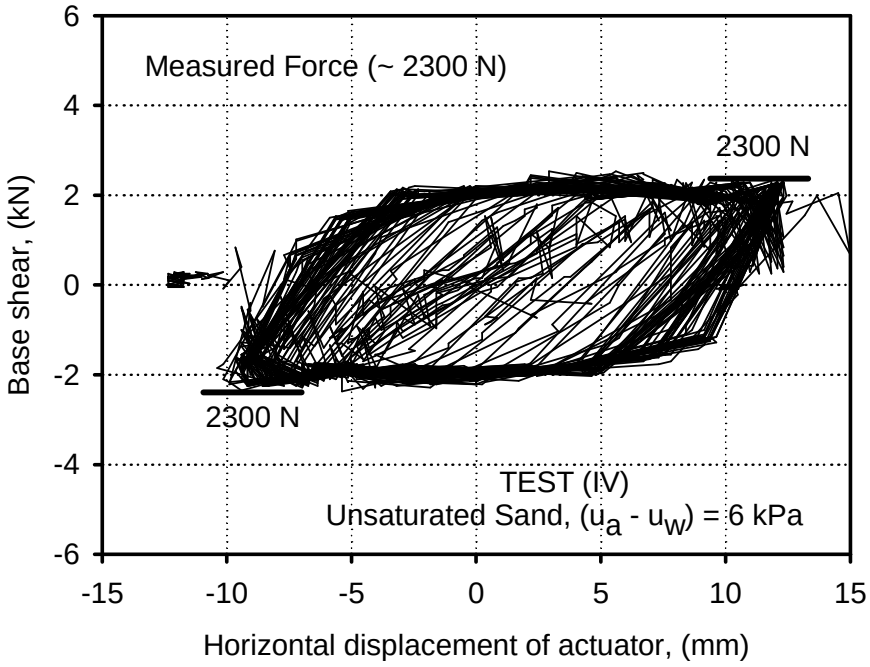

Figure 6.33 Measured base shear versus horizontal displacement the test conducted under unsaturated condition (Matric suction = 6 kPa)

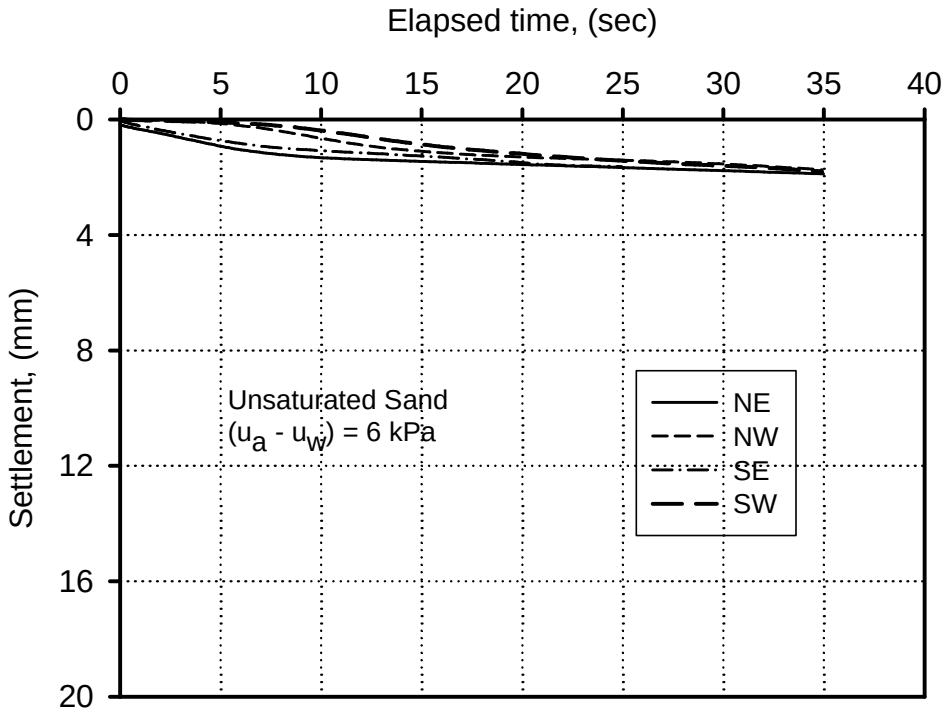

Figure 6.34 Measured settlement versus time of the model footing for the test conducted under unsaturated condition (Matric suction = 6 kPa)

6.11 Analysis and Discussion of Results

Past earthquake records show that severe damages of structures are usually caused by EQs with frequency, *f* in the range of 1 to 5 Hz and peak average amplitude of acceleration of 0.5*g* (Gopikrishna 2000). In this research program, a frequency value of 3 Hz was considered as an input for simulating the EQ shaking. A frequency of 3 Hz provides a level (i.e., intensity) of shaking as desired avoiding the resonance state. Based on the trial tests, an average double amplitude of displacement (in the positive and negative direction) of 20 mm was reasonable with an input frequency, *f* of 3 Hz to simulate an acceleration amplitude of ~ 0.5*g* approximately. A number of accelerometers were installed to record the acceleration values using accelerometers (capacity range ~ 2*g*) at two different locations (i.e., bottom and top) of the soil in the FLSB. The acceleration time history corresponding to the frequency of 3 Hz and amplitude of 20 mm

for each test (e.g., saturated or unsaturated condition) was measured using the DAQS. The maximum applied force recorded during the EQ shaking tests was in the range of 3000 N which is within the capacity of the MTS actuator.

Liquefaction initiated immediately after shearing of the saturated sand (e.g., Test I). In unsaturated sands, the liquefaction is achieved when the pore air pressure, u_a equals pore water pressure, u_w and also equals the total stress, σ (Unno 2008). As shown in Figure 6.35, the time for liquefaction initiation observed at the sand surface during testing unsaturated conditions has increased with an increase of matric suction. For the tests conducted in sand under unsaturated conditions; 2 kPa and 4 kPa, the liquefaction was observed after 20 sec and 25 sec, respectively. Table 6.10 summarizes the changes of matric suction in the stress bulb zone after the tests were completed. Changes of matric suction values are indications of changes in the response of the tested sand to the EQ loading during the duration of shaking.

Table 6.10 Input accelerations at three locations and the range of the applied force exerted by actuator for each test

Acceleration (m/sec^2)	Sat. Test (I)	Unsat. Test (II)	Unsat. Test (III)	Unsat. Test (IV)
	0 kPa	2 kPa	4 kPa	6 kPa
[1]BOTTOM	0.50g	0.50g	0.50g	0.45g
[2]TOP	0.25g	0.45g	0.52g	0.40g
Applied force by actuator (N)	1400-1500	2300-2400	1900-2300	2000-2300
Liquefaction	*Liquefaction occurred*	*Liquefaction occurred*	*Liquefaction occurred*	*No liquefaction was observed*

[1] Accelerometer located at the bottom of the soil; [2] Accelerometer located at the top of the soil

The matric suction values for Test (II) and Test (III) decreased as the water in the sand was squeezed upwards with time leading to the liquefaction (see Table 6.11).

Table 6.11 Changes of matric suction values after the tests were completed

Test #	Reading of Tensiometer before test started	Reading of Tensiometer after test complotted	Remarks
Test (I)	$(u_a - u_w)$ = 0.0 kPa	0.0 kPa	Liquefied
Test (II)	$(u_a - u_w)$ = 2.0 kPa	~ 0.0 kPa	Liquefied after 20 sec
Test (III)	$(u_a - u_w)$ = 4.0 kPa	~ 2.0 kPa	Liquefied after 25 sec
Test (IV)	$(u_a - u_w)$ = 6.0 kPa	6.0 kPa	No liquefaction

$(u_a - u_w)$ = average matric suction in the stress bulb zone of the model footing

From the experimental results of the undertaken research program in this Chapter, it can be seen that in addition to the cyclic loading (shaking) the excess pore water pressure generation leads to initiation of liquefaction of the tested sand. Several studies which focus on susceptibility of saturated sands to liquefaction were reported in geotechnical literature (Terzaghi and Peck 1948, Casagrande 1975, Dobry R. et al. 1982 and Vaid and Sivathayalan 1996).

In this experimental investigation, the focus was to study the model footing behaviour during seismic loading in unsaturated sandy soil. The matric suction (i.e., negative pore water pressure) was measured using Tensiometers before and at the completion of the tests as summarized in Table 6.11. The matric suction values of test (II) and Test (III) changed from 2 kPa and 4 kPa to 0 kPa and 2 kPa, respectively indicating excess pore water pressure of 2 kPa for the two cases, hence, and liquefaction occurred accordingly.

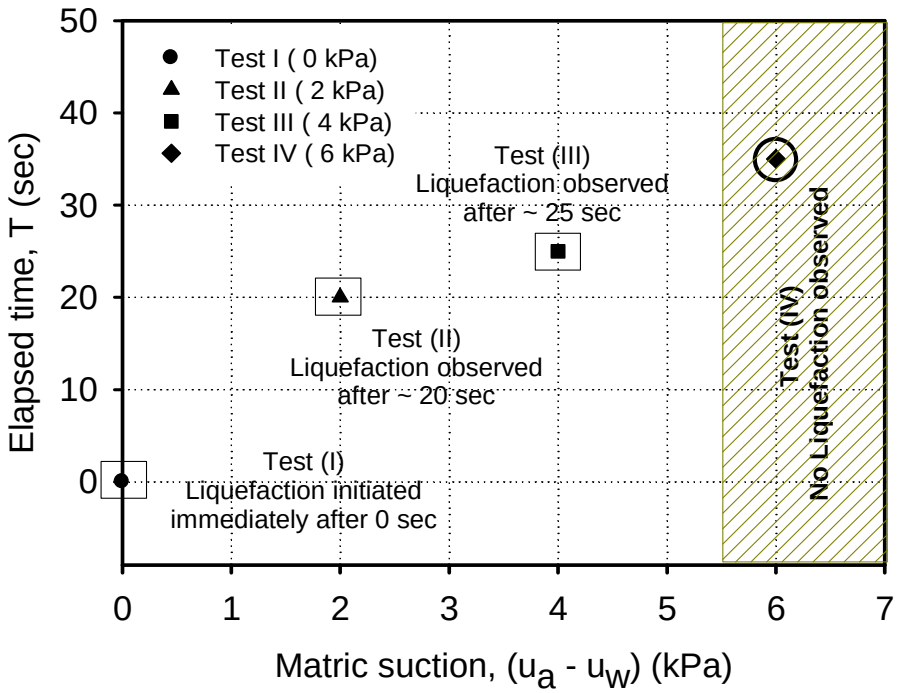

Figure 6.35 Liquefaction with time for tests conducted under saturated and unsaturated conditions (Matric suction = 0 kPa, 2 kPa, 4 kPa and 6 kPa)

The model footing on the saturated sand started sinking immediately after subjecting the FLSB to shaking. Measured settlements (i.e., liquefaction induced settlement) of the model footing were large for the saturated sand test (i.e., Test I). The settlement of the model footing during shaking increased with time (for 0 kPa, 2 kPa and 4 kPa conditions) due to liquefaction which was caused by the gradual increase of excess pore-water pressure (and decrease of matric suction in Test II and Test III) between the lower and upper layers of the tested sand. Because of the collapse of void spaces in the sand, the degree of saturation increased and the matric suction decreased leading to reductions in the effective stress and shear strength (i.e., shear modulus). On the other hand, measured settlements of the model footing were small in the case of unsaturated test under 6 kPa (i.e., Test IV) because the matric suction contributed to inter-particle forces between the soil grains. A relationship between the measured settlement with time for the model footing under different saturated and unsaturated conditions under similar EQ loading is presented in Figure 6.36.

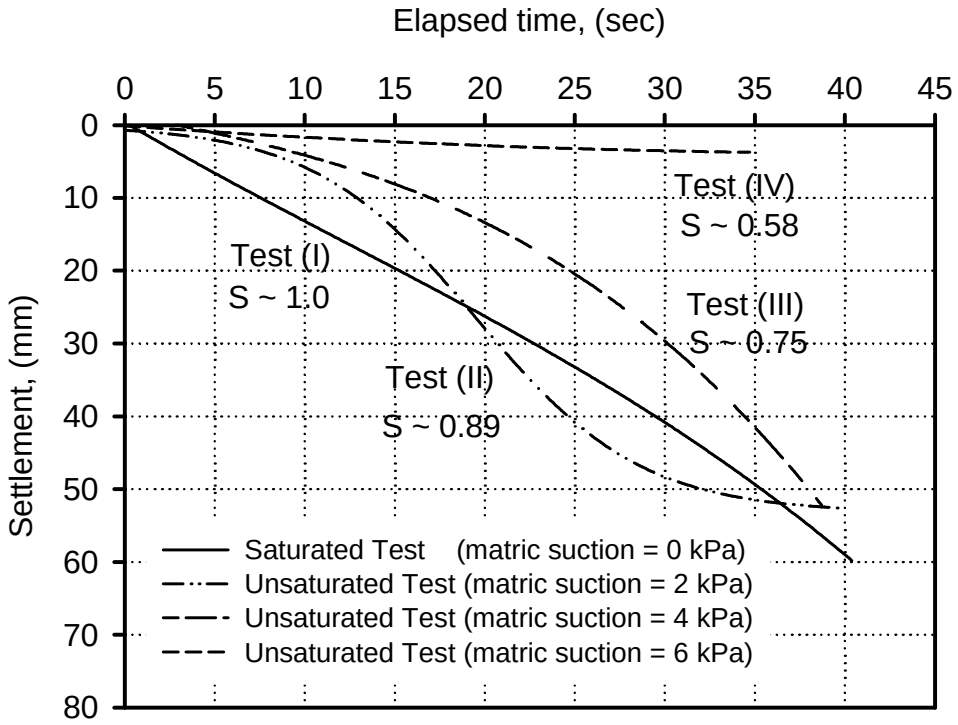

Figure 6.36 Measured settlement at the center of the footing with time for tests conducted under saturated and unsaturated conditions (matric suction = 0 kPa, 2 kPa, 4 kPa and 6 kPa)

The measured accelerations using the accelerometers (located at the bottom and top of the tested sand) and the applied forces (i.e., base shear) by the MTS actuator for the four conducted tests (see Table 6.10). The measured acceleration values at the top of the tested soil were lowered for all conditions (saturated or unsaturated). Such behaviour may be attributed to the effect of liquefaction which substantially reduced the contact between the soil grains and lower the effective stress as a result. Spikes of the acceleration amplitudes were seen in the unsaturated sand tests, showing a dilative behaviour of the sand particularly at the top portions of the sand.

The applied force by the MTS actuator on the base of the shake table during the saturated sand test was slightly lower in comparison to the applied forces for the case of

unsaturated sand tests indicating that the unsaturated sand was stiffer than the saturated sand.

The matric suction values (average value within the stress bulb zone) before and after each test (e.g., Test I, Test II, Test III, and Test IV) are presented in Table 6.10. Interestingly, in the unsaturated test in Test (IV) there was no change in the matric suction (6 kPa) from the Tensiometer readings. Such a response suggests the importance and effectiveness of maintaining the soil in an unsaturated condition. Figure 6.37 provides a summary of the range of matric suction range between 5.5 kPa to 6.5 kPa (i.e., transition zone) which is equivalent to the degrees of saturation of 30% and 60% respectively. Matric suction value falls within this zone is expected to provide sufficient if not optimum resistance to liquefaction for the studied sand. The behaviour of the model footing and the tested sand particularly for Test IV (small settlement and no liquefaction) can be attributed to the contribution of the matric suction to the shear strength of the sand. In the unsaturated sand structure, the water skeleton (i.e., meniscus or a film of water) makes the soil grains attracted to each other during the shaking, leading to an increase of the skeleton stress (i.e., effective stress). Unna (2008) reported that unsaturated sand specimens lose their effective stress under present cyclic shear loading when the degree of saturation is approximately 80%.

The soil-water characteristic curve (SWCC) can be divided into three zones namely; saturation zone, transition zone and residual zone as discussed in Vanapalli et al. (1996). Based on the results of this research program, a zone of low magnitude to no liquefaction zone can be suggested within the transition zone as highlighted on the SWCC of the tested sand (see Figure 6.37). Hence, sandy soils with a maintained matric suction range between 5.5 kPa and 6.5 kPa would dramatically improve the resistance of the soil to liquefaction and also reduce the settlement of footings during EQ ground shaking.

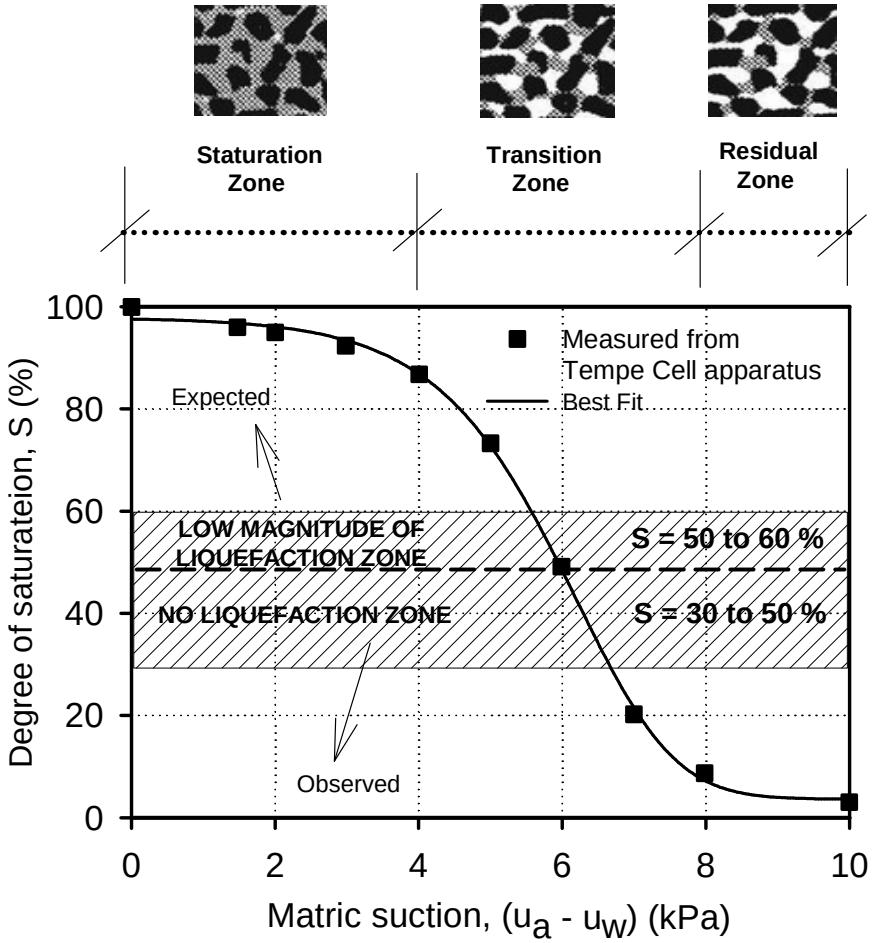

Figure 6.37 Anticipated effective unsaturated condition zone on the soil-water characteristic curve (SWCC) of the tested sand

(frequency = 3 Hz and acceleration ~ 0.42 m/sec^2)

6.12 Summary and Conclusions

During the last few decades there has been an extensive effort by several researchers to address the issue related to liquefaction phenomenon and seismically induced settlement of shallow foundations. The focus of the available studies in the geotechnical literature

was on saturated soils as these conditions most likely offer worst-scenarios to sand liquefaction in practice. Soil liquefaction may lead to intolerable deformations (settlement and/or tilting) that may affect not only the integrity of a structure built on but also the performance and the service it provides.

The National Building Code of Canada (NBCC-2010) specified five different categories of soil from Class A, hard rock to Class E, soft soil in addition to Class F which covers liquefiable soils. Different from saturated soils, the unsaturated soils have three phases, namely, pore water (which is negative), and pore air and solid. In addition, the mechanical behaviour of unsaturated soils is significantly different from that of saturated soils. However, limited research work was directed towards the performance of shallow foundations in unsaturated sands where EQs are expected to occur.

In the research program undertaken in this thesis, a Flexible Laminar Shear Box (FLSB) was designed and used to better understand the behaviour of shallow foundations (i.e., footings) particularly on unsaturated sandy soils. A model footing of 150 mm × 150 mm was used to mimic the behaviour of a prototype footing size that is commonly used in the field. The focus of the research was to simulate different saturated and unsaturated conditions of the tested sand prior to conducting tests under EQ loading. Tensiometers were also used to measure the matric suction values in the tested sand. The entire setup which consists of the FLSB and the shake table, was used to simulate an EQ shaking (e.g., sinusoidal wave form) that might occur in Ottawa region (model frequency and acceleration are 3 Hz and peak ground acceleration of ~ 0.42 m/sec^2, respectively).

Based on the obtained results and observations in this research program, the following conclusions can be drawn:

- The FLSB and the 1-*g* shake table combined assembly formed an economical and viable equipment to provide valuable insight for understanding the behaviour of shallow foundations built particularly on unsaturated sands in seismically active regions.

- The model footing which placed on the saturated soil (i.e., Test I; performed under saturated sand condition $(u_a - u_w) = 0$ kPa) experienced excessive settlement within 5 to 10 seconds due to the early initiation of liquefaction during the time of shaking.

- The model footing conducted under unsaturated conditions (Test II of 2 kPa, Test III of 4 kPa and Test IV of 6 kPa) experienced less settlement in comparison to the saturated condition. However, the settlement of the model footing for the 2 kPa test (i.e., Test II) was excessive after 20 seconds of the test initiation and the soil started liquefying due to the upward movement of the water table. Similar observation was noticed for the second unsaturated test of 4 kPa (i.e., Test III), however, within the stress bulb zone liquefaction was observed after 25 seconds from the initiation of shaking. For the case of 6 kPa test (i.e., Test IV), interestingly, a small settlement was experienced by the model footing and no liquefaction was noticed during the entire period of shaking of 35 seconds.

- During Test III and Test IV, the deformations of the model footing (settlements) were not observed when the shaking stopped. This may be due to the strain hardening behaviour of the sand.

- A range of matric suction value of 5.5 kPa and 6.5 kPa (within the transition zone of the SWCC) can be recommended to be maintained in unsaturated sandy soils in practice as a ground improvement technique to drastically reduce liquefaction potential and seismically induced settlement of shallow foundations. In reference to the capillary tension phenomenon, capillary barriers of unsaturated soils can be applied in engineering practice to take advantage of the matric suction contribution to shear strength and resistance of liquefaction for achieving safe and economical shallow foundation design.

- More studies using the same setup and input parameters for different types of soils (e.g., sensitive clay) would be valuable to researchers for better understanding the contribution towards the challenging area of geotechnical earthquake engineering.

6.13 References

Al-Karni, A. A., and Budhu, M. (2001). "An experimental study of seismic bearing capacity of shallow footings", Proceeding of the 4th International Conference on Recent Advances in Geotechnical Earthquake Engineering and Soil Dynamics, San Diego.

Asada, A. (1998). "Simplified prediction of liquefaction-induced damage to individual houses and its mitigation", 15-year anniversary of 1983 Nihonkai-chubu earthquake, Chap. 9 (in Japanese).

Bardet, J., Mace, N., and Tobita, T., (1999). "Liquefaction-induced ground deformation and failure." Report to PEER/PG and E., University of Southern California.

Castro G. (1969). "Liquefaction of sands", PhD Thesis, Harvard University, Cambridge, Massachusetts, USA.

Cetin, K. O., Bilge, H. T., Wu, J., Kammerer, A. M., and Seed, R. B. (2009). "Probabilistic model for the assessment of cyclically induced reconsolidation (volumetric) settlements". Journal of Geotechnical Geoenvironmental Engineering, 135 (3), 387 – 398.

Cutter, S. L., (2001). "American Hazardscapes: The Regionalization of Hazards and Disasters". Washington, D.C., Joseph Henry Press.

Das, B. M. and Omar M. T., (1994). "The effects of foundation width on model tests for the bearing capacity of sand with geogrid reinforcement", Geotechnical and Geological Engineering, 12 (2), 133 – 141.

Dashti, S., Bray J. D., Pestana, J. M., Reimer, M. and Wilson, D. (2010). “Mechanisms of seismically induced settlement of buildings with shallow foundations on liquefiable soil.” Journal of Geotechnical and Geoenvironmental Engineering, ASCE, 36 (1), 151 – 164.

D’Appolonia, E., (1970). “Dynamic loadings”. Journal of Soil Mechanics and Foundation Division, 96 (SMI), Paper (7010), 49 – 72.

Dobry, R., Ladd, R. S., Yokel, F. Y., Chung, R. M., and Powell, D. (1982). ‘‘Prediction of pore water pressure buildup and liquefaction of sands during earthquakes by the cyclic strain method.’’ NBS Build. Sci. Ser. 138, National Bureau of Standards, Gaithersburg.

Duku, P. M., Stewart, J. P., Whang, D. H., and Yee, E. (2008). “Volumetric strains of clean sands subject to cyclic loads”. Journal of Geotechnical and Geoenvironmental Engineering, 134 (8), 1073 –1085.

EERI (Earthquake Engineering Research Institute). (1999a). “The Izmit (Kocaeli) Turkey Earthquake of August 17, 1999”. EERI Special Earthquake Report, October 1999.

EERI (Earthquake Engineering Research Institute). (1999b). “The Chi-Chi Taiwan Earthquake of September 21, 1999”. EERI Special Earthquake Report Dec., 99.

Eseller-Bayat, E., E. (2009). “Seismic Response and Liquefaction Prevention of Sands Partially Saturated through Introduction of Gas Bubbles”, Ph.D. Thesis, Northeastern University, Boston, MA.

EQE. (1994). “The January 17, 1994 Northridge, CA Earthquake. EQE Summary Report.” March 1994.

EQE. (1989). “The October 17, 1989 Loma Prieta Earthquake”. EQE Report, October 1989.

Finn, W. D. L., and Byrne, P. M. (1976). “Estimating settlements in dry sand during earthquakes”. Canadian Geotechnical Journal, 13 (4), 355 – 363.

Ghayoomi, M., McCartney, J., and Ko, Hon-Yim. (2013). “Empirical methodology to estimate seismically induced settlement of partially saturated sand”. Journal of Geotechnical and Geoenvironmental Engineering, 139, 367 – 376.

Giardini, D., Grunthal, G., Shedlock, K. M., and Zhang, P. Z., (1999). “The GSHAP Global Seismic Hazard Map”, Annali Di Geofisica, Vol. (42): 1225 –1230.

Gibson, A. D. (1997). “Physical scale modeling of geotechnical structures at 1-*g*”. PhD Thesis. Pasadena, CA: California Institute of Technology.

Giddens, R. and Briaud, J. (1994). “Load tests on five large spread footings on sand and evaluation of prediction methods.” Federal Highway Administration Department of Civil Engineering, A&M University, TX., USA.

Finn, W. D. L., and Byrne, P. M. (1976). “Estimating settlements in dry sand during earthquakes.” Canadian Geotechnical Journal, (13): 355-363.

Gopikrishna, K. (2000). “An approach to assess severity of site damage using accelerograms.” M. Tech. Dissertation, Visvesvaraya Technological University, Karnataka.

Hamada, M., Towhata, I., Yasusa, S. and Isoyama, R. (1987) “Study on permanent ground displacement induced by seismic liquefaction.” Journal of Computers and Geotechnics, 4 (4), 197 – 220.

Hsu, C. C., and Vucetic, M. (2004). “Volumetric threshold shear strain for cyclic settlement.” Journal of Geotechnical and Geoenvironmental Engineering, 130 (1), 58 –70.

Iai, S. (1989). “Similitude for shaking table tests on soil-tests on soil-structure-field model in 1-g gravitational-field soils and foundations.” JSSMFE, 29(1): 105 – 118.

Ishihara, K., and Yoshimine, M. (1992). “Evaluation of settlements in sand deposits following liquefaction during earthquakes.” Soils and Foundation, 32 (1), 173 – 188.

Kokusho, T. (2003). “Current state of research on flow failure considering void redistribution in liquefied deposits.” Soil Dynamics and Earthquake Engineering, 23, 585 – 593.

Koga, Y. and Matsuo O. (1990). “Shaking table tests of embankments resting on liquefiable sandy ground.” Soils and Foundation, (30), 162–174.

Kramer, S. L. (1996). Geotechnical Earthquake Engineering. 1st Ed., Publisher: P. Prentice Hallrentice Hall, USA.

Liu, L., and Dobry, R. (1997). “Seismic response of shallow foundation on liquefiable sand.” Journal of Geotechnical Engineering, 123 (6), 557 – 567.

Lee, K. L., and Albaisa, A. (1974). “Earthquake induced settlement in saturated sands.” Journal Geotechnical Engineering, 100 (GT4), 387– 405.

Lu, L., Yamazaki, F., and Katama, T. (1992). “Soil amplification based on seismometer array and micrometer observations in Chiba, Japan.” Earthquake Engineering and Structural Dynamics, Institute of Industrial Science, The University of Tokyo, Japan, John Wiley and Sons, LTD.

Meymand, P. J. (1998). “Shaking table scale model tests of nonlinear soil-pile superstructure interaction in soft clay.” Ph.D. Dissertation, University of California, Berkeley, CA.

Matsuda, T., and Goto Y. (1988). “Studies on experimental technique of shaking table test for geotechnical problems.” Proceedings of the ninth World Conference on Earthquake Engineering, Tokyo-Kyoto, (8), 837 – 842.

Meymand, P. (1998). “Shaking table scale model test of nonlinear soil-pile-superstructure interaction in soft clay.” Ph.D. Dissertation, University of California Berkeley.

Mizuno, H., and Iiba M. (1982). “Shaking table testing of seismic building-pile-soil interaction.” Proceedings of 5th Japan Earthquake Engineering Symposium, 1713 – 1720.

Mileti, D. S. (1999). “Disasters by design: a reassessment of natural hazards in the United States.” Washington, D.C.: Joseph Henry Press.

Mohamed, F. M. O. and Vanapalli, S. K. (2006). “Laboratory investigations for the measurement of the bearing capacity of an unsaturated coarse-grained soil.” In Proceedings of the 59th Canadian Geotechnical Conference, Vancouver, B.C., 1 – 4 October 2006. Canadian Geotechnical Society, Richmond, B.C., (1), 219 – 226.

National Research Council of Canada (2010). “National Building Code of Canada: NBCC.” NRCC, Ottawa, Canada.

National Geophysical Data Centre (NGDC): USA (http://www.ngdc.noaa.gov/).

Network for Earthquake Engineering Simulation (NEES). (2004). Preventing Earthquake Disasters: The ground challenge in earthquake engineering. The National Academies Press, Washington, D.C. USA (www.nap.edu).

NIST (National Institute of Standards and Technology). (1996). January 17, 1995 Hyogoken- Nanbu (Kobe) Earthquake: Performance of Structures, Lifelines, and Fire Protection Systems. NIST SP 901, July. Gaithersburg, Md., NIST.

Okamura, M., and Teraoka, T. (2005). “Shaking table tests to investigate soil desaturation as a liquefaction countermeasure”, ASCE Geotechnical Special Publication, No.145, Seismic performance and simulation of pile foundations in liquefied and laterally spreading ground, 282 – 293.

Orense, R. P., Marimoto I., Yumiyama T., Yamamoto H., and Sugawara K. (2003). “Study on wall-type gravel drains as liquefaction countermeasure for underground structures.” Soil Dynamics and Earthquake Engineering, (23), 19 – 39.

Pradel, D. (1998). “Procedure to evaluate earthquake-induced settlements in dry sandy soils.” Journal Geotechnical Engineering, 124 (4), 364–368.

Prasad, S. K., Towhata, I., Chandradhara, G. P. and Nanjundaswamy, P. (2004). “Shaking table tests in earthquake geotechnical engineering.” Current Science, 87 (10), 1398 – 1404.

Pamuk, A., Gallagher, P. M., and Zimmie, T. F. (2007). “Remediation of piled foundations against lateral spreading by passive site stabilization technique.” Soil Dynamics and Earthquake Engineering, 27, 864 – 874.

Poulos, H. G. and Davis, E. H. (1974). “Elastic solutions for soil and rock mechanics.” John Wiley and Sons, New York.

Rollins, K. M., and Seed, H. B. (1990). “Influence of buildings on potential liquefaction damage.” Journal of Geotechnical Engineering, 116 (2), 165 – 185.

Rayhani**,** M. T. and El Naggar**,** M. H. (2007). “Centrifuge modeling of seismic response of layered soft clay.” Bulletin of Earthquake Engineering, 5 (4), 571 – 589.

Rayhani, M. T., and El Naggar, M H. (2008). “Numerical modeling of seismic response of rigid foundation on soft soil.” International Journal of Geomechanics, 8 (6), 336 – 346.

Silver, M. L., and Seed, H. B. (1971). “Volume changes in sands during cyclic loading.” Journal of Soil Mechanics and Foundation Division, 97 (SM9), 1171 – 1182.

Seed, H. B. and Silver, M. L. (1972). “Settlement of dry sands during earthquakes.” Journal of Geotechnical Engineering, 98(4), 381 – 397.

Seed, H. B., and Idriss, I. M. (1971). “Simplified procedure for evaluating soil liquefaction potential.” Journal of Soil Mechanics and Foundation Division, 97 (SM9), 1249 – 1274.

Sawada, S., Tsukamoto, Y., and Ishihara, K. (2006). "Residual deformation characteristics of partially saturated sandy soils subjected to seismic excitation." Soil Dynamic Earthquake Engineering, 26 (2 – 4), 175 – 182.

Sharma, R. S. and Mohamed, M. H. A. (2003). "An experimental investigation of LNAPL migration in unsaturated or saturated sand." Third British Geotechnical Society Geoenvironmental Engineering Conference, (70), 305 – 313.

Shen, C.K., Li, X.S., Ng, C.W.W., Van Laak, P. A., Kutter, B. L., Cappel, K. and Tauscher, R. C. (1998). "Development of a geotechnical centrifuge in Hong Kong Centrifuge." Tokyo, Japan, (1), 13 – 18.

Suleiman, A. S., Albini P., and Migliavacca, P. (2004). "A short introduction to historical earthquakes in Libya." Geophysics Department, Faculty of Science, Tripoli University, Tripoli, Libya and Istituto Nazionale di Geofisica e Vulcanologia, Sezione di Milano, Italy, Geophysics, 47 (23), 545 – 555.

Takahashi, A., Takemura, J., Suzuki, A. and Kusakabe, O. (2001). "Development and performance of an active type shear box in a centrifuge." International Journal of Physical Modeling in Geotechnics, 1 (2), 1 – 18.

Terzaghi, K., and Peck R. B. (1948/1967). Soil Mechanics in Engineering Practice. 2nd Ed. John Wiley and Sons, New York.

Thevanayagam, S., Kanagalingam, T., Reinhrn, A., Tharmendhira, R., Dobry, R., Pitman, M., Abdoun, T., Elgamal, A., Zeghal, M., Ecemis, N., and El Shamy U. (2009). "Lamiar Box system for 1-*g* physical modeling of liquefaction and lateral spreading." Geotechnical Testing Journal, 32, 5, 1 – 11.

Turan, A. (2009). "Physical modeling of seismic soil-structural interaction of embedded structures." Ph.D. Dissertation, University of Western Ontario, ON, Canada.

Towhata, I. (2008). "Geotechnical Earthquake Engineering." ISBN 978-3-540-35782-7, Springer Verlag- Berlin Heidelberg.

Tokimastsu, K., and Seed, H. B. (1987). “Evaluation of settlements in sands due to earthquake shaking.” Journal Geotechnical Engineering, 113 (8), 861 – 878.

Tsukamoto, Y., Ishihara, K., Saada, S., and Fujiwara, S. (2012). “Settlement of rigid circular foundations during seismic shaking in shaking table tests.” International Journal of Geomechanics, (12), 462–470.

Tutunchian, M. A., Shahnazari H., Salehzadeh H., and Asadi M. (2011). “Study on dynamic behavior of shallow foundations on liquefiable sand, using video processing technique.” Electronic Journal of Geotechnical Engineering, 16 (1), 945 – 960.

Ueng, T. S. and Chen, C. H. (2006). “Liquefaction of sand under multidirectional shaking table tests.” In: Ng, Zhang and Wang editors, Proceedings of the International Conference on Physical Modeling in Geotechnics, ICPMG 06, Hong Kong, 481.

University of Washington. (2001). “The Nisqually Earthquake of 28 February 2001: Preliminary Reconnaissance Report.” Seattle, Wash.: Nisqually Earthquake Clearinghouse Group.

Unno, T. (2008). “Liquefaction potential assessment for unsaturated soil based on liquefaction mechanism of unsaturated sand.” The 14th World Conference on Earthquake Engineering, Beijing, China.

Vaid Y. P., and Sivathayalan S. (1996). “Static and cyclic liquefaction potential of Fraser Delta sand in simple shear and triaxial tests.” Canadian Geotechnical Journal, (33), 281 – 289.

Van Laak, P., Taboada, V., Dobry, R. and Elgamal, A.W. (1994). “Earthquake centrifuge modeling using a laminar box.” In Ebelhar, R.J., Drnevich, V. and Kutter, B.L., Dynamic Geotechnical Testing: Second Volume, ASTM STP 1213, American Society for Testing and Materials, Philadelphia, 370 – 384.

Vanapalli S. K, Fredlund D. G, Pufahl D. E and Clifton A. W. (1996). “Model for the prediction of shear strength with respect to soil suction.” Canadian Geotechnical. Journal, 33 (3), 379 – 392.

Wang B., Zen K., Chen G. Q., and Kasama K. (2012). “Effects of excess pore pressure dissipation on liquefaction-induced ground deformation in 1-*g* shaking take test.” Geomechanics and Engineering, 4 (2), 91 – 103.

Wu, J., and Seed, R. B. (2004). “Estimating of liquefaction-induced ground settlement (case studies).” Proceeding of the 5th International Conference on Case Histories in Geotechnical Engineering, New York.

Whang, D. H., Moyneur, M. S., Duku, P., and Stewart, J. P. (2005). “Seismic compression behavior of non-plastic silty sands.” Proceeding of the, International Symposium on Advanced Experimental Unsaturated Soil Mechanics, A. Tarantino, E. Romero, and Y. J. Cui, eds., A.A. Balkema, Rotterdam, Netherlands, 257–263.

Wu, S., Gray, D. H., and Richart, F. E., J. (1984). “Capillary effects on dynamic modulus of sands and silts.” Journal of Geotechnical Engineering, 110 (9), 1188 – 1203.

Youd, T, L., (1970). “Densification and shear of sand during vibration.” Journal of Soil Mechanics and Foundation Division, 96(SM3), 863–880.

Yoshimi, Y. K. and Tokimatsu, K. (1977). “Settlement of buildings on saturated sand during earthquakes.” Soils and Found. Tokyo, Japan, 17 (1), 23 – 38.

CHAPTER 7

SUMMARY AND CONCLUSIONS

7.1 General

The bearing capacity equations proposed by Terzaghi (1943) and Meyerhof (1951) for saturated soils are used in conventional geotechnical engineering practice for unsaturated soils. Such a practice is considered to be conservative in approach; however, it some scenarios the design of foundations would be expensive. In addition, settlements estimation in unsaturated soils extending the relationships such as the Schmertmann et al. (1978) equation that does not consider the influence of capillary stresses (matric suction) for unsaturated soils is erroneous. For this reason, in this thesis a comprehensive experimental research work has been carried out using model footings of 100 mm × 100 mm, and 150 mm × 150 mm on sandy soil under saturated and unsaturated conditions to understand the bearing capacity and settlement behavior of unsaturated sands using specially designed bearing capacity equipment (UOBCE 2011). In addition, studies were also conducted to understand the influence of capillary stresses on sand under saturated and unsaturated conditions when they are subjected to seismic loads using the Flexible Laminar Shear Box (FLSB). The resistance of the tested unsaturated sand to deformations associated with the liquefaction under seismic loading was investigated using a model footing of 150 mm × 150 mm.

Based on extensive investigations, a general framework is proposed to interpret the bearing capacity of shallow foundations for unsaturated sandy soils modifying Terzaghi (1943) and Meyerhof (1951) equations. Furthermore, a semi-empirical model is proposed for predicting the variation of bearing capacity with respect to matric suction using the

saturated shear strength parameters, c' and ϕ' and the soil-water characteristic curve (SWCC).

In addition, several cone penetration tests (CPTs) were carried out in a controlled laboratory environment in sand under saturated and unsaturated conditions. Several SPTs and PLTs were also performed in-situ in saturated and unsaturated sandy soil at Carp region in Ottawa. Correlations based on the experimental results are developed between the SPTs and the bearing capacity of unsaturated sands.

In most cases of shallow foundations design, it is the settlement that is the governing parameter rather than the bearing capacity, particularly for sands. A simple CPT-based procedure is proposed to estimate the bearing capacity and settlement of shallow foundations in saturated and unsaturated conditions. The CPTs results were used for developing relationships between the modulus of elasticity, E_s and cone resistance, q_c. These relationships were used to modify Schmertmann et al. (1978) equation for settlement estimation of footings in both saturated and unsaturated sands.

In some cases, soils can be subjected to seismic loading in seismically active areas. Liquefaction is one of the primary reasons that contribute to intolerable deformations. Several tests were conducted to understand the behaviour and mechanism of failure of a model footing of 150 mm × 150 mm under seismic loading in a sandy soil under unsaturated conditions. The study suggests that a range of matric suction of 5.5 kPa and 6.5 kPa, if maintained in the sand, can drastically reduce seismically induced settlement and liquefaction in sands supporting shallow foundations.

7.2 Summary

The salient features of the research program presented in this thesis can be summarized as below:

7.2.1 Laboratory Investigation

7.2.1.1 Design and Construction of Bearing Capacity Equipment

The University of Ottawa Bearing Capacity Equipment (UOBCE-2011) was specially designed and successfully used for the research program to determine the variation of bearing capacity and settlement of sands with respect to matric suction using model footings which are interpreted similar to the plate load tests (PLTs). The equipment setup consists of a rigid-steel frame made of rectangular section pipes with thickness of 6 mm and a box of 1500 mm (length) × 1200 mm (width) × 1060 mm (depth). The test box can hold up to 3 tons of soil and the capacity of the loading machine (i.e., Model 244 MTS Hydraulic Actuator) is 28.5 kN. The PLTs results were used to develop the proposed relationships for estimating both bearing capacity and settlement of footings in saturated and unsaturated sands.

7.2.1.2 Bearing Capacity of Unsaturated Sands from PLTs

The focus of the study presented in Chapter 2 was directed towards understanding the influence of three parameters; namely, (i) matric suction, (ii) overburden stress, and (iii) dilation, on the bearing capacity of surface and embedded model footings (PLTs) in unsaturated sands. The results show that the bearing capacity of unsaturated sands is significantly influenced by all the three parameters. In addition, comparisons are provided between the predicted and measured bearing capacity values using the proposed semi-empirical equation modifying the Terzaghi (1943) and Meyerhof (1951) equations. There is a good comparison between the predicted and measured bearing capacity values using the proposed semi-empirical equation.

7.2.1.3 Bearing Capacity of Unsaturated Sands from CPTs

The CPTs are used to determine the bearing capacity of soils due to their reliability, simplicity and associated low costs in conventional engineering practice. The CPTs are also performed in unsaturated soils; however, the influence of matric suction towards the contribution of the bearing capacity is not evaluated or taken into account. An experimental program was undertaken in the UOBCE to determine the bearing capacity of sand under both saturated and unsaturated conditions using model PLTs and CPTs. These studies demonstrate that the bearing capacity of sands was significantly influenced by matric suction. Based on the studies presented in this research program, simple relationships were proposed between CPTs and the bearing capacity of sands for both saturated and unsaturated conditions.

7.2.1.4 Settlement of Footings on Unsaturated Sands Using the PLTs and the CPTs

Simple relationships are proposed by modifying the Schmertmann et al. (1978) equation for settlement estimations of footings (i.e., $B/L \approx 1$) carrying vertical loads in saturated and unsaturated sandy soils. The modified method is developed using model plate load tests (PLTs) and cone penetration tests (CPTs) results conducted in saturated and unsaturated sand in a controlled laboratory environment. Seven in-situ large-scale footings tested under both saturated and unsaturated conditions in sands were used to validate the proposed technique. The results of the study are encouraging as they provide reliable estimates of the settlement of shallow footings in both saturated and unsaturated sands using the conventional CPT results.

7.2.2 Field Investigation

7.2.2.1 Bearing Capacity of Unsaturated Sands from SPTs

The in-situ bearing capacity of sandy soils is conventionally determined or estimated using the plate load tests (PLTs), cone penetration tests (CPTs) or standard penetration tests (SPTs). The contribution of matric suction towards the bearing capacity of unsaturated sands is, however, not estimated from these tests. As a part of this research program, several SPTs and PLTs were conducted on sand in Ottawa, Canada under saturated and unsaturated conditions to demonstrate the contribution of matric suction on the bearing capacity results. In addition, relationships were proposed to estimate the bearing capacity of sands under both saturated and unsaturated conditions from the SPT and CPT results. Comparisons were provided between the measured and estimated bearing capacity values for three different sands using the model PLTs, large-scale footing load tests (FLTs), CPTs and SPTs data from the literature using the proposed relationships. The results of the studies suggest that the proposed simple relationships were reliable and can be used in the estimation of the bearing capacity of both saturated and unsaturated sands.

7.2.3 Investigation of the Behaviour of a Model Footing on Unsaturated Sand Subjected to Seismic Loading

Shallow foundations in saturated sands or sands with relatively high degree of saturation when subjected to earthquake loading conditions may liquefy due to the loss of the effective stress. A reliable, economical and effective way to understand the mechanisms leading to liquefaction in both saturated and unsaturated sands can be determined using Flexible Laminar Shear Box (FLSB) filled with sand on a shake table. A FLSB was specially designed, constructed and assembled at the University of Ottawa for this research program. The FLSB was used to better understand the behaviour of shallow

foundations (i.e., footings) particularly on unsaturated sandy soils as it has provisions for collecting the required data such as the deformation, water level in the box, matric suction below the surface footing, and density and water contents. Tensiometers were also used to directly measure the matric suction values in the tested sand.

A model footing of 150 mm × 150 mm with a mass of 40 kg was used to mimic a prototype footing size. The sand in the FLSB was first saturated and the water table was then lowered to a different level of depths from the soil surface to simulate different scenarios of saturated and unsaturated conditions below to model footing. The results of the study show that capillary stresses (i.e., matric suction) offers significant resistance to both settlement and liquefaction of the tested unsaturated sand.

7.3 Conclusions

Based on the research program presented in this thesis, the following conclusions can be drawn:

i. Bearing Capacity Equipment (UOBCE) was designed and built at the University of Ottawa to carry out surface and embedded PLTs in both saturated and unsaturated sand in a controlled laboratory environment. A semi-empirical equation was proposed to estimate the bearing capacity of footings in saturated and unsaturated sands with respect to variations of matric suction.
ii. Empirical correlations were proposed between the bearing capacity of shallow foundations and CPTs and SPTs data conducted in laboratory and in-situ in sand under saturated and unsaturated conditions.
iii. Simple relationships were proposed by modifying Schemrtmann et al. (1978) CPT-based equation for settlement estimation of footings using PLTs and CPTs data in unsaturated sands.
iv. The studies show that even low values of capillary stresses (i.e., matric suction in the range of 0 to ~ 6 kPa) increase the bearing capacity by two to four folds, and also significantly decrease the settlement of footings.

v. Flexible Laminar Shear Box (FLSB) was designed and constructed at the University of Ottawa and placed on a shake table to simulate and understand the behaviour of footings in both saturated and unsaturated soils under seismic loading.

vi. It was observed that the matric suction has a direct effect on the performance of the model footing and the tested soil when they are subjected to seismic loading conditions. Experimental studies demonstrate that the tested sand in unsaturated condition (with a matric suction value between 5.5 kPa and 6.5 kPa) offers significant resistance to liquefaction. The experimental results also suggest the measured settlements of the model footing during testing under unsaturated conditions were much lower in comparison to tests under saturated conditions. The settlements in the present study for Test I (0 kPa) and Test IV (6 kPa) at the 5^{th} sec of shaking were 6 mm and 1 mm, respectively. The settlements for Test I (0 kPa) and Test IV (6 kPa) after 10^{th} sec of shaking were 20 mm and 2 mm respectively.

vii. The studies summarized in this research program are promising and encouraging as they not only provide reliable and simple tools for interpreting the bearing capacity and settlement behaviour of shallow footings in both saturated and unsaturated sands but also enhance our understanding of the behaviour of shallow foundations subjected to seismic (i.e., EQ) loading conditions.

7.4 Limitations of the Research Undertaken in this Thesis

- Limited experimental investigations were undertaken both in laboratory and in-situ environment using three model footings (i.e., 100 mm × 100 mm, and 150 mm × 150 mm, and 200 mm × 200 mm).

- Full-scale footing tests were beyond the scope of the present thesis. Also, there were no full scale tests that were reported in the geotechnical literature with in-situ variations of matric suction with depth to analyze the results using the relationships proposed in the present study.

- The experimental program to study the influence of matric suction on settlement and liquefaction was carried out using one model footing using sand.

- More in-situ experimental studies are required to validate the proposed techniques before extending them into engineering practice.

7.5 Proposed Future Studies and Work

- The research program undertaken in this thesis shows that the bearing capacity, settlement and liquefaction of unsaturated sands were substantially influenced by matric suction. These studies are promising to stabilize infrastructure failure in liquefaction prone regions by maintaining capillary stresses within a depth zone of 1.5 times the width of shallow foundations. Capillary barriers can be used around the foundation in sandy soils to maintain unsaturated conditions to alleviate the problems associated with liquefaction; however, more experimental and numerical modeling studies will be useful to understand the strengths and limitation of using capillary barriers as a ground improvement technique.

- More cone penetration tests (CPTs), standard penetration tests (SPTs), and large scale plate load tests (PLTs) in-situ are required to provide comparisons with the predicted/estimated bearing values and settlement behaviour using the proposed framework presented in Chapters 2 through 5.

- More studies using different types of soils are required to validate the relationships proposed for estimating bearing capacity and settlement of shallow foundations built in unsaturated soils.

- More studies using larger FLSB and shake table to understand the influence of many other parameters such as the depth, width and shape of the foundations in several coarse- and fine-grained soils will be valuable.

- The testing program conducted in this research using peak ground acceleration (i.e., 0.42 m/sec^2 with a frequency of 3 Hz) which represents worst case scenario may occur in Ottawa region; however, it would be valuable to check the performance of model footings under lower accelerations values that are commonly encountered more frequently.

APPENDIX A

A.1 SAMPLE CALCULATION

A sample calculation of the sleeve friction along the influence zone applying equation [3.5] (for AVR matric suction of 6 kPa along a depth of 150 mm as shown in Figure 3.5 in Chapter 3) with *k* equal to 1 is summarized below:

$$Q_{fus} = 0.35\left(\frac{16 \times 0.15}{2}\right)(0.01885) + [(0.6)\{(0.58)(\tan 26\}](0.01885)) = 0.04\,kPa$$

By substituting the value of sleeve friction from Eq. [3.6] in Eq. [3.3], (in Chapter 3) the sleeve friction can be determined:

$$f_s = \frac{Q_{fus}}{A_s} = \frac{0.04}{0.01885} = 2.12\,kPa$$

$$Q_t = Q_c + Q_{fus} \qquad [3.7]$$

where:

Q_t : total applied force (taken by sleeve and cone), kN

For the experimental results conducted in this research, the average measured applied force, Q_t at a depth of 150 mm is 2.09 kN. Using Eq. [3.7] (in Chapter 3), the applied load on the cone can be determined as 2.05 kN. By substituting the value of Q_c value back in Eq. [3.2] (in Chapter 3), the cone resistance, q_c can be estimated.

$$q_c = \frac{Q_c}{A_c} = \frac{2.05}{0.00127 \times 1000} = 1.62\,MPa$$

APPENDIX B

B.1 TEST II and TEST III

6.13.1 Shake Table Test (II) for Unsaturated Condition ($(u_a - u_w)$ = 2 kPa)

The soil in the FLSB was first saturated as detailed in the earlier section. The water table was then lowered to a different depth from the soil surface to achieve matric suction values recorded by the Tensiometers of 2 kPa. Soil specimens from the small aluminum cups were collected and data and results are presented in Table B.1.

Figures B.1 to B.4 present the measured acceleration values, base shear versus horizontal displacement and measured settlements.

The measured acceleration at the top of the soil (i.e., ACC TOP, see Figure B.3) is close to the input acceleration recorded at the bottom of the sand (i.e., ACC TOP = 90 to 95 % ACC BOTTOM) due to the initiation of liquefaction of the unsaturated sand as the pore-water pressure increased due to shaking The recorded force during shaking the table back and forth by the MTS actuator which was 2200 N within the required amplitude of 20 mm as measured in the horizontal displacement (see Figure B.4). It can be seen that the settlement was increasing almost linearly with time during the shaking. The settlement (see Figure B.5) was not increasing during the first cycles of shaking due to the fact the sand was still in a state of unsaturated condition (2 kPa). Such a behaviour can be attributed to the higher shear strength for this case (i.e., Test II) compare to the previous case (i.e., saturated condition; Test I). It was noticed that the sand started to liquefy after the 5^{th} second of shaking. The amount of water seem to increase at a rapid rate on the soil surface. The model footing was gradually sinking in the sand as the liquefaction was propagating upwards the time shaking period ends. The settlement of the footing when it was placed on the sand (i.e., static settlement) and prior to shaking was 8 mm approximately. The water was seen gushing (after 20 seconds of shaking) from both of

the water supply pipes confirming excess pore water pressure in the sand. In addition, the reading of the Tensiometer located in the vicinity of the stress bulb of the model footing indicted zero matric suction at the end of the test and.

Table B. 1 Data from the tested sand (prior to shaking) for an average matric suction of 2 kPa in the stress bulb zone (i.e., 1.5*B*) surface model footing using FLSB on Shake Table

Parameter or Property (Test II)					
[1]D (mm)	[2]γ_t (kN/m^3)	[3]γ_d (kN/m^3)	[4]w (%)	[5]S (%)	[6]$(u_a - u_w)_{AVR}$ (kPa)
10	19.54	0.64	21.5	89	2.0
220	19.72	0.625	23	98	1.0
600	19.74	15.95	23.8	100	0.0

[1]Depth of a Tensiometer from the soil surface; [2]total unit weight; [3]dry unit weight; [4]water content; [5]degree of saturation, [6]average matric suction in the stress bulb zone.

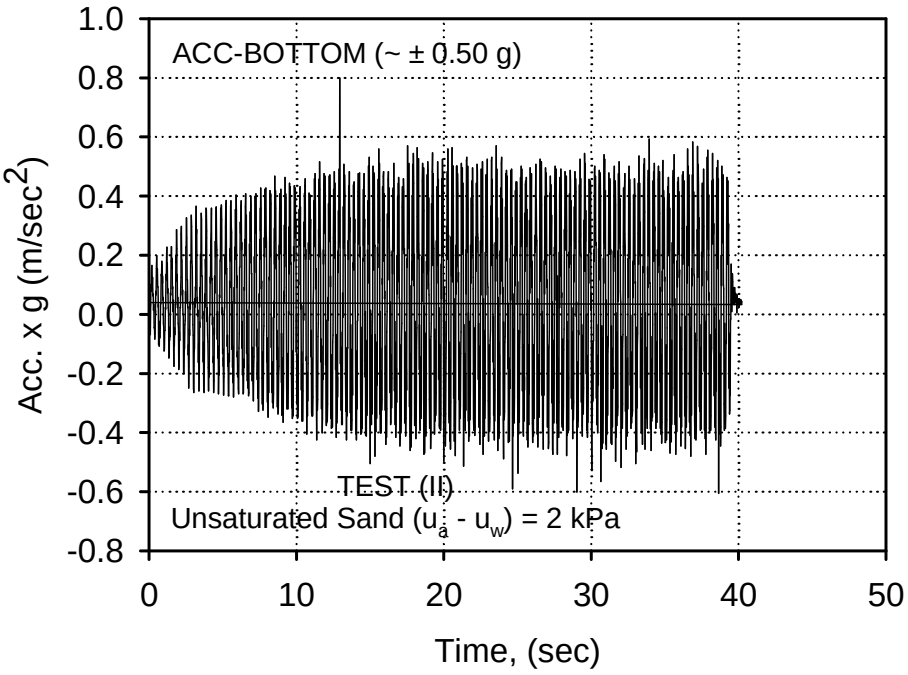

Figure B. 1 Measured accelerations time history at the bottom of the soil for unsaturated condition test (matric suction = 2 kPa)

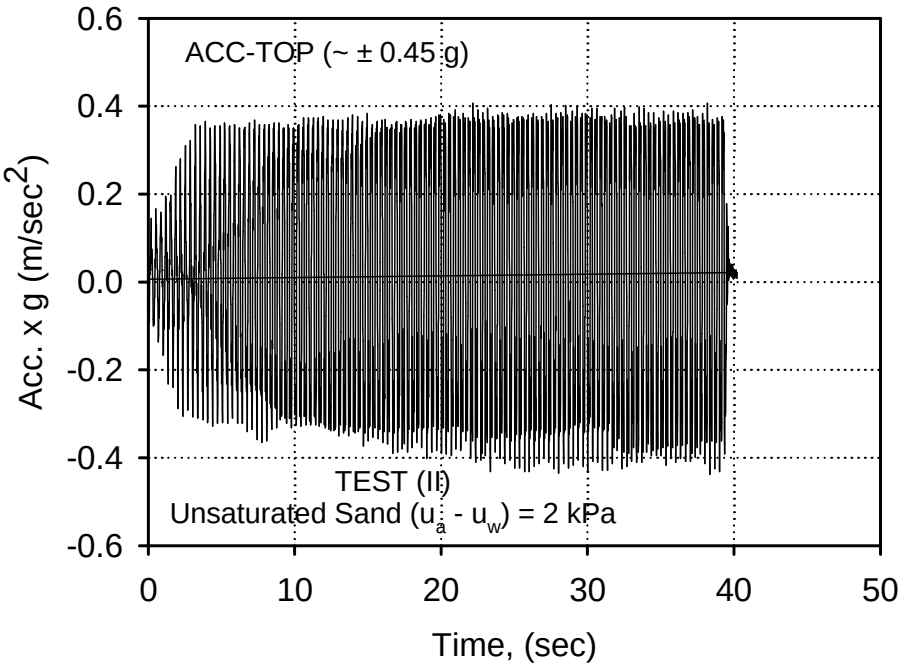

Figure B. 2 Measured accelerations time history at the top of the soil for unsaturated condition test (matric suction = 2 kPa)

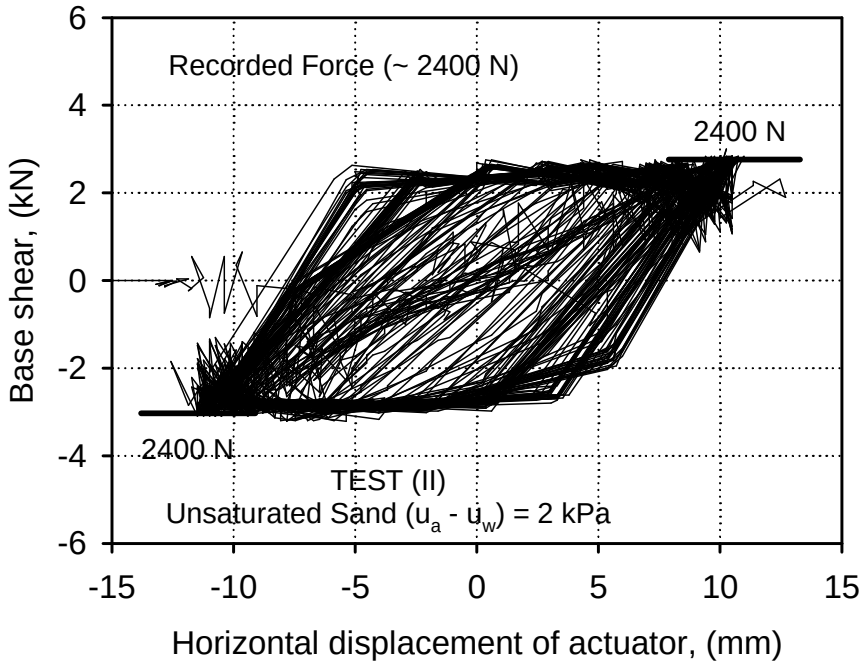

Figure B. 3 Measured actuator versus horizontal displacement (matric suction = 2 kPa)

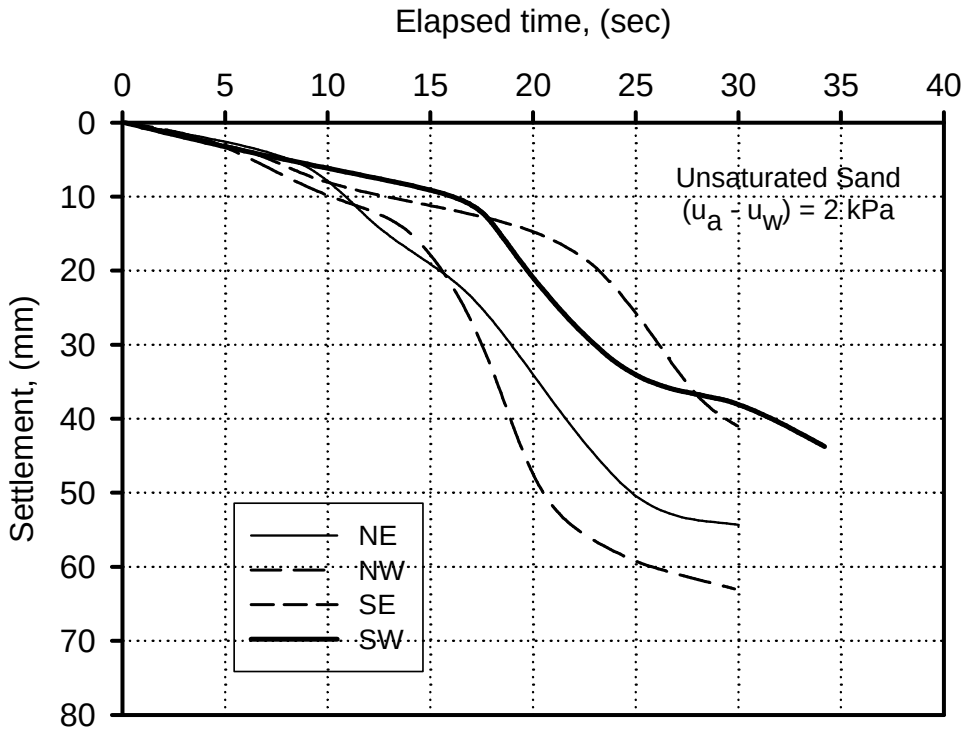

Figure B. 4 Measured settlement versus time of the model footing for saturated condition (matric suction = 2 kPa)

6.13.2 Shake Table Test (III) for Unsaturated Condition ($(u_a - u_w)$ = 4 kPa)

The procedure detailed in the previous section (6.13.1) was followed to simulate average matric suction of 4 kPa in the stress bulb zone of the model footing. Data from the tested sand and results are presented in Table B.2. Figures B.5 to A.8 that show the measured acceleration values, base shear versus horizontal displacement and measured settlements.

The measured acceleration at the top of the soil (i.e., ACC TOP, see Figure B.6) was close to the input acceleration recorded at the bottom of the sand (i.e., ACC TOP = 90 to 115 % ACC BOTTOM) showing large amplitude spikes. These spikes can be attributed to dilative response of the sand as there was low confinement at the shallow depths of the soil. This observation is consistent with the results reported by Wang et al. (2012).

The initiation of liquefaction of the unsaturated sand an increase in the pore-water pressure associated with the shaking was observed after 24 seconds of shaking initiation. The measured force during the back and forth shaking of the table by the MTS actuator was 1600 N within the required amplitude of 20 mm (Figure B.7). The settlements were measured at the four corners of the model footing. It can be seen that the settlement (Figure B.8) was increasing almost linearly with time during the shaking. The settlement was not increasing during the first cycles of shaking due to the fact the sand was still a state of unsaturated condition (4 kPa) which has higher shear strength compare to the previous case (i.e., 0 kPa and 2 kPa). Then, the sand started to liquefy after the 5th second of shaking. The model footing was sinking in the sand as the liquefaction propagates upwards. The settlement of the footing when it was placed on the sand (i.e., static settlement) and prior to shaking was 4 mm approximately. It was noticed that the matric suction dropped to zero after the test completed. In addition, water was also gushing (after the 20 second of shaking) from both of the water supply tubes confirming excess pore water pressure in the sand.

Table B. 2 Data from the tested sand (prior to shaking) for an average matric suction of 4 kPa in the stress bulb zone (i.e., 1.5*B*) surface model footing using FLSB on Shake Table

Parameter or Property (Test III)					
[1]D (mm)	[2]γ_t (kN/m^3)	[3]γ_d (kN/m^3)	[4]w (%)	[5]S (%)	[6]$(u_a - u_w)_{AVR}$ (kPa)
10	18.75	15.85	18.33	75.33	4.0
220	19.20	16.07	19.5	83.25	2.0
600	19.74	15.95	23.77	100	0.0

[1]Depth of a Tensiometer from the soil surface; [2]total unit weight; [3]dry unit weight; [4]water content; [5]degree of saturation, [6]average matric suction in the stress bulb zone.

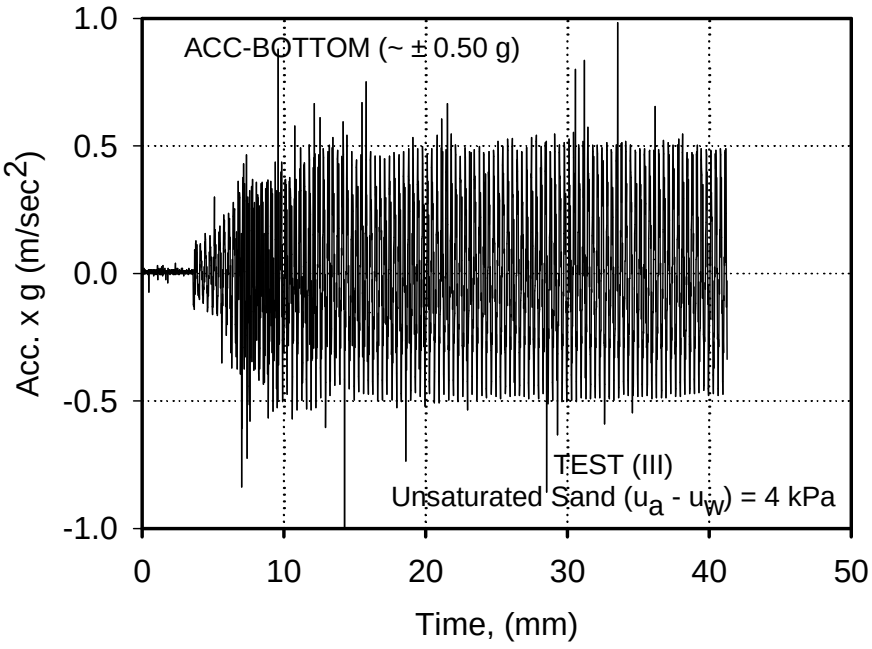

Figure B. 5 Measured accelerations time history at the bottom of the soil for unsaturated condition test (matric suction = 4 kPa)

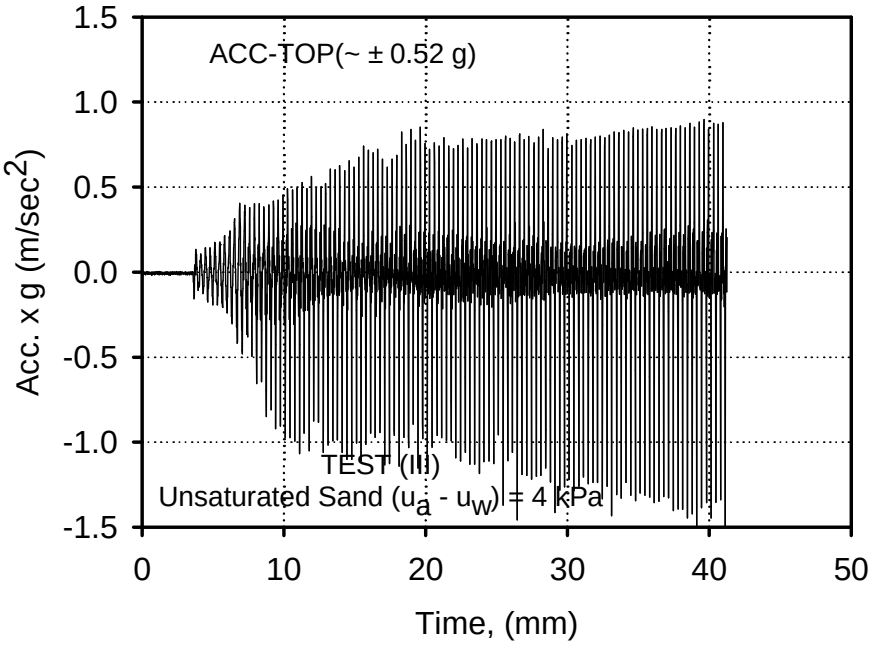

Figure B. 6 Measured accelerations time history at the top of the soil for unsaturated condition test (matric suction = 4 kPa)

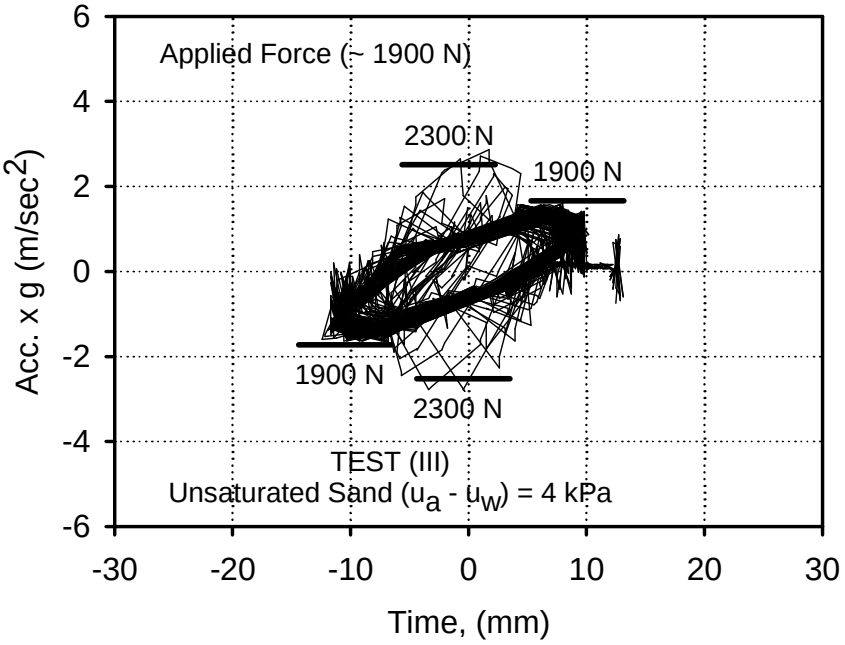

Figure B. 7 Measured actuator versus horizontal displacement (matric suction = 4 kPa)

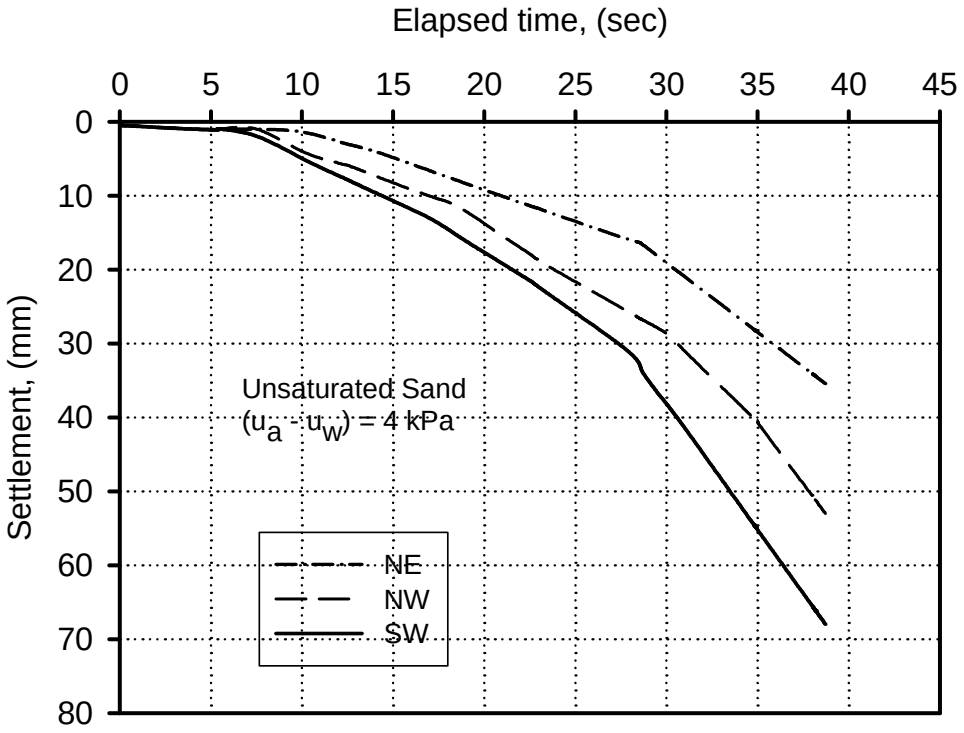

Figure B. 8 Measured settlement versus time of the model footing for saturated condition (matric suction = 4 kPa)